

WESTERN SYDNEY
UNIVERSITY



Hawkesbury Institute
for the Environment

**RESPONSES OF WHEAT PHOTOSYNTHESIS AND
YIELD TO ELEVATED CO₂ UNDER HEAT AND
WATER STRESS**

Sachin Gorakshnath Chavan

A thesis submitted in fulfilment of the requirements for the degree of Doctor of
Philosophy Degree

Hawkesbury Institute for the Environment
Western Sydney University
Australia

Dec 2017

This thesis is dedicated to my parents and supervisors for their endless support and encouragement.

ACKNOWLEDGEMENTS

It is with great pleasure that I wish to express my utmost gratitude to my principal supervisor, Assoc Prof Oula Ghannoum for her continuous encouragement, advice, and guidance. She has been a source of generosity, insight and inspiration; guiding me in all my efforts throughout my candidature. I owe my research achievements to her enthusiastic supervision. I acknowledge with great gratitude my co-supervisor Dr Remko Duursma who provided me with unflinching encouragement, support and feedback during the candidature. Successful completion of this thesis would not have been possible without their invaluable insights and comments on my work.

I gratefully acknowledge the Western Sydney University for granting me the Agriculture, Fisheries and Forestry Postgraduate Research Scholarship and DAFF, Filling the Research Gap for funding my PhD project. I also acknowledge the vibrant Hawkesbury Institute for the Environment and the ARC Centre of Excellence for Translational Photosynthesis for providing a stimulating academic environment and a platform to interact with renowned researchers in Photosynthesis.

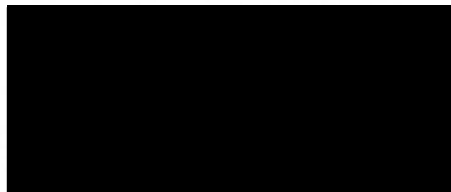
I acknowledge with great gratitude Prof Michael Tausz, Dr Sabine Tausz-Posch, Dr Markus Loew, Dr Maryse Bourgault and Osmin Torres Gutierrez from University of Melbourne, and Russel Argall and Sam Henty from DEPI, Horsham, for their valuable support in field data collection. I am thankful to Dr Craig Barton (HIE) for his assistance with the tuneable diode laser and carbon isotope discrimination measurements. I am also thankful to Mr Burhan Amiji and Ms Renee Smith (HIE) for their generous support with glasshouse experiments.

My gratitude also goes to staff at the Hawkesbury Institute for the Environment, Dr David Harland, Patricia Hellier, Lisa Davison, Jenny Harvey, Gavin McKenzie, David Thompson and Kerri Sherriff for their generous support on administrative and laboratory work. I wish to thank my research group colleagues Balasaheb Sonawane, Varsha Pathare Sonawane, Fiona Koller, Julius Sagun, Walter Israel, Dr Christie Foster, Dr Clémence Henry, Dr Javier Cano Martin and Dr Alex Watson-Lazowski for their friendship and support throughout my candidature. I am thankful to HIE-R user group and all my PhD colleagues at HIE and ANU.

As always, my heartfelt gratitude goes to my family members and friends for their love and constant support throughout my life and for motivating me to pursue an academic career.

STATEMENT OF AUTHENTICATION

The work presented in this thesis is, to the best of my knowledge and belief, original except as acknowledged in the text. I hereby declare that I have not submitted this material, either in full or in part, for a degree at this or any other institution

A large black rectangular box redacting the author's signature.

Author's Signature

TABLE OF CONTENTS

ACKNOWLEDGEMENTS	iii
STATEMENT OF AUTHENTICATION.....	iv
TABLE OF CONTENTS	v
LIST OF FIGURES	ix
LIST OF TABLES	xi
LIST OF SUPPLEMENTARY TABLES	xii
LIST OF SUPPLEMENTARY FIGURES	xiii
ABBREVIATIONS	xiv
GENERAL ABSTRACT	1
CHAPTER 1	3
GENERAL INTRODUCTION.....	3
1.1 Climate change	4
<i>1.1.1 Greenhouse gases and rising CO₂ concentrations.....</i>	<i>4</i>
<i>1.1.2 Climate warming.....</i>	<i>5</i>
<i>1.1.3 Extreme events and precipitation.....</i>	<i>6</i>
1.2 Wheat production in the context of climate change	8
<i>1.2.1 Production in Australia</i>	<i>8</i>
<i>1.2.2 Impact of climate change on wheat productivity</i>	<i>9</i>
1.3 Photosynthesis	10
<i>1.3.1 C₃ photosynthesis</i>	<i>11</i>
<i>1.3.2 Photorespiration</i>	<i>12</i>
<i>1.3.3 Rubisco properties</i>	<i>13</i>
<i>1.3.4 CO₂ diffusion.....</i>	<i>15</i>
<i>1.3.5 Biochemical models of C₃ photosynthesis.....</i>	<i>17</i>
1.4 Effect of climate change drivers on photosynthesis	19
<i>1.4.1 Elevated CO₂ effect on photosynthesis</i>	<i>19</i>
<i>1.4.2 Heat stress and eCO₂ response of photosynthesis</i>	<i>20</i>
<i>1.4.3 Water stress and eCO₂ response of photosynthesis</i>	<i>22</i>
1.5 AGFACE.....	24
1.6 Knowledge Gap	26
1.7 Aims and Objectives	27
1.8 Thesis format and structure.....	28

CHAPTER 2	29
ELEVATED CO₂ SIMILARLY STIMULATED BIOMASS AND YIELD OF TWO CONTRASTING WHEAT CULTIVARS WHILE MODERATE HEAT STRESS WAS NOT DETRIMENTAL	29
Abstract	30
2.1 Introduction	31
2.2 Materials and methods	35
2.2.1 <i>Plant culture and treatments</i>	35
2.2.2 <i>Growth and biomass measurements</i>	35
2.2.3 <i>Leaf gas exchange measurements</i>	36
2.2.4 <i>Mesophyll conductance and temperature response</i>	36
2.2.5 <i>Leaf nitrogen and carbon estimation</i>	38
2.2.6 <i>Statistical and temperature analysis</i>	38
2.3 Results	41
2.3.1 <i>Similar photosynthetic temperature responses at aCO₂ between the two wheat lines</i>	41
2.3.2 <i>eCO₂ stimulated wheat photosynthesis and reduced stomatal conductance despite causing a mild acclimation</i>	42
2.3.3 <i>HS did not inhibit photosynthesis at 25°C but slightly reduced photosynthesis at 35°C in aCO₂-grown plants</i>	42
2.3.4 <i>Larger Yitpi produced slightly more grain yield than faster Scout at current ambient CO₂</i>	43
2.3.5 <i>At anthesis, eCO₂ stimulated wheat biomass due to greater allocation to the stems</i>	44
2.3.6 <i>eCO₂ stimulated grain yield similarly in both wheat lines due to more grains per ear in Yitpi and more and bigger grains in Scout</i>	44
2.3.7 <i>eCO₂ did not stimulate the grain yield of HS plants and reduced grain N in Yitpi</i>	45
2.4 Discussion	46
2.4.1 <i>Two wheat lines with contrasting morphology and development, but similar photosynthesis and yield</i>	46
2.4.2 <i>Elevated CO₂ stimulated photosynthesis but reduced photosynthetic capacity in both lines</i>	46
2.4.3 <i>Elevated CO₂ tended to stimulate vegetative biomass more in Yitpi than Scout but grain yield stimulation was similar in both lines</i>	47
2.4.4 <i>Elevated CO₂ reduced grain N in Yitpi only</i>	47

2.4.5 HS was not harmful and increased biomass and grain yield in aCO ₂ grown plants.....	48
2.4.6 HS did not affect biomass and grain yield in eCO ₂ grown plants	49
2.5 Conclusions.....	50
CHAPTER 3.....	74
ELEVATED CO₂ REDUCES IMPACT OF HEAT STRESS ON WHEAT PHYSIOLOGY BUT NOT ON GRAIN YIELD	74
Abstract.....	75
3.1 Introduction.....	76
3.2 Material and methods.....	80
3.2.1 Plant culture and treatments.....	80
3.2.2 Temperature response of leaf gas exchange	80
3.2.3 Rubisco content determination	81
3.2.4 Leaf gas exchange measurements	81
3.2.5 Growth and biomass measurements	82
3.2.6 Statistical analysis	82
3.3 Results	84
3.3.1 eCO ₂ stimulated wheat photosynthesis with or without downregulation	84
3.3.2 Temperature response of gas exchange parameters in aCO ₂ and eCO ₂ grown plants.....	85
3.3.3 Leaf gas exchange and chlorophyll fluorescence response to eCO ₂ and HS	85
3.3.4 Response of biomass, morphological parameters and grain yield to eCO ₂ and HS	86
3.4 Discussion.....	88
3.4.1 Photosynthetic acclimation to eCO ₂ is a function of developmental stage	88
3.4.2 Elevated CO ₂ reduced photosynthetic capacity at higher temperature	89
3.4.3 Elevated CO ₂ protected plants from HS damage	90
3.4.4 Plant biomass recovered after HS but not the grain yield.....	91
3.5 Conclusions.....	92
CHAPTER 4.....	112
ELEVATED CO₂ DOES NOT PROTECT WHEAT FROM WATER STRESS IN DRYLAND CONDITIONS.....	112
Abstract.....	113
4.1 Introduction.....	114
4.2 Material and methods.....	117

3.2.1 Plant material	117
3.2.2 Site description.....	117
3.2.3 Experimental setup and general management	117
3.2.4 Biomass and grain yield measurements.....	118
3.2.5 Leaf gas exchange measurements	118
3.2.6 Data analysis	119
4.3 Results	121
4.3.1 Elevated CO ₂ did not affect soil water content under irrigated or rainfed conditions.....	121
4.3.2 Elevated CO ₂ stimulated photosynthesis and grain yield similarly under irrigated or rainfed conditions.....	121
4.3.3 Elevated CO ₂ reduced photosynthetic capacity only in 2015	122
4.3.4 Water stress equally reduced biomass and grain yield under aCO ₂ and eCO ₂	123
4.4 Discussion.....	124
4.4.1 Effect of eCO ₂ on soil water content	124
4.4.2 Effect of eCO ₂ and WS on photosynthesis.....	125
4.4.3 Elevated CO ₂ could not ameliorate WS damage.....	126
4.4.4 Response of photosynthesis, biomass and grain yield differed between the two growth seasons.....	126
4.4.5 Elevated CO ₂ and WS act antagonistically on grain quality.....	127
4.5 Conclusions.....	127
CHAPTER 5	144
GENERAL DISCUSSION	144
5.1 Overall thesis summary	145
5.2 Overall thesis conclusions.....	147
5.2.1. Scout and Yitpi responded to environmental factors differently in the glasshouse experiment and similarly in the field	147
5.2.2. Elevated CO ₂ interacted with slightly beneficial moderate HS and damaging severe HS under well-watered conditions.....	148
5.2.3. HS will more likely interact with eCO ₂ than WS under dryland field conditions	149
5.2.4 Elevated CO ₂ only marginally benefits wheat plants under severe HS or WS ..	150
5.3 Future prospects and implications	152
References.....	159

LIST OF FIGURES

Figure 1.1 Global carbon dioxide (CO ₂) emissions from fossil fuels responsible for warming since 1850 and enormous increase in the emissions in the last century (IPCC, 2014)	4
Figure 1.2 Emission scenarios and the resulting radiative forcing levels for the Representative Concentration Pathways (RCPs, lines) and the associated scenarios categories (IPCC, 2014)	5
Figure 1.3 Projected global average surface temperature change for the 2006–2100 period. Representative concentration pathways (RCP) describe four different pathways of greenhouse gas emissions for 21 st century (IPCC, 2014).....	6
Figure 1.4 Hot days over 35°C 2090 / RCP4.5 Relative to 1986-2005 (CSIRO and BOM, 2015)	7
Figure 1.5 Rainfall deciles for April to September 1997-2013, relative to the reference period 1900–2013 (source: BOM, 2014)	7
Figure 1.6 Wheat belt of Australia	8
Figure 1.7 Wheat export worldwide during 2016. The range from blue to red indicate export value in USD for different countries (AJG Simoes, CA Hidalgo)	9
Figure 1.8 Simulated water-limited wheat yield potential (Yw) trends in Australia from 1990 to 2015. Black dots indicate sites with no significant trend ($P > 0.1$); small coloured circles indicate stations with Yw decline ($P < 0.1$); large circles indicate stations with Yw decline ($P < 0.05$). Colour heat from yellow to red is used to indicate the rate of Yw decline in kg ha ⁻¹ yr ⁻¹	10
Figure 1.9 Light and dark reactions of photosynthesis transferring energy from the sun to fix atmospheric carbon	11
Figure 1.10 Calvin cycle depicting dark reactions of photosynthesis involving CO ₂ addition to RuBP by Rubisco to form 3-phosphoglycerate which is further phosphorylated and reduced to G-3-P. G-3-P is partly used to form carbohydrates and the rest recycled to regenerate RuBP	12
Figure 1.11 Photorespiration in higher plants	13
Figure 1.12 Mechanism of Rubisco catalyzed addition of CO ₂ and O ₂ to enolized RuBP	14
Figure 1.13 Pathway CO ₂ diffusion in leaves of C ₃ plants	16
Figure 1.14 Carbon isotope discrimination (Δ), over ratio of intercellular CO ₂ and ambient partial pressure of CO ₂ . The line drawn is equation 1 with $a = 4.4\%$ and $b = 27\%$	17
Figure 1.15 FvCB model depicting the response of CO ₂ assimilation rate over intercellular CO ₂ concentration limited by Rubisco and electron transport rate.....	18
Figure 1.16 Response of CO ₂ assimilation (A) to temperature (T) showing a specific optimum temperature (T _o) range.....	21
Figure 1.17 Aerial view of FACE site in Horsham, Victoria	24
Figure 1.18 Monthly mean maximum temperature trend for the year 2014 compared to all year records for highest and lowest monthly mean temperature.....	25
Figure 2.1 Glasshouse growth conditions	55
Figure 2.2 Glass house experimental design.....	56
Figure 2.3 Temperature response of photosynthetic parameters.....	57
Figure 2.4 Photosynthetic response of Scout and Yitpi to eCO ₂ measured at 25°C leaf temperature and various time points	58
Figure 2.5 Photosynthesis and chlorophyll fluorescence response of Scout and Yitpi to eCO ₂ measured during the two heat stress cycles	59
Figure 2.6 Response of photosynthetic parameters to eCO ₂ and heat stress measured at growth CO ₂ during anthesis (T ₃) in Scout and Yitpi	60
Figure 2.7 Booting and speed of development in Scout and Yitpi.....	61
Figure 2.8 Plant growth and morphological traits response to elevated CO ₂	62
Figure 2.9 Response of total dry mass and grain yield to growth at eCO ₂ and heat stress at final harvest (T ₄)	63
Figure 3.1 Glasshouse growth conditions and heat stress cycle	97

Figure 3.2 Photosynthetic response of Scout to eCO_2 measured thirteen weeks after planting (WAP) at two leaf temperatures and two CO_2 concentrations.....	98
Figure 3.3: Temperature response of V_{cmax} and J_{max} measured 13 weeks after planting (WAP).....	99
Figure 3.4 Response of V_{cmax} and J_{max} to growth at eCO_2 and HS measured 17 weeks after planting at the recovery stage of the HS cycle	100
Figure 3.5 Temperature response of spot gas exchange parameters measured thirteen weeks after planting (WAP).....	101
Figure 3.6 Photosynthetic response of aCO_2 and eCO_2 grown Scout measured before, during, after and at the recovery stage of the heat stress cycle	102
Figure 3.7 Chlorophyll fluorescence response of aCO_2 and eCO_2 grown Scout measured before, during, after and at the recovery stage of heat stress cycle	103
Figure 3.8 Response of biomass and ears (or tillers) to eCO_2 and HS across the life cycle of Scout	104
Figure 3.9 Response of plant total biomass and grain yield to elevated CO_2 and heat stress at the final harvest	105
Figure 4.1 Field growth conditions recorded during the growth season (GS) of 2014 and 2015.....	131
Figure 4.2 Effect of elevated CO_2 and irrigation on soil water content measured at different depths in 2014 and 2015	132
Figure 4.3 Effect of eCO_2 and irrigation on CO_2 assimilation rates (A_{sat}) and stomatal conductance (g_s) measured at common ($400 \mu l L^{-1}$) and growth CO_2 during 2014 and 2015	133
Figure 4.4 Effect of eCO_2 and irrigation on photosynthetic capacity during 2014 and 2015	134
Figure 4.5 Relationships between CO_2 assimilation rates (A_{sat}), stomatal conductance (g_s) and leaf nitrogen (N) content during 2014 and 2015.....	135
Figure 4.6 Relationships between A_{sat} per unit N, A_{sat} , C_i , g_s (measured at common CO_2) and soil water content	136
Figure 4.7 Effect of eCO_2 and irrigation on above ground dry matter and grain yield during 2014 and 2015	137
Figure 4.8 Effect of eCO_2 and irrigation on grain size and grain protein during 2014 and 2015	138
Figure 5.1 Fold change with eCO_2 in control and stresses plants for Photosynthesis, biomass and grain yield per plant.....	157
Figure 5.2 Modelling approach to consider interactive effects of eCO_2 with HS and WS	158

LIST OF TABLES

<i>Table 1.1 Monthly mean maximum temperatures for year 2014 compared to all year records for highest and lowest monthly mean temperature records for all years</i>	<i>25</i>
<i>Table 2.1 Summary of modelled parameters for temperature response of photosynthesis.....</i>	<i>51</i>
<i>Table 2.2 Summary of statistics for gas exchange parameters</i>	<i>52</i>
<i>Table 2.3 Response of plant dry mass, grain yield and nitrogen (N) content to elevated CO₂ and heat stress</i>	<i>53</i>
<i>Table 2.4 Summary of statistics for plant dry mass and morphological parameters</i>	<i>54</i>
<i>Table 3.1 Summary of modelled parameters for temperature response of photosynthesis.....</i>	<i>93</i>
<i>Table 3.2 Summary of statistics for gas exchange parameters</i>	<i>94</i>
<i>Table 3.3 Response of plant dry mass (DM) and morphological parameters to elevated CO₂ and heat stress</i>	<i>95</i>
<i>Table 3.4 Summary of statistics for plant dry mass (DM) and morphological parameters</i>	<i>96</i>
<i>Table 4.1 Summary of constants used for estimating gas exchange parameters</i>	<i>128</i>
<i>Table 4.2 Summary of statistics for gas exchange parameters</i>	<i>129</i>
<i>Table 4.3 Summary of statistics for plant dry matter (DM) and grain yield parameters.....</i>	<i>130</i>
<i>Table 5.1 Comparative responses to eCO₂ of two wheat cultivars grown in either the glasshouse in the field</i>	<i>154</i>
<i>Table 5.2 Comparative responses of the wheat cultivar Scout to eCO₂ and moderate or severe HS.....</i>	<i>155</i>
<i>Table 5.3 Comparative wheat responses to moderate HS, severe HS and WS.</i>	<i>156</i>

LIST OF SUPPLEMENTARY TABLES

<i>Table S 2.1 Response of Scout gas exchange parameters to elevated CO₂ and heat stress</i>	<i>64</i>
<i>Table S 2.2 Response of Yitpi gas exchange parameters to growth at elevated CO₂ and heat stress</i>	<i>65</i>
<i>Table S 2.3 Response of other plant dry mass and morphological parameters to elevated CO₂ and HS.....</i>	<i>66</i>
<i>Table S 2.4 Summary of plant nitrogen content parameters.....</i>	<i>68</i>
<i>Table S 3.1 Response of leaf gas exchange parameters to elevated CO₂ and heat stress Summary of leaf gas exchange parameters measured at different time points for Scout grown at ambient CO₂ (aCO₂) or elevated CO₂ (eCO₂) and exposed (H) or not exposed (control) to 5-day heat stress (HS) at the flowering stage. Values are means ± SE (n= 9-10).....</i>	<i>106</i>
<i>Table S 4.1 Response of Scout gas exchange parameters to elevated CO₂ and water stress during 2014 and 2015.....</i>	<i>139</i>
<i>Table S 4.2 Response of Yitpi gas exchange parameters to elevated CO₂ and water stress during 2014 and 2015.....</i>	<i>140</i>
<i>Table S 4.3 Response of plant dry matter (DM) and grain yield parameters to elevated CO₂ and water stress</i>	<i>141</i>

LIST OF SUPPLEMENTARY FIGURES

<i>Figure S 2.1 Relationships between gas exchange parameters at T3</i>	<i>69</i>
<i>Figure S 2.2 Photosynthetic response to growth at eCO₂ and heat stresses (H1 and H2).....</i>	<i>70</i>
<i>Figure S 2.3 Relationship between dry mass and morphological parameters measured at anthesis (T3) ...</i>	<i>71</i>
<i>Figure S 2.4 Relationship between grain protein content and yield</i>	<i>72</i>
<i>Figure S 2.5 Vapour pressure deficit (VPD) plotted over time during HS1 and HS2</i>	<i>73</i>
<i>Figure S 3.1 Relationship between biomass and morphological parameters measured 13 weeks after planting at the recovery stage of the HS cycle</i>	<i>107</i>
<i>Figure S 3.2 Response of grain size and morphology to heat stress at the final harvest</i>	<i>108</i>
<i>Figure S 3.3 Experimental design</i>	<i>109</i>
<i>Figure S 3.4 Radiation over time</i>	<i>110</i>
<i>Figure S 3.5 Grain yield of main shoot and tillers</i>	<i>111</i>
<i>Figure S 4.1 Carbon isotope discrimination values (d13C) for Scout and Yitpi.....</i>	<i>142</i>
<i>Figure S 4.2 Radiation profile for growth seasons 2014 and 2015</i>	<i>143</i>

ABBREVIATIONS

Δ	-	Photosynthetic carbon isotope discrimination
ΔS	-	Entropy term
$\delta^{13}\text{C}$	-	Leaf carbon isotope composition
$a\text{CO}_2$	-	Ambient CO_2
AGFACE	-	Australian Grains Free air CO_2 enrichment
A_{sat}	-	Light saturated CO_2 assimilation rate
A_{net}	-	Net CO_2 assimilation rate
a'	-	Combined fractionation factor through the leaf boundary layer and stomata
A-C_i	-	Response of CO_2 assimilation rate to intercellular CO_2 concentration
APSIM	-	Agricultural Production Systems SIMulator
ATP	-	Adenosine triphosphate
b'_3	-	Combined fractionation of Rubisco, respiration and photorespiration
b'_4	-	Fractionation occurring during PEP carboxylation
BIS	-	Bisphosphoglycerate
BOM	-	Bureau of Meteorology
C₃	-	C_3 photosynthesis pathway
CABP	-	2-carboxyarabinitol 1,5- bisphosphate
C_a	-	Ambient CO_2 concentration
C_i	-	Intercellular CO_2 concentration
C_c	-	Chloroplastic CO_2 concentration
CSIRO	-	Commonwealth Scientific and Industrial Research Organization
DEPI	-	Department of primary industries
eCO_2	-	Elevated CO_2
E_a	-	Activation energy (J mol^{-1})
EDTA	-	Ethylenediaminetetraacetic acid

EPSP	-	4-(2-Hydroxyethyl)-1-piperazinepropanesulfonic acid, 4-(2-Hydroxyethyl) piperazine-1-propanesulfonic acid, N-(2-Hydroxyethyl) piperazine-N'-(3-propanesulfonic acid)
FACE	-	Free air CO ₂ enrichment
<i>g_s</i>	-	Stomatal conductance
<i>g_m</i>	-	Mesophyll conductance
G3P	-	Glyceraldehyde 3 phosphate
<i>H_d</i>	-	Deactivation energy (J mol ⁻¹)
HS	-	Heat stress
IRGA	-	infrared gas analyzer
IPCC	-	Intergovernmental Panel on Climate Change
<i>J_{max}</i>	-	Maximal RuBP regeneration rate (μmol CO ₂ m ⁻² s ⁻¹)
<i>k₂₅</i>	-	Parameter rate at 25°C
<i>k_mk₂₅</i>	-	Michaelis Menten constant
LCF		leaf chamber fluorometer
MgCl₂	-	Magnesium chloride
MnCl₂	-	Manganese chloride
N	-	Nitrogen
Narea	-	Leaf nitrogen per unit area
NADH	-	β-Nicotinamide adenine dinucleotide
NaHCO₃	-	Sodium bicarbonate
NOAA	-	National Oceanic and Atmospheric Administration
NUE	-	Nitrogen use efficiency
NUE_b	-	Nitrogen use efficiency of biomass
NUE_g	-	Nitrogen use efficiency of grain yield
PGA	-	Phosphoglycerate
Plant DM	-	Plant dry mass
PNUE	-	Photosynthetic nitrogen use efficiency
PPFD	-	Photosynthetic photon flux density
ppm	-	Parts per million
PSI	-	Photosystem I
PSII	-	Photosystem II
PWUE	-	Photosynthetic water use efficiency

r^2	-	Regression coefficient
RH	-	Relative humidity
Rubisco	-	Ribulose-1, 5-bisphosphate carboxylase/ oxygenase
RuBP	-	Ribulose-1, 5-bisphosphate
SE	-	Standard error
$S_{c/o}$	-	Specificity factor
SWC	-	Soil water content
t	-	Ternary effects of transpiration rate on the carbon isotope
TDL	-	Tunable Diode Laser
T_o	-	Thermal optimum
VPD	-	Vapor pressure deficit
V_{cmax}	-	Maximal RuBP carboxylation rate ($\mu\text{mol CO}_2 \text{ m}^{-2} \text{ s}^{-1}$)
R_d	-	Dark respiration ($\mu\text{mol CO}_2 \text{ m}^{-2} \text{ s}^{-1}$)
WS	-	Water stress

GENERAL ABSTRACT

Climate change involves rising CO₂ and temperature, varying rainfall patterns as well as increased frequency and duration of heat stress (HS) and water stress (WS). It is important to assess the impact of climate change, including extreme events on crop productivity to manage future food security challenges. Elevated CO₂ (eCO₂) boosts leaf photosynthesis and plant productivity, however plant responses to eCO₂ depend on environmental conditions. The response of wheat to eCO₂ has been investigated in enclosures and in field studies; however, studies accounting for eCO₂ interactions with HS or WS are limited. My PhD project addresses this knowledge gap.

The broad aim of this thesis was to investigate the response of two commercial wheat cultivars with contrasting agronomical traits to future climate with eCO₂ and more extreme events, in order to develop a mechanistic approach that can potentially be incorporated in current crop models, which, so far, fail to predict accurate yields under stressful conditions. Consequently, I investigated the interactive effects of eCO₂ with either heat HS or WS on photosynthesis, crop growth and grain yield of the two wheat cultivars Scout and Yitpi grown either in the glasshouse or in a dryland field.

In the first glasshouse experiment, the two cultivars were grown at current ambient (450 ppm) and future elevated (650 ppm) CO₂ concentrations, 22/14°C day/night temperature, supplied with non-limiting water and nutrients and exposed to 3-day moderate HS cycles at the vegetative (38/14°C) and flowering stage (33/14°C). At aCO₂, both wheat lines showed similar photosynthetic temperature responses; while larger and greater-tillering Yitpi produced slightly more grain yield than early-maturing Scout. Elevated CO₂ stimulated wheat photosynthesis and reduced stomatal conductance despite causing mild photosynthetic acclimation, while moderate HS did not inhibit photosynthesis at 25°C but slightly reduced photosynthesis at 35°C in aCO₂-grown plants. Elevated CO₂ similarly stimulated final biomass and grain yield of the two wheat cultivars not exposed to moderate HS by variably affecting grain size and number. *The main distinct outcomes of this chapter were the insignificant effect of moderate HS on wheat yield and the reduced grain nutrient quality of high tillering Yitpi at eCO₂.*

In the second glasshouse experiment, a single cultivar Scout was grown at current ambient (419 ppm) and future elevated (654 ppm) CO₂ concentrations, 22/14°C day/night temperature, supplied with non-limiting water and nutrients and exposed to 5-day severe HS cycle at the flowering stage (39/23°C). Growth at eCO₂ led to downregulation of photosynthetic

capacity in Scout measured at common CO₂ and leaf temperature in control plants not exposed to severe HS. Severe HS reduced light saturated CO₂ assimilation rates (A_{sat}) in aCO₂ but not in eCO₂ grown plants. Growth stimulation by eCO₂ protected plants by increasing electron transport capacity under severe HS, ultimately avoiding the damage to maximum efficiency of photosystem II. Elevated CO₂ stimulated biomass and grain yield, while severe HS equally reduced grain yield at both aCO₂ and eCO₂ but had no effect on biomass at final harvest due to stimulated tillering. *In conclusion, eCO₂ protected wheat photosynthesis and biomass against severe HS damage at the flowering stage via increased maximal rate of RuBP regeneration (J_{max}), indicating an important interaction between the two components of climate change, however grain yield was reduced by severe HS in both CO₂ treatments due to grain abortion.*

The field experiment investigated the interactive effects of eCO₂ and WS on two wheat cultivars Scout and Yitpi grown under dryland field conditions using free air CO₂ enrichment (FACE). Plants were grown at two CO₂ concentrations (400 and 550 ppm) under rainfed or irrigated conditions over two growing seasons during 2014 and 2015. Irrigation in dryland field conditions created contrasting soil water conditions under aCO₂ and eCO₂. Elevated CO₂ and WS responses of biomass and grain yield differed in the two growing seasons. Elevated CO₂ stimulated photosynthesis, biomass and grain yield, but reduced photosynthetic capacity evident from lower maximal rate of RuBP carboxylation (V_{cmax}) and flag leaf N only in 2015. *Water stress reduced above-ground biomass and grain yield in both cultivars and CO₂ treatment more strongly in 2014 relative to 2015. However, marginal growth stimulation by eCO₂ did not protect plants from WS. Biomass, grain yield and grain quality were antagonistically affected by eCO₂ and WS.*

When all data were considered together, I observed that Scout and Yitpi responded differently to growth conditions in the glasshouse and responded similarly in the field. Under well-watered conditions, Scout and Yitpi slightly benefited from moderate HS but were adversely impacted by severe HS. At the flowering stage, severe HS caused grain abortion decreasing grain yield in both CO₂ treatments. Elevated CO₂ alleviated photosynthetic inhibition but did not stop grain yield damage caused by severe HS. Water stress reduced net photosynthesis, biomass and grain yield in both CO₂ treatments and no interaction between eCO₂ and WS was observed for any of the measured parameters. Grain yield was stimulated by eCO₂ more in the glasshouse than in the field. Grain nutrient quality was reduced by eCO₂ and unaffected by either HS or WS (in both season average).

CHAPTER 1

GENERAL INTRODUCTION

1.1 Climate change

Climate has been changing throughout history and most of these changes are attributed to very small changes in Earth's orbit that change the amount of solar energy the Earth receives from the Sun. However, the current trend of climate change being human induced is of particular significance as the rate of change is unprecedented in the past thousand years. Atmospheric concentrations of carbon dioxide (CO₂) have been steadily rising from 315 parts per million (ppm) in 1959 to a current atmospheric average of approximately 385 ppm (Keeling, et al., 2009). The evidence for climate change is compelling as the sea levels have risen by 17 cm in the last century. The rate in the last decade is twice as fast compared to last century. Warming oceans, shrinking ice sheets, declining arctic sea ice, glacial retreat, extreme events and ocean acidification are the other major evidences of global climate change.

1.1.1 Greenhouse gases and rising CO₂ concentrations

Carbon dioxide, methane, nitrous oxide and fluorinates are the most important greenhouse gases that have increased post industrial revolution. In the last century there is enormous increase in greenhouse gas emissions generated by fossil fuels (Figure 1.1, IPCC, 2014) that are heating the planet at a much faster rate than ever before.

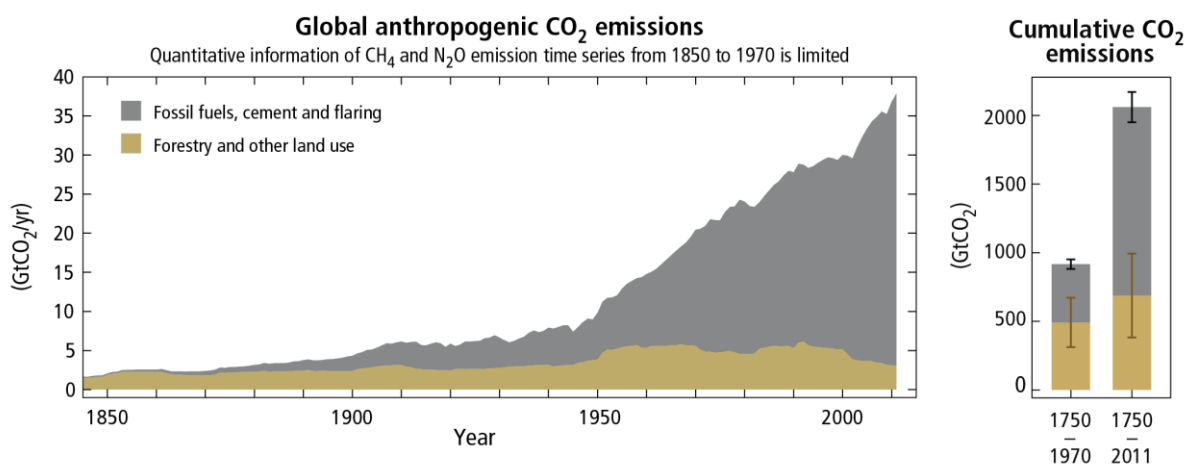


Figure 1.1 Global carbon dioxide (CO₂) emissions from fossil fuels responsible for warming since 1850 and enormous increase in the emissions in the last century (IPCC, 2014)

Given these gases remain in the atmosphere for longer periods, atmospheric greenhouse gas concentrations would continue to increase and remain elevated for hundreds of years. Given it is difficult to project far-off future emissions and other human factors that influence climate, the future CO₂ concentrations are projected based on various assumptions about future economic, social, technological, and environmental conditions (Figure 1.2, IPCC, 2014). By 2100 CO₂ is expected to reach 580 – 720 ppm according to the most likely emission scenario.

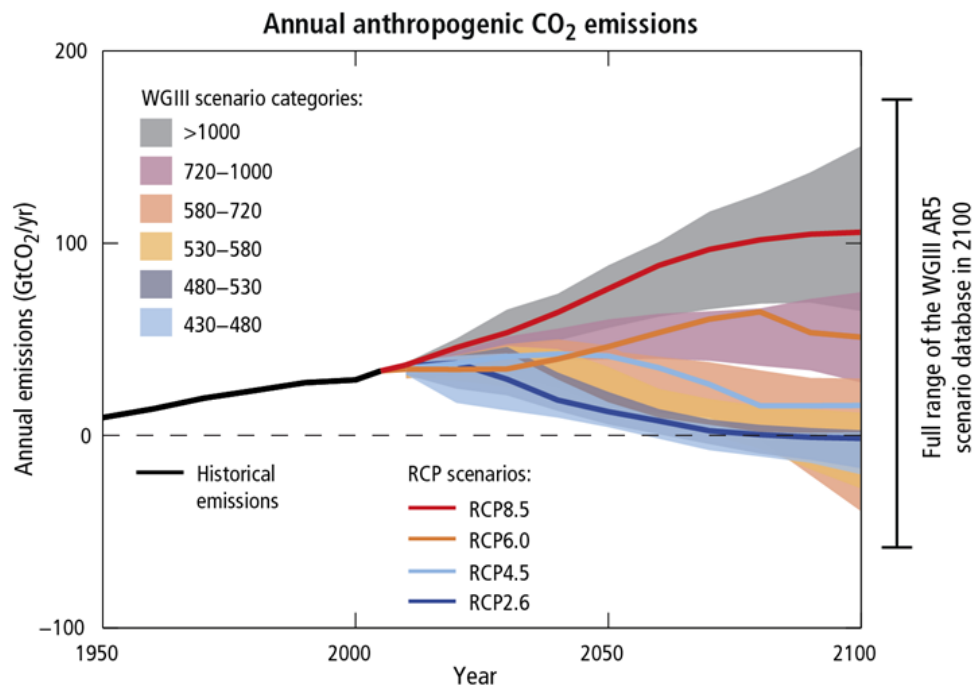


Figure 1.2 Emission scenarios and the resulting radiative forcing levels for the Representative Concentration Pathways (RCPs, lines) and the associated scenarios categories (IPCC, 2014)

1.1.2 Climate warming

Scientific studies predict that a global temperature rise of close to 3°C (above pre-industrial levels) could result in 25% of the Earth's animals and plants disappearing because they cannot adapt fast enough. Average temperatures on Earth have already warmed by 0.85°C. Global average temperatures projected with three different scenarios predict distinct rise in the temperature and observations till now follow the prediction trend (Figure 1.3). For example, global mean surface temperature is expected to increase by 1.1°C to 2.6°C by 2100 (IPCC, 2014). Since 1910, Australian temperatures have increased by 0.9°C, with more warming in night time minimum temperature than daytime maximum temperature (CSIRO and BOM, 2015).

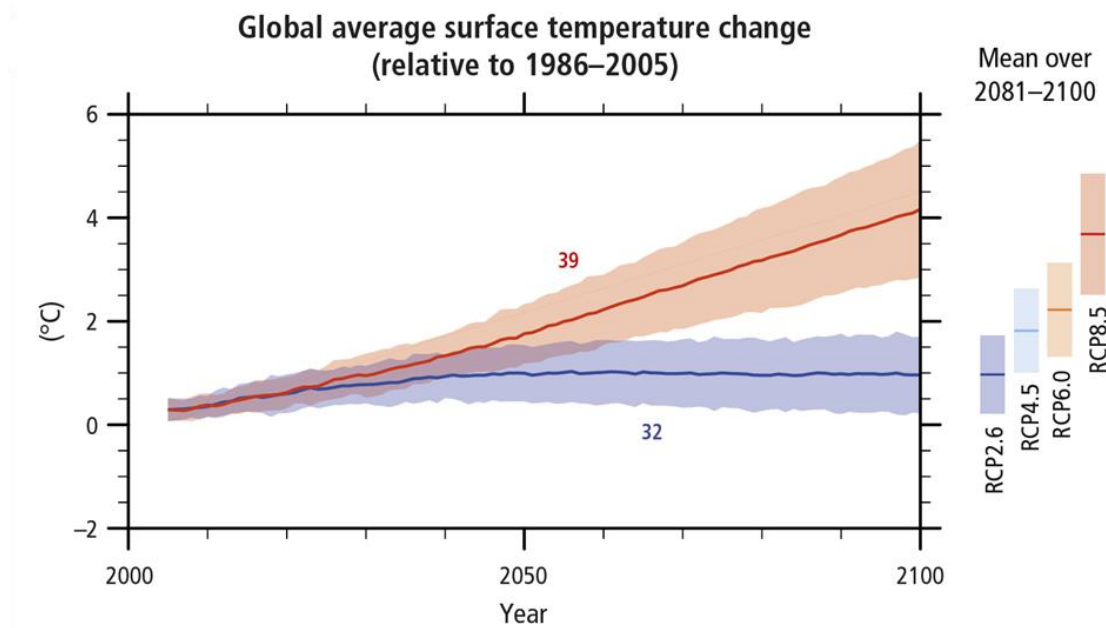


Figure 1.3 Projected global average surface temperature change for the 2006–2100 period. Representative concentration pathways (RCP) describe four different pathways of greenhouse gas emissions for 21st century (IPCC, 2014)

1.1.3 Extreme events and precipitation

In the near future hotter days, more severe storms, floods, snowfalls, droughts, fire and higher sea levels are expected (Rosenzweig et al., 2001). The average temperature changes have been accompanied by a large increase in extreme events. Patterns of precipitation and storm events, including both rain and snowfall are also likely to change. The amount of rain falling in heavy precipitation events is likely to increase in most regions, while storm tracks are projected to shift pole ward (Meehl et al 2007). Heat records do not linger anymore, 2016 was the warmest year on record relative to 20th century average which surpassed the previous recent records (NOAA, 2016). Australia had its warmest year in 2013 since the records began in 1910 (BOM, 2014), while 2016 was the 4th warmest and year of extreme events for Australia (NOAA, 2016 and BOM, 2017). Trends projected relative to observations recorded between 1986 and 2005 predict up to additional 3 - 100 more days above 35°C in major Australian cities (Figure 1.4, CSIRO and BOM, 2015).

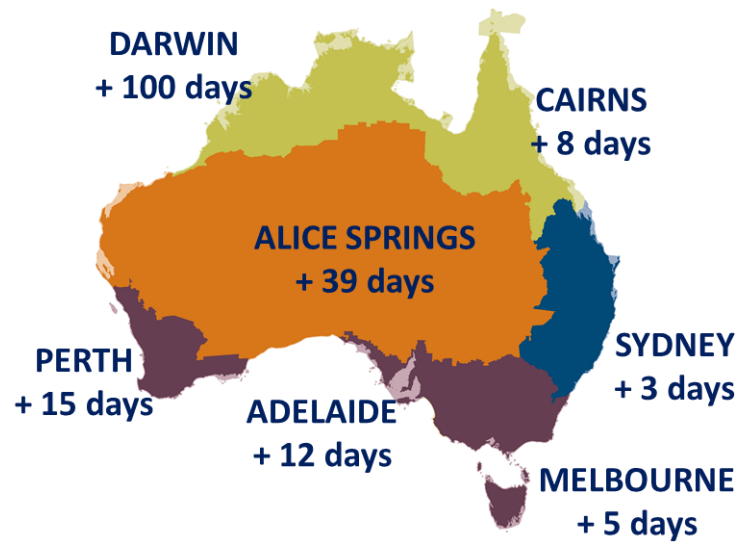


Figure 1.4 Hot days over 35°C 2090 / RCP4.5 Relative to 1986-2005 (CSIRO and BOM, 2015)

In addition, Australia has seen a linear decreasing trend in the rainfall over the entire 20th century. Rainfall declines over cooler months of the year in the south-west and south-east regions of Australia which is also the wheat growing belt (Figure 1.5). Rainfall is the major limiting factor for agriculture in Australian environment (CSIRO and BOM, 2015). These changes will adversely affect agricultural production and entire ecosystems.

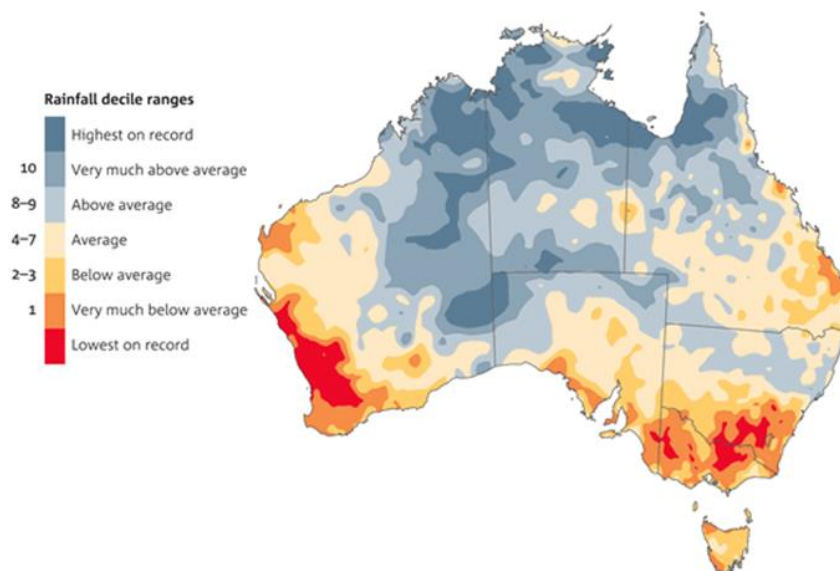


Figure 1.5 Rainfall deciles for April to September 1997-2013, relative to the reference period 1900–2013 (source: BOM, 2014)

1.2 Wheat production in the context of climate change

1.2.1 Production in Australia

Wheat (*Triticum aestivum*) is the major winter crop grown worldwide including Australia with major producing states including Western Australia, New South Wales, South Australia, Victoria and Queensland (Figure 1.6).

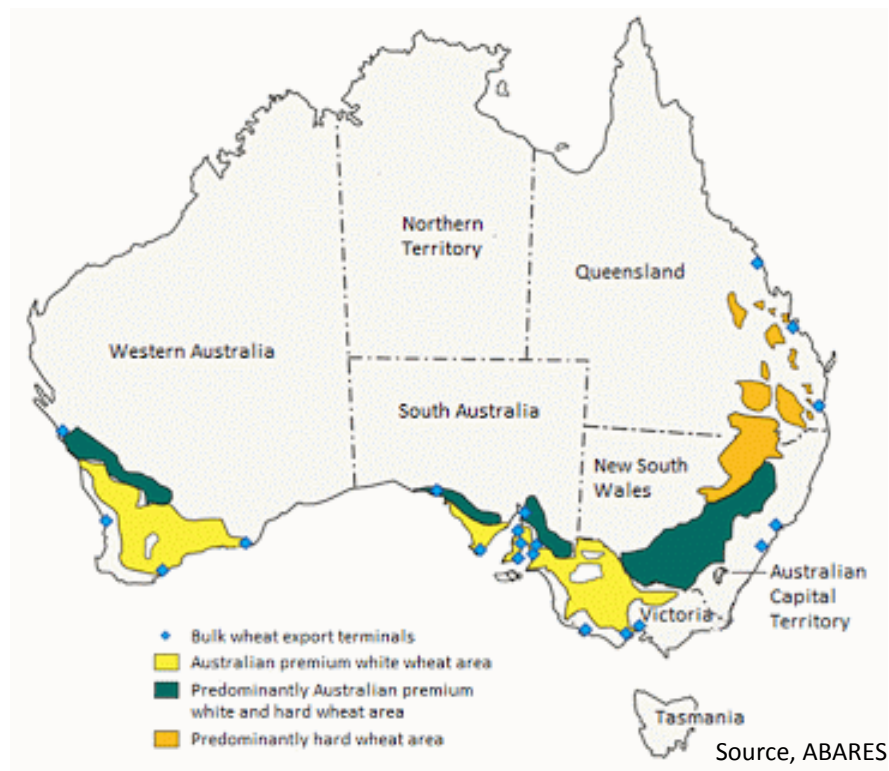


Figure 1.6 Wheat belt of Australia

Wheat is sown in autumn and harvesting depends on seasonal conditions, occurring in spring and summer. It is used for the production of breads, noodles and pastas. Australia produces just 3% of the world's wheat but accounts for 10-15% of the world's 100 million tonne annual global wheat trade. Most of Australian wheat is sold in overseas markets from Asia and Middle East regions with Western Australia the largest exporting state. Wheat is one of the largest contributors to Australian economy accounting \$3.5 billion export earnings for Australia in 2016 (Figure 1.7, *AJG Simoes, CA Hidalgo*). Australia is a key player in the world wheat market as wheat is one of the most valuable exports for Australia (PwC, Australia).

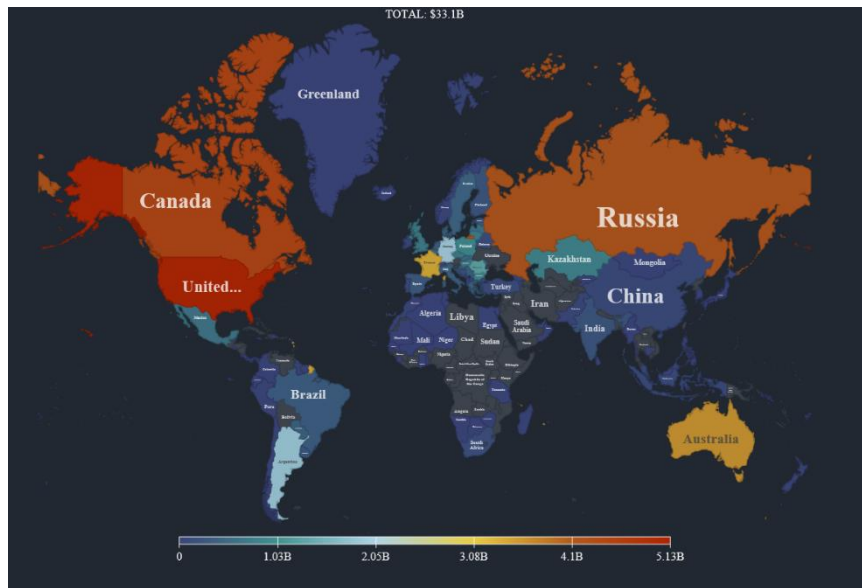


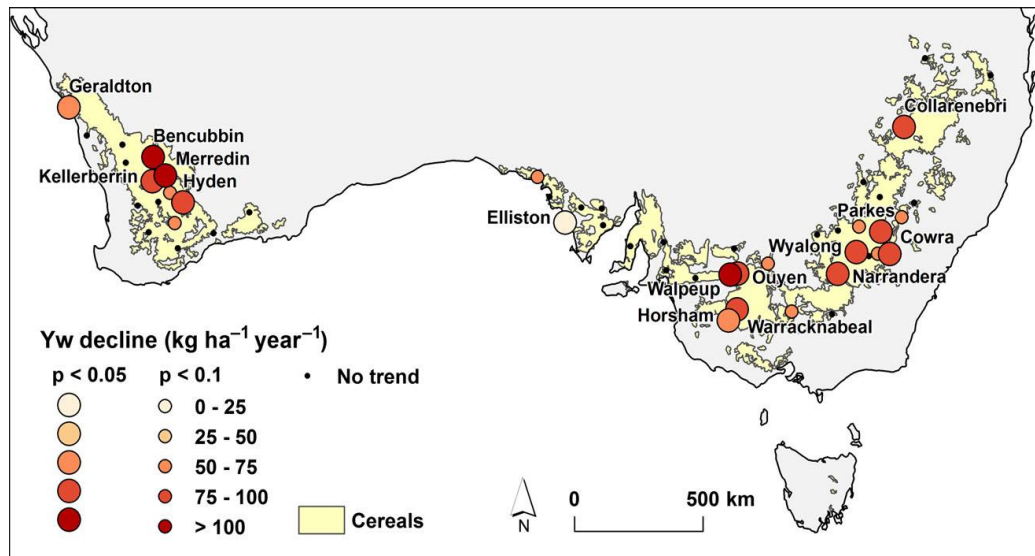
Figure 1.7 Wheat export worldwide during 2016. The range from blue to red indicate export value in USD for different countries (AJG Simoes, CA Hidalgo)

1.2.2 Impact of climate change on wheat productivity

The key drivers of crop responses to climate change are changes in atmospheric CO₂, temperature and precipitation (Asseng et al., 2013). The potential impacts of climate change on agriculture does not only depend on the mean values of expected climatic parameters but also on the probability, frequency, and severity of possible extreme events (Rosenzweig et al., 2001). Ongoing climate change has reduced wheat production and for every degree of temperature increase, global wheat production is expected to decrease by 6% (Asseng et al., 2015). Hochman et al., (2017) analysed the major limiting factors for wheat production in the recent years and showed that climate trends account for stalled wheat yields in Australia since 1990 (Figure 1.8).

It is difficult to accurately measure the effects of changes in climate on global crop production as agriculture is always changing, however current scientific understanding represents credible threat to sustainable crop productivity (Lobell and Gourdji, 2012). Crop models currently used such as APSIM (Agricultural Production Systems SIMulator) can predict the growth and yield under current environmental conditions (Holzworth et al., 2014; Keating et al., 2003). However, these crop models lack the mechanistic approach to consider stresses and their interaction to accurately predict the crop yield under eCO₂ and future extreme climate. Photosynthesis is a vital process affected by drivers of climate change and thus can be useful

in developing a mechanistic approach to improve the predictability of crop models (Wu et al., 2016, 2017; Yin and Struik, 2009).



Hochman et al., (2017)

Figure 1.8 Simulated water-limited wheat yield potential (Yw) trends in Australia from 1990 to 2015. Black dots indicate sites with no significant trend ($P > 0.1$); small coloured circles indicate stations with Yw decline ($P < 0.1$); large circles indicate stations with Yw decline ($P < 0.05$). Colour heat from yellow to red is used to indicate the rate of Yw decline in $\text{kg ha}^{-1} \text{ yr}^{-1}$

1.3 Photosynthesis

Photosynthesis is the primary physiological process that harvests energy from the sun to convert CO_2 into sugars. The chlorophyll pigments of chloroplasts in mesophyll tissue of leaves are the actual sites of photosynthesis. Photosynthesis consists of two types of reactions namely light reactions and the dark reactions (Figure 1.9). Thylakoid membranes of chloroplasts consist of protein-pigment complexes that together serve as an antenna, collecting light and transferring its energy to the reaction center, where chemical reactions store some of the energy by transferring electrons from a chlorophyll pigment to an electron acceptor molecule. The electron acceptor NADP is reduced to NADPH (nicotinamide adenine dinucleotide phosphate) and ATP (adenosine triphosphate) is produced using the proton gradient. NADPH and ATP are further utilized in carbon reduction. Thus, light reactions capture and convert sunlight to chemically usable form of energy to drive CO_2 assimilation and growth. The dark reactions take place in the stroma within the chloroplast that fix CO_2 in the form of carbohydrates. Dark reactions use the products of the light reactions (ATP and NADPH) (Taiz and Zeiger, 2010).

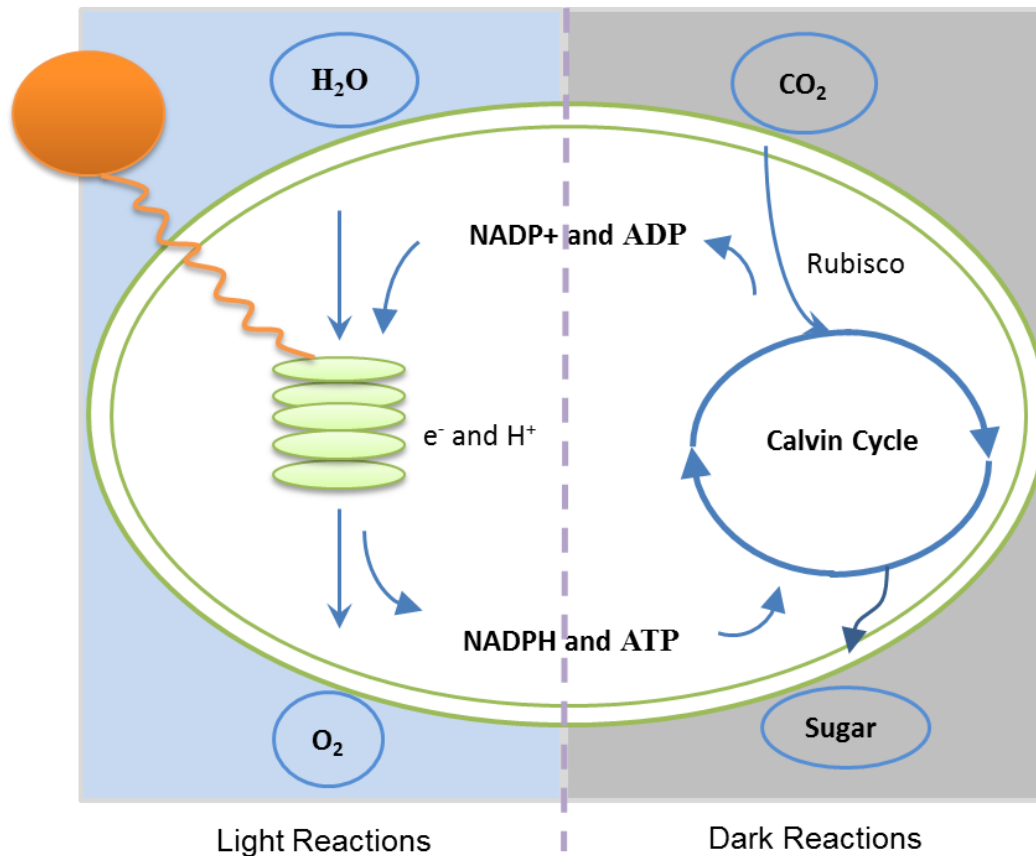
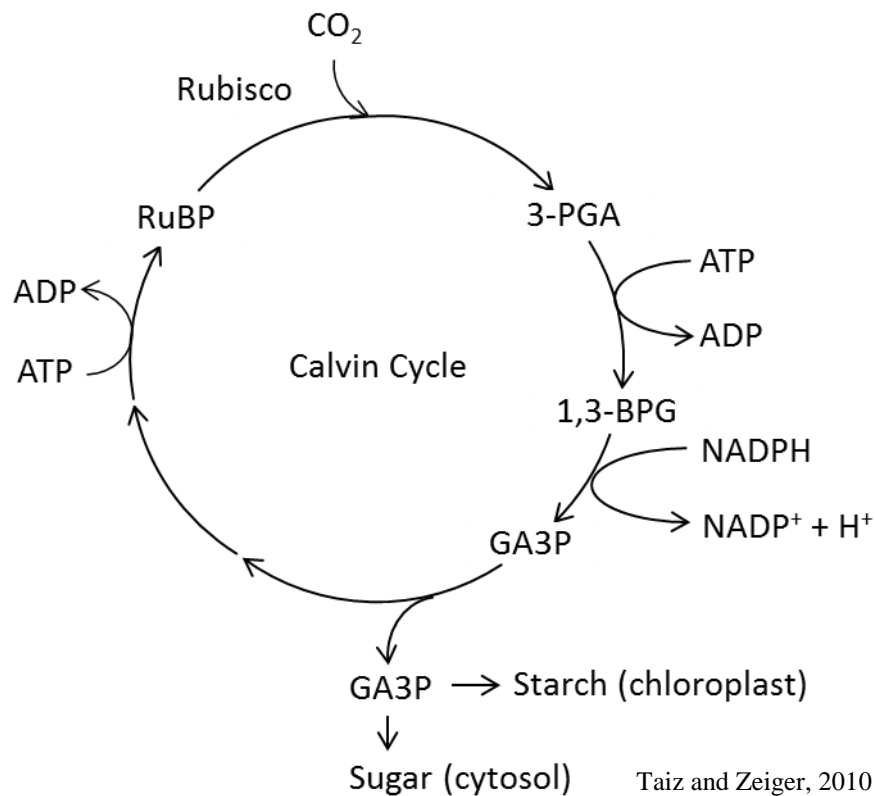


Figure 1.9 Light and dark reactions of photosynthesis transferring energy from the sun to fix atmospheric carbon

1.3.1 *C₃ photosynthesis*

The Calvin (C_3) cycle is the major pathway employed for carbon fixation by C_3 plants along with C_4 and CAM. C_3 photosynthesis employs the C_3 cycle also known as Calvin cycle or the photosynthetic carbon reduction cycle. The Calvin cycle comprises a series of chemical reactions categorized into CO_2 fixation, reduction, and regeneration (Figure 1.10). CO_2 is fixed using Ribulose-1, 5-bisphosphate carboxylase/oxygenase (Rubisco) enzyme leading to the formation of the first stable 3-carbon product, 3-Phosphoglycerate (3-PGA). 3-PGA is then phosphorylated by phosphoglycerate kinase using ATP to form 1, 3-bisphosphoglycerate (1, 3-BPG). 1, 3-BPG is reduced to glyceraldehyde-3-phosphate (G-3-P) using NADPH. G-3-P can be used in starch synthesis within the chloroplast or exported to the cytosol for sucrose synthesis. Finally, RuBP is regenerated at the expense of ATP molecules to continue the cycle.



Taiz and Zeiger, 2010

Figure 1.10 Calvin cycle depicting dark reactions of photosynthesis involving CO_2 addition to RuBP by Rubisco to form 3-phosphoglycerate which is further phosphorylated and reduced to G-3-P. G-3-P is partly used to form carbohydrates and the rest recycled to regenerate RuBP

1.3.2 Photorespiration

An important property of Rubisco is to catalyse both the carboxylation and oxygenation of RuBP. The oxygenation of RuBP leads to the formation of PGA and phosphoglycolate. Phosphoglycolate is dephosphorylated to glycolate by phosphoglycolate phosphatase inside the chloroplast. Glycolate oxidase in peroxisomes oxidises glycolate to glyoxylate which is further converted to glycine. Conversion of glycine to serine by glycine decarboxylase in mitochondria is a key step that leads to loss of CO_2 . Serine is then converted back to 3-PGA at the cost of energy in the form of ATP and NADPH (Ogren, 1984). This whole process that takes place in chloroplasts, peroxisomes and mitochondria is referred to as photorespiration (Figure 1.11). Photorespiration may cause loss of up to 50% of carbon fixed by Rubisco in C_3 plants (Zelitch, 1973).

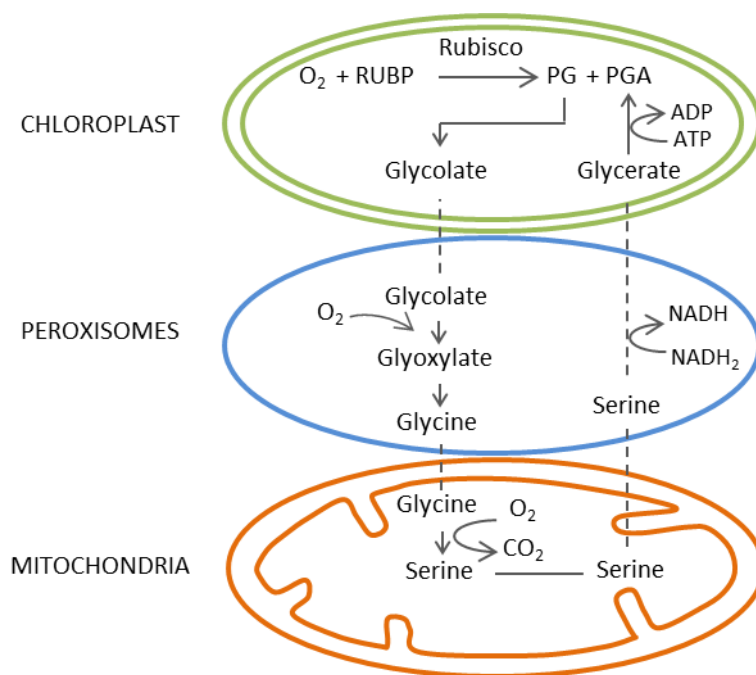


Figure 1.11 Photorespiration in higher plants

1.3.3 Rubisco properties

Activity of Rubisco is limited by its kinetic properties. Rubisco needs to be activated by carbamylation of conserved residue K201 which is further stabilized by Mg^{2+} binding. Rubisco activase acts as active site protection enzyme by removing the storage or inhibitory RuBP lacking carbamate (Portis and Salvucci, 2002). In addition, the rate of Rubisco activity is also regulated by CO_2 and phosphate. Rubisco is a slow catalyst as it has a very low turnover rate (K_{cat}) of 3 to 4 CO_2 molecules per second in most C_3 plants at $25^\circ C$. Hence it is the primary rate limiting step in the Calvin cycle. The affinity of the enzyme for its substrate can be determined by the Michaelis Menten (K_m) constant in enzyme kinetics. K_m is defined as the substrate concentration when the enzyme operates at half of its maximum rate. Michaelis Menten constants of Rubisco for CO_2 and O_2 are abbreviated as K_c and K_o respectively. O_2 competitively inhibits CO_2 , reducing the apparent affinity (K_m^{air}) of Rubisco for CO_2 . Apparent K_m is defined as " $K_c (1+O/K_o)$ ", where O is the O_2 concentration in the chloroplast.

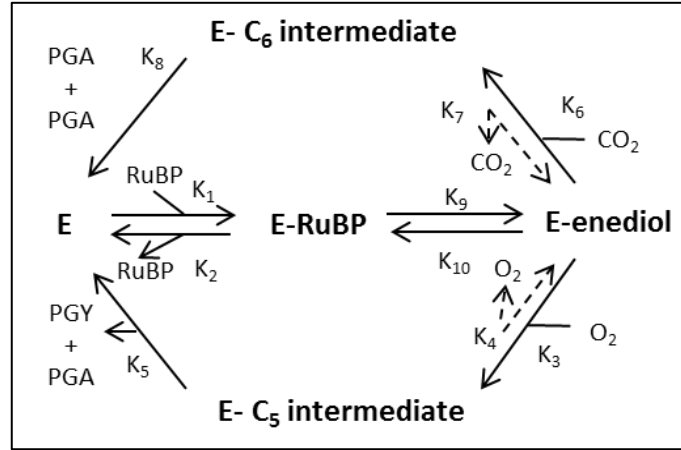


Figure 1.12 Mechanism of Rubisco catalyzed addition of CO₂ and O₂ to enolized RuBP

$$K_c = \frac{k_8}{k_6} \times \frac{k_9 + k_{10}}{k_9} \quad K_o = \frac{k_5}{k_3} \times \frac{k_9 + k_{10}}{k_9}$$

$$k_{cat}^c = k_8 \quad k_{cat}^o = k_5$$

$$\text{Carboxylation efficiency} = \frac{k_{cat}^c}{K_c} = k_6 \times \frac{k_9}{k_9 + k_{10}}$$

$$\text{Oxygenation efficiency} = \frac{k_{cat}^o}{K_o} = k_3 \times \frac{k_9}{k_9 + k_{10}}$$

$$\text{Specificity factor, } S_{c/o} = \frac{k_{cat}^c}{K_c} \times \frac{K_o}{k_{cat}^o}$$

(von Caemmerer, 2013)

Specificity factor ($S_{c/o}$) of Rubisco is a measure of its ability to catalyze carboxylation relative to oxygenation. $S_{c/o}$ is the carboxylation to oxygenation ratio at equal CO₂ and O₂ partial pressures (Jordan and Ogren, 1984; Von Caemmerer, 2013). Rubisco has evolved through natural selection in response to reducing atmospheric CO₂: O₂ ratios. This has improved the ability of Rubisco to catalyze carboxylation at the expense of catalytic turnover rate of carboxylase (Andrews and Lorimer, 1987). In spite of the selection pressure Rubisco has not succeeded in overcoming wasteful photorespiration which is attributed to O₂ sensitivity of the

2, 3-enediol form of RuBP to which CO₂ is added during carboxylation (Lorimer and Andrews, 1973). Despite being slow and confused, Rubisco might be optimally adapted to the biochemical conditions available in respective species (Figure 1.12; Tcherkez et al., 2006). However, recent survey of enzymes and comparisons with Rubisco's chemistry show that Rubisco is neither slow nor unspecific and warrants further research to improve understanding of Rubisco's mechanism and photosynthetic biochemical regulation (Bathellier et al., 2018).

1.3.4 CO₂ diffusion

Stomata are the pores found in the epidermis of leaves that enable CO₂ entry for photosynthesis. Stomata also act as exit for water molecules which provide the resistance for incoming CO₂ molecules. This exchange of CO₂ and water is controlled by adjusting the aperture of stomata in response to environmental variables of light, temperature and humidity (Evans and Caemmerer, 1996). CO₂ diffusion encounters resistance at various levels before it reaches the actual site of carboxylation in the chloroplast. CO₂ diffusion is restricted by boundary layer resistance due to unstirred layer of air at the leaf surface and stomata. After overcoming the boundary layer and stomatal resistance (g_s) the CO₂ molecules in intercellular air spaces then diffuse from sub stomatal cavities throughout the mesophyll and finally reach the stroma of chloroplast (Figure 1.13). The combined restrictions to CO₂ diffusion from intercellular air space to chloroplasts are termed as mesophyll conductance (g_m). Mesophyll conductance can be separated in two components gaseous phase and liquid phase. Gaseous phase resistance along the intercellular air space is generally assumed to be less significant than liquid phase resistance comprising water filled pores of cell wall, plasma membrane, cytosol, chloroplast envelop and stroma. Understanding CO₂ diffusion is crucial to estimate the CO₂ partial pressures at carboxylation sites (C_c) which further can predict the net photosynthetic rates (Evans et al., 2009). The decrease in CO₂ concentration in chloroplast increases the apparent K_m values for carboxylase activity of Rubisco and reduces the net rate of CO₂ fixation.

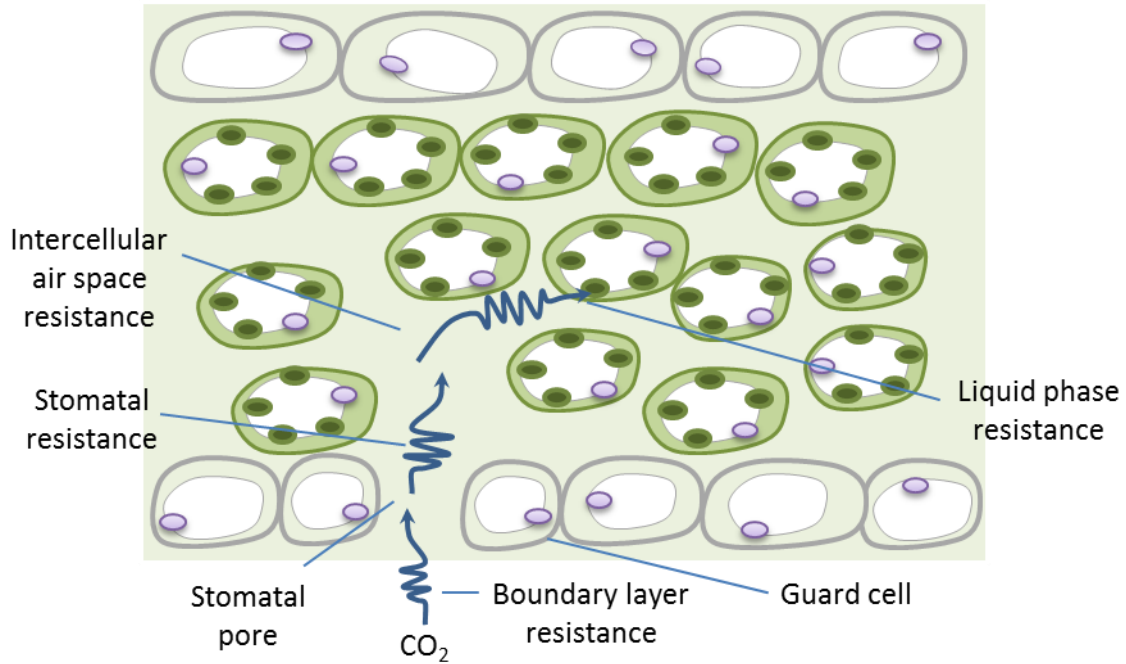


Figure 1.13 Pathway CO₂ diffusion in leaves of C₃ plants

Leaf anatomical variations also affect net photosynthetic rates. A leaf with high N content will have higher photosynthetic rates due to more exposed mesophyll surface area with more chlorophyll pigments. The drawdown in CO₂ from intercellular space to chloroplast as a result of g_m can be determined using concurrent gas exchange measurements with tunable diode laser (TDL) spectroscopy. The method based on ¹³C discrimination utilizes the preference of ¹²C over ¹³C by Rubisco and during carboxylation CO₂ fixed by Rubisco inside plant is deprived in ¹³C as compared to atmospheric CO₂. Isotopic composition of carbon isotopes (δ) in air (R_a) and plant (R_p) is altered and is used to define a new term Δ that accounts for discrimination by plant (Farquhar and Richards, 1984). Δ is deviation of R_a/R_p (α) from unity and independent of isotopic composition of standard used for measuring R_p and R_a . The discrimination correlates with the ratio of intercellular (C_i) to ambient (C_a) CO₂ concentration, C_i/C_a accounting to the following equation with its simplest form (Figure 1.14, Farquhar et al., 1982, 1989).

$$\Delta = a + (b - a) \frac{C_i}{C_a} \quad 1)$$

Where,

a = fractionation occurring due diffusion in air,

b = net fractionation caused by carboxylation

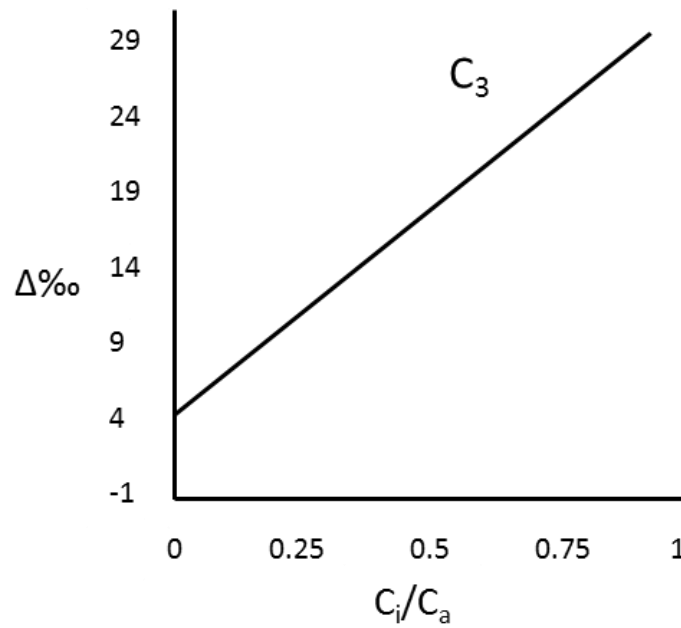


Figure 1.14 Carbon isotope discrimination (Δ), over ratio of intercellular CO_2 and ambient partial pressure of CO_2 . The line drawn is equation 1 with $a = 4.4\%$ and $b = 27\%$

The deviation of observed discrimination measured using TDL (tunable diode laser) spectroscopy from the theoretical discrimination considering no mesophyll conductance is used to calculate chloroplast CO_2 partial pressures (C_c) (Evans et al., 1986).

$$\delta_i - \delta_{atm} = \frac{27.2}{g_m C_a} A + X \quad (2)$$

where,

δ_i = isotopic composition of CO_2 in leaf

δ_{atm} = isotopic composition in atmospheric air

X = representative constant term.

1.3.5 Biochemical models of C_3 photosynthesis

Gas exchange studies at the leaf level provide information about biochemical aspects of CO_2 assimilation. Biochemical models of photosynthesis are equations derived to determine the CO_2 assimilation (A) rates using kinetic properties of Rubisco, light reactions and carbon reduction. The C_3 model developed to help interpret gas exchange measurements of CO_2 assimilation by Farquhar, von Caemmerer and Berry (FvCB) in 1980 is one such biochemical model. The C_3 model predicts net photosynthesis (A_{net}) as minimum of potential limitations to

CO₂ assimilation including maximum Rubisco activity (V_{cmax}), electron transport rate (J) or RuBP regeneration limitation and triose phosphate utilisation limitation (TPU) (Figure 1.15, Farquhar et al., 1980). According to the original version of the FvCB model (and given that TPU limitation (T_p) is less likely), the net CO₂ assimilation rate is minimum of two limiting rates:

$$A_{net} = \min(A_c, A_j) - R_d \quad (3)$$

Where, A_c is Rubisco limited or RuBP saturated rate of CO₂ assimilation, A_j is RuBP regeneration limited or electron transport limited rate of CO₂ assimilation and R_d is dark respiration.

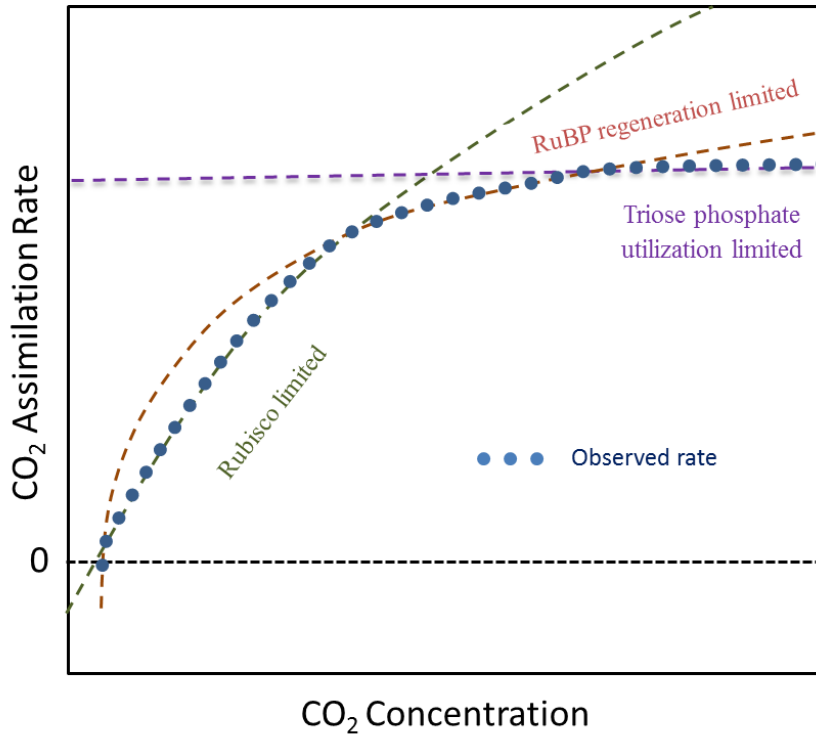


Figure 1.15 FvCB model depicting the response of CO₂ assimilation rate over intercellular CO₂ concentration limited by Rubisco and electron transport rate

Rubisco limited (A_c), Electron transport limited (A_j) and triose phosphate limited (T_p) photosynthesis are given by,

$$A_c = \frac{(C_c - \Gamma^*)V_{cmax}}{C_c + K_c(1 + O/K_o)} - R_d \quad (4)$$

$$A_j = \frac{(C_c - \Gamma^*)J}{4C_c + 8\Gamma^*} - R_d \quad (5)$$

$$A_p = 3T_p - R_d \quad (6)$$

Where, C_c and O_c are the CO_2 and O_2 partial pressures inside the chloroplast respectively, K_c and K_o are the Michelis Menten coefficients of Rubisco activity for CO_2 and O_2 respectively, Γ^* is the CO_2 compensation point in the absence of mitochondrial respiration and T_p is rate of inorganic phosphate supply. Compensation point is related to specificity factor by,

$$\Gamma^* = \frac{0.5O_c}{S_{c/o}} \quad (7)$$

The equations linking electron transport rate to light intensity are important and continuously modified with updated knowledge on photon requirements and ATP production (Farquhar et al., 1980). The C_3 model suggests that net CO_2 assimilation is limited by Rubisco at low CO_2 partial pressures and limited by electron transport at high CO_2 partial pressures (Long and Bernacchi, 2003). Initially C_i was used in the model in place of C_c . With the knowledge of significant drawdown of C_c relative to C_i , g_m was incorporated in the model using carbon isotope discrimination (Von Caemmerer, 2013). Modelled CO_2 assimilation as a function of C_i and light at different growth conditions are established as important tools to study photosynthesis. The FvCB model has been used for analyzing underlying C_3 leaf biochemistry and predicting photosynthetic fluxes of ecosystems in response to global climate change. However, this model has not been applied in crop growth models with the exception of a couple of attempts (Wu et al., 2016, 2017; Yin and Struik, 2009). Photosynthesis study is crucial in the context of assessing the impact of climate change on agro-ecosystem function and therefore, mechanistic quantification of photosynthesis process needs to be improved in the crop growth simulation models.

1.4 Effect of climate change drivers on photosynthesis

1.4.1 Elevated CO_2 effect on photosynthesis

Carbon dioxide concentrations regulate stomatal opening and closing. Open stomata allow CO_2 to diffuse into leaves for photosynthesis, but also provide pathway for water to diffuse out of leaves. Plants therefore regulate the degree of stomatal opening as a compromise between the high photosynthetic rates and low water loss rates. Elevated CO_2 levels in the atmosphere will allow more CO_2 diffusion with less frequent stomatal opening ultimately reducing the stomatal conductance and water loss through transpiration. Plants can maintain high photosynthetic rates under elevated CO_2 levels with relatively low stomatal conductance. Increased partial pressures

of CO₂ at carboxylation sites will result in higher photosynthetic rates. In addition, elevated CO₂ decreases competition with O₂ for Rubisco ultimately reducing the carbon loss through photorespiration (Leakey et al., 2009). Increased photosynthetic rates will enhance the growth and productivity of plants leading to increased leaf area and plants size. Thus, overall effect of elevated CO₂ may decrease water loss through transpiration and increase water use with enhanced plant size and biomass. Overall FACE (free air CO₂ enrichment) experiments show decreases in whole plant water use of 5-20% under elevated CO₂. Across a variety of FACE experiments, growth under elevated CO₂ decreases stomatal conductance of water by an average of 22% (Ainsworth and Rogers, 2007).

Elevated CO₂ increases the efficiency of Rubisco allowing plants to invest less N to achieve higher photosynthetic rates. This results in reduced amount of leaf N and Rubisco. However, decreased N reduces photosynthetic capacity. Plants may adapt to long term exposure to elevated CO₂ by decreasing the photosynthetic capacity due to decreased amount of Rubisco (acclimation) or by reducing activation of Rubisco and regulatory mechanisms without affecting the amount of Rubisco (down regulation). The failure of C₃ plants to sustain the stimulation in photosynthesis by elevated CO₂ due to acclimation is associated with carbohydrate accumulation and might be linked to decreased transcription of the Rubisco large subunit gene (Delgado et al., 1994).

The results from FACE experiments show that, despite small decreases in maximum carboxylation rate of Rubisco (V_{max}) and maximum electron transport rates for RuBP regeneration (J_{max}), the light-saturated rate of photosynthetic carbon uptake (A_{sat}) is markedly stimulated in C₃ plants grown at elevated CO₂ (Ainsworth and Rogers, 2007). However, there is variation in the increase of CO₂ uptake according to species and experimental conditions. FACE studies have reported smaller increases in grain yield of wheat compared to enclosure based studies (Ainsworth and Long, 2005).

1.4.2 Heat stress and eCO₂ response of photosynthesis

Photosynthesis can function between 0°C and 45°C in general with an optimum range in the middle of the non-harmful range and decreases when away from this thermal optimum (Figure 1.16). Changes in growth conditions may shift the thermal optimum (T_o) in some plants that show thermal acclimation (Berry and Bjorkman, 1980).

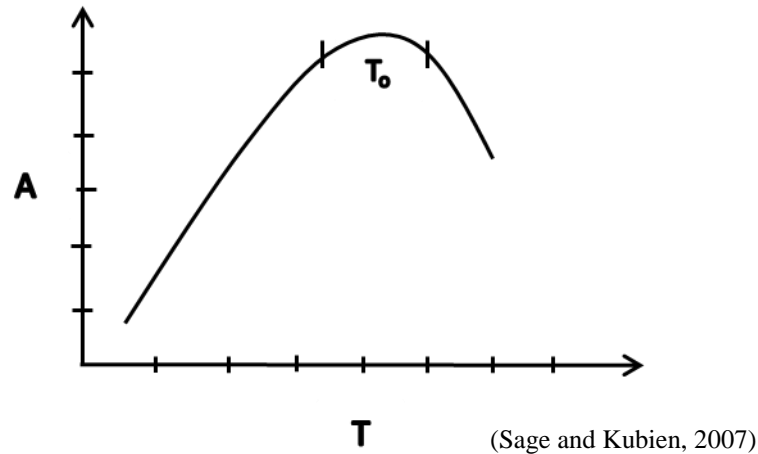


Figure 1.16 Response of CO₂ assimilation (A) to temperature (T) showing a specific optimum temperature (T_o) range

Temperature affects photosynthesis via enzymatic reactions. Rubisco is more sensitive to increased temperatures than the rest of enzymes involved in carboxylation. Although Rubisco catalytic activity increases with temperature, its low affinity for CO₂ and ability to act as an oxygenase limit the chance of increasing net photosynthesis with temperature (Jordan and Ogren, 1984). At high temperatures, the solubility of oxygen decreases to a lesser extent than CO₂, resulting in increased photorespiration relative to photosynthesis (Keys, 1986). Elevated CO₂ modifies the photosynthetic response to temperature (Long, 1991) and may shift the thermal optimum range. Modelled responses of net CO₂ assimilation to temperature at different CO₂ levels suggest that limitation photosynthesis shifts from Rubisco to electron transport at elevated CO₂ partial pressures (Sage and Kubien, 2007). Temperature effect on photosynthesis also depends on stomatal response to temperature which is influenced by water vapor pressure difference (VPD) and internal plant water status. Irrigated plants open stomata to a broader range of increasing temperatures as compared to dry plants (Berry and Bjorkman, 1980).

In addition to warming, abrupt temperature increases above the optimum range that cause injury or irreversible damage termed as ‘heat stress’ (Wahid et al., 2007) are also much likely to occur as a result of climate change (IPCC, 2014). Heat stress reduces photosynthesis through disruptions in the structure and function of chloroplasts, and reductions in chlorophyll content. The inactivation of chloroplast enzymes, mainly induced by oxidative stress, may also reduce the rate of photosynthesis. Oxidative stress may induce lipid peroxidation leading to protein degradation, membrane rupture and enzyme inactivation (Farooq et al., 2011).

Elevated CO₂ concentration stimulates photosynthesis and inhibits photorespiration in C₃ plants such as wheat, thus rising CO₂ concentrations are expected to stimulate wheat yield, if other factors are constant. However, warming generally reduces wheat yield, probably because of shorter grain filling period caused by more rapid development. Wheat crops in most production zones of Australia, and more specifically southern Australia, frequently experience temperatures which inhibit optimal plant growth (CSIRO and BOM, 2015). A major influence of temperature is the acceleration of development. In wheat, leaf appearance rates are faster and time to flowering is shortened by increase in temperature. The reason for accelerated development at higher temperatures is due to the cell cycle being shorter, leading to faster rates of cell division and initiation of leaf primordia. Heat stress during flowering and grain filling has been shown to adversely affect grain yield, through both of its constituents, grain number and grain weight (Farooq et al., 2011; Stone and Nicolas, 1996). Grain yields of C₃ wheat are likely to be substantially increased by rising levels of atmospheric CO₂ concentrations in areas where temperature is moderate to high. However, in areas, where the temperature is already marginal for yield, further increases will significantly reduce yield, irrespective of rising CO₂ concentrations because of greatly accelerated crop development and/or flower abortion. Heat stress during anthesis increases floret abortion, and during reproductive phase can cause pollen sterility, tissue dehydration, lower CO₂ assimilation and increased photorespiration. Stone and Nicolas, (1998) studied wheat response to short periods of very high temperature (> 35°C) and found that both heat susceptible and tolerant lines showed reduction in kernel mass linearly with number of short period heat stress events. While being beneficial for wheat grains by seed filling, eCO₂ can also prove to be detrimental as it affects climate variability and consequently affecting the grain filling window.

1.4.3 Water stress and eCO₂ response of photosynthesis

Reduced stomatal conductance is the primary cause of reduced photosynthesis rates during the initial part of water stress (WS). However major damage at later stages is attributed to tissue dehydration (Farooq et al., 2014) along with progressive down regulation of metabolic processes decreasing the RuBP content consequently limiting photosynthesis (Flexas and Medrano, 2002). ATP synthesis is sensitive to cellular dehydration due to WS. Water stress decreases ATP synthase which limit the RuBP regeneration ultimately inhibiting photosynthesis. Decrease in ATP synthesis is attributed to inhibition of coupling factor activity

(Lawlor and Cornic, 2002; Tezara et al., 1999). Water stress has no direct effect on PSII primary photochemistry and enhances the susceptibility of plants to photo inhibition. Decrease in the PSII functioning in water stressed plants is observed because of interaction between WS and other environmental stresses such as irradiance (Lu and Zhang, 1998). Elevated CO₂ can negate the adverse effects of moderate WS by stimulating photosynthesis and increasing water use efficiency as a result of reduced stomatal conductance; however, in severe WS, eCO₂ may not show any effect due to biochemical inhibition.

Grossman-Clarke et al., (2001) tested a model using FACE study data suggesting enhancement in elevated CO₂ effect on wheat under drought through lower transpiration rate, higher root biomass and dependence of CO₂ uptake on intercellular CO₂ concentration. A study on wheat demonstrated that plants grown under elevated CO₂ are better equipped to compensate WS (Wechsung et al., 1999). Kimball et al., (1995) reported 44% and 19% increase in CO₂ assimilation rates and 21% and 8% increase in grain yield of wheat in the dry and wet treatments, respectively under FACE. Dias de Oliveira et al., (2013) observed that elevated CO₂ with high temperature can compensate for the adverse effects of terminal drought on biomass accumulation and grain yield in wheat.

1.5 AGFACE

Most CO₂ enrichment studies have been carried out in controlled environment conditions. While valuable for treatments that require a high degree of environmental regulation such as heat stress, it is important to undertake studies under natural field conditions. For this reason, a grain crop field research facility (AGFACE) was established in Horsham in order to investigate the response of wheat (and other crops) to future environments under the natural dryland field conditions that are characteristic of Australia's agriculture (Figure 1.17).



Figure 1.17 Aerial view of FACE site in Horsham, Victoria

The field study described in chapter 4 was conducted at the Australian Free Air CO₂ Enrichment (AGFACE) research facility during 2014 and 2015. The AGFACE site is located 7 km west of Horsham, Victoria, Australia (36°45'07''S, 142°06'52''E; 127m above sea level), which is a semi-arid region of the Australian wheat belt. The region has a Mediterranean climate but with drier and cooler winters. The region receives 448 mm long-term (more than 100 years) average annual rainfall and has a minimum of 8.2°C, and a maximum of 21.5°C long-term average temperature.

Table 1.1 Monthly mean maximum temperatures for year 2014 compared to all year records for highest and lowest monthly mean temperature records for all years

Statistic	Jan	Feb	Mar	Apr	May	Jun	Jul	Aug	Sep	Oct	Nov	Dec
Mean	31.0	30.5	26.8	22.2	17.7	14.4	13.6	15.2	18.2	21.6	26.1	28.4
Highest monthly mean	34.0	32.9	30.1	25.8	19.1	15.5	14.8	17.0	20.1	25.5	30.4	30.3
Lowest monthly mean	26.9	27.3	24.4	19.2	15.7	13.1	12.3	13.0	15.9	17.5	22.8	24.2
Highest Daily	46.0 25 th 2003	47.4 7 th 2009	41.01 6 th 2008	36.5 1 st 2014	28.0 8 th 2002	24.0 8 th 2005	20.0 25 th 2007	26.0 27 th 2007	31.0 19 th 2006	38.0 12 th 2004	42.3 29 th 2012	46.0 31 st 2005
Lowest Daily	18.0 21 st 2002	16.0 3 rd 2005	15.0 21 st 2001	11.6 24 th 2012	9.0 28 th 2000	9.5 21 st 2012	8.0 23 rd 2004	8.5 1 st 2014	10.0 11 th 2004	10.0 1 st 2003	14.0 4 th 2004	15.2 19 th 2010

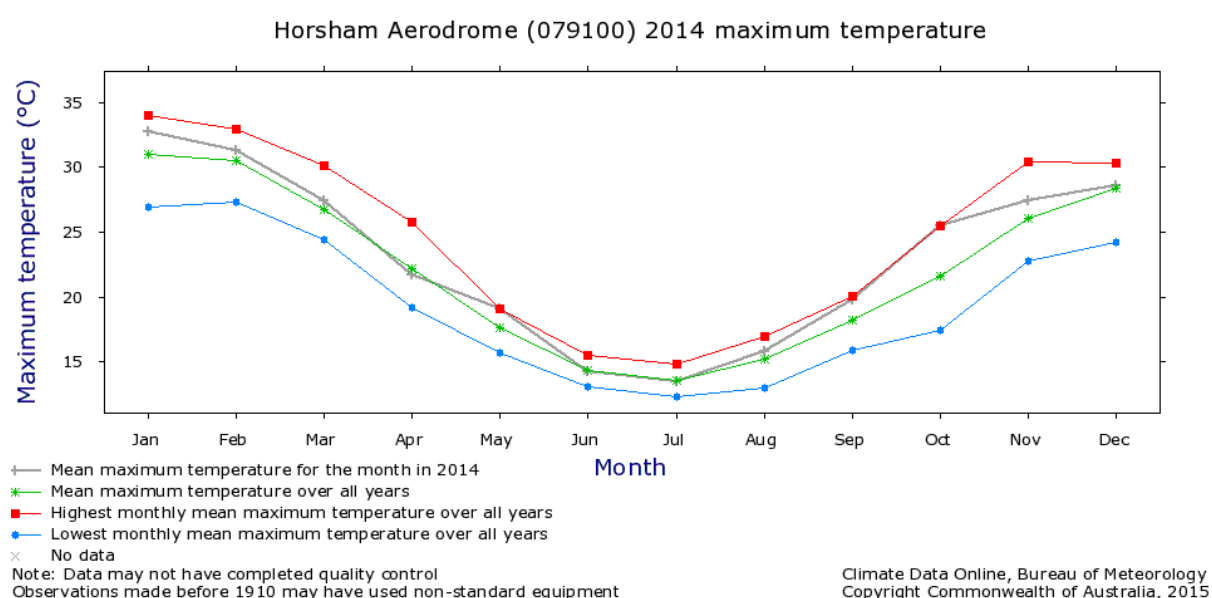


Figure 1.18 Monthly mean maximum temperature trend for the year 2014 compared to all year records for highest and lowest monthly mean temperature

Highest daily temperature records showed extreme temperature changes (Table 1.1 and Figure 1.18, Climate data online, BOM, 2015). Average temperature (22.3°C) of monthly mean maximum temperature from February 2014 to June 2014 was used as growth day temperature for the glasshouse experiments in this study conducted in the same period.

1.6 Knowledge Gap

Several studies have investigated the response of wheat to eCO₂ in enclosures and in field studies (Amthor, 2001; Hocking and Meyer, 1991; Hunsaker et al., 2000, 1996; Kimball, 1983; Kimball et al., 1995, 1999; Miglietta et al., 1996; Nie et al., 1995; Osborne et al., 1998). However, only a few studies have considered eCO₂ interaction with temperature increases in wheat (Cai et al., 2016; Delgado et al., 1994; Jauregui et al., 2015; Morison and Lawlor, 1999; Rawson, 1992) and rarely with the abrupt temperature increases or heat stress (Coleman et al., 1991; Wang et al., 2008).

Also, eCO₂ enhancement in growth is expected to ameliorate the negative impacts of drought (Hatfield et al., 2011), while similar CO₂ response under water stress or well-watered conditions has also been observed (Ghannoum et al., 2007). The eCO₂ response of crops varies under different soil moisture regimes (Ewert et al., 2002) and field studies addressing eCO₂ response of crops in the field are scarce covering limited number of locations and growing seasons with little to no drought stress, limiting their use in generalising predictions based on previously published literature (Hatfield et al., 2011; Leakey et al., 2012).

Crop models currently used such as APSIM can predict the growth and yield infield under normal environmental conditions. Recently, the FvCB model has been incorporated into APSIM (Wu et al., 2017). However, these crop models still lack the mechanistic approach to consider stresses and their interaction to accurately predict the yield under eCO₂ and future extreme climate. Despite several attempts and studies, the approach to improve models for future extreme climate conditions is still lacking. C₃ model developed by Farquhar et al., (1980) has the potential to mechanistically consider the effect of stresses and their interaction with elevated CO₂.

Thus, experimental validation of interactive effects of eCO₂ with heat (addressed in chapter 2 and 3) and WS (addressed in chapter 4) will be instrumental in addressing the challenge of predicting wheat crop production under the future extreme climate scenarios. The incorporation of comparative field and controlled environment data for the same wheat cultivars will also be a valuable addition to this field and help bridge our knowledge gap.

1.7 Aims and Objectives

The overall aim of this PhD project was to investigate the interactive effects of heat stress and water stress on the response to eCO₂ of photosynthesis, biomass and grain yield of two commercial wheat cultivars Scout and Yitpi grown in the glasshouse and in the field.

Outcomes of this project will greatly enhance our ability to predict wheat yield under future climates characterized by a high CO₂ atmosphere and frequent heat and water stress events.

The specific objectives of Chapter 2 were to:

- I. Determine the elevated CO₂ response of photosynthesis, biomass and grain yield of two glasshouse grown cultivars Scout and Yitpi,
- II. Investigate the temperature response of photosynthesis in Scout and Yitpi, and
- III. Determine the impact of moderate heat stress applied at the vegetative and flowering stage on the eCO₂ responses of photosynthesis, biomass and grain yield of glasshouse grown Scout and Yitpi

The specific objectives of Chapter 3 were to:

- I. Investigate the temperature response of photosynthesis under ambient and elevated CO₂ in glasshouse grown Scout, and
- II. Determine the impact of severe heat stress applied at the flowering stage on the eCO₂ responses of photosynthesis, biomass and grain yield of glasshouse grown Scout.

The specific objectives of Chapter 4 were to:

- I. Determine the elevated CO₂ response of photosynthesis, biomass and grain yield of two wheat cultivars Scout and Yitpi grown in dryland field conditions using free air CO₂ enrichment for two growing seasons,
- II. Determine the eCO₂ impact on soil water content in irrigated and rainfed conditions, and
- III. Determine the water stress impact on the eCO₂ responses of photosynthesis, biomass and grain yield of two field grown wheat cultivars Scout and Yitpi.

1.8 Thesis format and structure

Research undertaken during my PhD project is presented as a series of three experimental studies prepared for submission to peer-reviewed journals. There are five chapters in this thesis. In addition to three experimental chapters (Chapters 2, 3 and 4), there is an introductory literature review (Chapter 1) and a final synthesis and general discussion (Chapter 5) that contextualizes the research, discusses key findings and outlines prospects for future.

Chapters	Title
Chapter 1	General introduction and literature review
Chapter 2 (Experiment 1)	Elevated CO ₂ similarly stimulated biomass and yield of two contrasting wheat cultivars while moderate heat stress was not detrimental and water stress on photosynthesis of two field grown wheat lines Scout and Yitpi
Chapter 3 (Experiment 2)	Elevated CO ₂ reduces impact of heat stress on wheat physiology but not on grain yield
Chapter 4 (Experiment 3)	Elevated CO ₂ does not protect wheat from damage by water stress in dryland conditions
Chapter 5	General discussion and prospects
Bibliography	

CHAPTER 2

**ELEVATED CO₂ SIMILARLY STIMULATED BIOMASS AND YIELD
OF TWO CONTRASTING WHEAT CULTIVARS WHILE MODERATE
HEAT STRESS WAS NOT DETRIMENTAL**

Abstract

Climate change is increasing the frequency of extreme events such as heat waves, adversely affecting crop productivity. Elevated carbon dioxide (eCO₂) may alleviate the negative effects of environmental stresses by enhancing photosynthesis and reducing transpiration. While positive impacts of eCO₂ on crop productivity are evident, the interactive effects of eCO₂ and environmental stresses are still unclear. Accordingly, two commercial wheat lines (Scout and Yitpi) were grown under non-limiting water and nutrients at 22/15°C (day/night average) and ambient (450 ppm) or elevated (650 ppm) CO₂ in the glasshouse. Plants were exposed to one or two heat stress (HS) cycles (3-day long) at vegetative (H1, daytime average of 38.1°C) or flowering (H2, daytime average of 33.5°C) stage. At current ambient CO₂ (aCO₂), both wheat lines showed similar photosynthetic temperature responses; while larger and greater-tillering Yitpi produced only slightly more grain yield than early-maturing Scout. eCO₂ stimulated wheat photosynthesis and reduced stomatal conductance despite causing a mild photosynthetic acclimation (~12% reduction in rates measured at common CO₂). HS did not inhibit photosynthesis at 25°C but slightly reduced photosynthesis at 35°C in aCO₂-grown plants. At anthesis, eCO₂ stimulated wheat biomass due to greater allocation to the stems in Yitpi, while HS had no effect. At the final harvest, eCO₂ stimulated grain yield similarly in both wheat lines under control conditions, due to more grains per ear in Yitpi and more and bigger grains in Scout. HS mildly enhanced final biomass and grain yield of aCO₂ grown plants only, while eCO₂ reduced grain N in non-HS Yitpi plants. In conclusion, eCO₂ similarly stimulated final biomass and grain yield of two contrasting wheat cultivars not exposed to HS by variably affecting grain size and number. The insignificant effect of moderate HS on wheat yield and the reduced grain nutrient quality of high tillering Yitpi at eCO₂ warrant further research. This study highlights the complex HS x eCO₂ interactions on crop yield which must be incorporated when developing mechanistic leaf-to-canopy crop models.

Key words: Wheat, photosynthesis, grain yield, elevated CO₂, heat stress, climate change

2.1 Introduction

Wheat (*Triticum aestivum*) is a main staple crop grown worldwide including Australia. Ongoing climate change has reduced wheat production (Asseng et al., 2015). The key drivers of crop responses to climate change are changes in atmospheric carbon dioxide (CO₂), temperature and precipitation (Asseng et al., 2013). Rising atmospheric CO₂ is expected to reach 700 ppm by the end of this century and consequently increasing surface temperatures by 1.1°C to 2.6°C (IPCC, 2014). For every degree of temperature increase, global wheat production is expected to decrease by 6 – 10 % (Asseng et al., 2015; García et al., 2015). Crop models estimate the yield as a function of weather, soil, genotype and crop management practices, and are hence, important tools for assessing the impact of climate change (Asseng et al., 2013). However, current crop models lack the ability to consider plant genotype responses to elevated atmospheric CO₂ concentration (eCO₂) and their interaction with other environmental conditions. To improve current crop models, it is important to elucidate how plants respond to eCO₂ interactions with environmental stresses at the physiological and molecular level. Photosynthesis, a fundamental process driving crop growth and yield, is affected by both eCO₂ and environmental stresses. Thus, photosynthesis can partially explain the interactive effects of eCO₂ with environmental stresses and provide a mechanistic basis for crop models (Yin and Struik, 2009).

During photosynthesis, ribulose-1, 5-bisphosphate carboxylase (Rubisco) catalyzes the carboxylation of ribulose-1, 5-bisphosphate (RuBP) using sunlight and water. Increased partial pressure of CO₂ at the carboxylation site increases photosynthetic rates (A_{sat}) and reduces stomatal conductance (g_s) and consequently, transpiration rates. In addition to the carboxylation reaction, Rubisco can also take up oxygen (O₂) in the light and release CO₂ in a series of reactions termed as photorespiration (Ogren, 1984). Elevated CO₂ decreases the competition of O₂ for Rubisco sites, ultimately reducing carbon loss through photorespiration (Jordan and Ogren, 1984). Increased photosynthetic rates enhance the growth and productivity of plants leading to increased leaf area, plant size and crop yield (Krenzer and Moss, 1975; Sionit et al., 1981; Hocking and Meyer, 1991; Mitchell et al., 1993; Kimball et al., 1995; Mulholland et al., 1998; Cardoso- Vilhena and Barnes, 2001; Högy et al., 2009; Kimball, 2016; Fitzgerald et al., 2016; Kimball, 1983). Following long time exposure to eCO₂, plants may respond to CO₂ enrichment by reducing photosynthetic capacity due to lower amount of Rubisco in a process referred as ‘acclimation’ (Ainsworth et al., 2003; Nie et al., 1995; Rogers

and Humphries, 2000). Alternatively, plants may reduce photosynthetic capacity in response to eCO₂ by reducing activation of Rubisco and regulatory mechanisms without affecting the amount of Rubisco which can be termed as ‘down regulation’ (Delgado et al., 1994).

Optimum temperature range for wheat growth is 17-23°C, with a minimum of 0°C and maximum of 37°C (Porter and Gawith, 1999). Warming involves gradual increase in long-term mean temperature shifting phenological patterns of agricultural crops, and an increase in frequency of heat waves. Heat can reduce crop growth and disrupt reproduction depending on the timing, intensity and duration (Sadras and Dreccer, 2015). Higher temperatures (below damaging level) during daytime, increase photosynthesis up to an optimum temperature, above which photosynthesis decreases mainly due to higher photorespiration (Berry and Bjorkman, 1980; Long, 1991). High night time temperatures increase respiration and reduce net photosynthesis (Prasad et al., 2008). At the whole plant level, high temperatures accelerate growth (Fischer, 1980) and shorten crop duration (Hatfield and Prueger, 2015), hence reducing grain yield due to insufficient time to capture resources. Losses due to short crop duration are usually higher than benefits of growth stimulation at high temperature (Wardlaw and Moncur, 1995). In addition to warming, abrupt temperature increases above the optimum range that cause injury or irreversible damage termed as ‘heat stress’ (Wahid et al., 2007) are also much likely to occur as a result of climate change (IPCC, 2014). The severity of the damage due to heat stress (HS) depends on magnitude and duration of HS and also on the developmental stage of the plant at the time of exposure to HS. HS can directly damage cells, decrease chlorophyll content and reduce photosynthesis and also may increase grain abortion resulting in reduced growth, biomass and grain yield (Farooq et al., 2011; Stone and Nicolas, 1996, 1998; Wardlaw et al., 2002). Wheat is highly susceptible to damage by HS at the flowering stage and may lead to complete loss of grain yield due to pollen inactivation. HS may also reduce photosynthesis by impairing photosystem II (Berry and Bjorkman, 1980) and Rubisco activase in the Calvin-cycle (Eckardt and Portis, 1997).

The interactive effects of eCO₂ and HS can be positive, negative or neutral (Wang et al., 2008, 2011). Elevated CO₂ increases the temperature optima of photosynthesis (Alonso et al., 2009; Long, 1991) by reducing photorespiration and may increase tolerance to photo inhibition (Hogan et al., 1991). The impact of HS on photosynthesis in plants grown at eCO₂ will depend on whether Rubisco, electron transport or end-product synthesis is limiting to photosynthesis at higher temperatures (Sage and Kubien, 2007). Enhanced growth and leaf level water use efficiency (WUE) by eCO₂ may help compensate for the negative impact of HS; conversely,

heat-induced shortening of the grain-filling stage and grain abortion could limit the benefits of eCO₂ (Lobell and Gourdj, 2012).

Several studies have investigated the response of wheat to eCO₂ in enclosures and in field studies (Amthor, 2001; Hocking and Meyer, 1991; Hunsaker et al., 2000, 1996; Kimball, 1983; Kimball et al., 1995, 1999; Miglietta et al., 1996; Nie et al., 1995; Osborne et al., 1998). However, only a few studies have considered eCO₂ interaction with temperature increases in wheat (Rawson, 1992; Delgado et al., 1994; Morison and Lawlor, 1999; Jauregui et al., 2015; Cai et al., 2016) and rarely with the abrupt temperature increases or HS (Coleman et al., 1991; Wang et al., 2008). Studies considering heat stresses have addressed mainly the biomass or yield aspects and not the physiological processes such as photosynthesis (Stone and Nicolas, 1994, 1996, 1998). Interactive effects of eCO₂ and HS on photosynthesis have been reported in a limited number of studies (reviewed by Wang et al., 2008, 2011). Given that heat shocks are expected to occur more frequently in the near future, a clear understanding of the interactive effects of eCO₂ and HS on wheat growth and productivity is critically important.

To address this knowledge gap, we investigated the response of wheat growth and photosynthesis to eCO₂ and HS. Two commercial wheat lines, Scout and Yitpi with similar genetic background but distinct agronomic features were selected for analyzing the interactive effects of eCO₂ and HS on photosynthesis, growth, biomass and grain yield. Scout is a midseason maturity line with very good early vigor that can produce leaf area early in the season. Scout has a putative water-use efficiency (WUE) gene, which has been identified using carbon isotope discrimination. Yitpi is a good early vigor, freely tillering and long maturity line which flowers slightly later than the flowering frame (Bahrami et al., 2017; Pacificseeds, 2009; Seednet, 2005). Although Scout is known to be a high yielding variety with very good grain quality (Pacific seeds, 2009), we hypothesized that Yitpi might end up producing similar or higher grain yield due to its ability to produce more tillers and the longer time taken to flower and mature (Hypothesis 1).

As mentioned above, plants may respond to eCO₂ by decreasing photosynthetic capacity due to down-regulation or acclimation. Fast growing plants with high sink capacity show a greater eCO₂-induced growth stimulation (Poorter, 1993) and less photosynthetic acclimation due to lower accumulation of carbohydrates (Delgado et al., 1994) compared to slow growing and low sink capacity counterparts. Consequently, we hypothesized that Yitpi may show greater photosynthetic, growth and yield response to eCO₂ due to weaker acclimation as a result of its

free tillering habit and greater sink capacity relative to Scout (Hypothesis 2). Also, eCO₂ stimulates grain yield by increased tillering and thus produces more ears and grains (Amthor, 2001). Hence, we expect that eCO₂ will stimulate grain yield by increasing tillers in both lines (Hypothesis 3).

The potentially larger eCO₂ response due to larger sink capacity may buffer Yitpi against HS damage compared to Scout. In addition, eCO₂ reduces photorespiration and increases the tolerance to photo inhibition caused by HS (Hogan et al., 1991). Thus, HS (abrupt temperature increases above optimal growth temperatures) may decrease yield more in Scout grown at aCO₂ relative to Yitpi and eCO₂ (Hypothesis 4). Also, HS is more damaging at the flowering and reproductive stages relative to the vegetative developmental stage (Farooq et al., 2011). Hence, there may be less damage in plants exposed to HS at the vegetative stage relative to the flowering stage (Hypothesis 5).

To test these hypotheses, Scout and Yitpi were grown at ambient or elevated CO₂ conditions and subjected to one or two heat stresses at the vegetative (H1) and/or flowering (H2) stage. Growth, biomass and photosynthetic parameters were measured at different time points across the life cycle of the plants. Canopy scale eCO₂ stimulated grain yield of Scout and Yitpi while moderate canopy level HS was largely inconsequential.

2.2 Materials and methods

2.2.1 Plant culture and treatments

The experiment was conducted in the glasshouse facility located at the Hawkesbury campus of Western Sydney University (WSU). Seeds of commercial winter wheat lines Scout and Yitpi were procured from the department of primary industries (DEPI) Horsham, Victoria. Lines were selected based on their use in the Australian grains free air CO₂ enrichment (AGFACE) project investigating climate change impacts on wheat growth and yield. For germination, 300 seeds of each line were sterilized using 1.5 % NaOCl₂ for 1 min followed by incubation in the dark at 28°C for 48 hours in petri plates. Sprouted seeds were planted in germination trays using seed raising and cutting mix (Scotts, Osmocote®) at ambient growth conditions of CO₂ (aCO₂, 400 µl L⁻¹), temperature (22/14 °C day/night), RH (50 to 70%) and natural light (Figure 2.1). Two weeks old seedlings were transplanted to individual cylindrical pots (15 cm diameter and 35 cm height) using sieved soil collected from local site. At transplanting stage (T0) pots were distributed into two aCO₂ (400 µl L⁻¹) and two eCO₂ (650 µl L⁻¹) chambers (Figure 2.1B). Plants were exposed to two heat stress (HS) cycles at the vegetative (H1, 10 weeks after planting, WAP) and the flowering (H2, 15 WAP) stages for 3 days with temperature ramp up from 14°C night temperature (8 pm to 6 am) to 40°C during mid-day (10 pm to 4 pm) (Figure 2.1). Thrive all-purpose fertilizer (Yates) was applied monthly throughout the experiment to maintain similar nutrient supply in all treatment combinations. Pots were randomized regularly within and among chambers.

2.2.2 Growth and biomass measurements

The full factorial experimental design included four chambers (two chambers for each CO₂ treatment) and five destructive harvests at time points T0 (2 WAP), T1 (6 WAP), T2 (10 WAP), T3 (17) and T4 (25 WAP). Ten plants per treatment per line were measured and harvested at each time point (Figure 2.2). At each time point, morphological parameters were measured followed by determinations of root, shoot and leaf dry mass. Samples were dried for 48 hours in the oven at 60°C immediately after harvesting. Leaf area was measured at time point T1, T2 and T3 using a leaf area meter (LI-3100A, LI-COR, Lincoln, NE, USA). Plant height, leaf number, tiller number and ear (grain bearing plant organ) number along with developmental stage information (booting, half-emerged or fully emerged) were recorded at time points T2 and T3).

2.2.3 Leaf gas exchange measurements

Last expanded flag leaf was used to measure gas exchange parameters. Instantaneous steady state leaf gas exchange measurements were performed at time points T1, T2 and T3 using a portable open gas exchange system (LI-6400XT, LI-COR, Lincoln, USA) to measure light-saturated (PPFD=1500 PAR) photosynthetic rate (A_{sat}), stomatal conductance (g_s), ratio of intercellular to ambient CO₂ (C_i/C_a), leaf transpiration rate (E), dark respiration (R_d) and dark- and light-adapted chlorophyll fluorescence (F_v/F_m and F_v'/F_m' , respectively). Steady state leaf gas exchange measurements were also performed during and after heat shock along with recovery stage. Plants were moved to a neighboring chamber where air temperature was separately manipulated to achieve desired leaf temperature. The Licor 6400-40 leaf chamber fluorometer (LCF) was used to measure gas exchange at a photosynthetic photon flux density of 1500 $\mu\text{mol m}^{-2} \text{s}^{-1}$ at two CO₂ concentrations (400 and 650 $\mu\text{l L}^{-1}$) and two leaf temperatures (25 and 35 °C). Photosynthetic down regulation or acclimation was examined by comparing the measurements at common CO₂ (ambient and elevated CO₂ grown plants measured at 400 $\mu\text{l L}^{-1}$ CO₂ partial pressure) and growth CO₂ (aCO₂ grown plants measured at 400 $\mu\text{l L}^{-1}$ CO₂ partial pressure and eCO₂ grown plants measured at 650 $\mu\text{l L}^{-1}$ CO₂ partial pressure).

Dark respiration (R_d) was measured after a dark adaptation period of 15 minutes. Photosynthetic water use efficiency (PWUE) was calculated as A_{sat} ($\mu\text{mol m}^{-2} \text{s}^{-1}$)/ g_s ($\text{mol m}^{-2} \text{s}^{-1}$). The response of the A_{sat} to variations in sub-stomatal CO₂ mole fraction (C_i) (A-Ci response curve) was measured at T3 in 8 steps of CO₂ concentrations (50, 100, 230, 330, 420, 650, 1200 and 1800 $\mu\text{l L}^{-1}$) at leaf temperature of 25°C. Measurements were taken around mid-day (from 10 am to 3 pm) on attached last fully expanded flag leaves of the main stems. Before each measurement, the leaf was allowed to stabilize for 10-20 minutes until it reached a steady state of CO₂ uptake and stomatal conductance. Ten replications per treatment were measured.

2.2.4 Mesophyll conductance and temperature response

Mesophyll conductance (g_m) was determined by concurrent gas exchange and stable carbon isotope measurements using portable gas exchange system (LI-6400-XT, LI-COR, Lincoln, NE, USA) connected to a tunable diode laser (TDL) (TGA100, Campbell Scientific, Utah, USA) for two wheat lines grown at ambient atmospheric CO₂ partial pressures. A_{sat} and $^{13}\text{CO}_2/^{12}\text{CO}_2$ carbon isotope discrimination were measured after T1 at five leaf temperatures (15, 20, 25, 30 and 35°C) and saturating light (1500 $\mu\text{mol quanta m}^{-2} \text{s}^{-1}$). Leaf temperature

sequence started at 25°C decreasing to 15°C and then increased up to 35°C. Response of A_{sat} to variations in C_i was measured at each leaf temperature. Dark respiration was measured by switching light off for 20 minutes at the end of each temperature curve. Measurements were made inside a growth cabinet (Sanyo) to achieve desired leaf temperature. The photosynthetic carbon isotope discrimination (Δ) to determine g_m was measured as follows (Evans et al., 1986):

$$\Delta = \frac{1000\varepsilon(\delta^{13}C_{sam} - \delta^{13}C_{ref})}{1000 + \delta^{13}C_{sam} - \varepsilon(\delta^{13}C_{sam} - \delta^{13}C_{ref})} \quad (1)$$

Where,

$$\varepsilon = \frac{C_{ref}}{C_{ref} - C_{sam}} \quad (2)$$

C_{ref} and C_{sam} are the CO₂ concentrations of dry air entering and exiting the leaf chamber, respectively, measured by the TDL. g_m was calculated using correction for ternary and second-order effects (Evans and Von Caemmerer, 2013; Farquhar and Cernusak, 2012) following the next expression:

$$g_m = \frac{\frac{1+t}{1-t} \left(b - a_i - \frac{eR_d}{A + R_d} \right) \frac{A}{C_a}}{(\Delta_i - \Delta_o - \Delta_e - \Delta_f)} \quad (3)$$

Where, Δ_i is the fractionation that would occur if the g_m were infinite in the absence of any respiratory fractionation ($e = 0$), Δ_o is observed fractionation, Δ_e and Δ_f are fractionation of ¹³C due to respiration and photorespiration respectively (Evans and Von Caemmerer, 2013).

$$\Delta_i = \frac{1}{1-t} a' \frac{1}{(1-t)} ((1+t)b - a') \frac{C_i}{C_a} \quad (4)$$

$$\Delta_e = \frac{1+t}{1-t} \left(\frac{eR_d}{(A + R_d)C_a} (C_i - \Gamma^*) \right) \quad (5)$$

$$\Delta_f = \frac{1+t}{1-t} \left(f \frac{\Gamma^*}{C_a} \right) \quad (6)$$

Where,

$$t = \frac{(1+a')E}{2g_{ac}^t} \quad (7)$$

The constants used in the model were as follows: E denotes transpiration rate; g_{ac}^t is total conductance to diffusion in the boundary layer ($ab = 2.9\%$) and in air ($a = 4.4\%$); a' is the

combined fractionation of CO₂ across boundary layer and stomata; net fractionation caused by RuBP and PEP carboxylation ($b = 27.3\text{‰}$) (Evans et al., 1986); fractionation with respect to the average CO₂ composition associated with photorespiration ($f = 11.6\text{‰}$) (Lanigan et al., 2008) and we assumed null fractionation associated with mitochondrial respiration in light ($e = 0$).

2.2.5 Leaf nitrogen and carbon estimation

Leaf discs were cut from the flag leaves used for gas exchange measurements at time points T2 and T3 then oven dried. Leaf discs were processed for nitrogen and carbon content using elemental analyzer (EA Dumas method). Nitrogen and carbon were also estimated from other plant components including leaf, stem, root and grain harvested at T1, T3 and T4. Ground samples were processed for C & N with an CHN analyzer (LECO TruMac CN-analyser, Leco corporation, USA) using an automated dry combustion method (Dumas method). Leaf nitrogen (N) per unit area (N_{area}) was calculated as $N \text{ (mmol g}^{-1}) \times \text{LMA (g m}^{-2})$. Photosynthetic nitrogen use efficiency (PNUE) was calculated as $A_{\text{sat}} \text{ (}\mu\text{mol m}^{-2} \text{ s}^{-1}) / \text{leaf } N_{\text{area}} \text{ (mmol m}^{-2})$. Protein content was determined using N and multiplication factor of 5.7 (Bahrami et al., 2017; Mosse, 1990).

2.2.6 Statistical and temperature analysis

All data analyses and plotting were performed using R computer software (R Core Team, 2017). The effect of treatments and their interaction was analyzed using linear modeling with anova in R. Significance tests were performed with anova and post hoc Tukey test using the 'glht' function in the multcomp R package. Coefficient means were ranked using post-hoc Tukey test. The Farquhar-von Caemmerer-Berry (FvCB) photosynthesis model was fit to the A_{sat} response curves to C_i (A-C_i response curve) or chloroplastic CO₂ mole fraction (C_c), which was estimated from the g_m measurements (A-C_c response curve). g_m values were measured at five leaf temperatures (15, 20, 25, 30 and 35°C). We used the plantecophys R package (Duursma, 2015) to perform the fits, using measured g_m and R_d values, resulting in estimates of maximal carboxylation rate (V_{cmax}) and maximal electron transport rate (J_{max}) for D-ribulose-1,5-bisphosphate carboxylase/oxygenase (Rubisco) using measured R_d values. Temperature correction parameter (Tcorrect) was set to False while fitting A-C_i curves. Temperature response of V_{cmax} and J_{max} were calculated by Arrhenius and peaked functions, respectively (Medlyn et al., 2002). Estimated V_{cmax} and J_{max} values at five leaf temperatures were then fit

using nonlinear least square (nls) function in R to determine energy of activation for V_{cmax} (EaV) and J_{max} (EaJ) and entropy (ΔS). Temperature responses of V_{cmax} and R_d were fit using Arrhenius equation as follows,

$$f(Tk) = k_{25} \cdot \exp \left[\frac{E_a \cdot (Tk - 298)}{R \cdot 298 \cdot Tk} \right] \quad (8)$$

where E_a is the activation energy (in J mol^{-1}) and k_{25} is the value of R_d or V_{cmax} at 25 °C. R is the universal gas constant ($8.314 \text{ J mol}^{-1} \text{ K}^{-1}$) and Tk is the leaf temperature in °K. The activation energy term E_a describes the exponential rate of rise of enzyme activity with the increase in temperature. The temperature coefficient Q_{10} , a measure of the rate of change of a biological or chemical system as a consequence of increasing the temperature by 10 °C was also determined for R_d using the following equation:

$$R_d = R_{d25} \cdot Q_{10}^{[(T-25)/10]} \quad (9)$$

A peaked function (Harley et al., 1992) derived Arrhenius function was used to fit the temperature dependence of J_{max} , and is given by the following equation:

$$f(Tk) = k_{25} \cdot \exp \left[\frac{E_a \cdot (Tk - 298)}{R \cdot 298 \cdot Tk} \right] \left[\frac{1 + \exp \left(\frac{298 \cdot \Delta S - H_d}{298 \cdot R} \right)}{1 + \exp \left(\frac{Tk \cdot \Delta S - H_d}{Tk \cdot R} \right)} \right] \quad (10)$$

Where, E_a is the activation energy and k_{25} is the J_{max} value at 25 °C, H_d is the deactivation energy and S is the entropy term. H_d and ΔS together describe the rate of decrease in the function above the optimum. H_d was set to constant 200 kJ mol^{-1} to avoid over parametrization. The temperature optimum of J_{max} was derived from Eqn 10 (Medlyn et al., 2002) and written as follows:

$$T_{opt} = \frac{H_d}{\Delta S - R \cdot \ln \left[\frac{E_a}{(H_d - E_a)} \right]} \quad (11)$$

The temperature response of A_{sat} was fit using a simple parabola equation (Crous et al., 2013) to determine temperature optimum of photosynthesis:

$$A_{sat} = A_{opt} - b \cdot (T - T_{opt})^2 \quad (12)$$

Where, T is the leaf temperature of leaf gas exchange measurement for A_{sat} , T_{opt} represents the temperature optimum and A_{opt} is the corresponding A_{sat} at that temperature optimum. Steady state gas exchange parameters g_m , g_s , C_i and J_{max} to V_{cmax} ratio were fit using nls function with polynomial equation:

$$y = A + Bx + Cx^2 \quad (13)$$

2.3 Results

Two commercial wheat lines Scout and Yitpi were grown under current ambient ($450 \mu\text{l L}^{-1}$, day time average) and future elevated ($650 \mu\text{l L}^{-1}$, day time average) CO_2 conditions with 65% (daytime average) relative humidity, 22°C (day time average) growth temperature and natural light (500 PAR average daily maximum) (Figure. 2.1). Humidity was managed by using humidifiers set to operate between 50 to 70 % RH which reflects in vapor pressure deficit (VPD) (Figure S2.5). Both aCO_2 and eCO_2 grown plants were exposed to two 3-day heat stress (HS) cycles at the vegetative (H1, 10 WAP, daytime average of 38°C) and flowering stage (H2, 15 WAP, daytime average of 33.5°C). Heat stress 2 (H2) was lower in intensity relative to H2 due to the cool winter conditions. Grain filling started 17 WAP and final harvest occurred 25 WAP (Figures 2.1 and 2.2).

2.3.1 Similar photosynthetic temperature responses at aCO_2 between the two wheat lines

A- C_i curves together with mesophyll conductance were measured at five leaf temperatures in order to characterize the thermal photosynthetic responses of the two wheat lines grown at aCO_2 (Figure 2.3; Table 2.1). Overall, both lines had similar photosynthetic temperature response. A_{sat} , and g_s increased with leaf temperature up to an optimum (T_{opt}) around 23.4°C and decreased thereafter in both lines, while C_i decreased between 15°C and 35°C (Figures 2.3A-D). g_m increased up to 25°C and did not significantly change at higher temperatures. R_d increased with increasing temperature in both lines (Figure 2.3H). The modelled Q_{10} temperature coefficient (rate of change due increase by 10°C) of R_d was similar in both lines (Table 2.1). Scout had slightly higher A_{sat} , g_s , C_i and g_m than Yitpi at T_{opt} (Figures 2.3 A-D and H). V_{cmax} and J_{max} were calculated by fitting the response of A_{sat} to variations in chloroplast CO_2 concentration (C_c) (A- C_c response curve) using measured R_d and g_m . V_{cmax} increased with leaf temperature in both lines, while J_{max} increased up to T_{opt} (30°C) and decreased with further temperature increase in both lines (Figures 2.3E-F, Table 2.1). The ratio of $J_{\text{max}}/V_{\text{cmax}}$ was equal between Scout and Yitpi and decreased similarly with leaf temperature for both wheat lines (Figure 2.3G). There was no significant difference in V_{cmax} , J_{max} or their activation energy between the two wheat lines (Figure 2.3E-G, Table 2.1).

2.3.2 eCO₂ stimulated wheat photosynthesis and reduced stomatal conductance despite causing a mild acclimation

Overall, the two wheat lines had similar A_{sat} , g_s , PWUE (A_{sat}/g_s), R_d , Fv/Fm, V_{cmax} and J_{max} measured under most growth and measurement conditions (Figures 2.3 and 2.4, Tables 2.2, S2.1 and S2.2). To assess photosynthetic acclimation due to eCO₂, control plants were measured at common CO₂ and 25°C. Under these conditions, eCO₂ reduced A_{sat} (-12% at T2) and g_s in both lines; the downregulation of A_{sat} was observed at all stages in Yitpi but not at T3 in Scout (Figure 2.4, Tables 2.2, S2.1 and S2.2). When control plants were measured at growth CO₂ and 25°C, eCO₂ increased A_{sat} (+21% at T2) to a similar extent in both wheat lines, and reduced g_s in Yitpi (-28% at T2) slightly more than in Scout (-11% at T2) (Figure 2.4, Tables 2.2, S2.1 and S2.2).

2.3.3 HS did not inhibit photosynthesis at 25°C but slightly reduced photosynthesis at 35°C in aCO₂-grown plants

Photosynthesis was measured at growth CO₂ around both HS cycles (Figure 2.5). Overall, HS did not have negative effect on photosynthesis measured at 25°C during or after HS but showed significant interaction between temperature and CO₂ (Figure 2.5). A_{sat} measured during H1 and H2 at 35°C was higher relative to 25°C in Scout (10-14%) and Yitpi (12-18%) plants grown at eCO₂ but not at aCO₂ (Figure 2.5A-D). Dark-adapted chlorophyll fluorescence was measured to assess damage to PSII around the HS cycles. Fv/Fm measured at 25°C fluctuated little and tended to be lower in eCO₂ grown Yitpi. During H1 and H2, Fv/Fm decreased at 35°C relative to 25°C; this reduction was largest in aCO₂ grown Scout relative to the other treatments (Figure 2.5E-H).

To assess the long-term interactive effects of eCO₂ and HS, plants were measured at growth CO₂ at the conclusion of both H cycles around anthesis (Figure 2.6, Table 2.2). Elevated CO₂ stimulated A_{sat} in HS plants more than in control plants and in Yitpi more than Scout (Figure 2.6A-B), while the response of g_s to eCO₂ was weak in all plants (Figure 2.6C-D). Accordingly, PWUE was stimulated by eCO₂ in both wheat lines to various extent depending on the HS treatment (Figure 2.6E-F, Tables 2.2, S2.2 and S2.3). There was a good correlation between A_{sat} and g_s ($r^2=0.51$, $p < 0.001$) across all treatments (Figure S2.1A). The A-C_i response curves were measured at 25°C to assess the effects of eCO₂ and HS treatments on photosynthetic capacity at the recovery stage after H2. Growth at eCO₂ marginally reduced V_{cmax} in Scout (-

14%, $p = 0.09$) and Yitpi (-15%, $p = 0.06$) but had no effect on J_{max} in either line. HS did not affect V_{cmax} or J_{max} in either of the lines (Figure 2.4I-L). There was a good linear relationship between V_{cmax} and J_{max} (Figure S2.1B).

2.3.4 Larger Yitpi produced slightly more grain yield than faster Scout at current ambient CO_2

The two lines differed in phenology and growth habit. When compared at a CO_2 , the two wheat lines showed different growth characteristics. Scout developed faster and flowered earlier than Yitpi as evident from booting information at pre-anthesis stage (Figure 2.7). At T2, 43% of tillers had ears in Scout compared to 11% of the tillers in Yitpi (Figure 2.7). In addition, Scout elongated faster than Yitpi; at T2 Scout was 74% ($p < 0.001$) taller than Yitpi but at T3 both lines had similar height (Figure 2.8E, Tables 2.3 and 2.4). In contrast, Yitpi accumulated more biomass relative to Scout due to its higher tillering habit (Figures 2.8 and 2.9). Total plant biomass was 42% ($p < 0.005$) higher in Yitpi than Scout at T3. Similarly, Yitpi had 130% ($p < 0.001$) more tillers, 254% ($p < 0.001$) larger leaf area, 128% ($p < 0.001$) more leaves and 61% ($p < 0.001$) larger leaf size at T3 (Figure 2.8, Tables 2.3 and 2.4).

At the final harvest (T4), Yitpi produced significantly greater plant biomass (84%), tillers (88%) and grains (54%) but only 17% greater grain yield compared to Scout (Figure 2.9, Tables 2.3 and 2.4). This was partly due to larger grain size in Scout (+31%, $p < 0.001$) than Yitpi. Another factor was that 100% of the tillers developed ears and more ears filled grains in Scout compared to 88% in the higher tillering Yitpi (Tables 2.3, 2.4 and S2.3). Higher (178%, $p < 0.001$) harvest index (HI) in Scout than Yitpi may be due to Scout early maturity and consequent leaf senescence leading to loss of biomass at final harvest (T4). It is worth noting that the final harvest was undertaken 4 weeks after all the ears had matured on Scout to give ample time for grain filling in Yitpi (Figure 2.9, Tables 2.3 and 2.4).

These results partially support our first hypothesis which suggested that Scout and Yitpi will likely show similar grain yield despite their different growth habits. Biomass accumulation differed despite having similar photosynthetic parameters. In summary, Yitpi initiated more tillers but a lower proportion of these tillers produced ears and filled grains. In contrast, Scout produced less tillers but flowered earlier and matured faster which allowed enough time for all its tillers to produce ears and fill bigger grains by the final harvest.

2.3.5 At anthesis, eCO₂ stimulated wheat biomass due to greater allocation to the stems

Overall, eCO₂ stimulated plant biomass of both wheat lines differently at the various stages (Tables 2.3 and 2.4). By T3 (anthesis), eCO₂ stimulated plant biomass of high-tillering Yitpi (+29%) more than fast-developing Scout (+9%) under control conditions. This increase was not associated with the number of tillers, total leaf area, mean leaf size or leaf mass area which were not significantly affected by growth at eCO₂ in either line (Figure 2.9, Tables 2.4 and S2.3). Rather, eCO₂ increased allocation to stem biomass relative to leaf biomass particularly in Yitpi; this was evident from the strong correlation across treatments for stem biomass *versus* leaf biomass ($r^2 = 0.83$, $p < 0.001$) and total biomass *versus* leaf area ($r^2 = 0.83$, $p < 0.001$) in Scout but not in Yitpi. However, the two lines followed common relationship for root *versus* shoot biomass ($r^2 = 0.41$, $p < 0.001$) and leaf area *versus* leaf number ($r^2 = 0.82$, $p < 0.001$) across all treatments suggesting no effect of line, eCO₂ or HS on these common allometric relationships (Figure S2.3).

2.3.6 eCO₂ stimulated grain yield similarly in both wheat lines due to more grains per ear in Yitpi and more and bigger grains in Scout

By the final harvest at T4 (seed maturity), the difference in biomass between aCO₂ and eCO₂ grown plants under control conditions was marginally ($p = 0.02$) larger for Scout (+67%) than Yitpi (+28%) for two main factors (Figures 2.8 and 2.9, Tables 2.3 and 2.4). Firstly, Scout matured and senesced earlier which resulted in greater loss of leaf area and biomass by the final harvest, especially at aCO₂. Secondly, Yitpi continued to grow and develop allowing more time for the aCO₂ plants to catch up with eCO₂ counterparts at T4 (Figures 2.7 and 2.8, Tables 2.3 and 2.4).

Under control conditions, growth at eCO₂ stimulated grain yield and total grain number per plant similarly in Scout (+64% and +42%, respectively) and Yitpi (+50% and +32%, respectively) (Figure 2.9, Tables 2.3 and 2.4). In Yitpi, this increase was due to more grains per ear, while in Scout there were more ears and grains per ear as well as larger grain size at eCO₂. Harvest index was not affected by eCO₂ or HS treatments (Figure 2.7, Tables 2.3, 2.4 and S2.3).

2.3.7 eCO₂ did not stimulate the grain yield of HS plants and reduced grain N in Yitpi

In contrast to expectation, moderate HS (34-38°C) applied at 60% daytime relative humidity during the vegetative (H1) and flowering (H2) stages did not have negative impact on biomass accumulation of the two wheat lines at T3 at either CO₂ treatment. By T4, HS plants had larger biomass ($p < 0.01$) and grain yield ($p < 0.1$) relative to control plants under aCO₂ only due to a significant HS x CO₂ interaction. Consequently, control aCO₂ grown plants had the smallest plant dry mass and grain yield relative to the other treatment combinations (Figure 2.9, Tables 2.3 and 2.4).

Flag leaf N content was not significantly affected by either eCO₂ or HS in either line at T2 or T3. Under control conditions, eCO₂ significantly ($p < 0.001$) reduced grain N in Yitpi (-17%) but not in Scout, while HS had no effect on grain N content in either line (Table S2.4). The higher biomass accumulation in Yitpi may have exhausted the nutrient supply on further stimulation by eCO₂ leading to a significant reduction in N content.

2.4 Discussion

2.4.1 Two wheat lines with contrasting morphology and development, but similar photosynthesis and yield

The major aim of this study was to investigate the performance of two wheat cultivars with distinct agronomic features in future climate conditions with eCO₂ and heat stress (HS). Scout and Yitpi were grown at aCO₂ and eCO₂ and exposed to HS at the vegetative and/or flowering stage. Photosynthesis, chlorophyll fluorescence, biomass and grain yield were measured at four points along the life cycle of the plants. The two wheat lines had similar photosynthetic traits including the response to temperature and eCO₂. In contrast to expectations of higher WUE in Scout due to its selection based on carbon isotope discrimination gene (Condon et al., 2004), both wheat lines showed similar PWUE under most measurement and growth conditions in this study (Figure 2.6, Table 2.2). Free tillering Yitpi produced substantially more tillers, leaf area and biomass relative to the faster developing Scout. Accordingly, the first hypothesis predicted that Yitpi will have higher grain yield. This hypothesis was only partially supported because relative to Yitpi, Scout had higher harvest index (HI) due to its early maturing and senescing habit, and produced only slightly less grain yield due to its larger grain size. It is worth noting that some field trials have reported slightly higher grain yields in Scout than Yitpi (National variety trial report, GRDC, 2014). Thus, early vigor and maturity compared to high tillering capacity seem to be equally beneficial traits for high grain yield in the Australian environment.

2.4.2 Elevated CO₂ stimulated photosynthesis but reduced photosynthetic capacity in both lines

Elevated CO₂ similarly increased A_{sat} and reduced g_s in both lines when measured at growth CO₂. Further, eCO₂ reduced A_{sat} (-12%) in both lines when measured at common CO₂ (400 μ L L⁻¹) suggesting equivalent downregulation or acclimation of photosynthesis (Delgado et al., 1994; Leakey et al., 2009). This result countered the second hypothesis suggesting that Yitpi will show less photosynthetic acclimation due to its higher sink capacity. The observed photosynthetic acclimation in response to growth at eCO₂ in this study was relatively small and was underpinned by an insignificant reduction of leaf N in Yitpi only (Table S2.4). It is likely that the larger sink capacity in Yitpi, further increased by eCO₂, entailed greater N demand, leading to acclimation (Rogers and Humphries, 2000). In contrast, Scout may have undergone photosynthetic downregulation rather than acclimation in response to eCO₂ (Delgado et al., 1994) because there was no significant reduction in N or V_{cmax} . Photosynthetic responses of

wheat in current study are in agreement with earlier enclosure studies which generally have higher response to eCO₂ than the FACE studies (Kimball et al., 1995; Hunsaker et al., 1996; Osborne et al., 1998; Kimball et al., 1999; Long et al., 2006; Cai et al., 2016).

2.4.3 Elevated CO₂ tended to stimulate vegetative biomass more in Yitpi than Scout but grain yield stimulation was similar in both lines

In accordance with the second hypothesis, eCO₂ stimulated plant biomass slightly more in Yitpi, the line with higher sink capacity, relative to Scout at anthesis. In partial support of the third hypothesis, the biomass stimulation was related to greater tillering in Scout only (1 extra tiller per plant). Yitpi produced lots of tillers at aCO₂; at eCO₂ the cultivar allocated more biomass to the existing tillers rather than produced more of them. Importantly, at seed maturity, eCO₂ stimulated grain yield similarly in both lines as result of the trade-off between yield components (Dias de Oliveira et al., 2015), particularly grain number and size. While grain number increased in both lines, eCO₂ stimulated grain size in Scout only. In line with the current study, grain yield of twenty wheat lines that differed in tillering propensity, water soluble carbohydrate accumulation, early vigor and transpiration efficiency have been found to respond similarly to eCO₂ (Bourgault et al., 2013; Ziska et al., 2004). Generally, eCO₂ stimulates grain yield by increasing the number of tillers and consequently, ears per plant (Bennett et al., 2012; Zhang et al., 2010), which has also been reported in FACE studies (Högy et al., 2009; Fitzgerald et al., 2016). However, in the current study, the increase in grain yield at eCO₂ was mainly caused by increased grain number due to the increase in the number of grains per ear.

2.4.4 Elevated CO₂ reduced grain N in Yitpi only

Increase in grain yield causes reduction in N and thus protein concentration due to the trade-off between yield and quality (Pleijel and Uddling, 2012; Taub et al., 2008). Stimulation in grain yield by eCO₂ (Bahrami et al., 2017; Seneweera and Conroy, 1997) also results in reduction of grain N content which is known as ‘dilution effect’.

Scout being high yielding cultivar with bigger grain size accumulated less N than Yitpi and eCO₂ affected plant N content differently in Scout and Yitpi. eCO₂ decreased leaf N (21.4%, $p < 0.001$) at T3 and grain N at T4 (20 % $p < 0.001$) in Yitpi but not in Scout. This is consistent with the results from FACE study with same cultivars which reported 14% reduction in N content by eCO₂ in above ground dry mass in Yitpi but not in Scout under well-watered conditions. The FACE study involved investigation of grain protein and N uptake for Scout

and Yitpi grown under two CO₂ (aCO₂ and eCO₂) and two water regimes (rainfed and irrigated) in which eCO₂ effect was marginally significant for grain protein ($p = 0.06$) and non-significant for N uptake, while water treatment significantly affected both grain protein concentration ($p = 0.028$) and N uptake ($p = 0.001$) (Bahrami et al., 2017).

Early vigor wheat cultivars such as Scout have been shown to have greater root biomass accumulation as well as greater early N uptake which may have avoid dilution effect (Bahrami et al., 2017; Liao et al., 2004). Yitpi being a free tillering cultivar with large biomass shows strong dilution effect due to further enhancement by eCO₂. Grain yield increase is strongly associated with increase in grain number per unit area (Bennett et al., 2012; Zhang et al., 2010) which reduces the amount of N translocated.

2.4.5 HS was not harmful and increased biomass and grain yield in aCO₂ grown plants

We did not find negative impact of heat stresses (either H1, H2 or H1+H2) on photosynthesis, chlorophyll fluorescence, biomass and grain yield. Unchanged maximum efficiency of PS II (Fv/Fm) confirmed that the plants were not stressed during or after the HS rejecting the hypothesis that HS will reduce photosynthesis, biomass and yield. This is in contrast to previously reported studies where HS reduced the grain yield and negatively affected the growth and development (Stone and Nicolas, 1996, 1998; Farooq et al., 2011; Coleman et al., 1991). In field conditions, during heat wave the vapor pressure deficit (VPD) increases and soil moisture decreases leading to lower stomatal conductance and consequently lower transpiration. Thus, plants are unable to cool down and leaf temperatures rise beyond optimum levels causing damage. As leaf temperatures were not measured in current study we speculate that leaf temperatures might not have increased beyond damaging levels and the HS in current study may have been acute temperature increase below damaging level. As the leaf temperatures were not measured the term HS also refers to the impact of VPD.

Interestingly, HS tended to increase biomass and grain yield in the aCO₂ grown plants in current study. The positive effect of HS in current study could be explained by the ability of plants to cool themselves down at moderate relative humidity by transpiration in well-watered conditions. During HS, leaf temperatures might not have increased beyond damaging levels even with air temperatures reaching up to 40°C. Well-watered crops can maintain grain-filling rate, duration and size under HS (Dupont et al., 2006), and high temperatures can increase crop yields if not exceeding critical optimum growth temperature (Welch et al., 2010). Also, in

current study the night temperatures were not increased during HS which favors plant growth by reducing respiratory losses (Prasad et al., 2008).

Non- stressful heat wave compels to do another experiment with modified conditions to make sure leaf temperatures increase like field conditions in order to study eCO₂ interaction with HS.

2.4.6 HS did not affect biomass and grain yield in eCO₂ grown plants

Plant development is generally accelerated by increased temperature, eCO₂ can accelerate it even further in some instances, or eCO₂ may have neutral or even retarding effects in other cases (Rawson, 1992). The interactive effects of eCO₂ and temperature on the physiology and growth of plants have been investigated, although mostly for increases in mean temperatures (Morison and Lawlor, 1999; Delgado et al., 1994; Kimball, 2016; Dias de Oliveira et al., 2015) rather than for short term heat waves (Wang et al., 2008; Coleman et al., 1991).

Although HS was not severe enough to negatively affect the photosynthesis, interactive effects of eCO₂ and HS were observed in the photosynthetic measurements during HS at growth CO₂. A_{sat} measured during HS at 35°C relative to 25°C leaf temperature was higher in eCO₂ but not in aCO₂ grown plants. Higher g_s during HS at moderate RH in well-watered conditions increased A_{sat} in both aCO₂ and eCO₂ grown plants. However, lower photorespiration under eCO₂ (Long, 1991) allows further increase in A_{sat} with temperature when measured at 35°C relative to 25°C, while under aCO₂ photorespiration increases with temperature reducing the A_{sat} measured at 35°C relative to 25°C. Also, less decrease in photosynthetic quantum efficiency under eCO₂, compared with its decrease under aCO₂ supports increase in A_{sat} at higher temperatures in eCO₂ grown plants relative to aCO₂ (Yin et al., 2014).

Biomass parameters also showed significant interactive effects of eCO₂ and HS. The HS in current study which was apparently an acute temperature increase below damaging level, stimulated biomass and grain yield in aCO₂ but not in eCO₂ grown plants. No stimulation in biomass by HS under eCO₂ grown plants could be explained by nutrient limitation due to eCO₂ stimulation. Plants may have exhausted available nutrients due to increased demand by eCO₂ stimulated sink capacity. And the temperature increase below damaging level was unable to further stimulate the biomass and grain yield. Also, eCO₂ induced acclimation reduces V_{cmax} and N content (Leakey et al., 2009; Rogers and Humphries, 2000) which may limit further stimulation by increased temperature. In addition, environmental variation in grain yield of wheat crops is associated with change in the number of kernels per unit land area (Fischer,

1985). Elevated CO₂ and temperature interactions can be complex, dynamic and difficult to generalize as they can go in any direction depending on plant biochemical composition and other environmental conditions (Rawson, 1992).

2.5 Conclusions

The two wheat lines, Scout and Yitpi differed in growth and development but produced similar grain yields. Elevated CO₂ stimulated biomass and yield similarly in both cultivars Scout and Yitpi. Overall, HS at moderate RH in well-watered conditions was not damaging to growth, photosynthesis, biomass or grain yield. However, the HS interacted with eCO₂ positively affecting only aCO₂ grown plants leading to similar biomass and grain yields in both aCO₂ and eCO₂ grown plants exposed to HS. Heat stress interaction with eCO₂ allowed eCO₂ grown plants to increase A_{sat} at higher temperatures but not aCO₂ grown plants. Considering the non-harmful HS, we speculate that HS in current study was mild and plants were able to cool down and maintain lower leaf temperatures despite high air temperatures during HS. Thus, HS experiment with modified conditions is required to understand interaction between eCO₂ and negatively affecting HS which is common in natural conditions (Wang et al., 2008, 2011).

Table 2.1 Summary of modelled parameters for temperature response of photosynthesis

Summary of coefficients derived using nonlinear least square fitting of CO₂ assimilation rates and maximal rate of carboxylation (V_{cmax}) and maximal rate of RuBP regeneration (J_{max}) determined using A-C_i response curves and dark respiration measured at five leaf temperatures 15, 20, 25, 30 and 35°C. Values are means with standard errors. Derived parameters include temperature optima (T_{opt}) of photosynthesis (A_{opt}); activation energy for carboxylation (EaV); activation energy (EaJ), entropy term (ΔSJ) and T_{opt} and corresponding value for J_{max} with deactivation energy (Hd) assumed constant; and activation energy (EaR) and temperature coefficient (Q_{10}) for dark respiration. Letters indicate significance of variation in means.

Parameter	Constant	Scout	Yitpi
A_{sat} ($\mu\text{mol m}^{-2} \text{s}^{-1}$)	T_{opt} (°C)	23.4 ± 1 a	23.4 ± 0.7 a
	A_{opt}	24.6 ± 1 a	22 ± 0.6 b
V_{cmax} ($\mu\text{mol m}^{-2} \text{s}^{-1}$)	V_{cmax} at 25°C	192.7 ± 17.1 a	198.4 ± 17.7 a
	EaV (kJ mol^{-1})	43.3 ± 8.74 a	46.4 ± 8.7 a
J_{max} ($\mu\text{mol m}^{-2} \text{s}^{-1}$)	J_{max} at 25°C	187.9 ± 13.1 a	186.1 ± 5.7 a
	T_{opt} (°C)	29.6 ± 0.3 a	30.5 ± 0.3 a
	J_{max} at T_{opt}	205.7 ± 10.2	215.4 ± 13.4
	EaJ (kJ mol^{-1})	37.7 ± 13.2 a	41.1 ± 5.8 a
	ΔSJ ($\text{J mol}^{-1} \text{K}^{-1}$)	648.3 ± 5.3 a	647 ± 2.4 a
	Hd (kJ mol^{-1})	200	
Rd ($\mu\text{mol m}^{-2} \text{s}^{-1}$)	Rd at 25°C	1.25 ± 0.02 a	1.25 ± 0.02 a
	EaR (kJ mol^{-1})	30.9 ± 1.6 a	33.2 ± 1.7 a
	Q_{10}	1.51 ± 0.03 a	1.56 ± 0.04 a

Table 2.2 Summary of statistics for gas exchange parameters

Summary of statistical analysis using anova test in R for effect of line, elevated CO₂ and heat stress (HS) on gas exchange parameters measured at 25°C leaf temperature at three-time points. Growth CO₂ measurements refer to measurement of ambient CO₂ grown plants at 400 (ul L⁻¹) and elevated CO₂ grown plants at (650 ul L⁻¹). Significance levels are: *** = $p < 0.001$; ** = $p < 0.01$; * = $p < 0.05$; † = $p < 0.1$; ns $p > 1$.

Time Point	Parameter	Meas CO ₂ (μl L ⁻¹)	Main Effects			Interactions			
			Line	Growth CO ₂	HS	Line*CO ₂	CO ₂ *HS	Line*HS	Line*CO ₂ *HS
T1	A _{sat} (μmol m ⁻² s ⁻¹)	400	ns	**		ns			
		650	ns	**		*			
	g _s (mol m ⁻² s ⁻¹)	400	ns	***		ns			
		650	ns	***		ns			
	PWUE (A _{sat} /g _s) (μmol mol ⁻¹)	400	ns	*		ns			
		650	ns	**		ns			
	Fv/Fm	400	ns	ns		ns			
	Fv'/Fm'	400	***	ns		ns			
	Rd (μmol m ⁻² s ⁻¹)	400	ns	ns		ns			
T2	A _{sat} (μmol m ⁻² s ⁻¹)	400	*	**	ns	ns	ns	ns	ns
		650	**	*	ns	ns	ns	ns	ns
	g _s (mol m ⁻² s ⁻¹)	400	ns	†	ns	ns	ns	ns	ns
		650	ns	ns	ns	ns	ns	ns	ns
	PWUE (A _{sat} /g _s) (μmol mol ⁻¹)	400	†	ns	ns	ns	ns	ns	ns
		650	**	ns	ns	ns	ns	ns	ns
	Fv/Fm	400	**	ns	ns	ns	**	ns	ns
	Fv'/Fm'	400	*	*	ns	ns	ns	ns	ns
	Rd (μmol m ⁻² s ⁻¹)	400	***	ns	†	ns	†	ns	ns
T3	A _{sat} (μmol m ⁻² s ⁻¹)	400	*	***	*	ns	ns	ns	ns
		650	***	*	**	ns	ns	ns	ns
	g _s (mol m ⁻² s ⁻¹)	400	*	***	***	ns	ns	***	ns
		650	***	**	***	ns	ns	***	ns
	PWUE (A _{sat} /g _s) (μmol mol ⁻¹)	400	ns	ns	**	*	ns	***	**
		650	ns	ns	**	ns	ns	***	ns
	Fv/Fm	400	***	ns	ns	***	*	†	*
	Fv'/Fm'	400	ns	†	ns	ns	ns	ns	ns
	Rd (μmol m ⁻² s ⁻¹)	400	***	ns	ns	*	**	*	ns
T3	A _{sat} (μmol m ⁻² s ⁻¹)	Growth CO ₂	*	***	*	ns	ns	ns	ns
	g _s (mol m ⁻² s ⁻¹)		*	***	***	ns	ns	***	ns
	PWUE (A _{sat} /g _s) (μmol mol ⁻¹)		ns	ns	**	*	ns	***	**
	Rd (μmol m ⁻² s ⁻¹)		***	ns	ns	*	**	*	ns

Table 2.3 Response of plant dry mass, grain yield and nitrogen (N) content to elevated CO₂ and heat stress

Summary of biomass and N parameters measured at different time points in Scout and Yitpi grown at ambient CO₂ (aCO₂) or elevated CO₂ (eCO₂) and exposed to 1 and/or 2 heat stresses (HS) at the vegetative (H1) or flowering (H2) stages, respectively. Values are means \pm SE (n= 9-10). Heat stress levels include plants not exposed to any HS (control), plants exposed to only HS 1 (H1), HS 2 (H2) and both HS (H1+H2).

Parameter	Time Point	Line HS	Scout				Yitpi			
			Control	H1	H2	H1 + H2	Control	H1	H2	H1 + H2
Total Plant DM (g plant ⁻¹)	T0	aCO ₂	0.04 \pm 0.001				0.04 \pm 0.003			
	T1	aCO ₂	0.82 \pm 0.18				1.16 \pm 0.15			
		eCO ₂	1.17 \pm 0.17				1.32 \pm 0.15			
	T2	aCO ₂	9.9 \pm 1.0	7.8 \pm 0.8			12.8 \pm 0.8	13.6 \pm 0.9		
		eCO ₂	10.6 \pm 0.5	9.7 \pm 0.3			14.8 \pm 1.1	14.9 \pm 1.3		
	T3	aCO ₂	16.8 \pm 1.8	12.2 \pm 1.1	14.0 \pm 2.2	16.1 \pm 2.0	23.9 \pm 1.1	26.1 \pm 0.7	24.4 \pm	23.1 \pm 1.0
		eCO ₂	18.3 \pm 1.3	21.0 \pm 1.4	18.1 \pm 2.0	20.0 \pm 2.1	30.8 \pm 1.9	31.1 \pm 1.2	31.6 \pm	28.9 \pm 1.8
	T4	aCO ₂	14.9 \pm 1.8		22.3 \pm 3.4	19.2 \pm 2.7	29.8 \pm 3.1		38.6 \pm	35.7 \pm 1.7
		eCO ₂	24.9 \pm 0.8		20.0 \pm 1.1	17.1 \pm 0.6	38.1 \pm 2.5		44.1 \pm 2.3	36.0 \pm 3.4
Grains Per Ear (plant ⁻¹)	T4	aCO ₂	29 \pm 2		31 \pm 3	29 \pm 3	22 \pm 2		30 \pm 2	27 \pm 2
		eCO ₂	36 \pm 4		32 \pm 1	26 \pm 1	29 \pm 1		28 \pm 2	27 \pm 2
Total Grain Number (plant ⁻¹)	T4	aCO ₂	230 \pm 15		273 \pm 34	247 \pm 36	328 \pm 32		471 \pm 41	405 \pm 7
		eCO ₂	326 \pm 11		287 \pm 19	237 \pm 8	433 \pm 37		458 \pm 27	364 \pm 38
Mean Grain Size (mg grain ⁻¹)	T4	aCO ₂	37 \pm 1		38 \pm 1	43 \pm 1	28 \pm 1		28 \pm 1	27 \pm 1
		eCO ₂	42 \pm 2		40 \pm 2	38 \pm 1	32 \pm 1		32 \pm 1	35 \pm 2
Grain yield (g plant ⁻¹)	T4	aCO ₂	8.5 \pm 0.6		10.9 \pm 2.0	10.7 \pm 1.7	9.1 \pm 1.0		13.2 \pm	11.1 \pm 0.4
		eCO ₂	14.0 \pm 0.6		11.6 \pm 0.9	9.0 \pm 0.5	13.7 \pm 1.0		14.8 \pm	12.8 \pm 1.3
Harvest Index	T4	aCO ₂	0.58 \pm 0.01		0.49 \pm 0.03	0.56 \pm 0.01	0.31 \pm 0.01		0.35	0.32 \pm 0.01
		eCO ₂	0.57 \pm 0.01		0.52 \pm 0.01	0.53 \pm 0.01	0.36 \pm 0.01		0.35	0.37 \pm 0.02
Total N uptake (g N plant ⁻¹)	T3	aCO ₂	0.21 \pm 0.02			0.19 \pm 0.04	0.41 \pm 0.06			0.53 \pm 0.04
		eCO ₂	0.21 \pm 0.02			0.32 \pm 0.06	0.37 \pm 0.02			0.57 \pm 0.06
	T4	aCO ₂	0.31 \pm 0.02			0.47 \pm 0.04	0.50 \pm 0.04			0.70 \pm 0.1
		eCO ₂	0.54 \pm 0.03			0.31 \pm 0.01	0.77 \pm 0.06			0.60 \pm 0.07
Grain Protein (%)	T4	aCO ₂	18 \pm 0.6			18.1 \pm 0.1	22.5 \pm 0.2			20.3 \pm 0.6
		eCO ₂	18 \pm 1			18 \pm 0.6	18.7 \pm 0.3			20.1 \pm 0.8
N utilization efficiency (g yield (g N uptake) ⁻¹)	T4	aCO ₂	28.1 \pm 1.1			25.7 \pm 2	18.1 \pm 0.8			16.9 \pm 2
		eCO ₂	26.0 \pm 1			26.6 \pm 1.2	17.9 \pm 0.2			21.8 \pm 2.1

Table 2.4 Summary of statistics for plant dry mass and morphological parameters

Summary of statistical analysis using anova test in R for effect of line, elevated CO₂ and heat stress (HS) on plant dry mass (DM) and morphological parameters measured at four-time points. Significance levels are: *** = $p < 0.001$; ** = $p < 0.01$; * = $p < 0.05$; † = $p < 0.1$; ns $p > 1$.

Time Point	Parameter (Mean plant ⁻¹)	Main Effects			Interactions			
		Line	CO ₂	HS	Line × CO ₂	CO ₂ × HS	Line × HS	Line × CO ₂ × HS
T1	Leaf number (n)	***	ns		ns			
	Leaf area (cm ²)	*	ns		ns			
	Leaf DM (g)	*	*		ns			
	Stem DM (g)	**	ns		ns			
	Root DM (g)	ns	ns		ns			
	Shoot DM (g)	**	*		ns			
	Total DM (g)	ns	ns		ns			
T2	Tiller number	***	ns	ns	ns	ns	ns	ns
	Leaf number	***	ns	ns	ns	ns	ns	ns
	Leaf area (cm ²)	***	ns	†	ns	ns	ns	ns
	Leaf DM (g)	***	ns	ns	ns	ns	ns	ns
	Stem DM (g)	ns	**	ns	ns	ns	ns	ns
	Root DM (g)	***	ns	ns	ns	ns	ns	ns
	Shoot DM (g)	***	**	ns	ns	ns	ns	ns
T3	Total DM (g)	***	*	ns	ns	ns	ns	ns
	Tiller number	***	ns	ns	*	ns	ns	ns
	Leaf number	***	**	ns	ns	ns	ns	ns
	Leaf area (cm ²)	***	ns	ns	ns	ns	ns	ns
	Leaf DM (g)	***	**	ns	ns	ns	ns	ns
	Stem DM (g)	***	***	ns	ns	ns	ns	ns
	Root DM (g)	***	**	ns	ns	ns	†	ns
T4	Shoot DM (g)	***	***	ns	ns	ns	ns	ns
	Total DM (g)	***	***	ns	ns	ns	ns	ns
	Total N uptake (g plant ⁻¹)	***	ns	**	ns	ns	†	ns
	Tiller number	***	ns	ns	ns	ns	ns	ns
	Ear no/tiller no (ratio)	**	ns	ns	ns	ns	ns	ns
	Root DM (g)	***	ns	ns	ns	ns	ns	ns
	Shoot DM (g)	***	**	**	ns	*	ns	ns
T4	Total DM (g)	***	*	**	ns	*	ns	ns
	Grain yield (g)	*	**	†	ns	*	ns	ns
	Grain number	***	ns	*	ns	**	ns	ns
	Grain size (mg grain ⁻¹)	***	**	ns	*	ns	ns	**
	Harvest index	***	ns	ns	ns	ns	*	ns
	Grain Protein (%)	***	*	ns	**	ns	*	*
	Total N uptake (g plant ⁻¹)	***	ns	ns	ns	***	ns	ns
	N utilization efficiency (g yield (g N uptake) ⁻¹)	***	ns	ns	ns	†	ns	ns

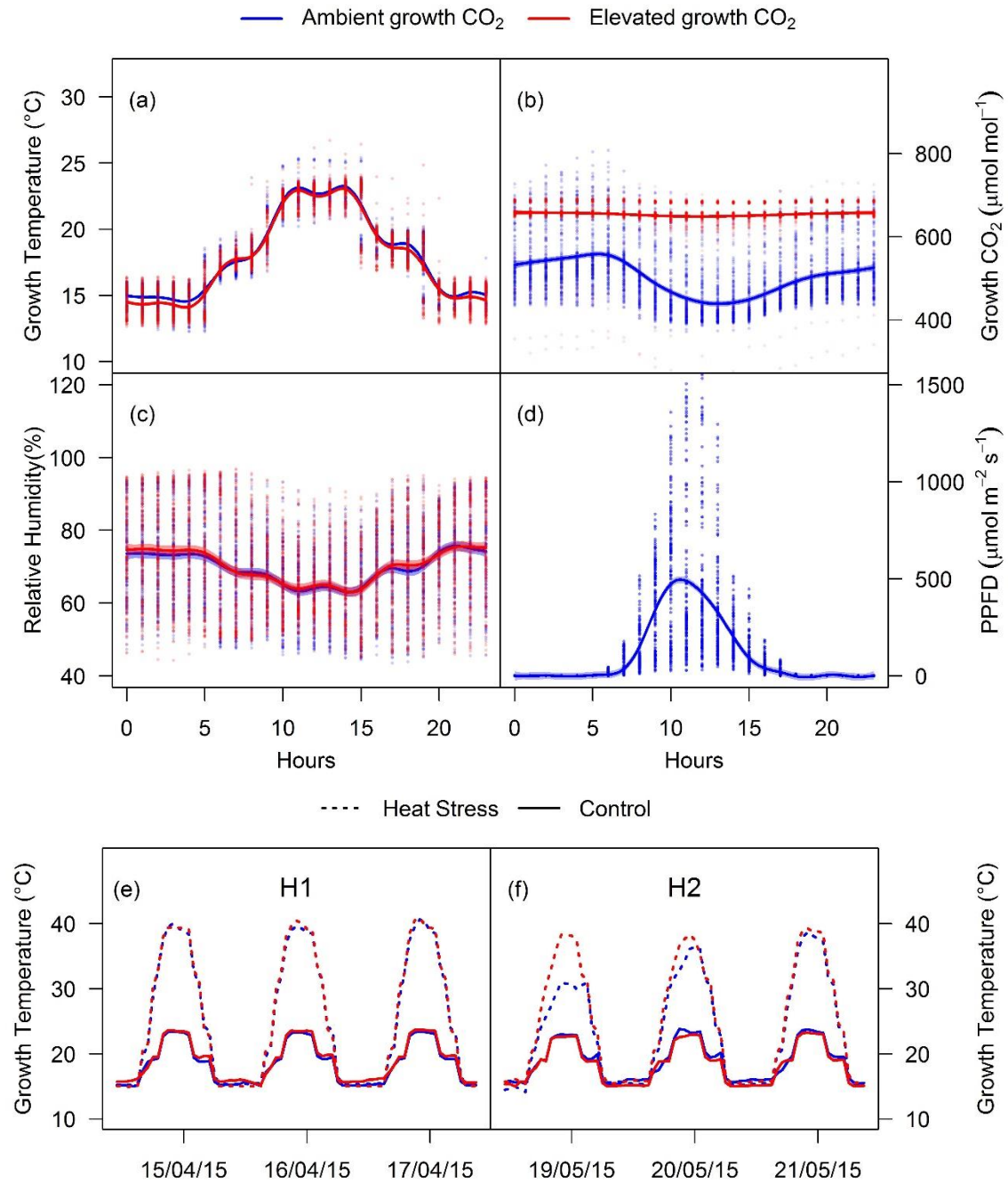


Figure 2.1 Glasshouse growth conditions

Glasshouse conditions during the experimental growth period; growth temperature (a), growth CO₂ (b), relative humidity (c) and PPFD (d). In panels a, b, c and d, the solid lines represent the growth averages, while the faint data points show all collected values. For heat stresses H1 (e) and H2 (f), the solid lines represent control temperature and dotted lines represent the heat stress temperature. Ambient and elevated CO₂ are depicted in blue and red color, respectively.

Time point (week period)	Weeks After Planting (WAP)	Growth Stage
T0 (W ₀ - W ₂)	2	Transplanting: 2 leaves unfolded
T1 (W ₂ - W ₇)	7	Tillering: Main shoot and 6/8 tillers, 6/8 leaves unfolded
H1	10	Vegetative stage
T2 (W ₇ - W ₁₂)	12	Pre-anthesis: 4 th node detectable
H2	15	Flowering stage
T3 (W ₁₂ - W ₁₇)	17	Anthesis: 50 % flowering
T4 (W ₁₇ - W ₂₅)	25	Grain filling: Seed maturity

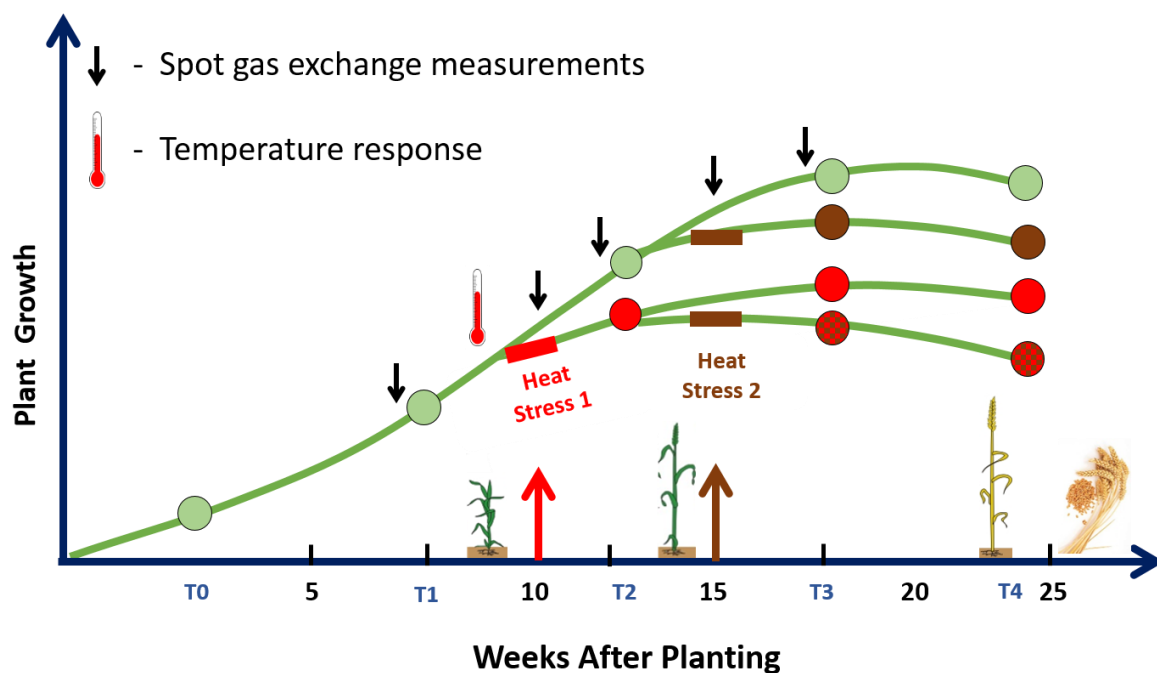


Figure 2.2 Glass house experimental design

Experimental design depicting plant growth plotted over 5-time points (T0, T1, T2, T3 and T4) across the wheat life cycle till maturity. The circles represent harvest of 10 plants at corresponding time point. Green circles on the top line represent control plants grown at ambient or elevated CO₂. Upward directed red and brown arrows point to timing and duration of two heat stresses (HS), H1 (vegetative stage) and H2 (flowering stage) respectively. The red circles represent plants subjected to heat stress 1 and brown circles represent plants subjected to heat stress 2. Red and brown dotted circles represent plants subjected to both heat stresses. Downward facing small black arrows represent timing of single point gas exchange measurements. Thermometer symbol represents timing of temperature response measurements.

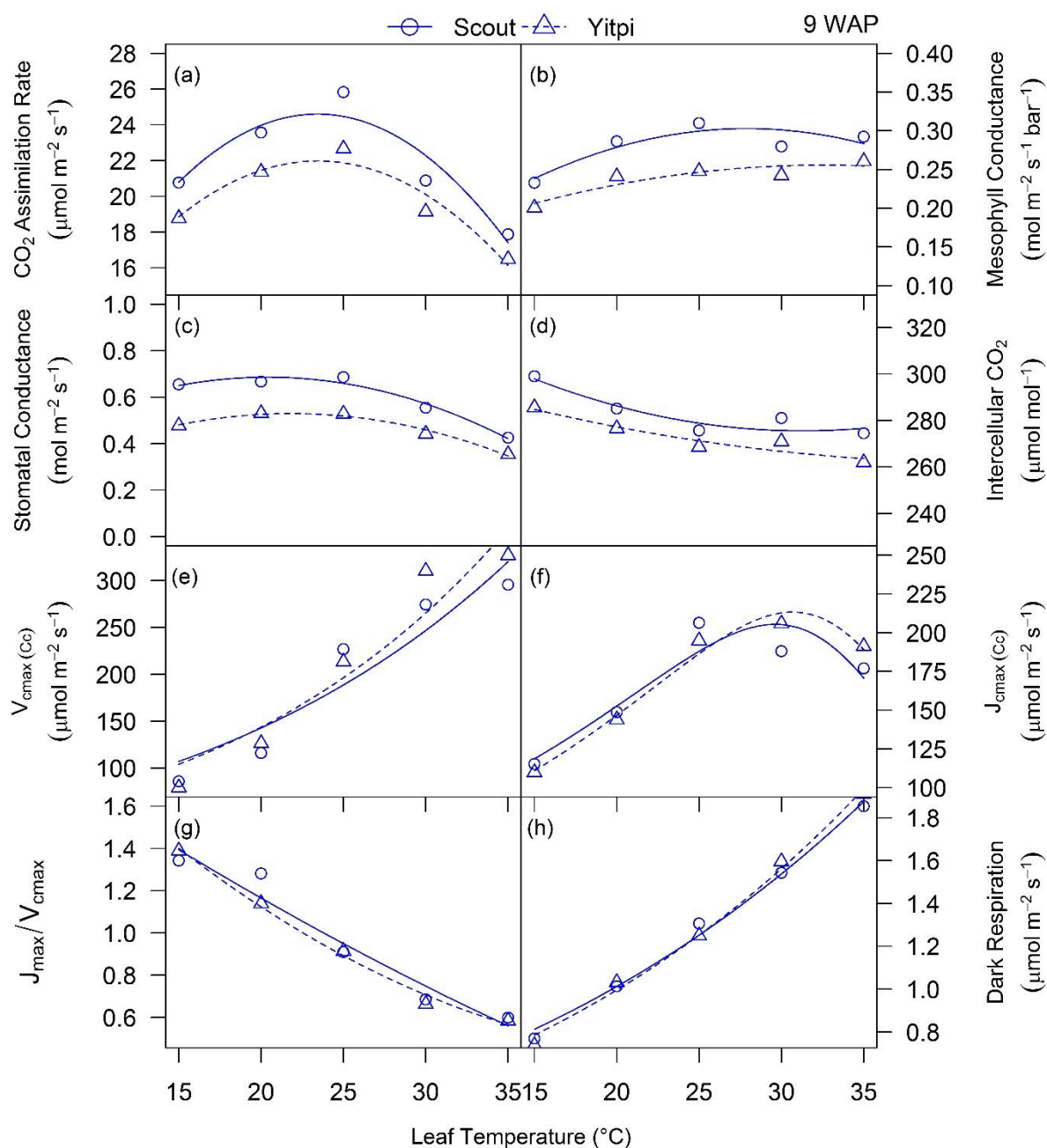


Figure 2.3 Temperature response of photosynthetic parameters

CO₂ assimilation rate (a), mesophyll conductance (b), stomatal conductance (c) and intercellular CO₂ (d), V_{cmax} (e), J_{max} (f), J_{max} / V_{cmax} (g) and dark respiration (h) over leaf temperatures (15, 20, 25, 30 and 35 °C) in plants grown at aCO₂. Scout and Yitpi are depicted using circles with solid lines and triangles with broken lines respectively. Lines in panels (a), (b), (c), (d), (e), (f) and (h) are fit using nonlinear least square (nls) function in R.

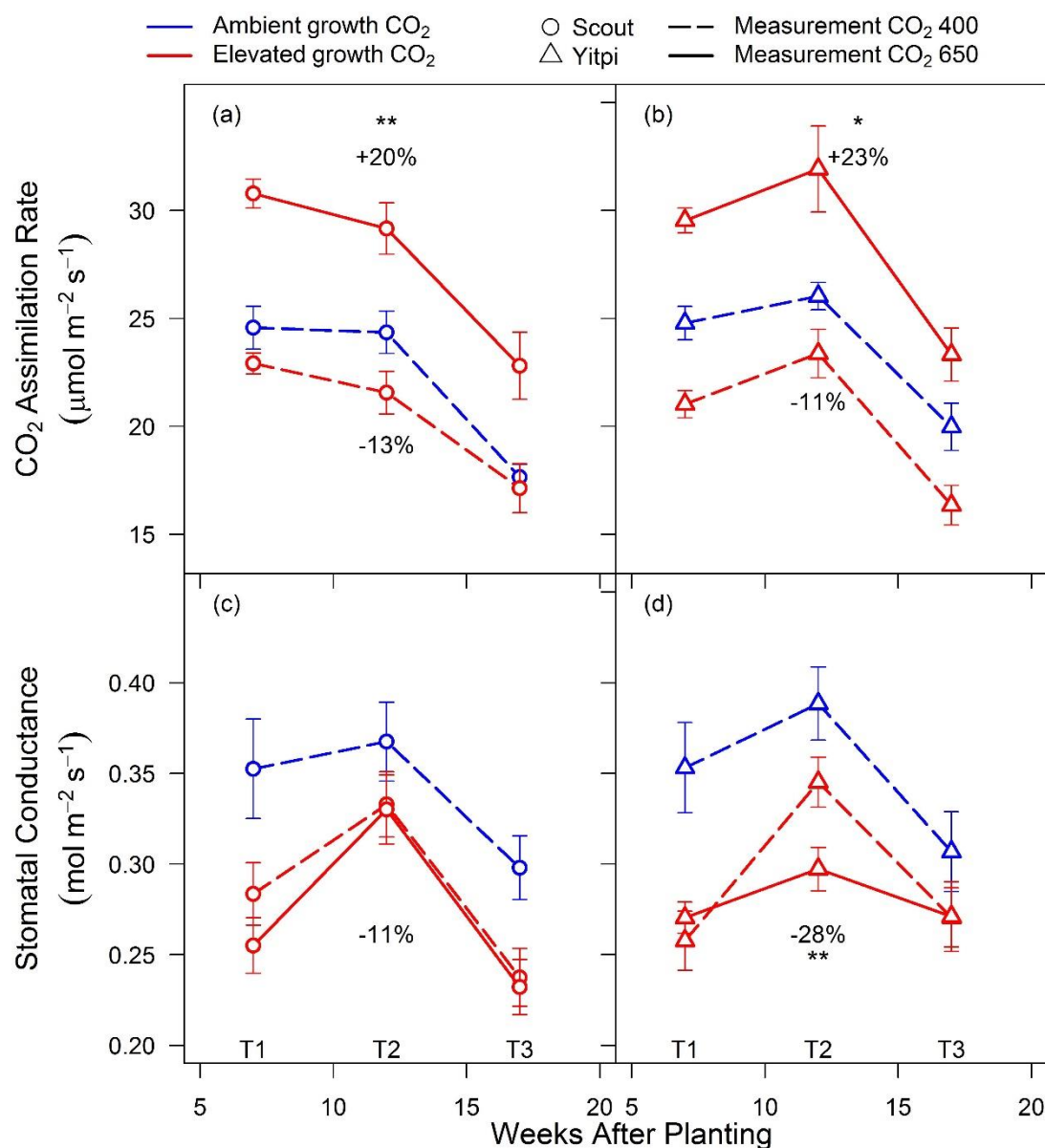


Figure 2.4 Photosynthetic response of Scout and Yitpi to eCO₂ measured at 25°C leaf temperature and various time points

CO₂ assimilation rates in Scout (a, b) and Yitpi (c, d) and stomatal conductance in Scout (e, f) and Yitpi (g, h) at various time points. Leaf gas exchange was measured at common CO₂ (dashed lines; both aCO₂ and eCO₂ grown plants measured at 400 μl CO₂ L⁻¹) and growth CO₂ (continuous lines; aCO₂ grown plants measured at 400 μl CO₂ L⁻¹ and eCO₂ grown plants measured at 650 μl CO₂ L⁻¹). Ambient and elevated CO₂ are depicted in blue and red color, respectively. Scout and Yitpi are depicted using circles and triangles, respectively. Statistical significance levels (t-test) for the growth condition within each line are shown and they are: * = $p < 0.05$; ** = $p < 0.01$; *** = $p < 0.001$.

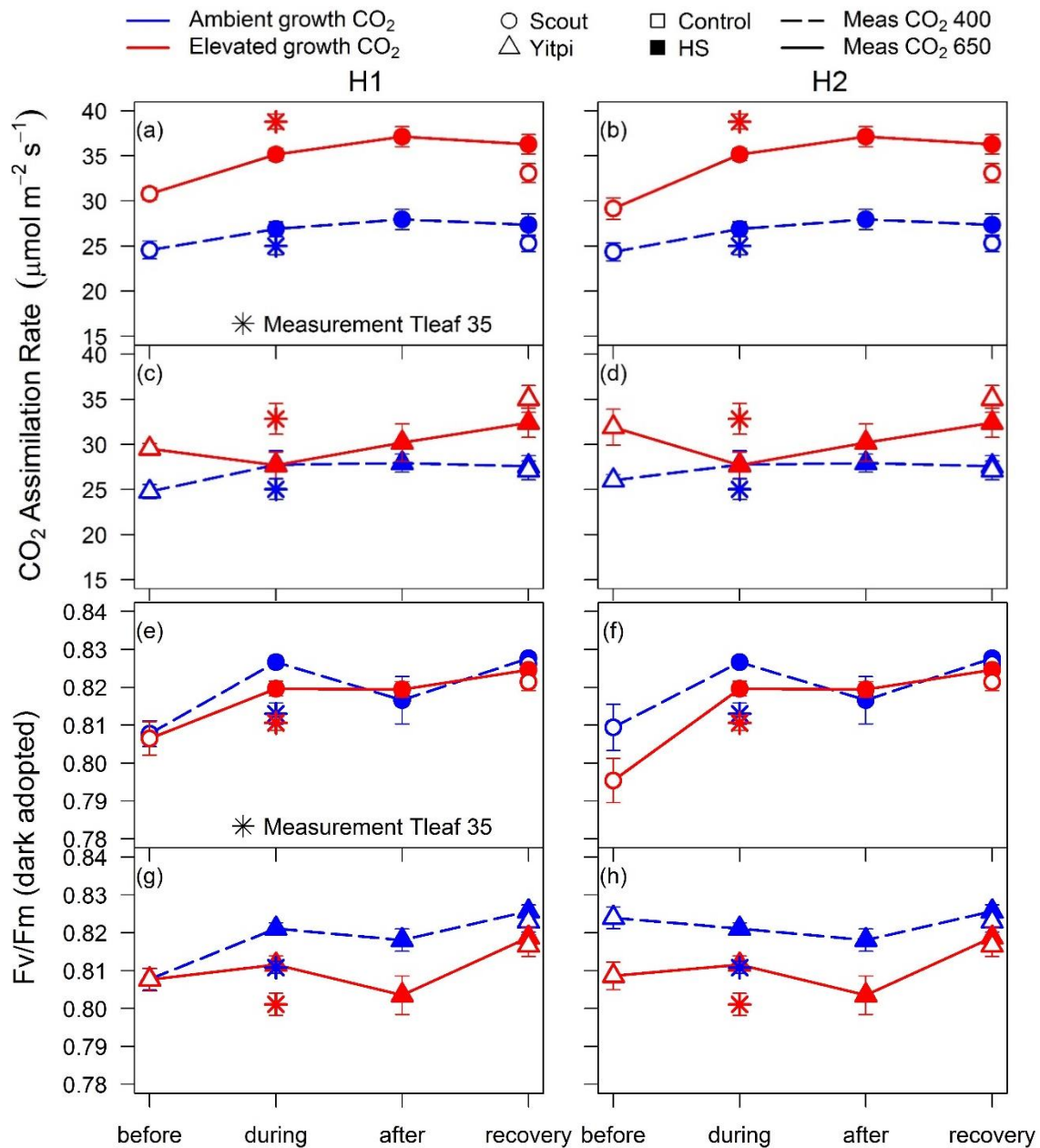


Figure 2.5 Photosynthesis and chlorophyll fluorescence response of Scout and Yitpi to eCO₂ measured during the two heat stress cycles

CO₂ assimilation rates (a, b, c, d) and dark-adapted chlorophyll fluorescence, Fv/Fm (e, f, g, h) measured at growth CO₂ (aCO₂ grown plants measured at 400 $\mu\text{L L}^{-1}$ and eCO₂ grown plants measured at 650 $\mu\text{L L}^{-1}$ CO₂ partial pressure). Left and right panels depict H1 and H2, respectively. Ambient and elevated CO₂ are depicted in blue and red color, respectively. Scout and Yitpi are depicted using circles and triangles, respectively. Open and closed symbols represent control and HS plants, respectively. All measurements were performed at leaf temperature of 25 °C except for measurements during heat stress denoted by * which were measured at 35°C.

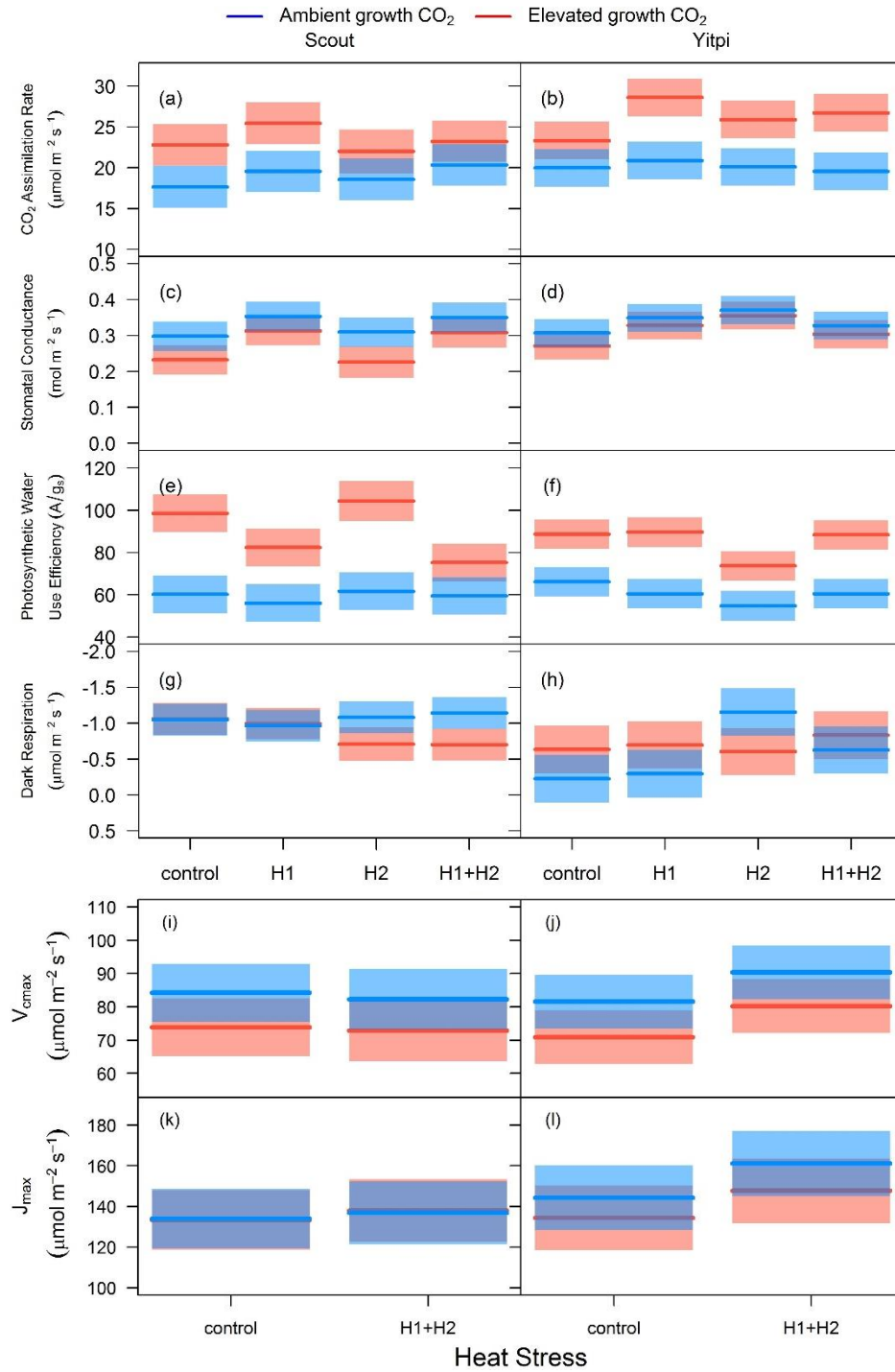


Figure 2.6 Response of photosynthetic parameters to eCO_2 and heat stress measured at growth CO_2 during anthesis (T3) in Scout and Yitpi

Means for CO_2 assimilation rate (a, b), stomatal conductance (c, d), photosynthetic water use efficiency (e, f), dark respiration (g, h), V_{max} (i, j) and J_{max} (k, l) plotted using visreg package in R. Lines indicate means and shaded region is 95% confidence interval. Ambient and elevated CO_2 are depicted in blue and red color, respectively. V_{max} and J_{max} were calculated using FvCB model fitted with measured R_d . Heat stress levels include plants not exposed to any heat stress (control), plants exposed to heat stress 1 (H1), plants exposed to heat stress 2 (H2) and plants exposed to both heat stresses (H1 + H2).

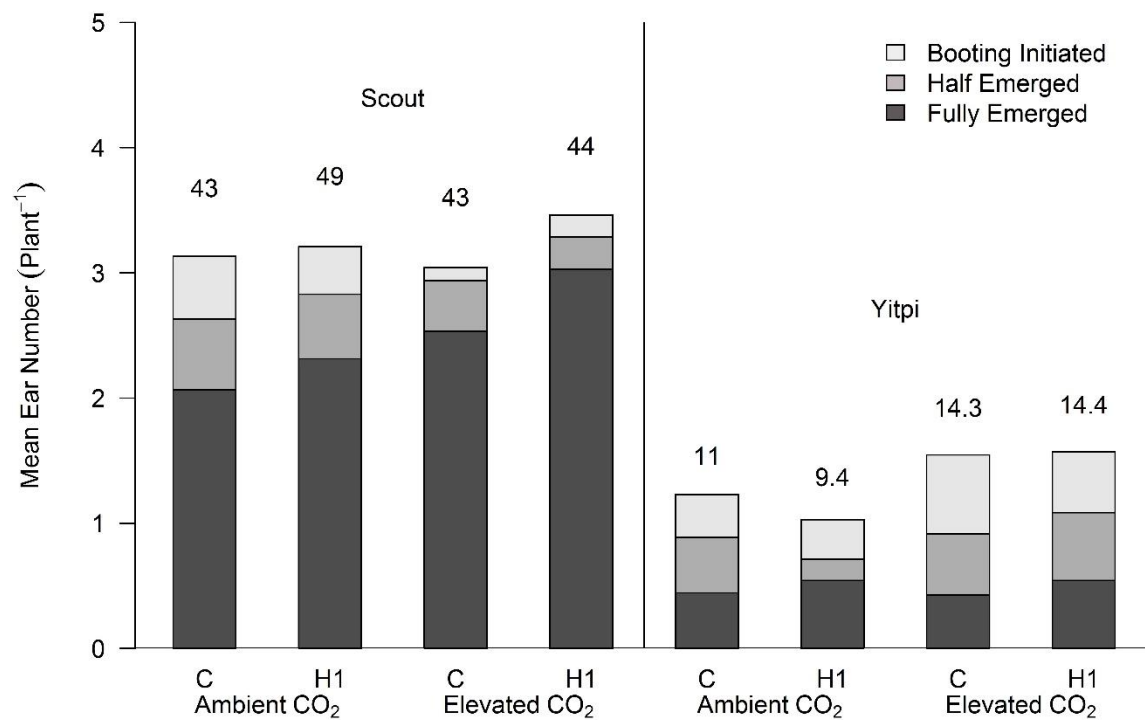


Figure 2.7 Booting and speed of development in Scout and Yitpi

Mean ear number counted at time point T2 for Scout and Yitpi grown at ambient and elevated CO₂ and exposed to heat stress 1 (H1). Number above each bar denotes the percentage of ears out of total number of tillers.

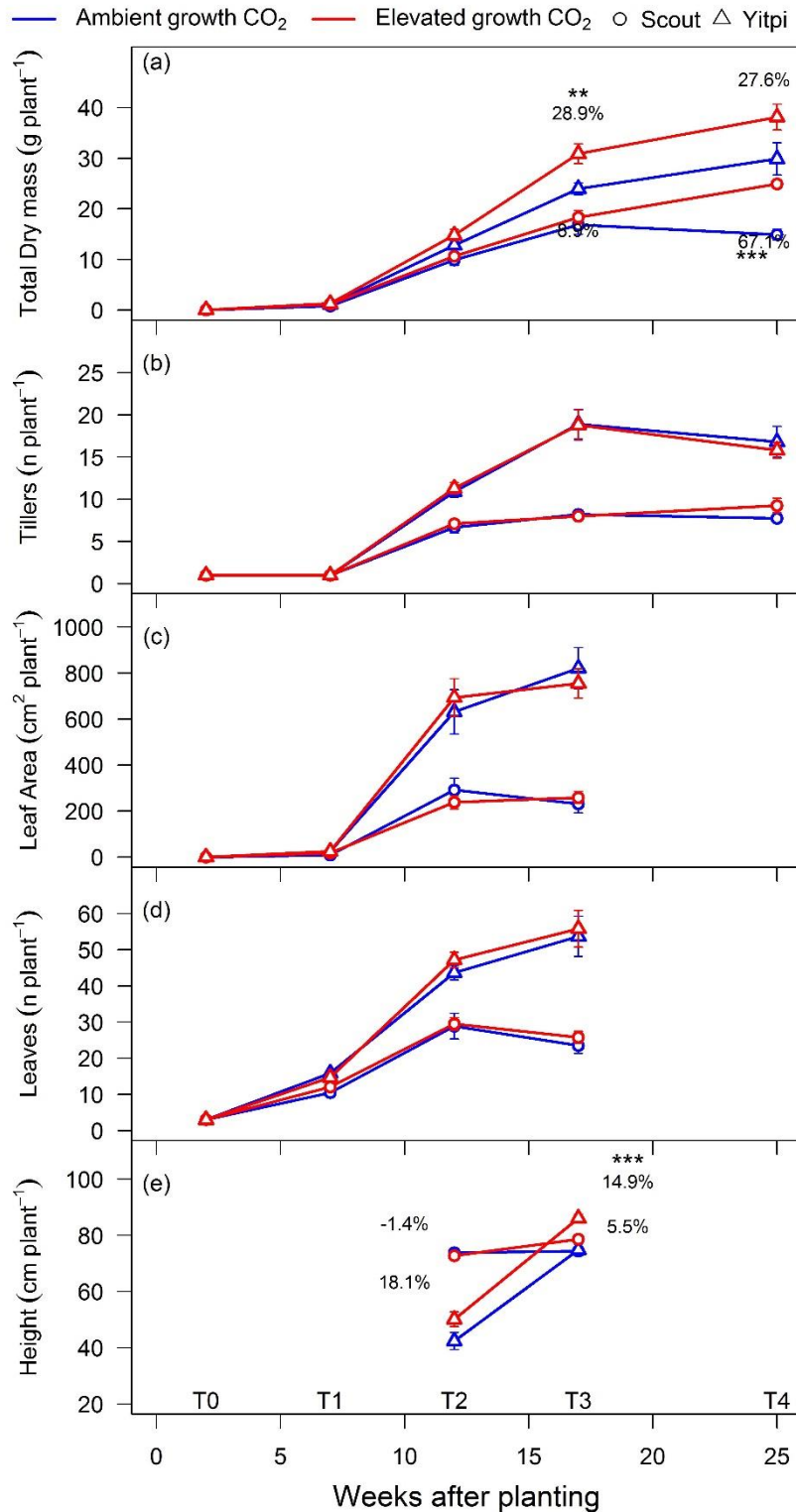


Figure 2.8 Plant growth and morphological traits response to elevated CO₂

Response of total dry mass (a), tillers or number of tillers (b), leaf area (c), leaf number (d) and height (e) to growth under eCO₂ at different time points across the life cycle of wheat lines Scout and Yitpi. Circles depict Scout and triangles depict Yitpi. Ambient and elevated CO₂ are depicted in blue and red color respectively. Statistical significance levels (t-test) for the growth condition within each line are shown and they are: * = $p < 0.05$; ** = $p < 0.01$; *** = $p < 0.001$.

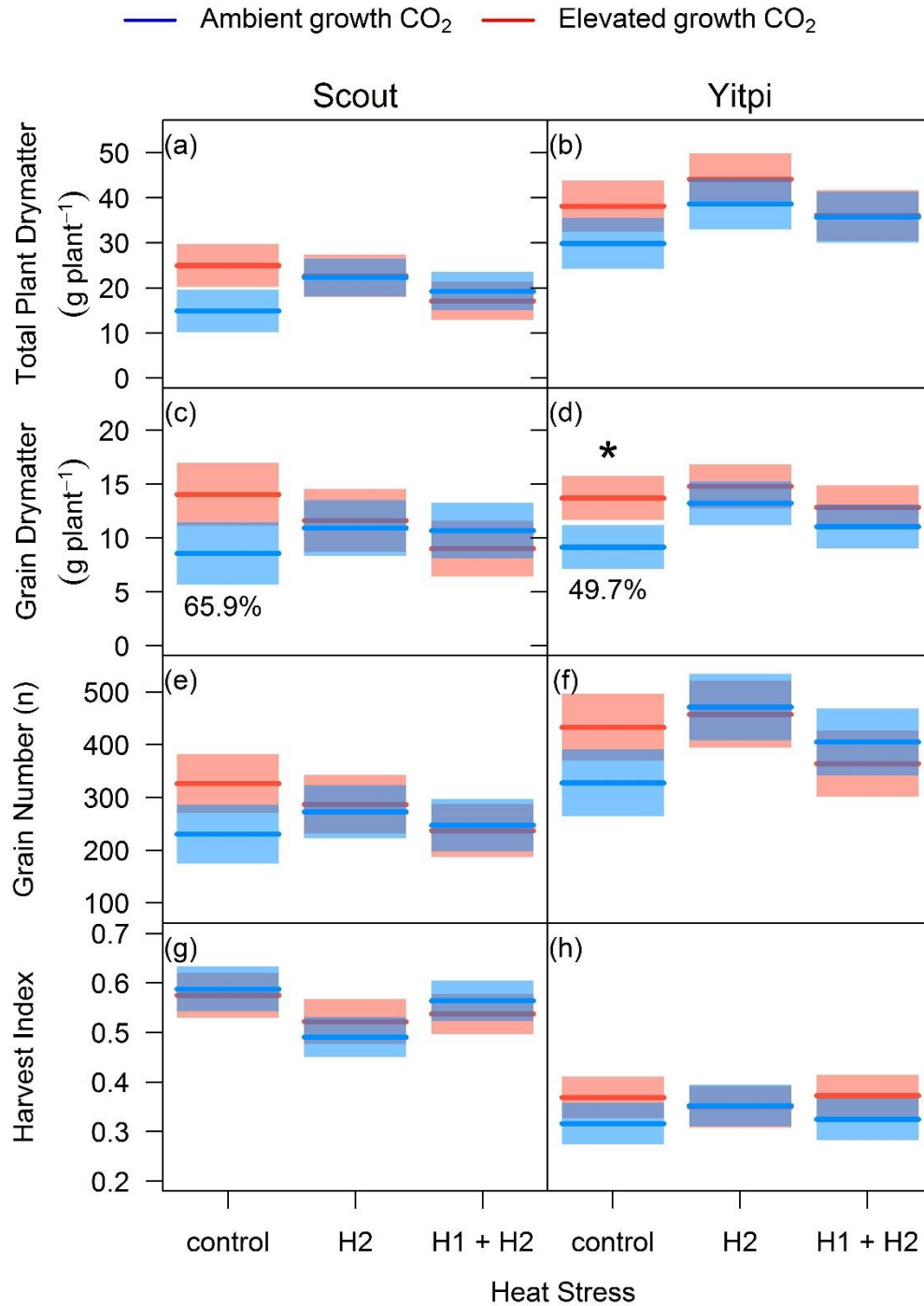


Figure 2.9 Response of total dry mass and grain yield to growth at eCO₂ and heat stress at final harvest (T4)

Means for total dry mass (a, b), grain dry mass (c, d), grain number (e, f) and harvest index (g, h) plotted using visreg package in R. Lines indicate means and shaded region is 95% confidence interval. Ambient and elevated CO₂ are depicted in blue and red color respectively. Heat stress levels include plants not exposed to any heat stress (control) and plants exposed to heat stress 2 (H2) or both heat stresses (H1 + H2). Left and right panels depict Scout and Yitpi, respectively.

Table S 2.1 Response of Scout gas exchange parameters to elevated CO₂ and heat stress

Summary of leaf gas exchange measured at two CO₂ (400 and 650 $\mu\text{l L}^{-1}$) partial pressures and 25°C leaf temperature for Scout grown at ambient CO₂ (aCO₂) or elevated CO₂ (eCO₂) and exposed to 1 and/or 2 heat stresses. Values are means \pm SE (n= 9-10). Heat stress treatments include plants not exposed to any heat stress (control), plants exposed to heat stress 1 (H1), heat stress 2 (H2) and both heat stresses (H1+H2).

Scout Parameters	Time Point	Growth CO ₂	Ambient				Elevated			
		Meas CO ₂ / Heat	Control	HS1	HS2	HS1_HS2	Control	HS1	HS2	HS1_HS2
A ($\mu\text{mol m}^{-2}\text{s}^{-1}$)	T1	400	24.6 \pm 0.99				22.9 \pm 0.49			
		650	31.4 \pm 1.2				30.8 \pm 0.67			
	T2	400	24.4 \pm 0.99	22.8 \pm 0.84			21.6 \pm 0.99	21.8 \pm 1.02		
		650	32.4 \pm 1.40	30.1 \pm 1.51			29.2 \pm 1.19	29 \pm 1.09		
	T3	400	17.6 \pm 0.59	19.5 \pm 0.64	18.6 \pm 1.04	14.8 \pm 1.12	17.1 \pm 1.14	19.1 \pm 0.96	14.8 \pm 1.12	17 \pm 1.29
		650	22.5 \pm 0.74	26.1 \pm 0.97	25 \pm 1.51	20.8 \pm 1.47	22.8 \pm 1.55	25.5 \pm 1.47	20.8 \pm 1.47	23.2 \pm 1.9
g_s ($\text{mol m}^{-2}\text{s}^{-1}$)	T1	400	0.35 \pm 0.02				0.28 \pm 0.01			
		650	0.36 \pm 0.04				0.25 \pm 0.01			
	T2	400	0.36 \pm 0.02	0.36 \pm 0.02			0.33 \pm 0.01	0.33 \pm 0.02		
		650	0.31 \pm 0.01	0.33 \pm 0.01			0.33 \pm 0.01	0.33 \pm 0.01		
	T3	400	0.29 \pm 0.01	0.35 \pm 0.01	0.31 \pm 0.02	0.20 \pm 0.02	0.23 \pm 0.01	0.34 \pm 0.02	0.20 \pm 0.02	0.31 \pm 0.02
		650	0.26 \pm 0.01	0.34 \pm 0.01	0.27 \pm 0.01	0.20 \pm 0.02	0.23 \pm 0.01	0.31 \pm 0.02	0.20 \pm 0.02	0.30 \pm 0.02
PWUE (A _{sat} /g _s) ($\mu\text{mol mol}^{-1}$)	T1	400	71.9 \pm 3.3				83.2 \pm 4.6			
		650	95.9 \pm 10				123.5 \pm 6.2			
	T2	400	67.6 \pm 3.7	65.2 \pm 3.9			65.3 \pm 2.2	66.6 \pm 3.2		
		650	106 \pm 9.5	90.6 \pm 5.4			89.7 \pm 4.0	86.9 \pm 2.3		
	T3	400	60.2 \pm 2.3	56.0 \pm 2.6	61.7 \pm 3.6	81.0 \pm 8.1	72.7 \pm 3.4	56.6 \pm 2.9	81.0 \pm 8.1	55.3 \pm 2.7
		650	90.5 \pm 6.3	77.4 \pm 5.2	92.9 \pm 4.3	125 \pm 23.0	98.6 \pm 4.2	82.4 \pm 3.9	125 \pm 23.0	75.3 \pm 3.6
Rd ($\mu\text{mol m}^{-2}\text{s}^{-1}$)	T1	400	-1.11 \pm 0.09				-1.19 \pm 0.08			
	T2	400	-0.54 \pm 0.16	-0.65 \pm 0.16			-0.76 \pm 0.09	-0.76 \pm 0.14		
	T3	400	-1.04 \pm 0.09	-0.96 \pm 0.08	-1.08 \pm 0.09	-0.71 \pm 0.15	-1.06 \pm 0.09	-0.99 \pm 0.16	-0.71 \pm 0.15	-0.70 \pm 0.05
Fv/Fm	T1	400	0.81 \pm 0.00				0.81 \pm 0.00			
	T2	400	0.81 \pm 0.01	0.80 \pm 0.01			0.80 \pm 0.01	0.82 \pm 0.00		
	T3	400	0.79 \pm 0.01	0.79 \pm 0.01	0.79 \pm 0.01	0.78 \pm 0.01	0.76 \pm 0.01	0.79 \pm 0.01	0.78 \pm 0.01	0.75 \pm 0.02
Fv'/Fm'	T1	400	0.48 \pm 0.01				0.49 \pm 0.01			
	T2	400	0.48 \pm 0.01	0.48 \pm 0.00		0.45 \pm 0.02	0.50 \pm 0.01	0.50 \pm 0.00		
	T3	400	0.50 \pm 0.01	0.50 \pm 0.01	0.49 \pm 0.01	0.52 \pm 0.01	0.52 \pm 0.02	0.50 \pm 0.01	0.45 \pm 0.02	0.48 \pm 0.02

Table S 2.2 Response of Yitpi gas exchange parameters to growth at elevated CO₂ and heat stress

Summary of leaf gas exchange measured at two CO₂ (400 and 650 $\mu\text{L L}^{-1}$) partial pressures and 25°C leaf temperature for Yitpi grown at ambient CO₂ (aCO₂) or elevated CO₂ (eCO₂) and exposed to 1 and/or 2 heat stresses. Values are means \pm SE (n= 9-10). Heat stress treatments include plants not exposed to any heat stress (control), plants exposed to heat stress 1 (H1), heat stress 2 (H2) and both heat stresses (H1+H2).

Yitpi Parameters	Time Point	Growth CO ₂ Meas CO ₂ / Heat	Ambient				Elevated			
			Control	HS1	HS2	HS1_HS2	Control	HS1	HS2	HS1_HS2
A ($\mu\text{mol m}^{-2} \text{s}^{-1}$)	T1	400	24.8 \pm 0.77				21 \pm 0.63			
		650	33.9 \pm 0.93				29.5 \pm 0.57			
	T2	400	26 \pm 0.63	24.2 \pm 1.01			23.4 \pm 1.12	22.9 \pm 1.49		
		650	36.2 \pm 0.84	34 \pm 1.30			31.9 \pm 1.99	32.5 \pm 2.18		
	T3	400	20 \pm 1.09	20.9 \pm 1.13	20.1 \pm 0.69	18.3 \pm 0.81	16.3 \pm 0.91	20.2 \pm 1.20	18.3 \pm 0.81	18.4 \pm 0.81
		650	27.6 \pm 1.64	29.2 \pm 1.46	27.7 \pm 0.92	25.9 \pm 1.36	23.3 \pm 1.22	28.6 \pm 1.49	25.9 \pm 1.36	26.7 \pm 1.14
g_s ($\text{mol m}^{-2} \text{s}^{-1}$)	T1	400	0.35 \pm 0.02				0.25 \pm 0.01			
		650	0.37 \pm 0.02				0.27 \pm 0.01			
	T2	400	0.38 \pm 0.02	0.33 \pm 0.02			0.34 \pm 0.01	0.31 \pm 0.01		
		650	0.35 \pm 0.01	0.31 \pm 0.01			0.29 \pm 0.01	0.30 \pm 0.02		
	T3	400	0.30 \pm 0.02	0.34 \pm 0.02	0.37 \pm 0.01	0.35 \pm 0.01	0.27 \pm 0.01	0.33 \pm 0.02	0.35 \pm 0.01	0.29 \pm 0.01
		650	0.29 \pm 0.02	0.34 \pm 0.01	0.38 \pm 0.01	0.35 \pm 0.01	0.27 \pm 0.01	0.32 \pm 0.02	0.35 \pm 0.01	0.30 \pm 0.01
PWUE (A_{sat}/g_s) ($\mu\text{mol mol}^{-1}$)	T1	400	72.4 \pm 3.8				84.1 \pm 5.1			
		650	93.1 \pm 5.6				110 \pm 3.6			
	T2	400	68.3 \pm 3.0	75.7 \pm 4.4			68.3 \pm 3.5	71.9 \pm 3.9		
		650	103 \pm 5.9	110 \pm 6.1			108 \pm 7.0	109 \pm 6.3		
	T3	400	66.1 \pm 2.3	60.5 \pm 2.2	54.8 \pm 1.9	52.0 \pm 1.8	61.1 \pm 2.3	61.1 \pm 2.5	52.0 \pm 1.8	62.7 \pm 2.9
		650	94.1 \pm 4.6	85.9 \pm 2.6	73.3 \pm 2.7	73.8 \pm 3.3	88.7 \pm 6.1	89.7 \pm 4.2	73.8 \pm 3.3	88.5 \pm 2.9
Rd ($\mu\text{mol m}^{-2} \text{s}^{-1}$)	T1	400	-1.15 \pm 0.59				-1.19 \pm			
	T2	400	-0.69 \pm 0.10	-1.24 \pm 0.14			-1.06 \pm	-1.06 \pm 0.08		
	T3	400	-0.23 \pm 0.28	-0.30 \pm 0.15	-1.16 \pm 0.13	-0.61 \pm 0.06	-0.63 \pm	-0.70 \pm 0.05	-0.61 \pm 0.06	-0.83 \pm 0.24
Fv/Fm	T1	400	0.81 \pm 0.00				0.81 \pm 0.00			
	T2	400	0.82 \pm 0.00	0.81 \pm 0.00			0.81 \pm 0.00	0.82 \pm 0.00		
	T3	400	0.81 \pm 0.00	0.77 \pm 0.01	0.81 \pm 0.00	0.81 \pm 0.01	0.80 \pm 0.00	0.81 \pm 0.00	0.81 \pm 0.01	0.81 \pm 0.00
Fv'/Fm'	T1	400	0.46 \pm 0.00				0.45 \pm 0.00			
	T2	400	0.48 \pm 0.00	0.47 \pm 0.01		0.50 \pm 0.01	0.48 \pm 0.01	0.48 \pm 0.01		
	T3	400	0.50 \pm 0.01	0.50 \pm 0.01	0.51 \pm 0.00	0.51 \pm 0.01	0.50 \pm 0.01	0.48 \pm 0.01	0.50 \pm 0.01	0.49 \pm 0.01

Table S 2.3 Response of other plant dry mass and morphological parameters to elevated CO₂ and HS

Summary of plant dry mass (DM) and morphological parameters measured at different time points for Scout and Yitpi grown at ambient CO₂ (aCO₂) or elevated CO₂ (eCO₂) and exposed to 1 and /or 2 heat stresses. Values are means \pm SE (n= 9-10). Heat stress levels include plants not exposed to any heat stress (control), plants exposed to heat stress 1 (H1), heat stress 2 (H2) and both heat stresses (H1+H2).

Parameter	Time Point	CO ₂ /	Scout				Yitpi			
			Control	H1	H2	H1 + H2	Control	H1	H2	H1 + H2
Leaf DM (g plant ⁻¹)	T1	aCO ₂	0.21 \pm 0.03				0.34 \pm 0.04			
		eCO ₂	0.34 \pm 0.03				0.40 \pm 0.04			
	T2	aCO ₂	1.6 \pm 0.2	1.3 \pm 0.2			4.3 \pm 0.2	4.3 \pm 0.4		
		eCO ₂	1.6 \pm 0.1	1.7 \pm 0.1			4.5 \pm 0.1	4.7 \pm 0.2		
	T3	aCO ₂	1.4 \pm 0.2	1.1 \pm 0.1	1.2 \pm 0.2	1.5 \pm 0.2	4.3 \pm 0.3	4.8 \pm 0.3	3.9 \pm 0.4	4.4 \pm 0.3
		eCO ₂	1.5 \pm 0.1	2.0 \pm 0.2	1.6 \pm 0.2	1.8 \pm 0.2	4.7 \pm 0.5	4.7 \pm 0.4	5.4 \pm 0.3	4.9 \pm 0.2
Stem DM (g plant ⁻¹)	T1	aCO ₂	0.21 \pm 0.03				0.34 \pm 0.04			
		eCO ₂	0.13 \pm 0.02				0.18 \pm 0.01			
	T2	aCO ₂	7.2 \pm 0.6	5.8 \pm 0.5			5.8 \pm 0.5	6.6 \pm 0.7		
		eCO ₂	8.0 \pm 0.4	7.1 \pm 0.2			8.0 \pm 0.4	7.4 \pm 0.7		
	T3	aCO ₂	14.5 \pm 1.5	10.6 \pm 0.9	12.2 \pm 1.8	13.9 \pm 1.6	17.8 \pm 1.2	19.0 \pm 1.1	18.9 \pm 1.2	16.7 \pm 1.3
		eCO ₂	16.0 \pm 1.1	18.1 \pm 1.1	15.6 \pm 1.6	17.3 \pm 1.7	24.3 \pm 1.6	23.7 \pm 1.2	24.1 \pm 0.7	21.1 \pm 1.4
Shoot DM (g plant ⁻¹)	T1	aCO ₂	0.31 \pm 0.03				0.50 \pm 0.05			
		eCO ₂	0.48 \pm 0.04				0.59 \pm 0.06			
	T2	aCO ₂	8.8 \pm 0.9	7.1 \pm 0.7			10.2 \pm 0.7	11.0 \pm 0.8		
		eCO ₂	9.7 \pm 0.4	8.8 \pm 0.3			12.5 \pm 0.9	12.1 \pm 0.9		
	T3	aCO ₂	15.9 \pm 1.7	11.7 \pm 1.0	13.4 \pm 2.0	15.4 \pm 1.9	22.2 \pm 1.2	21.5 \pm 2.5	22.8 \pm 1.1	21.1 \pm 1.0
		eCO ₂	17.6 \pm 1.2	20.1 \pm 1.3	17.2 \pm 1.1	19.1 \pm 1.9	29.0 \pm 1.9	28.5 \pm 1.2	29.5 \pm 0.7	26.1 \pm 1.5
	T4	aCO ₂	14.5 \pm 1.1		21.8 \pm 3.4	18.7 \pm 2.6	28.8 \pm 2.9		37.6 \pm 2.8	34.2 \pm 1.5
		eCO ₂	24.3 \pm 0.8		22.1 \pm 1.1	16.7 \pm 0.7	37.1 \pm 2.3		42.8 \pm 2.0	34.7 \pm 3.2
Root DM (g plant ⁻¹)	T1	aCO ₂	0.5 \pm 0.1				0.6 \pm 0.1			
		eCO ₂	0.6 \pm 0.1				0.7 \pm 0.1			
	T2	aCO ₂	1.1 \pm 0.23	0.7 \pm 0.12			2.5 \pm 0.37	2.5 \pm 0.19		
		eCO ₂	0.9 \pm 0.09	0.9 \pm 0.06			2.2 \pm 0.24	2.7 \pm 0.39		
	T3	aCO ₂	0.8 \pm 0.18	0.5 \pm 0.07	0.6 \pm 0.16	0.6 \pm 0.14	1.7 \pm 0.13	2.1 \pm 0.32	1.5 \pm 0.13	1.9 \pm 0.24
		eCO ₂	0.7 \pm 0.09	0.9 \pm 0.13	0.8 \pm 0.22	0.8 \pm 0.16	1.8 \pm 0.12	2.6 \pm 0.39	2.1 \pm 0.23	2.8 \pm 0.44
	T4	aCO ₂	0.3 \pm 0.07		0.4 \pm 0.08	0.5 \pm 0.13	1 \pm 0.32		1.0 \pm 0.17	1.4 \pm 0.28
		eCO ₂	0.4 \pm 0.09		0.4 \pm 0.10	0.3 \pm 0.12	1.0 \pm 0.19		1.2 \pm 0.29	1.3 \pm 0.29
Leaf Area (cm ² plant ⁻¹)	T1	aCO ₂	8.7 \pm 2.3				24.9 \pm 6.6			
		eCO ₂	18.6 \pm 3.8				24.9 \pm 6.5			
	T2	aCO ₂	291 \pm 51	159 \pm 24			630 \pm 96	560 \pm 18		
		eCO ₂	237 \pm 28	204 \pm 20			693 \pm 81	648 \pm 25		
	T3	aCO ₂	231 \pm 39	170 \pm 29	184 \pm 47	240 \pm 51	820 \pm 89	981 \pm 98	754 \pm 114	902 \pm 89
		eCO ₂	258 \pm 26	321 \pm 44	248 \pm 52	287 \pm 45	754 \pm 63	870 \pm 96	1015 \pm 51	910 \pm 50

Leaf Mass Area (g m ⁻²)	T1	aCO ₂	333 ± 98				239 ± 62			
		eCO ₂	316 ± 87				269 ± 56			
	T2	aCO ₂	47 ± 12 130 ± 61				81 ± 1 79 ± 9			
		eCO ₂	75 ± 7 96 ± 17				73 ± 7 72 ± 3			
	T3	aCO ₂	64 ± 2 68 ± 3 76 ± 06 79 ± 10				54 ± 2 51 ± 2 54 ± 2 50 ± 1			
		eCO ₂	62 ± 2 64 ± 2 75 ± 11 69 ± 03				62 ± 0.3 56 ± 3 53 ± 1 55 ± 1			
Leaf Size (cm ² plant ⁻¹)	T1	aCO ₂	0.9 ± 0.2				1.5 ± 0.3			
		eCO ₂	1.6 ± 0.3				1.6 ± 0.3			
	T2	aCO ₂	9.2 ± 1.3 7.0 ± 1.0				15.0 ± 2.0 12.3 ± 0.7			
		eCO ₂	8.1 ± 0.8 7.2 ± 0.8				14.7 ± 1.7 14.0 ± 0.8			
	T3	aCO ₂	9.4 ± 0.9 7.6 ± 0.6 8.1 ± 1.3 8.2 ± 1.1				15.2 ± 0.6 16.0 ± 1.2 13.9 ± 1.0 16.4 ± 1.2			
		eCO ₂	10.2 ± 1.0 8.3 ± 0.5 9.5 ± 1.2 8. ± 1.0				14.1 ± 1.1 15.3 ± 0.8 16.3 ± 0.7 16.2 ± 1.3			
Leaf Number (plant ⁻¹)	T1	aCO ₂	10.4 ± 0.9				15.9 ± 0.5			
		eCO ₂	12.1 ± 0.9				14.7 ± 0.9			
	T2	aCO ₂	28.8 ± 3.5 25.8 ± 3.4				43.6 ± 2.0 46.3 ± 2.4			
		eCO ₂	29.5 ± 1.7 29.3 ± 2.4				47.2 ± 2.1 47.6 ± 3.1			
	T3	aCO ₂	23.5 ± 2.1 21.3 ± 1.9 20.2 ± 1.7 26.0 ± 2.9				53.7 ± 5.5 60.8 ± 3.6 53.6 ± 6.5 54.4 ± 3.0			
		eCO ₂	25.8 ± 1.6 37.4 ± 3.43 24.1 ± 2.6 31.8 ± 2.4				55.8 ± 5.0 57.5 ± 5.9 62.5 ± 3.1 58.1 ± 3.9			
Tiller Number (plant ⁻¹)	T2	aCO ₂	6.7 ± 0.7 6.8 ± 0.7				10.8 ± 0.6 11.0 ± 0.6			
		eCO ₂	7.1 ± 0.4 8.1 ± 0.3				11.3 ± 0.6 11.5 ± 0.4			
	T3	aCO ₂	8.2 ± 0.3 6.9 ± 0.5 7.2 ± 0.5 7.7 ± 1.1				18.9 ± 1.7 20.2 ± 0.9 20.1 ± 1.5 19.3 ± 1.3			
		eCO ₂	8.0 ± 0.5 11.5 ± 1.0 7.5 ± 0.5 10.5 ± 0.8				18.8 ± 1.7 19.6 ± 1.0 20.0 ± 1.0 18.8 ± 1.2			
	T4	aCO ₂	7.2 ± 0.4 8.8 ± 0.8 8.4 ± 0.5				16.8 ± 1.8 16.2 ± 1.1 18.2 ± 2.4			
		eCO ₂	8.6 ± 0.9 8.4 ± 0.6 9.2 ± 0.3				15.8 ± 0.9 17.6 ± 0.7 13.6 ± 0.9			
Ear Number (plant ⁻¹)	T2	aCO ₂	3.2 ± 0.2 3.7 ± 0.2				0.6 ± 0.1 1.7 ± 0.3			
		eCO ₂	3 ± 0.1 3.5 ± 0.2				1.7 ± 0.3 2 ± 0.2			
	T3	aCO ₂	8.2 ± 0.3 6.9 ± 0.5 7.2 ± 0.5 8.5 ± 0.8				10.2 ± 0.7 10.3 ± 0.4 11.6 ± 0.7 10.9 ± 0.7			
		eCO ₂	7.9 ± 0.5 11.5 ± 1.0 8 ± 0.6 10.3 ± 0.8				12.8 ± 0.6 12.3 ± 0.9 12.5 ± 0.5 11.4 ± 0.7			
	T4	aCO ₂	7.7 ± 0.2 8.8 ± 0.8 8.4 ± 0.6				14.8 ± 1.2 15.8 ± 1 15.2 ± 1			
		eCO ₂	9.2 ± 0.8 9 ± 0.7 9 ± 0.3				15 ± 1 16.6 ± 1.1 13.4 ± 1			
Ear No / Tiller No (ratio)	T2	aCO ₂	0.50 ± 0.04 0.59 ± 0.05				0.07 ± 0.02 0.16 ± 0.03			
		eCO ₂	0.44 ± 0.04 0.43 ± 0.02				0.16 ± 0.04 0.17 ± 0.03			
	T3	aCO ₂	1 ± 0 1 ± 0 1 ± 0 1 ± 0				0.58 ± 0.06 0.52 ± 0.03 0.56 ± 0.04 0.58 ± 0.05			
		eCO ₂	0.99 ± 0.01 1 ± 0 1 ± 0 0.98 ± 0.02				0.72 ± 0.05 0.63 ± 0.04 0.63 ± 0.03 0.62 ± 0.04			
	T4	aCO ₂	1 ± 0 1 ± 0 1 ± 0 1 ± 0.04				0.89 ± 0.05 0.98 ± 0.01 0.86 ± 0.06			
		eCO ₂	1 ± 0 1 ± 0.04 0.98 ± 0.02				0.95 ± 0.03 0.94 ± 0.03 0.98 ± 0.02			

Table S 2.4 Summary of plant nitrogen content parameters

Summary of nitrogen content determined from flag leaf measured for gas exchange from Scout and Yitpi grown at ambient or elevated CO₂ and exposed to 1 and /or 2 heat stresses (HS). Values are means \pm SE (n= 9-10). Heat stress levels include plants not exposed to any heat stress (control), plants exposed to only HS 1 (H1), HS 2 (H2) and both HS (H1+H2).

Parameter	Time Point	Line Heat Stress CO ₂	Scout				Yitpi			
			Control	H1	H2	H1 + H2	Control	H1	H2	H1 + H2
Grain N (mg g ⁻¹)	T4	aCO ₂	31 \pm 1			31 \pm 0	39 \pm 0			35 \pm 1
		eCO ₂	31 \pm 1			32 \pm 0	32 \pm 0			35 \pm 1
Flag Leaf LMA (g m ⁻²)	T2	aCO ₂	32 \pm 6	40 \pm 1			42 \pm 2	43 \pm 3		
		eCO ₂	42 \pm 2	41 \pm 1			42 \pm 2	42 \pm 2		
	T3	aCO ₂	33 \pm 1	47 \pm 4	37 \pm 4	35 \pm 3	34 \pm 1	39 \pm 9	29 \pm 6	37 \pm 2
		eCO ₂	32 \pm 1	37 \pm 2	36 \pm 3	32 \pm 4	34 \pm 1	38 \pm 2	37 \pm 1	37 \pm 2
Flag Leaf N (mg g ⁻¹)	T2	aCO ₂	42 \pm 1	37 \pm 1			41 \pm 2	37 \pm 2		
		eCO ₂	39 \pm 1	37 \pm 1			37 \pm 2	36 \pm 1		
	T3	aCO ₂	29 \pm 2	31 \pm 1	33 \pm 2	32 \pm 2	30 \pm 1	27 \pm 1	32 \pm 2	30 \pm 1
		eCO ₂	33 \pm 2	35 \pm 1	30 \pm 2	32 \pm 1	26 \pm 2	29 \pm 1	30 \pm 1	27 \pm 1
Flag Leaf Narea (mmol m ⁻²)	T2	aCO ₂	97 \pm 20	108 \pm 4			125 \pm 7	114 \pm 3		
		eCO ₂	121 \pm 8	112 \pm 4			113 \pm 7	109 \pm 5		
	T3	aCO ₂	70 \pm 7	104 \pm 5	87 \pm 12	82 \pm 12	74 \pm 4	71 \pm 16	63 \pm 13	81 \pm 6
		eCO ₂	76 \pm 6	92 \pm 5	79 \pm 11	73 \pm 6	65 \pm 8	80 \pm 5	79 \pm 3	71 \pm 5
Leaf N (mg g ⁻¹)	T1	aCO ₂	48 \pm 2			35 \pm 3	4.9 \pm 0.16			
		eCO ₂	53 \pm 1				5.3 \pm 0.1			
	T3	aCO ₂	35 \pm 1			31 \pm 3	34 \pm 1			33 \pm 1
		eCO ₂	36 \pm 1			36 \pm 2	28 \pm 1			30 \pm 1
	T4	aCO ₂	9.6 \pm 1			10 \pm 1	7.4 \pm 0.5			8 \pm 0.4
		eCO ₂	12 \pm 1			11 \pm 1	7.5 \pm 0.7			6 \pm 0.1
Stem N (mg g ⁻¹)	T1	aCO ₂	31 \pm 2				39 \pm 2			
		eCO ₂	38 \pm 4				39 \pm 1			
	T3	aCO ₂	11 \pm 1			13 \pm 1	14 \pm 3			23 \pm 1
		eCO ₂	11 \pm 1			16 \pm 1	11 \pm 1			16 \pm 1
	T4	aCO ₂	9.7 \pm 1.3			6.8 \pm 1.6	6 \pm 1			5.6 \pm 2
		eCO ₂	10.1 \pm 1			11 \pm 2	3 \pm 0.3			6.7 \pm 2
Root N (mg g ⁻¹)	T1	aCO ₂	12 \pm 1				15 \pm 1			
		eCO ₂	14 \pm 1				12 \pm 0			
	T3	aCO ₂	15 \pm 0			14 \pm 0	14 \pm 1			17 \pm 1
		eCO ₂	17 \pm 2			16 \pm 0	12 \pm 1			11 \pm 0
	T4	aCO ₂	11 \pm 1			14 \pm 0	15 \pm 0			13 \pm 1
		eCO ₂	13 \pm 1			14 \pm 1	10 \pm 1			11 \pm 1

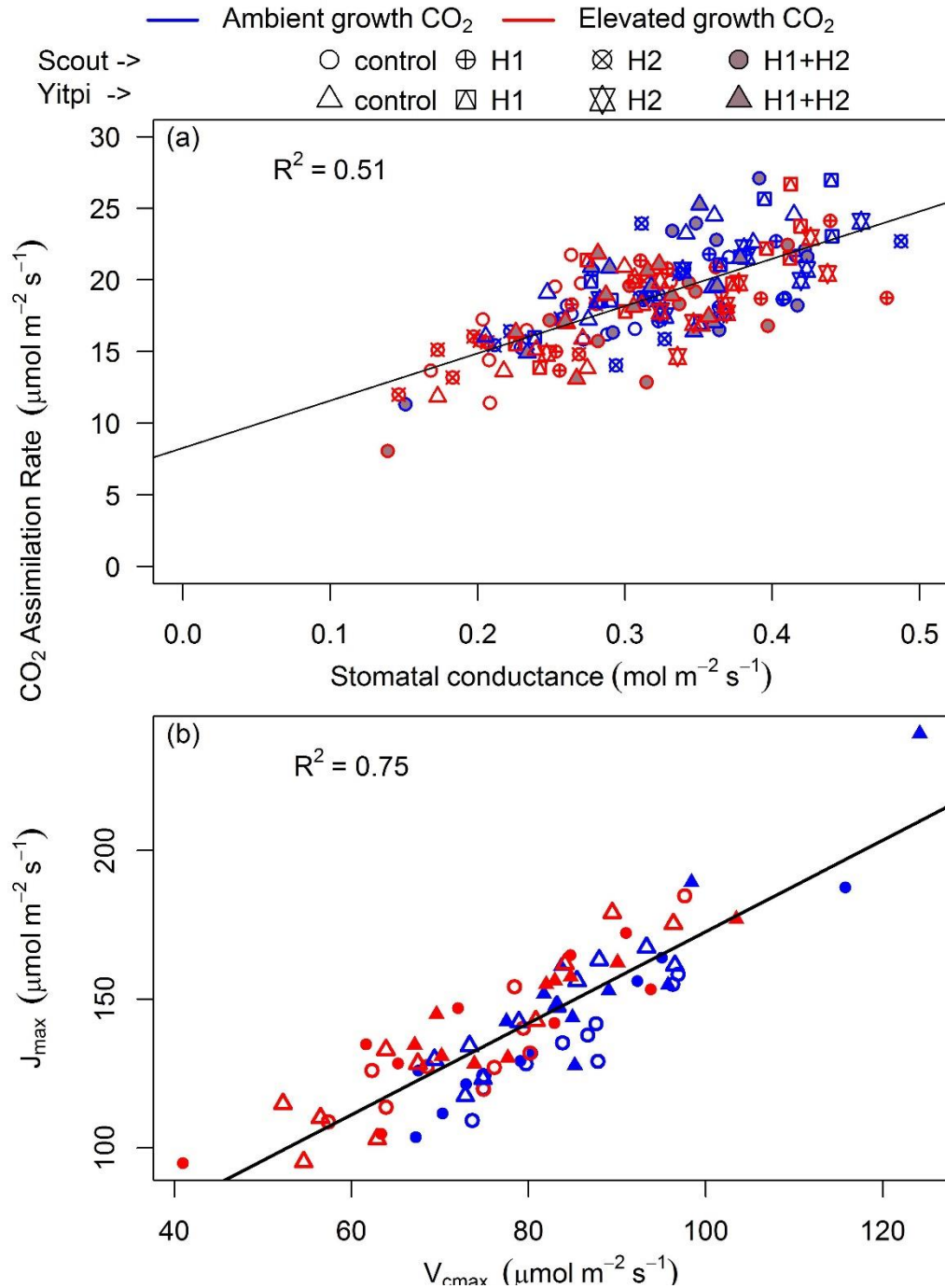


Figure S 2.1 Relationships between gas exchange parameters at T3

CO₂ assimilation rate plotted as a function of stomatal conductance measured at common (400 $\mu\text{l L}^{-1}$) CO₂ (a) and J_{max} plotted as a function of V_{cmax} (b). Scout and Yitpi are depicted using circles and triangles respectively. Ambient and elevated CO₂ are depicted in blue and red, respectively. Control and heat stressed plants depicted using open and closed symbols.

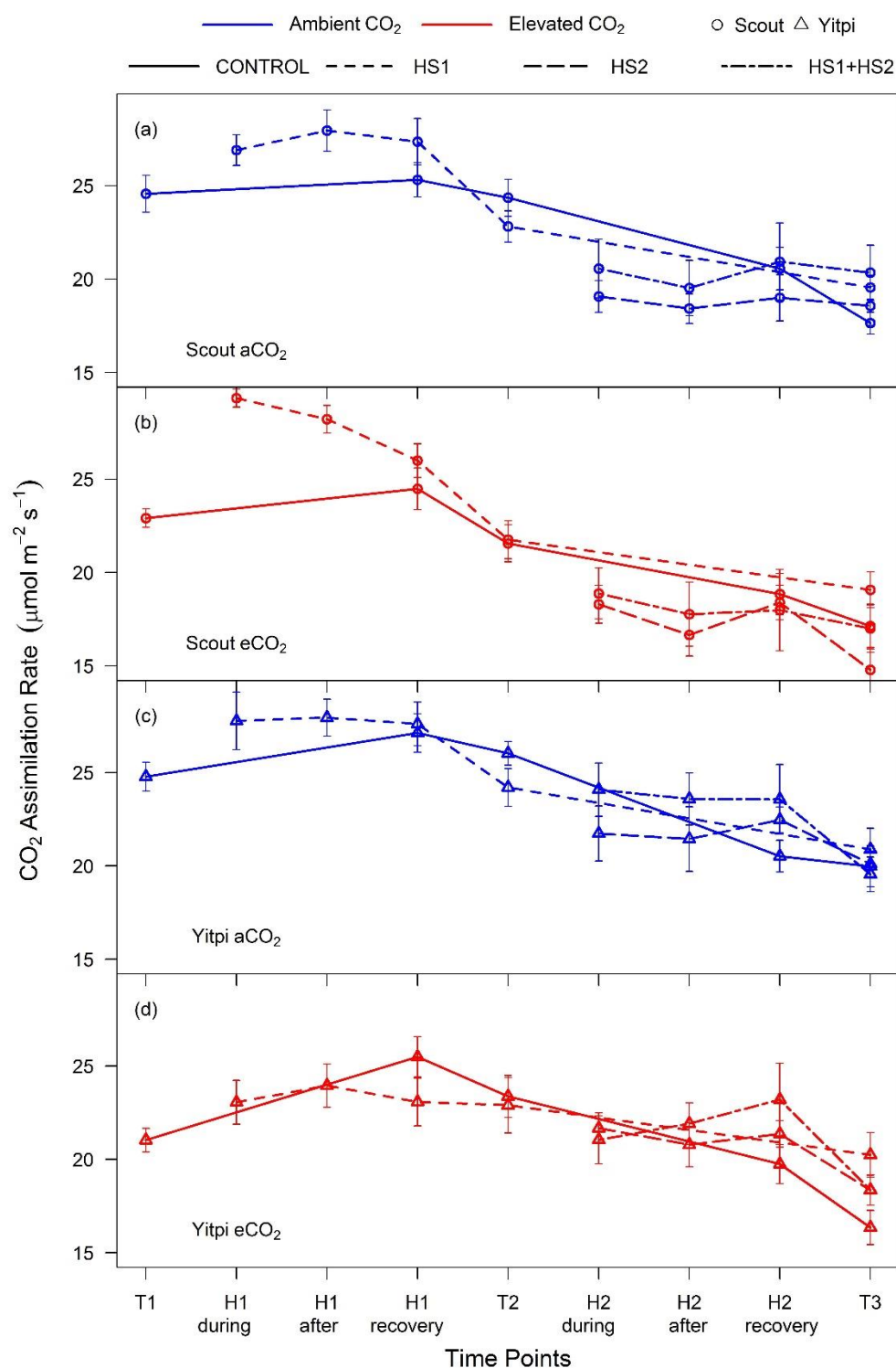


Figure S 2.2 Photosynthetic response to growth at eCO₂ and heat stresses (H1 and H2)

CO₂ assimilation rates measured at common CO₂ (400 $\mu\text{L L}^{-1}$) and leaf temperature (25°C) in aCO₂ grown Scout (a), eCO₂ grown Scout (b), aCO₂ grown Yitpi and eCO₂ grown Yitpi (d). Ambient and eCO₂ CO₂ grown plants are depicted in blue and red, respectively. Measurements were performed during, after, at recovery stage of heat stress and at time points T1, T2 and T3.

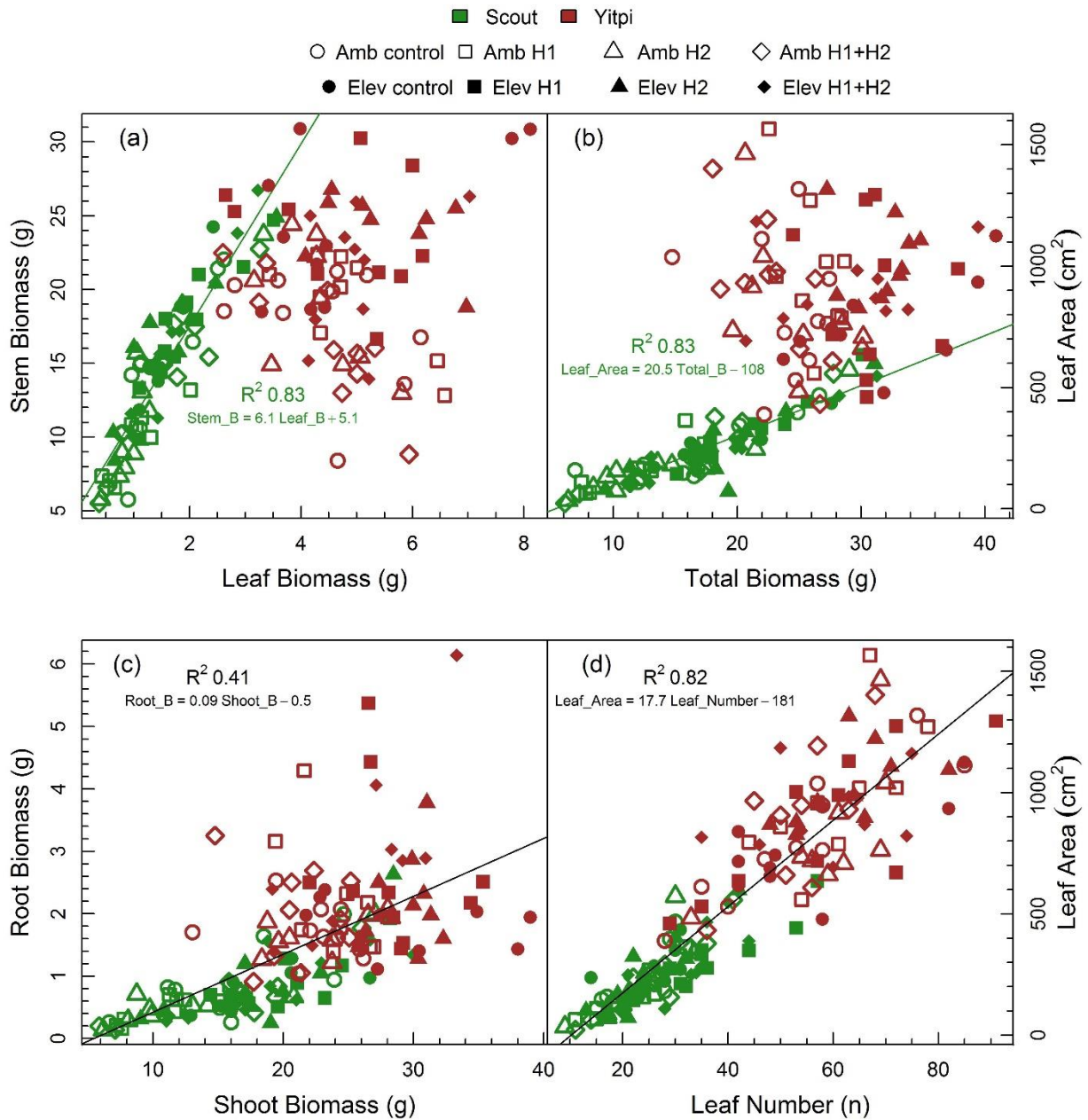


Figure S 2.3 Relationship between dry mass and morphological parameters measured at anthesis (T3)

Linear regression plotted for relationships between stem dry mass and leaf dry mass (a), total dry mass and leaf area (b), root dry mass and shoot (stem + leaf) dry mass (c) and leaf number and leaf area (d). Scout and Yitpi are depicted using green and brown color respectively. Ambient CO₂ and eCO₂ grown plants are depicted with open closed symbols, respectively. Heat stress levels are depicted in different shapes and include plants not exposed to any heat stress (control), plants exposed to heat stress 1 (H1), plants exposed to heat stress 2 (H2) and plants exposed to both the heat stresses (H1+H2).

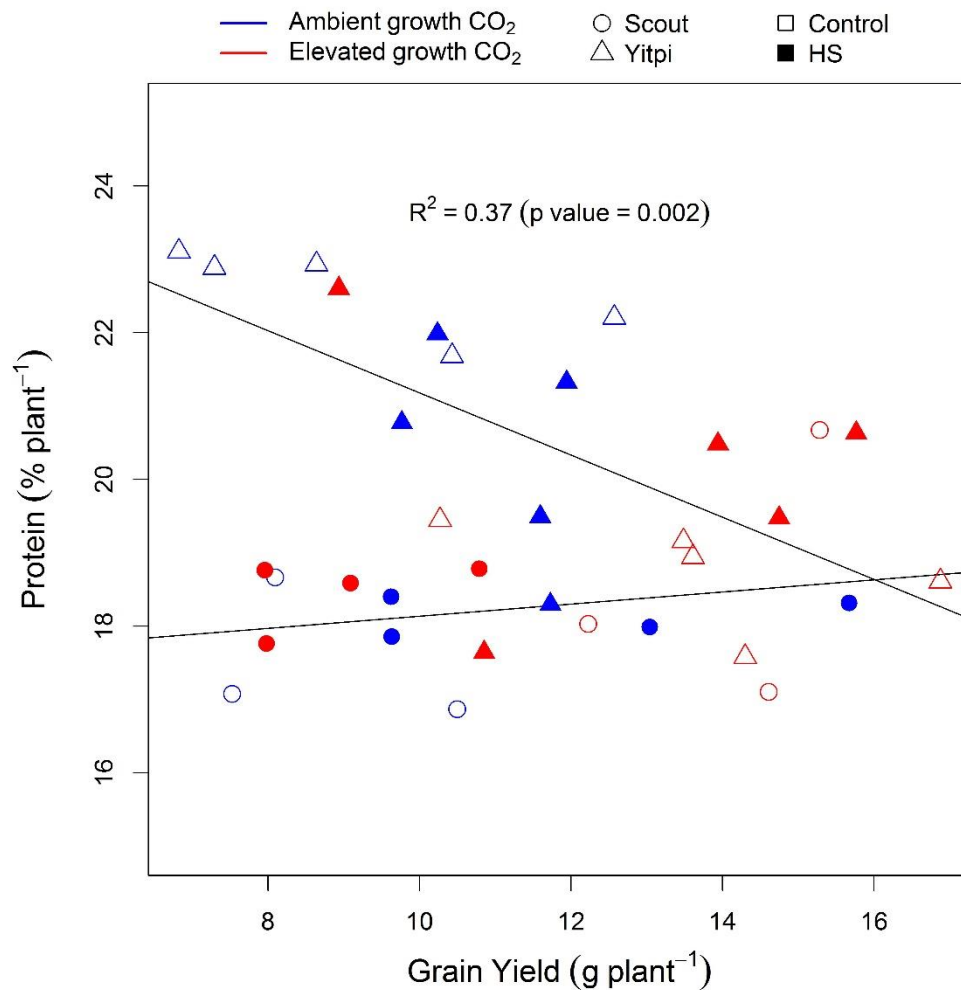


Figure S 2.4 Relationship between grain protein content and yield

Grain protein plotted as a function of yield measured at final harvest. Scout and Yitpi are depicted using circles and triangles respectively. Ambient and elevated CO₂ are depicted in blue and red, respectively. Control and heat stressed plants depicted using open and closed symbols.

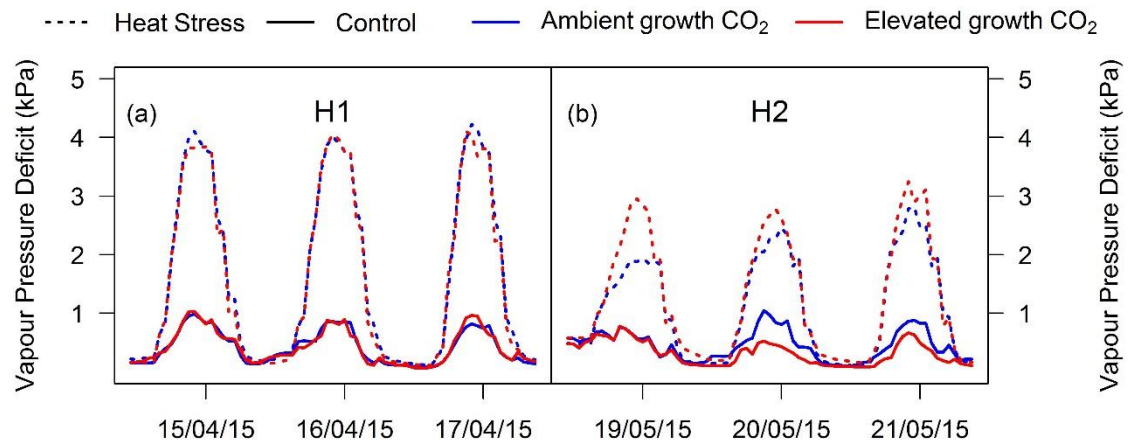


Figure S 2.5 Vapour pressure deficit (VPD) plotted over time during HS1 and HS2

Vapour pressure deficit (VPD) during heat stresses H1 (a) and H2 (b), the solid lines represent [LIST OF FIGURES](#) control temperature and dotted lines represent the heat stress temperature. Ambient and elevated CO₂ are depicted in blue and red color, respectively.

CHAPTER 3

ELEVATED CO₂ REDUCES IMPACT OF HEAT STRESS ON WHEAT PHYSIOLOGY BUT NOT ON GRAIN YIELD

Abstract

Rising atmospheric CO₂ concentration is expected to boost photosynthesis and consequently the productivity and yield of crops. However, the climate is expected to have more frequent heat stress (HS), droughts and floods that negatively affects crop growth and yield. Hence, understanding interactive effects of climate change variables including elevated CO₂ (eCO₂) and HS on the yield of key crops such as wheat is critically important to develop cultivars ready for future climate. We grew the commercial wheat line Scout under well-watered and fertilized conditions at 22/15°C (day/night average) and ambient (419 µl L⁻¹, day average) or elevated 654 µl L⁻¹, day average) CO₂ in the glasshouse. Plants were exposed to HS (40/24°C day/night average) at the flowering stage for five consecutive days. We measured leaf gas exchange and chlorophyll fluorescence before, during, after and at the recovery stage of the HS cycle along with the instantaneous temperature response of photosynthesis in both ambient CO₂ (aCO₂) and eCO₂ grown plants. We also measured biomass before HS, at the recovery stage after HS and both biomass and grain yield at maturity. Growth at eCO₂ led to a downregulation of photosynthetic capacity in Scout indicated by reduced (-12%) CO₂ assimilation rates (A_{sat}) measured at common CO₂ (400 µl L⁻¹) and leaf temperature (25°C) in control plants not exposed to HS. HS reduced A_{sat} (-42%) in aCO₂ but not in eCO₂ grown plants. Growth stimulation by eCO₂ protected plants by increasing electron transport capacity under HS, ultimately avoiding the damage to the maximum efficiency of photosystem II. Elevated CO₂ stimulated biomass (+35%) and grain yield (+30%). HS equally reduced grain yield in both aCO₂ (-38%) and eCO₂ (-41%) grown plants but had no effect on biomass at final harvest due to stimulated tillering. In summary, while eCO₂ protected wheat photosynthesis and biomass against HS damage at the flowering stage via increased J_{max} , grain yield was reduced by HS in both CO₂ treatments due to grain abortion, indicating an important interaction between the two components of climate change.

Key words: Wheat, photosynthesis, elevated CO₂, heat stress, climate change

3.1 Introduction

Rising atmospheric CO₂ concentration is the primary cause of increasing global mean surface temperatures. Along with rising mean surface temperatures, increasing frequency, duration and intensity of abrupt temperature increases (heat waves) are also expected. The future extreme climate conditions pose a big threat to the globally important wheat crop (Asseng et al., 2015). The interactive effects of eCO₂ and heat stress (HS) have been tested in a limited number of studies that showed variable effects due to variability in growth conditions and location (Fitzgerald et al., 2016; Wang et al., 2008, 2011). The FACE study by Fitzgerald et al., (2016) involved similar cultivars, however the HS was natural heat wave rather than a experimentally imposed treatment and highlighted need of experimentally imposed HS to investigate interactive effects of eCO₂ on growth and productivity.

Crop models are one of the important tools to assess the impact of climate change on crop productivity. However, current crop models lack the ability to consider interactive effects of elevated CO₂ (eCO₂) and environmental stresses. Crop models can be improved by incorporating mechanistic methods to account for the interactive effects of eCO₂ and stresses. Photosynthesis is a vital process affected by eCO₂ and temperature and thus may provide a mechanistic approach to improving the predictability of crop models (Wu et al., 2016, 2017; Yin and Struik, 2009).

Photosynthesis is highly sensitive to temperature and operates within a physiological range of 0 to 45°C with a thermal optimum determined by the genotype and growth conditions (Berry and Bjorkman, 1980). The C₃ wheat plant has a photosynthetic thermal optimum varying between 15 to 35°C depending on growth temperature with maximum photosynthesis observed in leaves developed at 25°C (Yamasaki et al., 2002). According to the C₃ model, photosynthesis is the minimum of maximal rate of RuBP carboxylation (V_{cmax}), maximal rate of RuBP regeneration or electron transport (J_{max}) and triose phosphate utilization (TPU) limitation (Farquhar et al., 1980; Sharkey, 1985). Photosynthesis is mainly limited by V_{cmax} at low CO₂ across a wide range of temperatures. At eCO₂, the photosynthesis limitation shifts to TPU at suboptimal temperatures and either J_{max} or Rubisco activation above the optimum temperatures (Sage and Kubien, 2007).

Heat stress is defined as the temperature increase beyond a threshold level causing irreversible damage to plant growth and development (Wahid et al., 2007). HS can inhibit both light and

dark processes of photosynthesis via numerous mechanisms (Farooq et al., 2011). Temperature above 45°C can damage photosystem II (PSII) (Berry and Bjorkman, 1980); while moderate increases can reduce photosynthetic rates by increasing photosystem I (PSI) electron flow (Haque et al., 2014). High temperatures reduce photosynthesis by increasing photorespiration and decreasing Rubisco activation (Eckardt and Portis, 1997). V_{max} is not negatively affected by high temperature but J_{max} decreases above optimal temperatures. HS can also inhibit photosynthesis by irreversibly damaging cells and decreasing chlorophyll content (Stone and Nicolas, 1998; Wardlaw et al., 2002; Stone and Nicolas, 1996). Plants may acclimate and acquire thermo-tolerance to HS lasting for one to a few days, by activating stress response mechanisms and expressing heat shock proteins to repair the damage caused by HS. However, the acquired thermo-tolerance is cost intensive and compromises plant growth and development (Wahid et al., 2007).

Elevated CO₂ stimulates photosynthesis by increasing carboxylation and suppressing oxygenation of Rubisco (Leakey et al., 2009). The effect of eCO₂ may become greater at high temperatures where photorespiration is high (Long, 1991). Also, eCO₂ increases the temperature optimum of photosynthesis and photosynthesis dependence on temperature (Alonso et al., 2008; Borjigidai et al., 2006; Ghannoum et al., 2010). At eCO₂, the response of photosynthesis to temperature moves from TPU limitation to electron transport (J_{max}) and Rubisco activation limitation (Sage and Kubien, 2007). Therefore the temperature optimum of photosynthesis will reflect that of J_{max} in non TPU limited plants grown at eCO₂. I predict that eCO₂ will increase the thermal optimum of photosynthesis, and at above optimum temperatures, the decrease in A_{sat} would be sharper at eCO₂ than aCO₂ as a consequence of shift to J_{max} limitation which is negatively affected at higher temperatures (Hypothesis 1).

Following long term exposure to eCO₂, plants may acclimate to CO₂ enriched environment and reduce photosynthetic capacity by decreasing a number of photosynthetic proteins including Rubisco, in a process known as ‘acclimation’ (Ainsworth et al., 2003; Nie et al., 1995; Rogers and Humphries, 2000). In response to eCO₂ plants invest more in photosynthetic components other than Rubisco to achieve maximum benefits of the high CO₂ environment. Thus, acclimation is associated with reduced V_{max} , J_{max} , leaf nitrogen (N) and Rubisco content. Alternatively, plants may reduce photosynthetic capacity in response to eCO₂ by reducing activation of Rubisco and regulatory mechanisms without affecting the amount of Rubisco which can be termed as ‘down regulation’ (Delgado et al., 1994). Acclimation or downregulation can be considered as a biochemical adjustment that improves the overall

performance of a plant in a high CO₂ environment rather than physiological dysfunction and acclimation is observed in limited resource conditions (Sage, 1994).

Acclimation to long term eCO₂ can modulate plant responses to high temperature (Ghannoum et al., 2010). Growth at eCO₂ reduces V_{cmax} and photorespiration in contrast to the instantaneous increase in temperature which enhances V_{cmax} and photorespiration. The changes due to acclimation under eCO₂ may lead to increased vulnerability to HS relative to non-acclimated plants. In contrast, increased sink capacity at eCO₂ allows plants to utilize the increased electron flow due to high temperatures during HS. Thus, eCO₂ may prevent photo-damage (Hogan et al., 1991) to photosynthetic apparatus due to HS by increasing electron transport. Hence, I predict that positive direct effects of eCO₂ on photosynthesis will override possible negative effects of acclimation, and hence alleviate HS damage to photosynthesis under eCO₂ (Hypothesis 2).

HS effects on plant biomass and grain yield depend on the magnitude and duration of HS along with the developmental stage of the plant. HS at the vegetative stage decreases biomass and grain yield mainly by speeding up plant development and reducing the time available to capture resources and by reducing the photosynthetic rates at higher temperatures (Lobell and Gourdj, 2012). At the flowering or anthesis stage, HS may reduce grain number due to pollen abortion, while at the grain filling stage HS reduces grain weight by affecting assimilate translocation and shortening the grain filling duration (Farooq et al., 2011; Prasad and Djanaguiraman, 2014; Wahid et al., 2007). However, eCO₂ may alleviate the negative impact of HS on biomass and grain yield through various mechanisms such as protection of photosynthetic apparatus from damage by HS, stimulation of photosynthesis and improvement in plant water status during HS due to a reduction in stomatal conductance and transpiration. Furthermore, increased levels of sucrose and hexoses in plants grown at eCO₂ are associated with increase in spike biomass and fertile florets (Dreccer et al., 2014), which have been observed to increase osmotic adjustment (Wahid et al., 2007) which can increase HS tolerance (Shanmugam et al., 2013). Also, eCO₂ may not only prevent damage due to HS but can also help in recovery after HS. Thus, I hypothesize that HS will reduce biomass more in aCO₂ relative to eCO₂ grown plants. Given that HS at the flowering stage reduces grain yield due to pollen abortion, eCO₂ is expected to prevent HS induced reduction in grain yield (Hypothesis 3).

The current study builds on the previous chapter, which investigated the responses of photosynthesis, biomass and grain yield in two wheat genotypes Scout and Yitpi to the

interactive effects eCO₂ and HS at the vegetative and flowering stage. However, the HS at moderate RH under well-watered conditions was not stressful enough and proved beneficial to aCO₂ grown plants. We concluded that leaf temperatures were maintained below damaging levels by transpirational cooling. To generate more stressful conditions, we designed a second HS experiment where a high relative humidity was used to reduce transpiration, and thus limit transpirational cooling by plants during the heatwave. Wheat plants (Scout) were grown at current ambient and future eCO₂ conditions followed by exposure to 5-day HS at flowering stage. Elevated CO₂ stimulated photosynthesis, biomass and grain yield. HS reduced biomass more in aCO₂ than eCO₂ grown plants but biomass recovered at the final harvest in both aCO₂ and eCO₂ grown plants. In contrast, HS equally reduced grain yield in both aCO₂ and eCO₂ grown plants.

3.2 Material and methods

3.2.1 Plant culture and treatments

The experiment was conducted in a glasshouse located at the Hawkesbury campus of Western Sydney University, Richmond, New South Wales. The commercial wheat line Scout, which has a putative transpiration use efficiency gene was selected for the current experiment. For germination, 300 seeds were sterilized using 1.5 % NaOCl₂ for 1 min followed by incubation in the dark at 28°C for 48 hours in Petri plates. Sprouted seeds were planted in germination trays using seed raising and cutting mix (Scotts, Osmocote®) at ambient CO₂ (400 µl L⁻¹), temperature (22/14 °C day/night), RH (50 to 70%) and natural light (Figure 3.1). Two week old seedlings were transplanted to individual cylindrical pots (15 cm diameter and 35 cm height) using sieved soil collected from the local site. The plant density was 24 plants per meter square. At the transplanting stage, pots were randomly distributed into aCO₂ (400 µl L⁻¹) and eCO₂ (650 µl L⁻¹) chambers. Plants were exposed to heat stress (HS) at the flowering stage for five days by increasing temperature to 43°C during the midday (10 am to 4 pm) and to 24°C during the night period (8 pm to 6 am) (Figure S3.3). Relative humidity (RH) was maintained between 50 and 70% during most of the experimental period (Figure 3.1). To minimize transpirational cooling and ensure high leaf temperature, RH was increased up 90% during the 5-day HS treatments. The glasshouse humidifier increased RH up to 85 %, while trays filled with water were placed in the chambers to further raise RH up to 90%. Thrive all-purpose fertilizer (Yates) was applied monthly throughout the experiment. Pots were randomized regularly within and among the glasshouse chambers.

3.2.2 Temperature response of leaf gas exchange

The response of light saturated (photosynthetic photon flux density (PPFD) = 1800 µmol m⁻² s⁻¹) CO₂ assimilation rate (A_{sat}) to variations in sub-stomatal CO₂ mole fraction (C_i) was measured at five leaf temperatures (15, 20, 25, 30 and 35°C) before the HS treatment was applied in both aCO₂ and eCO₂ grown plants. Leaf temperature sequence started at 25°C decreasing to 15°C and then increased up to 35°C. Dark respiration (R_d) was measured by switching light off for 20 minutes at the end of each temperature curve. Measurements were made inside a growth cabinet (Sanyo) to achieve desired leaf temperature.

3.2.3 *Rubisco content determination*

Following gas exchange measurements, leaf discs were collected from the flag leaves, rapidly frozen in liquid nitrogen and stored at -80°C until analyzed. Each leaf disc was extracted in 0.8 mL of ice-cold extraction buffer [50 mM EPPS-NaOH (pH 7.8), 5 mM DTT, 5 mM MgCl₂, 1 mM EDTA, 10 µl protease inhibitor cocktail (Sigma), 1% (w/v) polyvinyl polypyrrolidone] using a 2 mL Tenbroeck glass homogenizer kept on ice. The extract was centrifuged at 15,000 rpm for 1 min and the supernatant used for the assay of Rubisco content. Samples were first activated in buffer [50 mM EPPS (pH 8.0), 10 mM MgCl₂, 2 mM EDTA, 20 mM NaHCO₃] for 15min at room temperature. Rubisco content was estimated by the irreversible binding of [¹⁴C]-CABP to the fully carbamylated enzyme (Sharwood et al., 2008).

3.2.4 *Leaf gas exchange measurements*

Instantaneous steady state leaf gas exchange measurements were performed before, during, after and at the recovery stage of the HS cycle using a portable open gas exchange system (LI-6400XT, LI-COR, Lincoln, USA). Parameters measured included A_{sat} , stomatal conductance (g_s), the ratio of intercellular to ambient CO₂ (C_i/C_a), leaf transpiration rate (E), dark respiration (R_d) dark- and light-adapted chlorophyll fluorescence (F_v/F_m and F_v'/F_m' , respectively). Control plants were also measured for these parameters at the recovery stage following HS. Plants were moved to a neighboring chamber to achieve desired leaf temperature. Instantaneous steady state leaf gas exchange measurements were performed using Licor 6400 with a leaf chamber fluorometer (LCF) at a PPFD of 1800 µmol m⁻² s⁻¹ with two CO₂ concentrations (400 and 650 µl L⁻¹) and two leaf temperatures (25 and 35 °C). Photosynthetic down regulation or acclimation was examined by comparing the measurements at common CO₂ (ambient and elevated CO₂ grown plants measured at 400 µl CO₂ L⁻¹) and growth CO₂ (aCO₂ grown plants measured at 400 µl CO₂ L⁻¹ and eCO₂ grown plants measured at 650 µl CO₂ L⁻¹). R_d was measured after a 15-20 minute dark adaptation period. Photosynthetic water use efficiency (PWUE) was calculated as A_{sat} (µmol m⁻² s⁻¹)/ g_s (mol m⁻² s⁻¹). The response of the A_{sat} to variations in sub-stomatal CO₂ mole fraction (C_i) ($A-C_i$ response curve) was measured at T3 in 8 steps of CO₂ concentrations (50, 100, 230, 330, 420, 650, 1200 and 1800 µl L⁻¹) at leaf temperature of 25°C. Measurements were taken around mid-day (from 10 am to 3 pm) on attached last fully expanded flag leaves of the main stems. Before each measurement, the leaf was allowed to stabilize for 10-20 minutes until it reached a steady state of CO₂ uptake and stomatal conductance. Ten replications per treatment were measured.

3.2.5 Growth and biomass measurements

The full factorial experimental design included harvest of ten plants per treatment at three-time points including before HS (B), after recovery from HS (R) and at the final harvest after maturity (M). At each harvest, morphological parameters were measured and the biomass was harvested separately for roots, shoots and leaves. Samples were dried for 48 hours in the oven at 60°C immediately after harvesting. Leaf area was measured before HS and at the recovery stage of HS using leaf area meter (LI-3100A, LI-COR, Lincoln, NE, USA). Plant height, leaf number, tiller number and ear (grain bearing plant organ) number were also recorded. Leaf mass per area (LMA, g m⁻²) was calculated as total leaf dry mass/total leaf area.

3.2.6 Statistical analysis

All data analyses and plotting were performed using R computer software (R Core Team, 2017). The effect of treatments and their interactions were analyzed using linear modeling with anova in R. Significance tests were performed with anova and post hoc Tukey test using the 'glht' function in the multcomp R package. Coefficient means were ranked using post-hoc Tukey test. The Farquhar-von Caemmerer-Berry (FvCB) photosynthesis model was fit to the A_{sat} response curves to C_i (A- C_i response curve) or chloroplastic CO₂ mole fraction (C_c), which was estimated from the g_m measurements performed in a previous experiment (A- C_c response curve). We used the plantecophys R package (Duursma, 2015) to perform the fits, using measured g_m and R_d values, resulting in estimates of maximal carboxylation rate (V_{cmax}) and maximal electron transport rate (J_{max}) for D-ribulose-1,5-bisphosphate carboxylase/oxygenase (Rubisco) using measured R_d values. Temperature correction parameter (Tcorrect) was set to False while fitting A- C_i curves. Temperature response of V_{cmax} and J_{max} were calculated by Arrhenius and peaked functions, respectively (Medlyn et al., 2002). Estimated V_{cmax} and J_{max} values at five leaf temperatures were then fit using nonlinear least square (nls) function in R to determine energy of activation for V_{cmax} (EaV) and J_{max} (EaJ) and entropy (ΔS_J). Temperature responses of V_{cmax} and R_d were fit using Arrhenius equation as follows,

$$f(Tk) = k_{25} \cdot \exp \left[\frac{H_a \cdot (Tk - 298)}{R \cdot 298 \cdot Tk} \right] \quad (8)$$

where Ea is the activation energy (in J mol⁻¹) and k₂₅ is the value of R_d or V_{cmax} at 25 °C. R is the universal gas constant (8.314 J mol⁻¹ K⁻¹) and Tk is the leaf temperature in K. The activation energy term Ea describes the exponential rate of rise of enzyme activity with the increase in

temperature. The temperature coefficient Q_{10} , a measure of the rate of change of a biological or chemical system as a consequence of increasing the temperature by 10 °C was also determined for R_d using the following equation:

$$R_d = R_{d25} \cdot Q_{10}^{[(T-25)/10]} \quad (1)$$

A peaked function (Harley et al., 1992) derived Arrhenius function was used to fit the temperature dependence of J_{max} , and is given by the following equation:

$$f(Tk) = k_{25} \cdot \exp\left[\frac{H_a \cdot (Tk - 298)}{R \cdot 298 \cdot Tk}\right] \left[\frac{1 + \exp\left(\frac{298 \cdot \Delta S - H_d}{298 \cdot R}\right)}{1 + \exp\left(\frac{Tk \cdot \Delta S - H_d}{Tk \cdot R}\right)} \right] \quad (2)$$

Where, H_a is the activation energy and k_{25} is the J_{max} value at 25 °C, H_d is the deactivation energy and S is the entropy term. H_d and ΔS together describe the rate of decrease in the function above the optimum. H_d was set to constant 200 kJ mol⁻¹ to avoid over parameterization. The temperature optimum of J_{max} was derived from Eqn 2 (Medlyn et al., 2002) and written as follows:

$$T_{opt} = \frac{H_d}{\Delta S - R \cdot \ln\left[\frac{E_a}{(H_d - E_a)}\right]} \quad (3)$$

The temperature response of A_{sat} was fit using a simple parabola equation (Crous et al., 2013) to determine temperature optimum of photosynthesis:

$$A_{sat} = A_{opt} - b \cdot (T - T_{opt})^2 \quad (4)$$

Where, T is the leaf temperature of leaf gas exchange measurement for A_{sat} , T_{opt} represents the temperature optimum and A_{opt} is the corresponding A_{sat} at that temperature optimum. Steady state gas exchange parameters g_m , g_s , C_i and J_{max} to V_{cmax} ratio were fit using nls function with polynomial equation:

$$y = A + Bx + Cx^2 \quad (5)$$

3.3 Results

Wheat line Scout was grown under the current ambient ($419 \mu\text{l L}^{-1}$, day time average) and elevated ($654 \mu\text{l L}^{-1}$, day time average) CO_2 conditions with 62 % (daytime average) relative humidity, $22.3/14.8^\circ\text{C}$ (day/night average) growth temperature and natural light (800 PAR average daily maximum) (Figure 3.1, Figure S3.4). Both aCO_2 and eCO_2 grown plants were successfully exposed to a five-day heat stress (HS) at the flowering stage with $39.8/23.7^\circ\text{C}$ (day/night average) growth temperature (Figure 3.1) and 71% (daytime average) relative humidity (RH) (Figure 3.1A-E). High RH (reaching up to 90%) was maintained during most of the HS period to keep stomata open, thus minimizing transpirational cooling and maximizing leaf temperature. This strategy was effective. The leaf temperatures measured using Infrared camera were significantly higher ($+6^\circ\text{C}$) in HS (42.5 , day average) relative to control plants (28.4 , day average). Also, leaf temperatures were similar in aCO_2 and eCO_2 grown plants in both control and HS treatments (Figure 3.1F).

3.3.1 eCO_2 stimulated wheat photosynthesis with or without downregulation

To assess photosynthetic acclimation due to eCO_2 , control plants were measured at peak growth period and after anthesis at common CO_2 . At peak growth period (13 weeks after planting (WAP)) eCO_2 downregulated photosynthesis at both 25°C and 35°C (-12% , $p = 0.004$ and -13.3% , $p = 0.01$, respectively) (Figure 3.2A-B, Table 3.2) without reduction in photosynthetic capacity evident from unchanged V_{cmax} and J_{max} at 25°C along with no significant change in Rubisco sites determined by enzyme assays in measured leaves (Figure 3.3 Table 3.2). When control plants were measured at growth CO_2 , eCO_2 increased A_{sat} at both 25°C ($+25\%$, $p = 0.003$) and 35°C ($+39\%$, $P < 0.001$) (Figure 3.2A-B).

After anthesis (17 WAP), there was no significant downregulation in A_{sat} (Tables 3.2 and S3.1) measured at common CO_2 and 25°C or 35°C in spite of mild downregulation in photosynthetic capacity evident from reduced V_{cmax} (-36% , $p = 0.07$) and J_{max} (-23% , $p = 0.04$) in leaves measured thirteen weeks after planting (Figure 3.4). When control plants were measured at growth CO_2 and, eCO_2 increased A_{sat} at 25°C ($+36\%$, $p < 0.001$) but not at 35°C (Tables 3.2 and S3.1).

Interestingly, eCO_2 did not affect g_s measured in control plants during peak growth period or after anthesis at common or growth CO_2 (Figure 3.2, Tables 3.2 and S3.1).

3.3.2 Temperature response of gas exchange parameters in aCO₂ and eCO₂ grown plants

A-C_i curves were measured at five leaf temperatures in order to characterize the thermal photosynthetic responses of the wheat plants grown at ambient and elevated CO₂ (Figures 3.3 and 3.5; Table 3.1). Overall, Scout had similar photosynthetic temperature response up to 25°C under ambient or elevated CO₂ but at higher temperatures eCO₂ grown plants showed reduction in all photosynthetic parameters. A_{sat} and g_s increased with temperature up to temperature optimum (T_{opt}) around 23.5°C leaf temperature and decreased more under eCO₂ relative to aCO₂ at higher temperatures. Relative to aCO₂, plants grown under eCO₂ had higher A_{sat} up to T_{opt} but similar A_{sat} at higher temperatures (Figure 3.5A). R_d increased with temperature under both aCO₂ and eCO₂, however rate of increase was slower at higher temperatures under eCO₂ resulting in lower R_d under eCO₂ relative to aCO₂ at 30 and 35°C leaf temperatures. Energy of activation for R_d (EaR) was significantly lower under eCO₂ relative to aCO₂. The modelled Q₁₀ temperature coefficient (rate of change due increase by 10°C) of R_d was similar under aCO₂ or eCO₂ (Figure 3.5B, Table 3.1). Plants grown under eCO₂ had higher C_i at all temperatures and C_i decreased at higher temperatures under eCO₂ but not under aCO₂ (Figure 3.5D).

V_{cmax} and J_{max} were calculated by fitting the response of A_{sat} to variations in chloroplast CO₂ concentration (C_c) (A-C_c response curve) using measured R_d and g_m . V_{cmax} increased with leaf temperature, while J_{max} increased up to T_{opt} (28°C) and decreased with further temperature increase. However, eCO₂ reduced both V_{cmax} and J_{max} at higher temperatures relative to aCO₂ (Figure 3.3). The ratio of J_{max}/V_{cmax} was higher under eCO₂ relative to aCO₂ at lower temperatures and decreased similarly with leaf temperature under aCO₂ or eCO₂ (Figure 3.3). There was no significant difference in V_{cmax} at 25°C, J_{max} at 25°C or their activation energy under aCO₂ or eCO₂ (Figure 3.3, Table 3.1).

3.3.3 Leaf gas exchange and chlorophyll fluorescence response to eCO₂ and HS

Overall, HS reduced photosynthesis and HS was more damaging in aCO₂ than eCO₂ plants (Figures 3.6 and 3.7, Table S3.1). Just before the HS (15 WAP), eCO₂ increased both A_{sat} (+43%, $p < 0.001$) and g_s (+20%, $p = 0.032$) measured at growth CO₂. Heat stress reduced A_{sat} measured during and after the HS in both aCO₂ and eCO₂ grown plants. In contrast, HS increased g_s measured during HS and reduced g_s after HS in both aCO₂ and eCO₂ grown plants. One week after heat stress, both A_{sat} and g_s had completely recovered in eCO₂ grown plants but not in aCO₂ grown plants, which still showed significant reductions in A_{sat} (-42%, $p = 0.017$) and g_s (-32%, $p = 0.006$) (Figure 3.6, Tables 3.2 and S3.1).

The reduction in photosynthesis due to HS at the recovery stage was supported by the reduction in V_{cmax} (-53%, $p = 0.002$) in aCO₂ grown plants. In contrast, HS did not affect V_{cmax} in eCO₂ grown plants but increased J_{max} (+37%, $p = 0.001$) which may be the reason for photosynthetic recovery in eCO₂ grown plants. Also, HS did not affect J_{max} in aCO₂ grown plants suggesting that eCO₂ may have helped plants tolerate the damage due to HS by increasing J_{max} (Figure 3.4). Interestingly, HS significantly increased the ratio of J_{max}/V_{cmax} in both aCO₂ and eCO₂ grown plants, but it was not affected by growth CO₂.

Measurements of chlorophyll fluorescence confirmed the persistent damage to photosynthesis by HS in aCO₂ relative to eCO₂ grown plants. Heat stress reduced light adapted Fv'/Fm' measured after and at the recovery stage of HS in aCO₂ (-29%, $p = 0.019$) but not in eCO₂ grown plants (Figure 3.6B). Dark adapted Fv/Fm decreased more consistently due to HS in aCO₂ relative to eCO₂ grown plants (Figure 3.7A).

3.3.4 Response of biomass, morphological parameters and grain yield to eCO₂ and HS

The eCO₂ treatment stimulated rate of development, biomass and grain yield. Faster development was evident from the larger number of ears in eCO₂ relative to aCO₂ grown plants harvested 13 WAP (before HS) (Figure 3.8) (+127%, $p < 0.001$). Elevated CO₂ significantly stimulated the total biomass harvested throughout the growing period (Figure 3.8; Tables 3.3 and 3.4). Biomass stimulation was contributed by the overall increase in biomass components including root, stem and leaf biomass along with an increase in leaf area, leaf number, tiller number and ear number (Tables 3.3 and 3.4). At the final harvest, eCO₂ grown plants had 35% ($p < 0.001$) more biomass and 30% higher grain yield ($p = 0.001$) than aCO₂ grown plants (Figure 3.8, Tables 3.3 and 3.4). The increase in grain yield was due to increased number of tillers and consequently ears (+22%, $p < 0.001$) under eCO₂ (Table 3.3).

Heat stress reduced the biomass of aCO₂ plants (-30%, $p < 0.001$) more than eCO₂ plants (-10%, $p = 0.09$) harvested at 17 WAP following the HS (Figure 3.8, Table 3.3). Response of grain yield from tillers was stronger than main shoot grains indicating heat stress strongly affected grains in the early developmental stage (Figure S3.5). Interestingly, heat stressed plants recovered and had similar biomass relative to control plants grown under both aCO₂ and eCO₂ at the final harvest. This recovery in biomass was driven by the HS induced stimulation of new tillers and consequent new ears (Figure 3.8). Despite the recovery in biomass, the grain yield was greatly reduced in both aCO₂ (-38%, $p < 0.001$) and eCO₂ (-41%, $p < 0.001$) grown plants due to grain abortion in old ears and insufficient time for grain filling in new ears (Figure

3.9, Table 3.3). HS caused grain abortion leading to empty ears without grains or damaged and shrunk grains (Figure S3.2) evident from reduction in grain per ear (-53%, $p < 0.001$) and average grain weight (-25%, $P < 0.001$) under both aCO₂ or eCO₂.

3.4 Discussion

The current study investigated the interactive effects of eCO₂ and HS on photosynthesis, biomass and grain yield in the wheat line Scout. Scout was grown at ambient or elevated CO₂ conditions followed by exposure to 5-day HS at the flowering stage. A high RH during HS helped minimize transpirational cooling and ensured effective HS application. Although heat waves are associated with low relative humidity in natural field conditions we chose to increase humidity to achieve higher leaf temperature in order to separate heat stress from water stress. Elevated CO₂ stimulated photosynthesis, biomass and grain yield, while HS reduced photosynthetic rates during HS under both aCO₂ and eCO₂. Elevated CO₂ facilitated the recovery of photosynthesis and biomass following the HS, but the reduction in grain yield was similar under either growth CO₂ treatment because of grain abortion due to HS at anthesis.

3.4.1 Photosynthetic acclimation to eCO₂ is a function of developmental stage

Photosynthetic responses to eCO₂ are well documented (Ainsworth et al., 2003) and it is established that eCO₂ increases net photosynthesis and productivity, despite frequent down regulation or acclimation (Leakey et al., 2009), which are biochemical adjustment that improve the overall performance of a plant in eCO₂ (Sage, 1994). Acclimation generally occurs due to limited resources or when growth is restricted (Arp, 1991; Sage, 1994).

In the current study, during the peak growth stage (13 WAP), eCO₂ downregulated photosynthesis without changing photosynthetic capacity which was evident from unchanged V_{cmax} and J_{max} . After anthesis (17 WAP), the eCO₂-induced reduction in photosynthetic rates was due to acclimation as evident from the reduced V_{cmax} and J_{max} . These results partially support our first hypothesis that Scout will show downregulation but not acclimation. This suggests that plants may undergo photosynthetic down regulation during the initial growth period by reducing Rubisco activation or regulatory mechanisms. As the plant growth rate slows down, eCO₂ decreases photosynthetic capacity as a result of acclimation. This is consistent with free air CO₂ enrichment (FACE) study investigating photosynthetic acclimation in wheat under field conditions which reported that acclimation is a function of developmental stage (Zhu et al., 2012). They found no acclimation to eCO₂ in newly matured flag leaves, onset of acclimation at anthesis associated with lower V_{cmax} and J_{max} and complete acclimation at maturity with no stimulation under eCO₂.

Photosynthetic downregulation in the current study (-12%) is much lower than what is reported in a previous open top chamber study with wheat in tropical environmental conditions which found 43% and 66% reduction in photosynthetic rates in the Kalyansona and Kundan cultivars, respectively (Sharma-Natu et al., 1998). The differences in the acclimation could be due to difference in cultivars and growth environment conditions.

3.4.2 Elevated CO₂ reduced photosynthetic capacity at higher temperature

Elevated CO₂ modulates instantaneous temperature response of photosynthesis (Ghannoum et al., 2010). In the current study, at optimal and suboptimal temperatures, all gas exchange parameters showed similar temperature responses under aCO₂ or eCO₂. However, temperatures higher than the optimum reduced photosynthetic capacity as evident from lower V_{cmax} and J_{max} more under eCO₂ relative to aCO₂ grown plants. Consequently, lower V_{cmax} and J_{max} at higher temperatures reduced photosynthetic rates under eCO₂. At higher temperatures and eCO₂, Rubisco activation is known to limit photosynthesis. However, the decline in Rubisco activation state is a regulated response to a limitation in electron transport capacity, rather than a consequence of a direct effect of temperature on the integrity of Rubisco activase (Sage and Kubien, 2007).

Reduction in J_{max} under eCO₂ can be caused by a decrease in RuBP regeneration or electron transport. Low photorespiratory conditions under eCO₂ may lead to inorganic phosphate limitation, slowing down RuBP regeneration (Sage and Sharkey, 1987; Ellsworth et al., 2015). Also, the lower activation energy of J_{max} is associated with decreased membrane fluidity which is reduced by lipid saturation (Niinemets et al., 1999). Elevated CO₂ has been found to increase lipid saturation (Huang et al., 1999) suggesting that eCO₂-induced lipid saturation may have decreased membrane fluidity leading to a higher reduction in J_{max} .

Plants grown at aCO₂ or eCO₂ had similar photosynthetic thermal optimum (Table 3.1), which is in contrast to my hypothesis that eCO₂ will increase photosynthetic thermal optimum. Lower J_{max} and V_{cmax} at higher temperatures may have prevented the increase in thermal optimum under eCO₂. In contrast, Alonso et al., (2008, 2009) reported increased V_{cmax} at higher temperatures, as well as reduction and increase in J_{max} at suboptimal and supraoptimal temperatures, respectively under eCO₂. The contrasting responses in the studies by Alonso et al., (2008, 2009) could be due to the increase in V_{cmax} in response to eCO₂.

3.4.3 Elevated CO₂ protected plants from HS damage

Acclimation to long term eCO₂ can modulate photosynthetic response to temperature (Ghannoum et al., 2010) and the HS lasting for a few days during vegetative stage or flowering stage (Wahid et al., 2007). In the current study, eCO₂ downregulated photosynthesis while HS decreased photosynthesis in both aCO₂ and eCO₂ grown plants. However, two weeks after HS, eCO₂ grown plants showed complete recovery in photosynthesis rates, no change in Fv'/Fm' and lesser reduction in Fv/Fm, indicating that HS transiently reduced photosynthetic rates but did not damage the photosynthetic apparatus of eCO₂ grown plants.

The recovery of photosynthesis under eCO₂ can be explained by increased sink capacity which allows plants to utilize increased electron flow during HS and prevent the damage to photosynthetic apparatus by non-photochemical quenching. Increased electron transport rate in eCO₂ grown plants exposed to HS, as evidenced by increased J_{max} , may have avoided the damage to the maximum efficiency of photosystem II. Unchanged V_{cmax} at the recovery stage in eCO₂ grown plants exposed to HS also confirmed that photosynthetic capacity was not damaged by HS. Interactive effects of eCO₂ and HS have been studied in only a few studies (reviewed by Wang et al., 2011) and eCO₂ has been found to increase thermal tolerance of photosynthesis (Hogan et al., 1991; Wang et al., 2008). Increases in photosynthetic thermal tolerance with high CO₂ in C₃ plants including wheat were observed in both cool- and warm-season species indicating CO₂ effects were related to photosynthetic pathway rather than the plant habitat (Wang et al., 2008).

In contrast, the photosynthetic rate of aCO₂ grown plants did not recover and showed reduced Fv'/Fm' and Fv/Fm after HS, indicating damage to photosynthetic, which was also evident from the reduction in V_{cmax} . A reduction in Fv/Fm and Fv'/Fm' is an indicator of stress and has generally been found to decrease after HS (Sharkova, 2001; Haque et al., 2014). Reduction in net photosynthetic rates due to HS is consistent with earlier studies in wheat (Wang et al., 2008) however, photosynthetic responses to HS vary widely among cultivars (Sharma et al., 2014).

Growth CO₂ did not affect the J_{max}/V_{cmax} ratio, but HS equally increased J_{max}/V_{cmax} ratio in both aCO₂ and eCO₂ grown plants, suggesting that plants increased resource allocation to RuBP regeneration or electron transport in response to HS irrespective of growth CO₂. Conserved J_{max}/V_{cmax} ratio under ambient or elevated CO₂ is consistent with earlier studies which have found coordination between J_{max} and V_{cmax} to avoid photoinhibition (Walker et al., 2014).

3.4.4 Plant biomass recovered after HS but not the grain yield

Elevated CO₂ stimulated total plant biomass, but HS reduced the biomass of aCO₂ more than eCO₂ grown plants. A larger decrease in biomass under aCO₂ is consistent with the irreversible damage to photosynthetic capacity by HS, reducing carbon uptake. The reduction in biomass can also be attributed to HS-induced senescence (Farooq et al., 2011). Growth at eCO₂ can help prevent the damage to the photosynthetic apparatus by HS and thus showed only a slight reduction in biomass. In contrast, Coleman et al., (1991) did not find interactive effects of eCO₂ and HS on biomass in the C₃ plant *Arbutilon theophrasti* and reported equal decrease in biomass under both aCO₂ or eCO₂, following exposure to HS, suggesting that interactive effects are variable among species and growth conditions. Interestingly, the biomass of heat stressed plants recovered under both aCO₂ and eCO₂ due to HS induced stimulation of new tillers (Bányai et al., 2014) and consequent new ears in the current study. Wheat changes number of tillers depending on environmental conditions which allows plants to create new sinks and involves translocation of resources to grain from structural components during grain filling. However, if the grain development is stalled, plants try to utilize captured resources to develop new grains by initiating new tillers. Tillering in response to HS can be attributed to non-harmful effect of HS that may have promoted formation of new tillers. Hence, grain abortion due to HS was compensated by the production of new tillers contributing to the recovery in biomass at final harvest. However, the new tillers produced in the field conditions do not produce good quality grains as the plants run out of soil water and there is not enough time for grain filling.

Elevated CO₂ stimulated grain yield to a similar magnitude relative to the overall biomass stimulation. However, despite the recovery of biomass in plants exposed to HS, the grain yield was greatly reduced in both aCO₂ and eCO₂ grown plants due to grain abortion in the old ears and insufficient time for grain filling in the new ears. In response to HS, some ears had completely lost grains and ears with developing grains could not fill leading to shrunk and damaged grains (Figure S3.2). Earlier studies in wheat exposed to HS at flowering stage have reported a decrease in grain yields under aCO₂ in enclosure studies (Spiertz et al., 2006; Stone and Nicolas, 1996, 1996, 1998). However, the interactive effects of eCO₂ and HS have been examined in only a few studies under field conditions (Fitzgerald et al., 2016) which found the positive interaction between eCO₂ and HS during grain filling stage. However, the FACE study by Fitzgerald et al., (2016) was an opportunistic study involving naturally occurring heat wave

with lower intensity than the HS in the current study and needed experimentally imposed HS validation.

3.5 Conclusions

Elevated CO₂ stimulated photosynthesis, biomass and grain yield in Scout. The stimulation by eCO₂ was associated with downregulation of photosynthesis through regulatory mechanisms during the initial growth period and with acclimation during the later developmental stage. Instantaneous temperature response of photosynthesis under eCO₂ showed a reduction in photosynthetic capacity at higher temperatures and eCO₂ did not increase thermal optimum of photosynthesis. HS decreased photosynthesis and biomass more under aCO₂ than eCO₂ due to eCO₂ interaction with HS which protected plants from photosynthetic damage due to HS. However, biomass completely recovered under both aCO₂ and eCO₂ due to the initiation of new tillers and ears, which did not have enough time to develop and fill grains. Importantly, HS at the flowering stage equally reduced grain yield under aCO₂ and eCO₂ due to grain abortion. Thus, usefulness of eCO₂ benefits under HS are subjected to intensity, duration and timing of HS. Elevated CO₂ can ameliorate negative effects of HS on growth, physiology and yield if the HS occurs at developmental stages other than the most critical flowering stage. The current study demonstrates interactive effects of eCO₂ and severe HS impact on wheat growth and productivity at 50% anthesis stage, however the HS can occur over a wide window from booting to late grain filling stage affecting yield in variable ways, thus limiting the generalization of results on grain yield. Nonetheless, current study provides insights on interactive effects of eCO₂ and HS on photosynthesis which can be predicted to occur over a wide range of scenarios and will be useful in improving crop models to incorporate interactive effects of eCO₂ and HS.

Table 3.1 Summary of modelled parameters for temperature response of photosynthesis

Summary of coefficients derived using nonlinear least square fitting of CO₂ assimilation rates and maximal rate of carboxylation (V_{cmax}) and maximal rate of RuBP regeneration (J_{max}) determined using A-C_i response curves and dark respiration measured at five leaf temperatures (15, 20, 25, 30 and 35°C). Values are means with standard errors. Derived parameters include temperature optima (T_{opt}) of photosynthesis (A_{opt}); activation energy for carboxylation (EaV); activation energy (EaJ), entropy term (ΔSJ) and T_{opt} and corresponding value for J_{max} with deactivation energy (Hd) assumed constant; and activation energy (EaR) and temperature coefficient (Q_{10}) for dark respiration. Letters indicate significance of variation in means.

Parameter	Constant	Ambient Growth CO ₂	Elevated Growth CO ₂
A_{sat} ($\mu\text{mol m}^{-2} \text{s}^{-1}$)	T_{opt} (°C)	23.7 ± 1.1 a	23.4 ± 1.3 a
	A_{opt}	25.5 ± 1.3 a	30.9 ± 2.7 b
V_{cmax} ($\mu\text{mol m}^{-2} \text{s}^{-1}$)	V_{cmax} at 25°C	227 ± 36 a	174 ± 19 a
	EaV (kJ mol^{-1})	61 ± 15 a	54 ± 11 a
J_{max} ($\mu\text{mol m}^{-2} \text{s}^{-1}$)	J_{max} at 25°C	207 ± 12 a	196 ± 22 a
	T_{opt} (°C)	29.5 ± 0.7 a	27.5 ± 0.9 a
	J_{max} at T_{opt}	233 ± 6	210 ± 11 a
	EaJ (kJ mol^{-1})	40 ± 11 a	36 ± 22 a
	ΔSJ ($\text{J mol}^{-1} \text{K}^{-1}$)	647 ± 5 a	651 ± 8 a
	Hd (kJ mol^{-1})	200	
Rd ($\mu\text{mol m}^{-2} \text{s}^{-1}$)	Rd at 25°C	2.4 ± 0.1 a	2.2 ± 0.1 a
	EaR (kJ mol^{-1})	41 ± 3 a	31 ± 6 a
	Q_{10}	1.73 ± 0.07 a	1.50 ± 0.13 a

Table 3.2 Summary of statistics for gas exchange parameters

Summary of statistical analysis using anova for the effects of elevated CO₂ and heat stress on leaf gas exchange parameters. Significance levels are *** = $p < 0.001$; ** = $p < 0.01$; * = $p < 0.05$; † = $p < 0.1$; ns = $p > 1$.

Parameter (mean plant ⁻¹)	Measurement		T1	T2		
	Temp	CO ₂	Main effects	Main		Interaction
			CO ₂	CO ₂	HS	CO ₂ × HS
A (μmol m ⁻² s ⁻¹)	25	400	**	*	*	**
		650	**	**	*	**
	35	400	**	ns	ns	*
		650	**	ns	ns	*
Rd (μmol m ⁻² s ⁻¹)	25	400	ns	ns	ns	ns
	35	400	*			
g_s (mol m ⁻² s ⁻¹)	25	400	ns	*	*	ns
		650	ns	**	**	*
	35	400	ns	ns	ns	ns
		650	ns	ns	ns	ns
PWUE (A/gs)	25	400	ns	ns	ns	†
		650	ns	ns	ns	ns
	35	400	ns	ns	*	*
		650	ns	†	ns	ns
Fv/Fm	25	400	ns	*	ns	ns
Fv'/Fm'	25	400	ns	**	**	*
A (μmol m ⁻² s ⁻¹)	25	Growth CO ₂	**	***	†	**
	35		***	**	ns	*
Rd (μmol m ⁻² s ⁻¹)	25		***			
	35		*			
g_s (mol m ⁻² s ⁻¹)	25		ns	***	**	*
	35		ns	ns	ns	ns
PWUE (A/gs)	25		***	***	ns	*
	35		**	***	ns	ns

Table 3.3 Response of plant dry mass (DM) and morphological parameters to elevated CO₂ and heat stress

Summary of plant biomass and morphological parameters measured at different time points for Scout grown at ambient CO₂ (aCO₂) or elevated CO₂ (eCO₂), with some plants exposed to heat stress (HS) at the flowering stage. Values are means \pm SE (n= 9-10).

Parameter (Mean plant ⁻¹)	Time	T1	T2 (Anthesis)		T3 (Maturity)	
	Heat Stress	Control	Control	HS	Control	HS
	Growth CO ₂					
Tiller Number	aCO ₂	9.2 \pm 0.6	10.9 \pm 0.5	16.3 \pm 0.7		
	eCO ₂	12.9 \pm 0.7	12.3 \pm 0.8	28.3 \pm 1.6		
Leaf Area (cm ²)	aCO ₂	338 \pm 27	338 \pm 40	296 \pm 47		
	eCO ₂	680 \pm 59	441 \pm 58	650 \pm 55		
Leaf Number	aCO ₂	33.8 \pm 2.6	26.9 \pm 0.8	37 \pm 3.1		
	eCO ₂	49.5 \pm 2.8	27.6 \pm 2.2	66.7 \pm 4.4		
Leaf Size (cm ²)	aCO ₂	27 \pm 7	32 \pm 5	38 \pm 5		
	eCO ₂	24 \pm 2	24 \pm 3	42 \pm 5		
Leaf Mass Area (g m ⁻²)	aCO ₂	58 \pm 1	56 \pm 2	68 \pm 1		
	eCO ₂	52 \pm 2	48 \pm 3	60 \pm 1		
Leaf DM (g)	aCO ₂	1.9 \pm 0.1	1.8 \pm 0.1	2.0 \pm 0.3		
	eCO ₂	3.5 \pm 0.2	1.8 \pm 0.1	3.9 \pm 0.3		
Stem DM (g)	aCO ₂	3.9 \pm 0.1	9.6 \pm 0.3	9.3 \pm 0.7		
	eCO ₂	8.5 \pm 0.6	11.4 \pm 0.8	17.1 \pm 0.7		
Root DM (g)	aCO ₂	1.4 \pm 0.2	1.6 \pm 0.1	1.9 \pm 0.2	0.6 \pm 0.1	2 \pm 0.3
	eCO ₂	2.0 \pm 0.2	2.4 \pm 0.4	3.8 \pm 0.8	0.6 \pm 0.1	1.2 \pm 0.1
Shoot DM (g)	aCO ₂	8.1 \pm 0.3	32.9 \pm 1.3	22.1 \pm 0.8	9.3 \pm 0.4	10.3 \pm 0.4
	eCO ₂	16.8 \pm 1.1	41.2 \pm 1.9	35.5 \pm 0.8	12.7 \pm 0.7	18.9 \pm 1.5
Total DM (g)	aCO ₂	9.5 \pm 0.4	34.5 \pm 1.5	24.1 \pm 1.0	33.7 \pm 1.5	31.4 \pm 1.1
	eCO ₂	18.8 \pm 1.3	43.6 \pm 2.2	39.3 \pm 0.9	45.5 \pm 2.2	48.8 \pm 2.2
Ear Number	aCO ₂				10.2 \pm 0.3	16.7 \pm 1
	eCO ₂				12.5 \pm 0.4	22.6 \pm 0.8
Grains Per Ear	aCO ₂				41 \pm 1	21 \pm 1
	eCO ₂				41 \pm 1	17 \pm 1
Total Grain Number	aCO ₂				415 \pm 21	352 \pm 15
	eCO ₂				511 \pm 20	384 \pm 30
Mean Grain Size (mg grain ⁻¹)	aCO ₂				44 \pm 1	32 \pm 1
	eCO ₂				46 \pm 1	35 \pm 1
Grain yield (g)	aCO ₂				18.1 \pm 0.9	11.2 \pm 0.4
	eCO ₂				23.5 \pm 1.1	13.7 \pm 1.1
Harvest Index	aCO ₂				0.536 \pm 0.006	0.357 \pm 0.009
	eCO ₂				0.518 \pm 0.002	0.281 \pm 0.021

Table 3.4 Summary of statistics for plant dry mass (DM) and morphological parameters

Summary of statistical analysis using anova for the effects of elevated CO₂ and heat stress (HS) on biomass and morphological parameters for plants harvested at various time points. Significance levels are *** = $p < 0.001$; ** = $p < 0.01$; * = $p < 0.05$; † = $p < 0.1$; ns = $p > 1$.

Time Point	Parameter (Mean plant ⁻¹)	Main Effects		Interaction
		CO ₂	HS	CO ₂ * HS
T1	Tiller number	**		
	Leaf Number	***		
	Leaf Area (cm ²)	***		
	Ear Number	***		
	Ear DM (g)	***		
	Leaf DM (g)	***		
	Stem DM (g)	***		
	Roots DM (g)	†		
	Shoot DM (g)	***		
	Total DM (g)	***		
T2	Tiller Number	***	***	***
	Leaf Number	***	***	***
	Leaf Area (cm ²)	***	†	**
	Ear Number	***	***	***
	Ear DM (g)	***	***	ns
	Leaf DM (g)	***	***	***
	Stem DM (g)	***	***	***
	Roots DM (g)	***	**	*
	Shoot DM (g)	***	***	†
	Total DM (g)	***	***	†
T3	Ear Number	***	***	*
	Ear DM (g)	***	***	ns
	Roots DM (g)	†	***	†
	Shoot DM (g)	***	***	**
	Total DM (g)	***	ns	ns
	Main stem grain yield (g)	ns	***	ns
	Grain Yield (g)	***	***	ns
	Grain Number	**	***	ns
	Grains Per Ear	ns	***	†
	Grain Size (mg grain ⁻¹)	**	***	ns
	Harvest Index	**	***	*

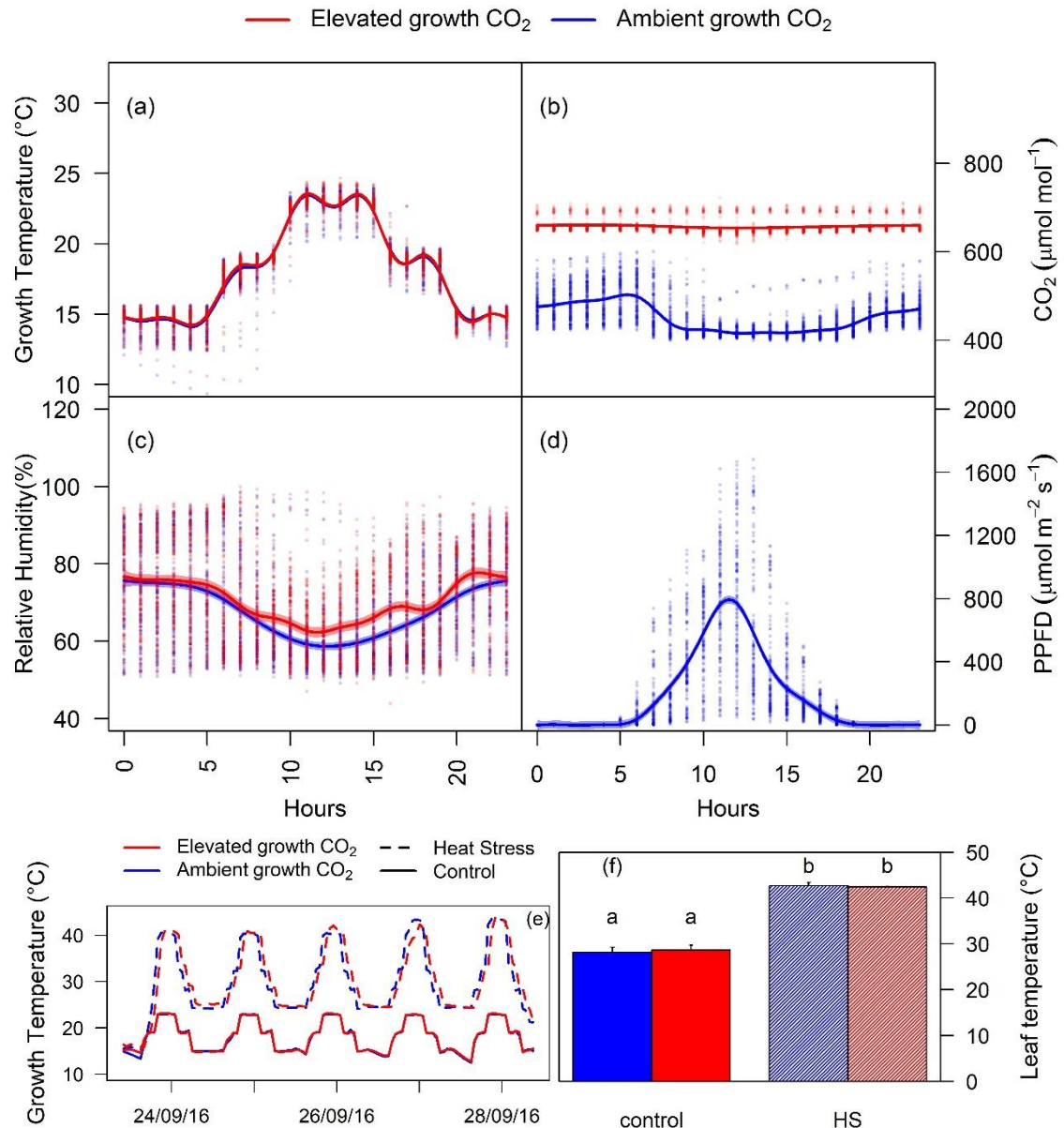


Figure 3.1 Glasshouse growth conditions and heat stress cycle

Daily averages of growth temperature (a), CO_2 (b), relative humidity (c) and PPFD (d). In panels, a, b, c and d solid lines represent the growth averages, while the faint data points show recorded observations. Lower panel (e) illustrates the 5-day heat stress cycle at the flowering stage. Growth temperatures recorded in control and heat stress chambers during heat stress are depicted using solid and dotted lines, respectively. Bar plot of means for leaf temperature (f) of a two-way analysis of variance (ANOVA). Values represent means \pm standard error. Bars sharing the same letter in the individual panel are not significantly different according to Tukey's HSD test at the 5% level. Ambient and elevated CO_2 treatments are depicted in blue and red, respectively.

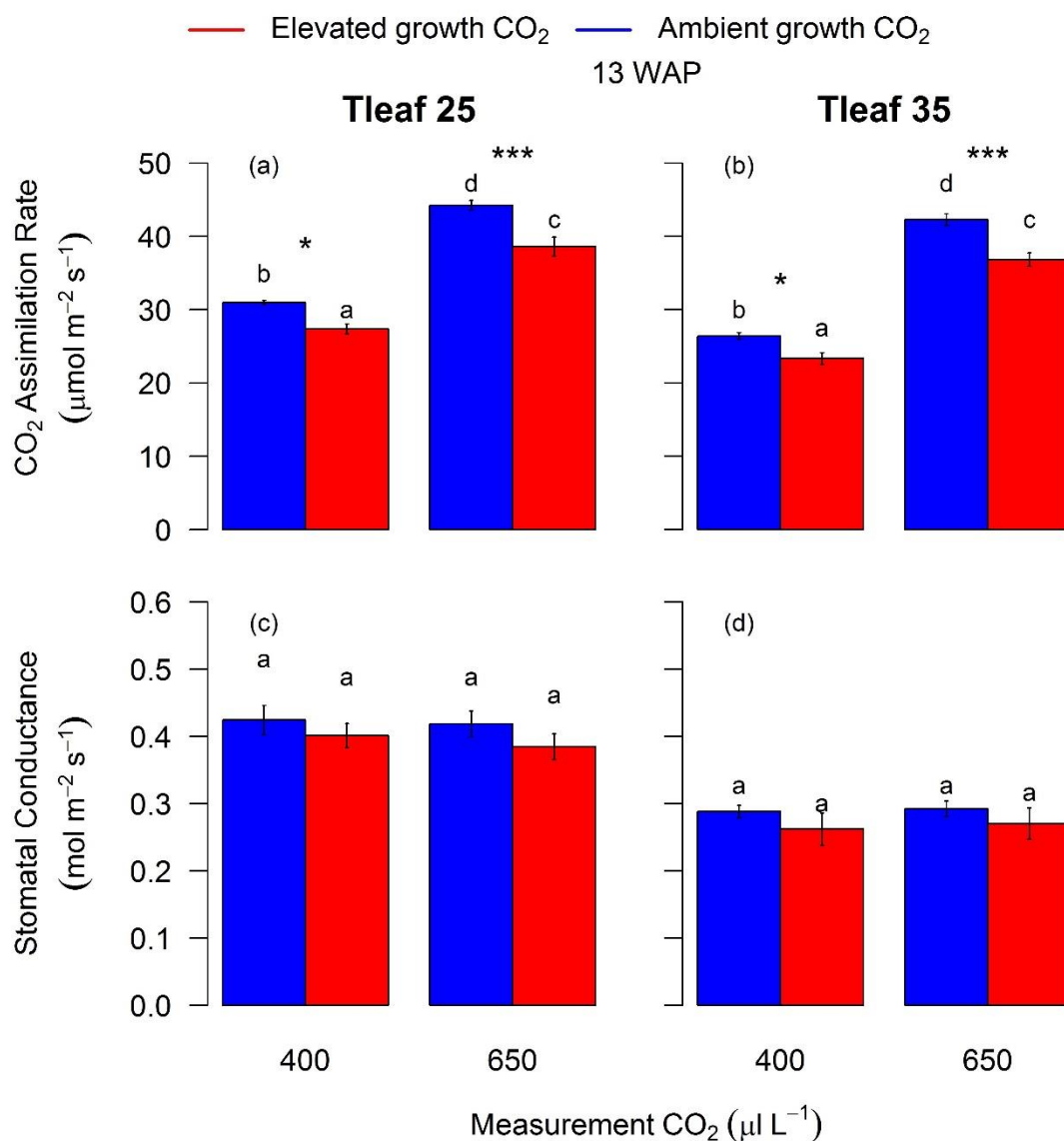


Figure 3.2 Photosynthetic response of Scout to eCO₂ measured thirteen weeks after planting (WAP) at two leaf temperatures and two CO₂ concentrations

Bar plot of means for CO₂ assimilation rate (a and b) and stomatal conductance (c and d) calculated using two-way analysis of variance (ANOVA). The error bars indicate standard error (SE) of the mean. Ambient and elevated CO₂ grown plants are depicted in blue and red color respectively. Grouping is based on measurement CO₂ (400 or 650 400 µL⁻¹) and leaf temperature (25 or 35°C). Bars sharing the same letter in the individual panel are not significantly different according to Tukey's HSD test at the 5% level. Statistical significance levels (t-test) for eCO₂ effect are shown and they are: * = p < 0.05; ** = p < 0.01; *** = p < 0.001.

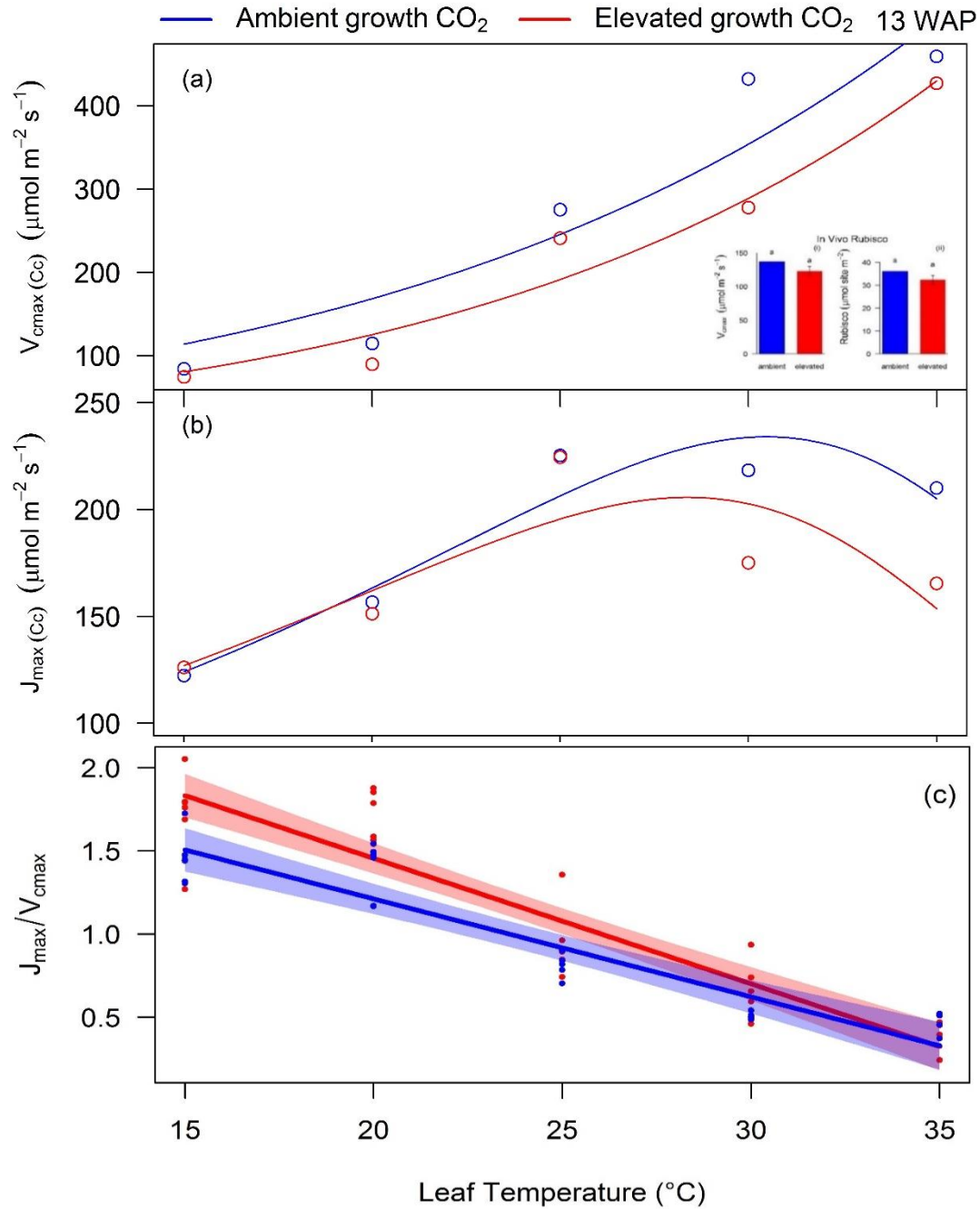


Figure 3.3: Temperature response of V_{cmax} and J_{max} measured 13 weeks after planting (WAP)

Maximum velocity of carboxylation, V_{cmax} (a), maximum velocity of RuBP regeneration, J_{max} (b) and ratio of J_{max}/V_{cmax} (c) determined using the response of CO₂ assimilation to variation in chloroplastic CO₂ (Cc) at five leaf temperatures (15, 20, 25, 30 and 35 °C) in Scout. Inset in panel (a) is a bar plot showing in vivo V_{cmax} (i) and Rubisco sites (ii) measured in flag leaf discs harvested at same time point. For panels a and b, values are mean \pm SE. The ratio of J_{max}/V_{cmax} (c) is plotted using visreg package in R. Solid lines are means with 95% confidence intervals. Ambient and elevated CO₂ grown plants are shown in blue and red, respectively.

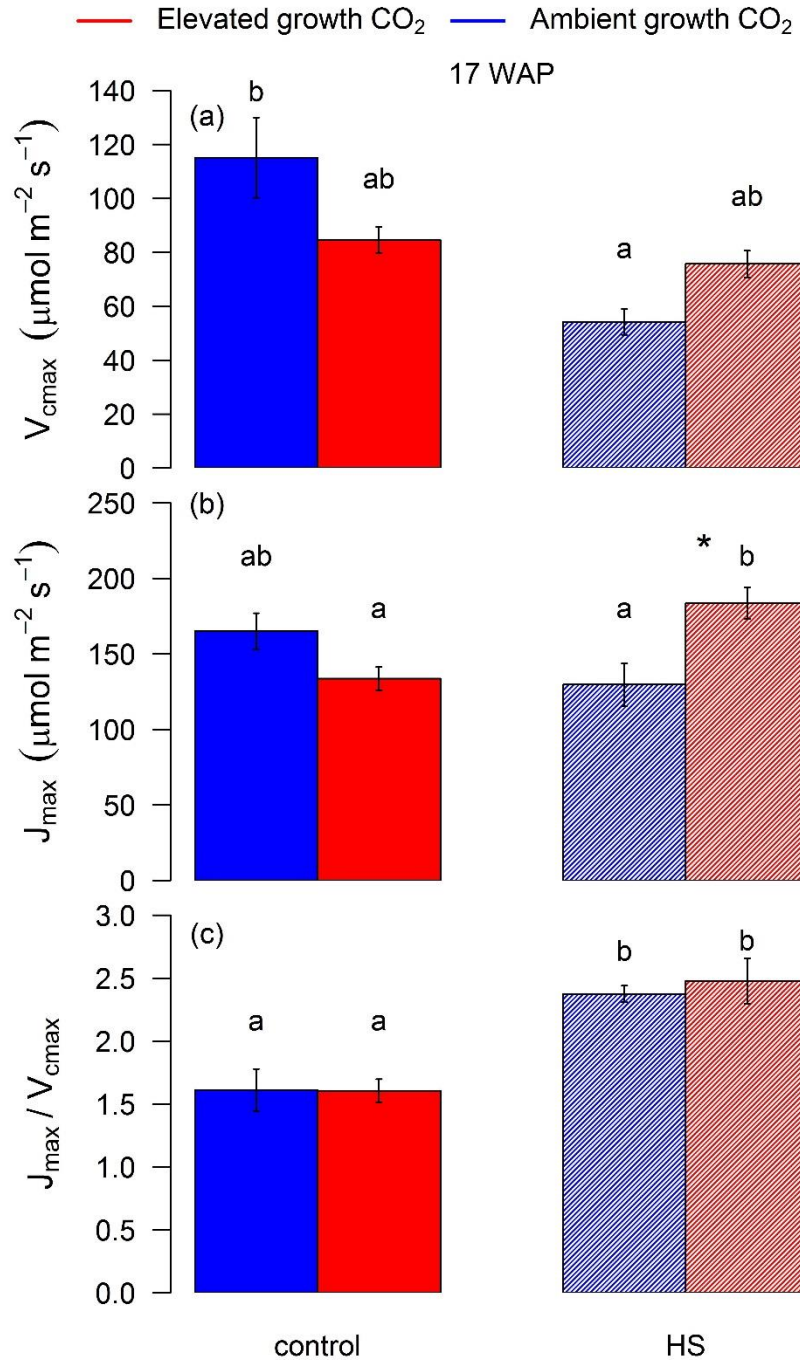


Figure 3.4 Response of V_{cmax} and J_{max} to growth at eCO₂ and HS measured 17 weeks after planting at the recovery stage of the HS cycle

Bar plot of means \pm standard error for V_{cmax} (a), J_{max} (b) and V_{cmax}/J_{max} (c) using two-way analysis of variance (ANOVA). Leaf gas exchange was measured in ambient (blue) and elevated (red) CO₂ grown plants exposed (HS) or not exposed (Control) to 5-day HS. Bars sharing the same letter in the individual panel are not significantly different according to Tukey's HSD test at the 5% level. Statistical significance levels (t-test) for eCO₂ effect are shown and they are: * = $p < 0.05$; ** = $p < 0.01$; *** = $p < 0.001$.

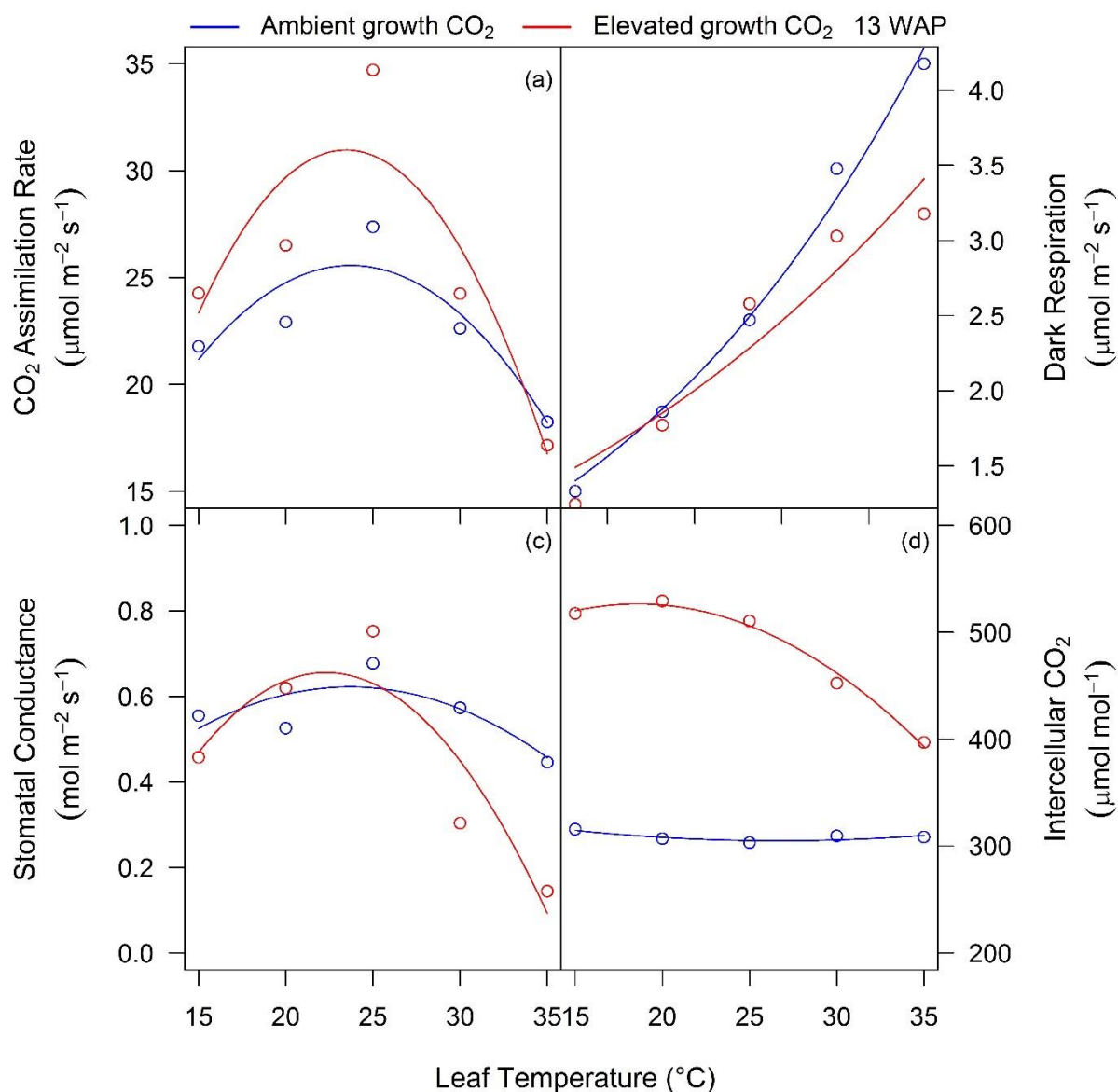


Figure 3.5 Temperature response of spot gas exchange parameters measured thirteen weeks after planting (WAP)

CO₂ assimilation rate (a), dark respiration (b), stomatal conductance (c) and intercellular CO₂ (d) measured at growth CO₂ and five leaf temperatures (15, 20, 25, 30 and 35 °C) in Scout. Values are mean ± SE. Ambient and elevated CO₂ grown plants are depicted in blue and red, respectively.

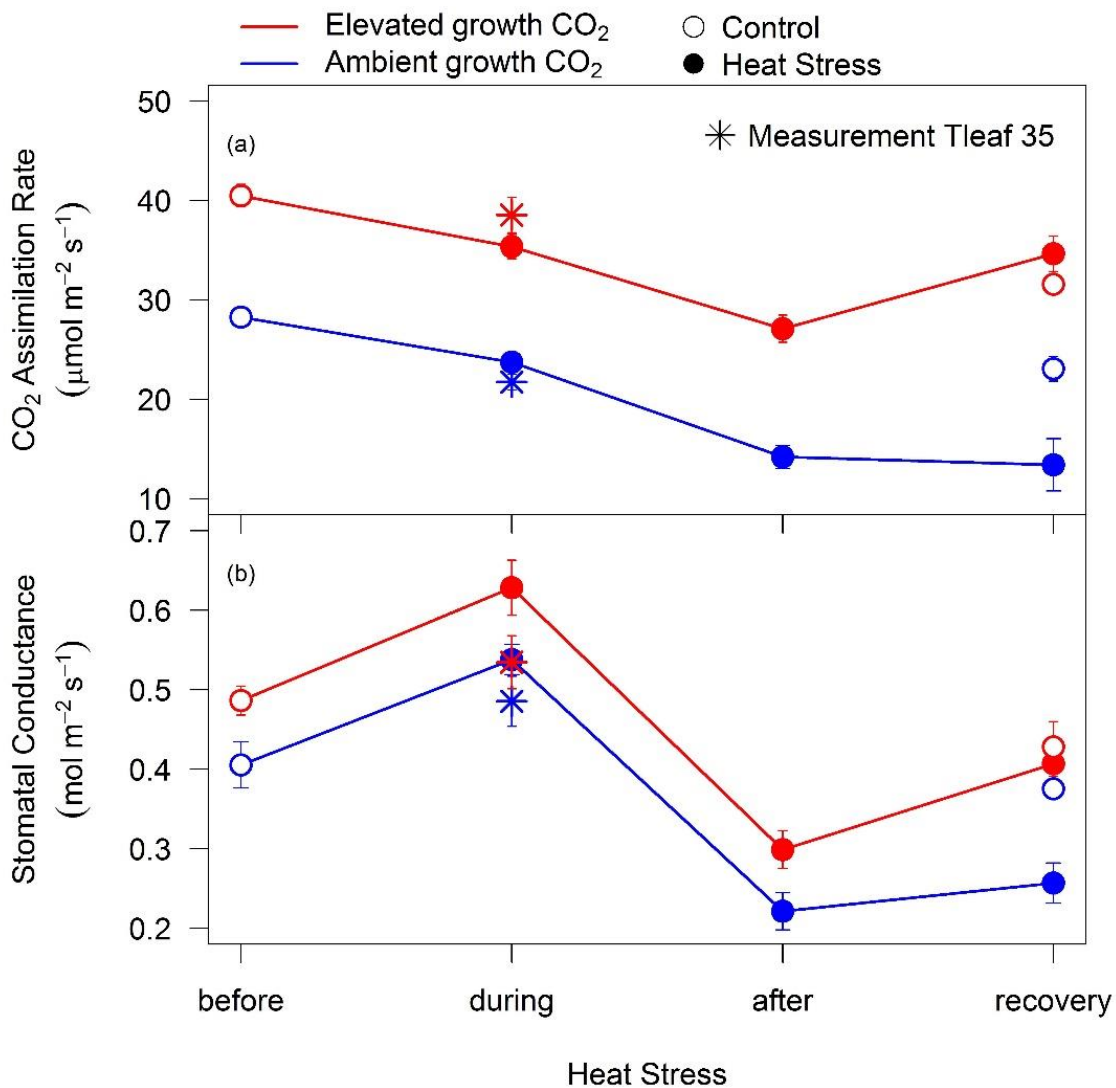


Figure 3.6 Photosynthetic response of aCO₂ and eCO₂ grown Scout measured before, during, after and at the recovery stage of the heat stress cycle

CO₂ assimilation rates (a) and stomatal conductance (b) measured at growth CO₂ (aCO₂ grown plants measured at 400 $\mu\text{l L}^{-1}$ and eCO₂ grown plants measured 650 $\mu\text{l L}^{-1}$). Ambient and elevated CO₂ grown plants are depicted in blue and red, respectively. Open and solid circles represent control and heat stressed plants respectively. The circle and star symbols depict CO₂ assimilation rates measured at 25°C and 35°C, respectively.

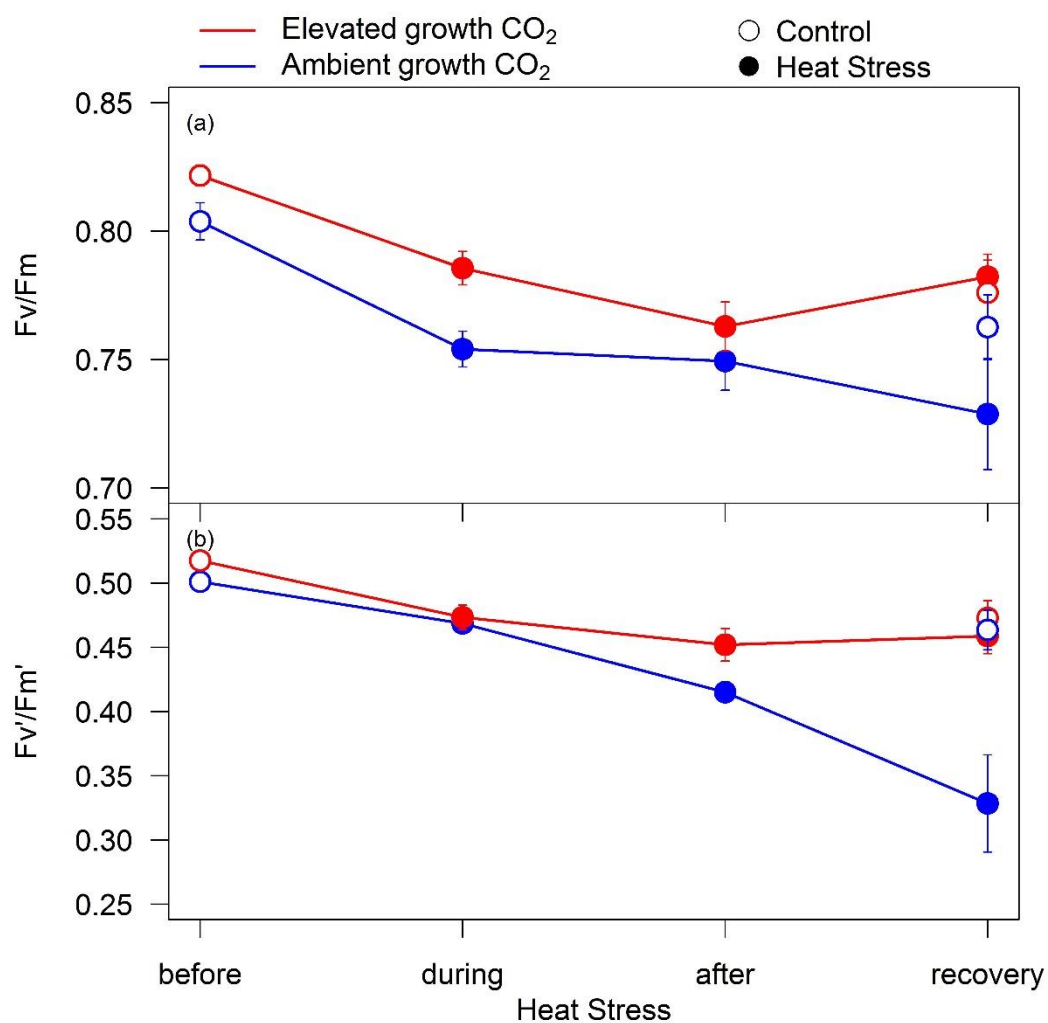


Figure 3.7 Chlorophyll fluorescence response of aCO₂ and eCO₂ grown Scout measured before, during, after and at the recovery stage of heat stress cycle

The ratio of F_v/F_m (a) in dark adapted leaves and F_v'/F_m' (b) in light adapted leaves measured at 25°C leaf temperature. Ambient and elevated CO₂ grown plants are depicted in blue and red, respectively. Open and solid circles represent control and heat stressed plants, respectively.

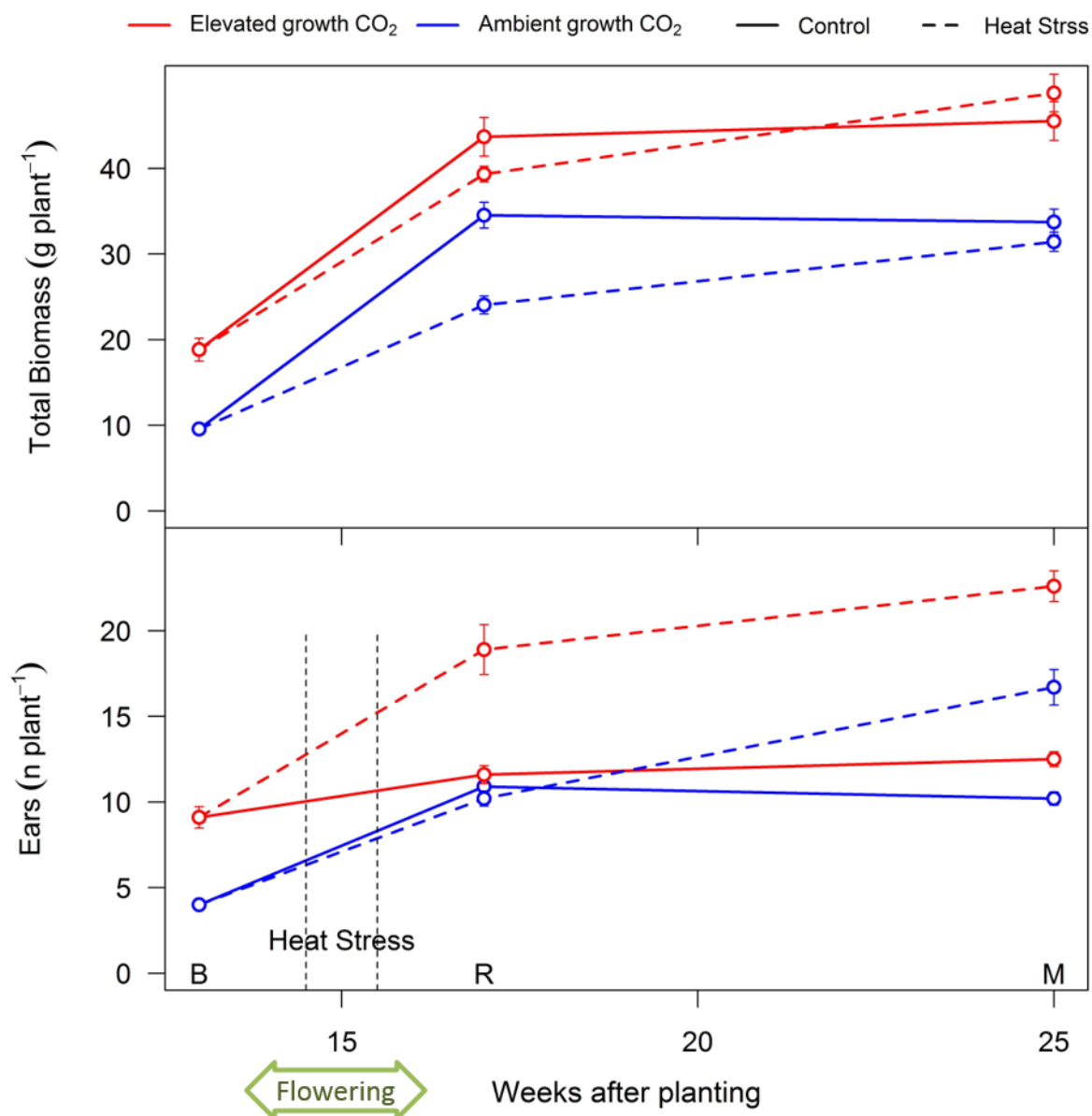


Figure 3.8 Response of biomass and ears (or tillers) to eCO₂ and HS across the life cycle of Scout

Response of total biomass (a) and ear number (b) to eCO₂ and HS at three time points; before HS (B), after recovery from HS (R) and at the final harvest after maturity (M). Ambient and elevated CO₂ grown plants are depicted in blue and red, respectively. Solid and dotted lines represent control and heat stressed plants, respectively. Vertical black dotted lines show the timing of HS. Symbols are means per plant \pm standard errors.

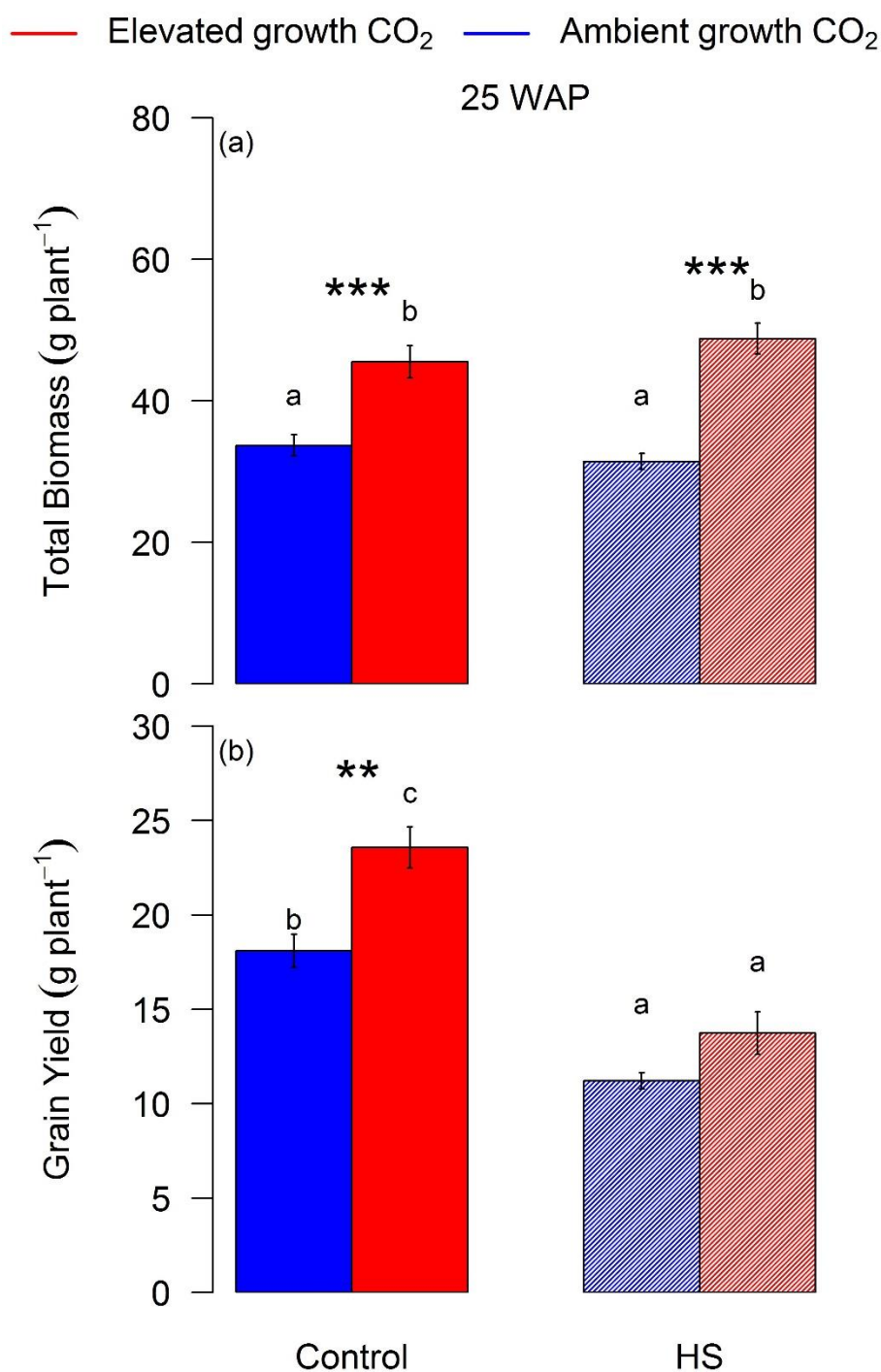


Figure 3.9 Response of plant total biomass and grain yield to elevated CO₂ and heat stress at the final harvest

Bar plot of means \pm standard error for total biomass (a) and grain yield (b) using two-way analysis of variance (ANOVA) measured in ambient (blue) and elevated (red) CO₂ grown plants exposed (HS) or not exposed (Control) to 5-day HS. Bars sharing the same letter in the individual panel are not significantly different according to Tukey's HSD test at the 5% level. Statistical significance levels (t-test) for eCO₂ effect are shown and they are: * = $p < 0.05$; ** = $p < 0.01$; *** = $p < 0.001$.

Table S 3.1 Response of leaf gas exchange parameters to elevated CO₂ and heat stress Summary of leaf gas exchange parameters measured at different time points for Scout grown at ambient CO₂ (aCO₂) or elevated CO₂ (eCO₂) and exposed (H) or not exposed (control) to 5-day heat stress (HS) at the flowering stage. Values are means \pm SE (n= 9-10).

Parameter (mean plant ⁻¹)	Growth CO ₂	Measurement		T1 (13WAP)	HS Cycle (15WAP)			T2 (17WAP)	
		Temp	CO ₂	Control	Before	During (HS)	After (HS)	Recovery	Control
A ($\mu\text{mol m}^{-2}\text{s}^{-1}$)	aCO ₂	25	400	31 \pm 0.3	28.3 \pm 0.8	23.7 \pm 0.8	14.2 \pm 1.2	13.4 \pm 2.6	23.1 \pm 1.2
		25	650	44.2 \pm 0.7	38.1 \pm 1.1	30 \pm 1.1	20.2 \pm 1.4	19.1 \pm 3.3	31.8 \pm 1.9
		35	400	26.4 \pm 0.4	25.4 \pm 0.7	21.7 \pm 0.8	15.6 \pm 1.1	11.2 \pm 2	18.6 \pm 1.9
		35	650	42.3 \pm 0.8	39.8 \pm 0.8	33.1 \pm 1.1	25.9 \pm 1.8	19.8 \pm 2.9	28.7 \pm 2.6
	eCO ₂	25	400	27.4 \pm 0.7	27.1 \pm 0.8	28 \pm 1.1	18.7 \pm 1	22.9 \pm 1	22 \pm 0.9
		25	650	38.6 \pm 1.3	40.5 \pm 1.1	35.4 \pm 1.2	27.1 \pm 1.4	34.6 \pm 1.8	31.6 \pm 1
		35	400	23.3 \pm 0.8	24 \pm 0.7	24.9 \pm 1.2	19.2 \pm 1.1	17.4 \pm 2.1	13.6 \pm 1.9
		35	650	36.8 \pm 0.9	38.9 \pm 1	38.5 \pm 1.8	30 \pm 2.2	29.8 \pm 3.2	22.7 \pm 4
Rd ($\mu\text{mol m}^{-2}\text{s}^{-1}$)	aCO ₂	25	400	-2.4 \pm 0.2	-1.8 \pm 0.1	-2.5 \pm 0.1	-2.4 \pm 0.1	-1.9 \pm 0.3	-1.8 \pm 0.1
		35	400	-4.0 \pm 0.2	-2.9 \pm 0.2	-3.7 \pm 0.1	-3 \pm 0.2	-2.6 \pm 0.2	-2.8 \pm 0.2
	eCO ₂	25	400	-1.9 \pm 0.2	-2.6 \pm 0.2	-2.3 \pm 0.1	-2.9 \pm 0.1	-2.3 \pm 0.2	-2.1 \pm 0.1
		35	400	-3.1 \pm 0.3	-3.7 \pm 0.1	-3.9 \pm 0.2	-4.5 \pm 0.2		-3.3 \pm 0.2
g_s ($\text{mol m}^{-2}\text{s}^{-1}$)	aCO ₂	25	400	0.42 \pm 0.02	0.41 \pm 0.03	0.54 \pm 0.02	0.22 \pm 0.02	0.26 \pm 0.03	0.38 \pm 0.01
		25	650	0.42 \pm 0.02	0.4 \pm 0.03	0.54 \pm 0.02	0.23 \pm 0.02	0.25 \pm 0.02	0.41 \pm 0.02
		35	400	0.29 \pm 0.01	0.4 \pm 0.03	0.49 \pm 0.03	0.41 \pm 0.03	0.26 \pm 0.03	0.23 \pm 0.03
		35	650	0.29 \pm 0.01	0.39 \pm 0.02	0.47 \pm 0.03	0.44 \pm 0.04	0.25 \pm 0.02	0.23 \pm 0.03
	eCO ₂	25	400	0.4 \pm 0.02	0.47 \pm 0.03	0.66 \pm 0.04	0.31 \pm 0.02	0.39 \pm 0.04	0.41 \pm 0.04
		25	650	0.38 \pm 0.02	0.49 \pm 0.02	0.63 \pm 0.03	0.3 \pm 0.02	0.41 \pm 0.02	0.43 \pm 0.03
		35	400	0.26 \pm 0.02	0.43 \pm 0.02	0.54 \pm 0.03	0.36 \pm 0.02	0.24 \pm 0.04	0.19 \pm 0.04
		35	650	0.27 \pm 0.02	0.43 \pm 0.02	0.53 \pm 0.03	0.35 \pm 0.04	0.24 \pm 0.04	0.19 \pm 0.05
PWUE (A_{sat}/g_s) ($\mu\text{mol mol}^{-1}$)	aCO ₂	25	400	74 \pm 3	72 \pm 4	44 \pm 2	66 \pm 3	51 \pm 5	61 \pm 2
		25	650	107 \pm 6	98 \pm 6	56 \pm 3	89 \pm 3	74 \pm 7	77 \pm 4
		35	400	92 \pm 4	65 \pm 3	46 \pm 3	39 \pm 3	43 \pm 6	83 \pm 10
		35	650	146 \pm 6	105 \pm 5	72 \pm 5	61 \pm 4	78 \pm 9	127 \pm 7
	eCO ₂	25	400	69 \pm 2	58 \pm 2	43 \pm 2	62 \pm 4	61 \pm 6	55 \pm 4
		25	650	101 \pm 3	84 \pm 3	57 \pm 3	95 \pm 7	85 \pm 3	75 \pm 5
		35	400	91 \pm 6	57 \pm 2	48 \pm 3	54 \pm 4	75 \pm 6	75 \pm 11
		35	650	139 \pm 10	93 \pm 4	75 \pm 5	99 \pm 15	132 \pm 14	134 \pm 25
Fv'/Fm'	aCO ₂	25	400	0.48 \pm 0.02	0.5 \pm 0.01	0.47 \pm 0.01	0.41 \pm 0.01	0.33 \pm 0.04	0.46 \pm 0.02
		35	400	0.42 \pm 0.01	0.45 \pm 0.01	0.42 \pm 0.02	0.35 \pm 0.01	0.31 \pm 0.04	0.4 \pm 0.01
	eCO ₂	25	400	0.48 \pm 0.03	0.52 \pm 0.01	0.47 \pm 0.01	0.45 \pm 0.01	0.46 \pm 0.01	0.47 \pm 0.01
		35	400	0.41 \pm 0.01	0.47 \pm 0.01	0.41 \pm 0.01	0.41 \pm 0.01	0.42 \pm 0.01	0.37 \pm 0.04
Fv/Fm	aCO ₂	25	400	0.82 \pm 0.01	0.8 \pm 0.01	0.75 \pm 0.01	0.75 \pm 0.01	0.73 \pm 0.02	0.76 \pm 0.01
		35	400	0.79 \pm 0.01	0.8 \pm 0	0.73 \pm 0.02	0.72 \pm 0.01	0.72 \pm 0.04	0.78 \pm 0.01
	eCO ₂	25	400	0.8 \pm 0.02	0.82 \pm 0	0.79 \pm 0.01	0.76 \pm 0.01	0.78 \pm 0.01	0.78 \pm 0.01
		35	400	0.79 \pm 0.01	0.81 \pm 0	0.75 \pm 0.01	0.76 \pm 0.01		0.74 \pm 0.04

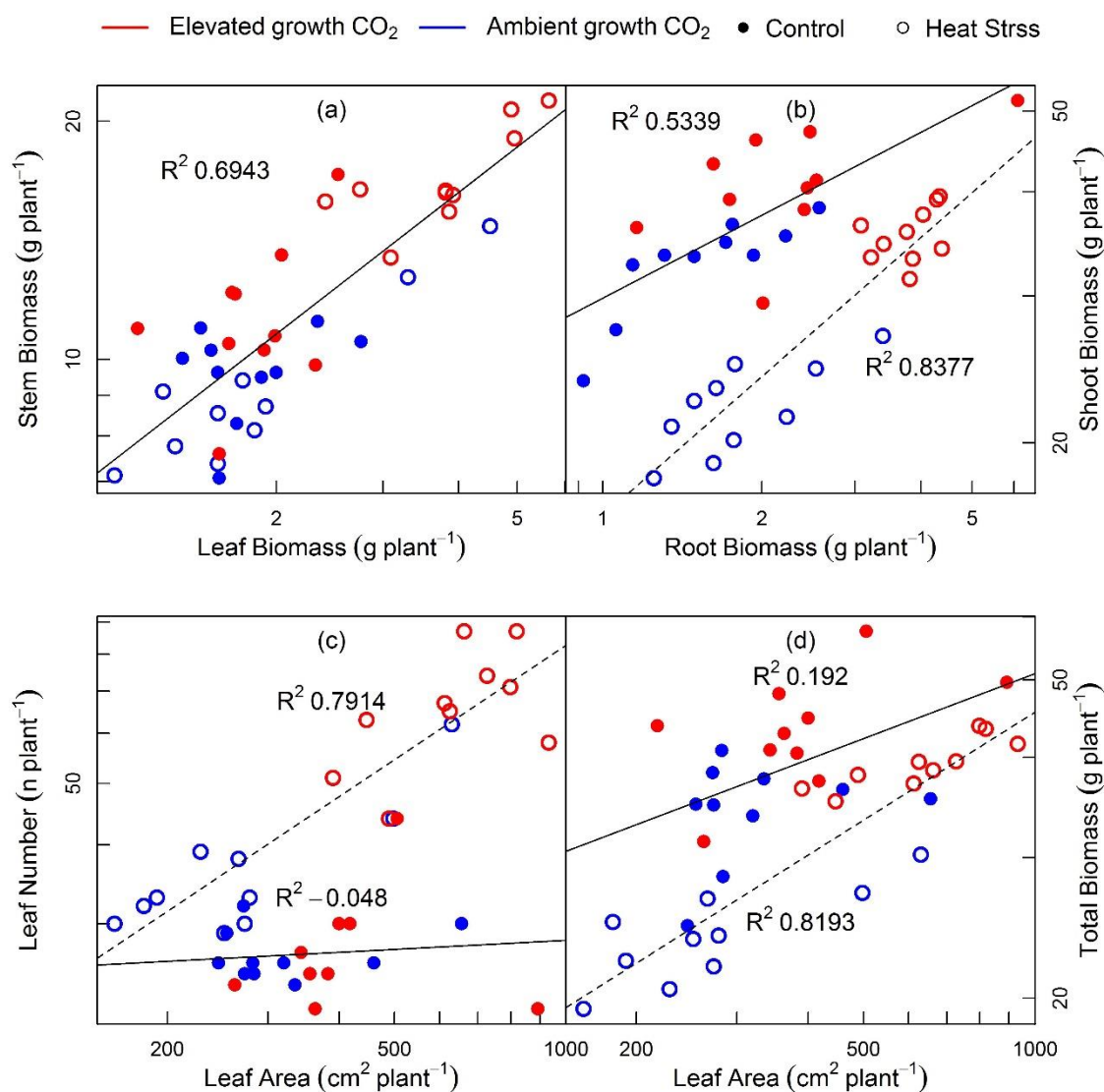


Figure S 3.1 Relationship between biomass and morphological parameters measured 13 weeks after planting at the recovery stage of the HS cycle

The relationships between stem biomass and leaf biomass (a), between root biomass and shoot (stem + leaf) biomass (b), between leaf number and leaf area (c) and between total biomass and leaf area (d). Linear regressions were plotted using log values. Ambient CO₂ and eCO₂ grown plants are depicted in blue and red, respectively. Closed and open circles represent control and heat stressed plants, respectively.







Heat Stress →	Control	HS	
CO ₂ ↓		Old tillers	New tillers
Ambient	(a) 	(b) 	(c) 
Elevated	(d) 	(e) 	(f) 

Figure S 3.2 Response of grain size and morphology to heat stress at the final harvest

Heat stress effect on grain size and morphology from old tillers and new tillers developed after HS under ambient (a, b, c) and elevated CO₂ (d, e, f).

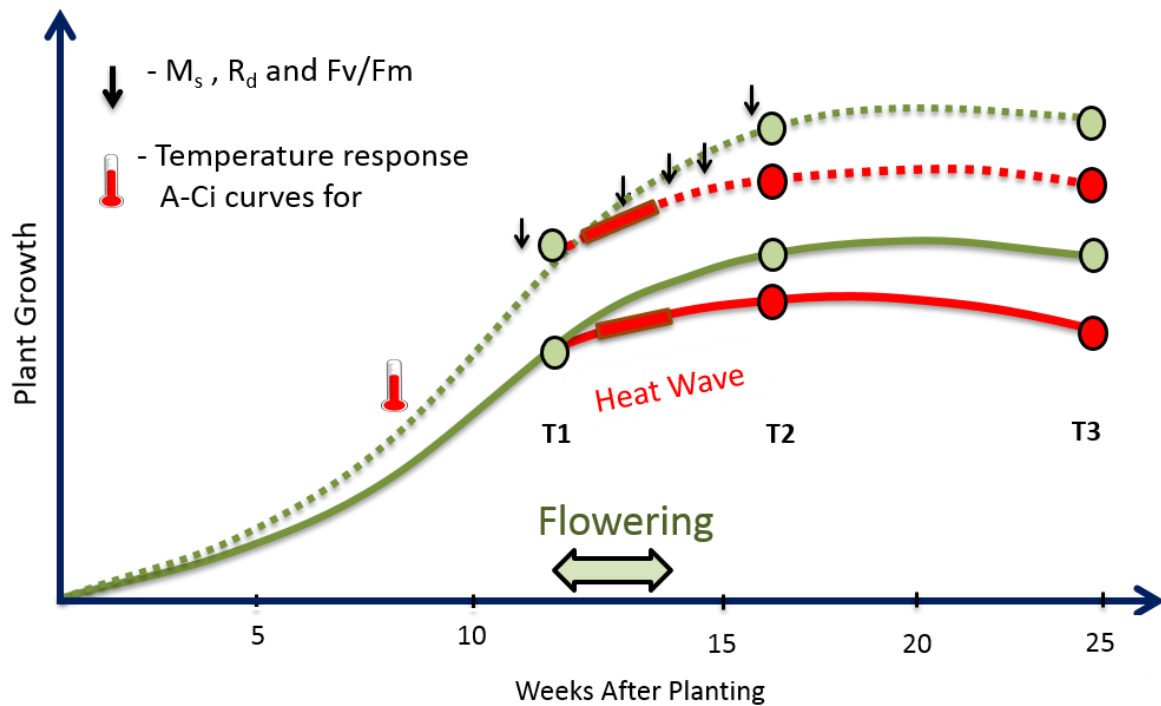


Figure S 3.3 Experimental design

Experimental design depicting plant growth plotted over time showing harvesting at 3-time points (T1, T2 and T3) across the wheat life cycle till maturity, timing of heat stress and measurements. The circles represent harvest of 10 plants at corresponding time point. Green circles on the green solid and dotted lines represent control plants grown at ambient and elevated CO₂ respectively. Red rectangles point to timing and duration of the heat stress (HS) at flowering stage. The red circles on red solid and dotted lines represent plants subjected to heat stress and grown at ambient and elevated CO₂ respectively. Thermometer symbol represents timing of temperature response measurements.

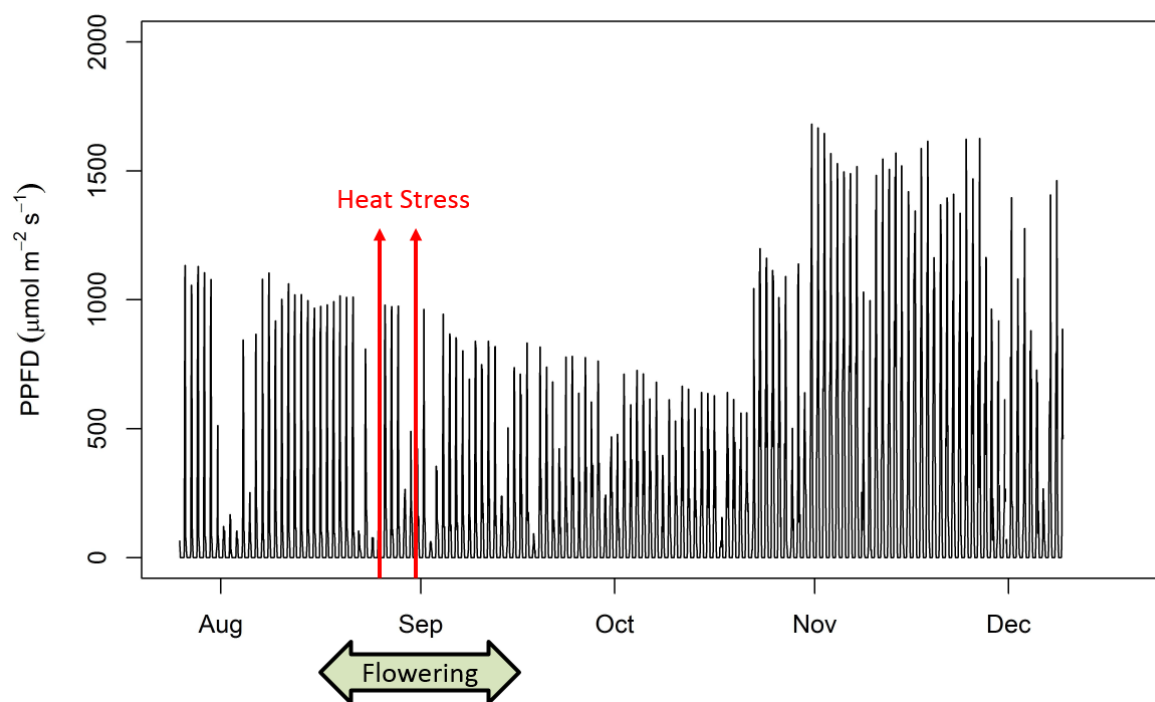


Figure S 3.4 Radiation over time

Radiation over time depicting the radiation load during the experiment highlighted for flowering and heat stress.

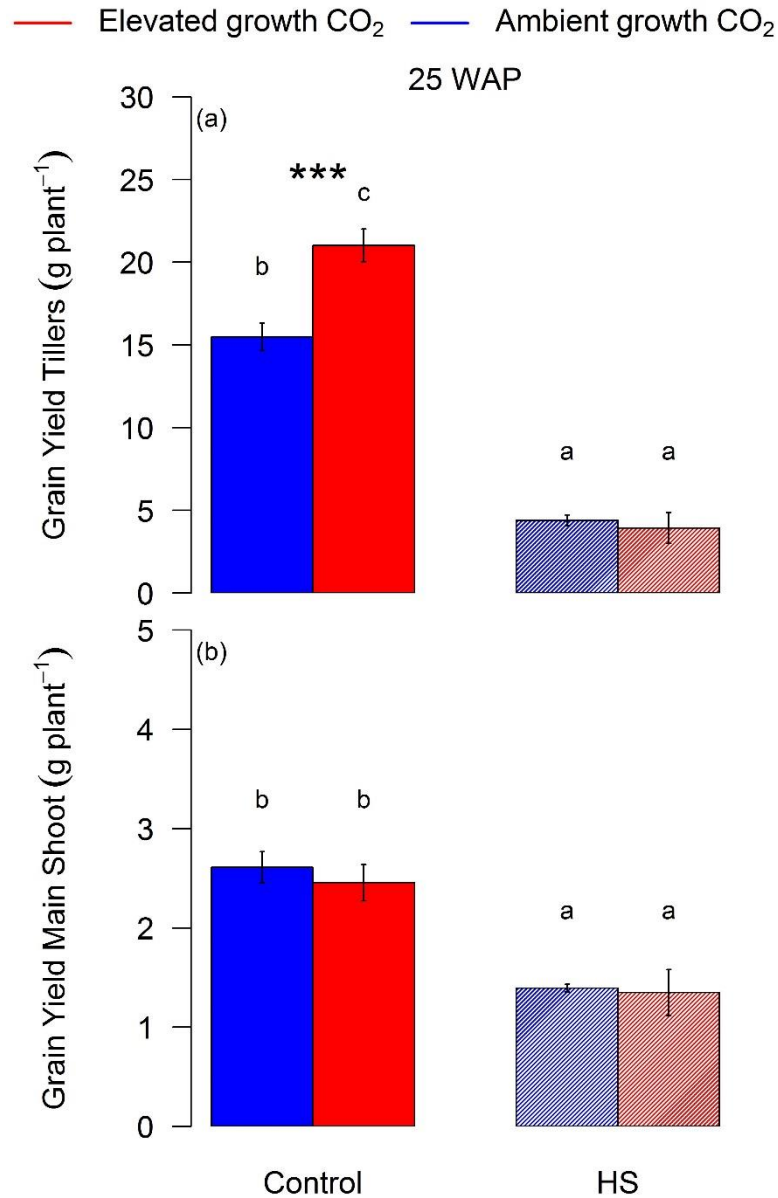


Figure S 3.5 Grain yield of main shoot and tillers

Bar plot of means \pm standard error for grain yield of tillers (a) and main shoot (b) using two-way analysis of variance (ANOVA) measured in ambient (blue) and elevated (red) CO₂ grown plants exposed (HS) or not exposed (Control) to 5-day HS. Bars sharing the same letter in the individual panel are not significantly different according to Tukey's HSD test at the 5% level. Statistical significance levels (t-test) for eCO₂ effect are shown and they are: * = $p < 0.05$; ** = $p < 0.01$; *** = $p < 0.001$.

CHAPTER 4

ELEVATED CO₂ DOES NOT PROTECT WHEAT FROM WATER STRESS IN DRYLAND CONDITIONS

Abstract

Elevated atmospheric CO₂ (eCO₂) concentration is predicted to stimulate the yield of C₃ crops, counteracting the negative impacts of drought on crop productivity. Key mechanisms of how eCO₂ may alleviate the negative effects of drought on photosynthesis, biomass accumulation and grain yield include direct stimulation of photosynthetic CO₂ assimilation rate (A_{sat}); and decreased stomatal conductance (g_s) followed by lower transpiration leading to soil moisture conservation (Ainsworth and Long, 2005). Considering the important interactive effects of eCO₂ and water stress (WS) on agricultural crop production in the context of climate change and food security, more field experiments in dryland cropping systems are urgently required (Gray et al., 2016; Hatfield et al., 2011). To address this knowledge gap, the AGFACE (Agricultural free air CO₂ enrichment) research facility was established in Horsham, Victoria (Australia). In the current study, two commercial wheat cultivars (Scout and Yitpi) were grown at current ambient (400 ppm) and future elevated CO₂ (550 ppm) under rainfed or irrigated field conditions for two growing seasons during 2014 and 2015 to investigate the interactive effects of eCO₂ and WS on photosynthesis, biomass, N content and yield. Leaf gas exchange, volumetric soil water content (SWC), flag leaf area, flag leaf and grain N content, aboveground biomass and grain yield were measured. Irrigation under dryland field conditions created contrasting soil water conditions under both CO₂ conditions. The two seasons received different amount of total rainfall at different times of the developmental stage of the crop. The response of photosynthesis, biomass and grain yield to eCO₂ and WS differed between the two growing seasons. Elevated CO₂ stimulated photosynthesis (+37%), biomass (+17%) and grain yield (+12%), and reduced photosynthetic capacity evident from lower V_{cmax} (-16%) and flag leaf N (-21%) only in 2015. Water stress reduced above-ground dry matter (-55% and -28%) and grain yield (-62% and -32%) in both cultivars and CO₂ treatments in 2014 and 2015, respectively. In conclusion, while the effects of eCO₂ on photosynthesis were more evident in 2015 and the effects of WS were stronger in 2014, the marginal growth stimulation by eCO₂ did not alleviate the negative impacts of WS on photosynthesis and crop biomass and grain yield. Overall there were no interactions between eCO₂ and WS on any of the measured parameters. Consequently, biomass, grain yield and grain quality were oppositely affected by elevated CO₂ and WS.

4.1 Introduction

Ongoing climate change with rising atmospheric CO₂ (eCO₂) concentrations is expected to increase the intensity and frequency of extreme events such as drought which poses a major challenge to agricultural crop production (Asseng et al., 2013; Lobell and Gourdji, 2012). Sustainable production of wheat, a major C₃ crop is highly important for global food security and the world's economy. The direct effects of eCO₂ and environmental stresses on crop growth and productivity are well established, but the interactive effects are still uncertain due to their dependence on the species (or genotypes) and growing conditions which are highly variable. Crop models are widely used to assess the impact of climate change on productivity. However, they cannot consider interacting stresses and their impact on crop productivity. Crop models can be improved by incorporating mechanistic approaches that can account for interactive effects of stresses. Photosynthesis, a key process driving crop growth has the potential to provide a mechanistic approach to crop models as it responds to interactive effects of elevated eCO₂ and drought (Wu et al., 2016, 2017; Yin and Struik, 2009).

During photosynthesis, Rubisco catalyses the capture of atmospheric CO₂ using sunlight and water. Elevated CO₂ stimulates CO₂ assimilation rate (A_{sat}) leading to greater biomass accumulation and crop yield, and often leads to a decrease in stomatal conductance (g_s) which can result in reduced transpiration and soil moisture conservation (Kimball, 1983, 2016; Kimball et al., 1995; Krenzer and Moss, 1975; Mitchell et al., 1993; Sionit et al., 1981). Following long term exposure to eCO₂, plants may 'acclimate' to CO₂ enrichment by reducing photosynthetic capacity due to the lower amount of Rubisco (Ainsworth et al., 2003; Nie et al., 1995; Rogers and Humphries, 2000). According to the C₃ model, photosynthesis is the minimum of three rates: maximal rate of RuBP carboxylation (V_{cmax}), maximal rate of RuBP regeneration or electron transport (J_{max}) and rate of triose phosphate utilisation (TPU) (Farquhar et al., 1980; Sharkey, 1985).

Water stress adversely affects plant growth and productivity mainly by reducing photosynthesis by both stomatal and nonstomatal limitations and plants adapted to arid conditions respond differently than others (Zhou et al., 2013; Zivcak et al., 2013). The photosynthetic decrease is expected to be progressive with decreasing relative water content. Water stress can directly affect photosynthesis by decreasing the availability of CO₂ via reduced stomatal conductance (g_s) (Chaves et al., 2003; Flexas and Medrano, 2002; Flexas et al., 2004) or by metabolic changes (Lawlor and Cornic, 2002; Tezara et al., 1999). Metabolic

changes involve a reduction in ATP content and ribulose biphosphate (RuBP) which are important components of photosynthetic reactions (Tezara et al., 1999). Also, reduction in photosynthesis with decreasing water content causes increase in the number of unutilised electrons generated during light reactions. Unutilised electrons produce reactive oxygen species that may cause structural damage to thylakoid membranes (Lawlor and Cornic, 2002). Consequently, during the initial stomatal phase, eCO₂ can enhance photosynthesis by alleviating the CO₂ limitation due to reduced stomatal conductance. As WS progresses below a certain threshold, photosynthetic reduction cannot be reversed by increasing CO₂ due to metabolic limitation (Lawlor and Cornic, 2002). Therefore, the interactive effects of WS and eCO₂ on crop productivity depends on the severity and duration of the drought period.

Elevated CO₂ enhancement in growth is expected to ameliorate the negative impacts of drought (Hatfield et al., 2011). However, the eCO₂ response of crops varies under different soil moisture regimes (Ewert et al., 2002) and field studies addressing eCO₂ response of crops in the field are scarce covering limited number of locations and growing seasons with little to no drought stress, limiting their use in generalising predictions based on previously published literature (Hatfield et al., 2011; Leakey et al., 2012). Given that droughts are expected to occur more frequently in the near future, improving our understanding of the interactive effects of eCO₂ and drought on wheat growth and productivity is critically important.

To address this knowledge gap, we investigated the response of wheat growth and photosynthesis to eCO₂ and drought in the typical dryland field conditions of the Australian wheat belt. Two commercial wheat lines, Scout and Yitpi, with similar genetic background but distinct agronomic features, were selected for analysing the interactive effects of eCO₂ and drought on photosynthesis, biomass and grain yield. Scout is a midseason maturity line with very good early vigour that can produce leaf area early in the season. Scout has a putative water-use efficiency (WUE) gene, which has been identified using carbon isotope discrimination. Yitpi is a line with good early vigour, freely tillering and long maturity which flowers slightly later than the flowering frame (Seednet, 2005).

Stomata regulate water loss by transpiration. In response to WS, leaf rolling is observed in wheat, which reduces the effective leaf area and transpiration, and thus, is a potentially useful drought avoidance mechanism in arid areas (Clarke, 1986). Plant water use response to eCO₂ depends on how the leaf transpiration, leaf area index (LAI) and canopy temperature respond to eCO₂ (Hatfield et al., 2011). Elevated CO₂ is expected to decrease g_s and save water loss

through transpiration, leading to increased soil water (Leakey et al., 2009). Thus, I hypothesised that leaf level water use efficiency will increase under eCO₂ and soil may retain higher water due to decreased plant water use (hypothesis 1).

Long term exposure to eCO₂ has been associated with photosynthetic acclimation in previous FACE studies, resulting in reduced photosynthetic capacity and N content. Acclimation is usually observed under N limitation but not under adequate N supply (Ainsworth and Long, 2005; Seneweera, 2011). Thus, I predicted that eCO₂ will stimulate photosynthesis without acclimation under the well-fertilised conditions of the AGFACE (hypothesis 2).

Water stress has been found to progressively reduce photosynthesis with a decrease in relative water content via stomatal and nonstomatal reductions involving metabolic changes such as reduction in RuBP synthesis (Flexas et al., 2004; Lawlor and Cornic, 2002). Hence, it is expected that WS will reduce net photosynthesis and growth leading to reduced grain yield due to both reduced g_s and biochemical limitations such as reduced J_{max} (hypothesis 3).

Elevated CO₂ is predicted to stimulate the yield, counteracting the negative impacts of drought on crop productivity by direct stimulation of A_{sat} leading to greater biomass accumulation and yield, and indirectly by decreasing g_s and leaf transpiration leading to soil moisture conservation. Many studies have shown that the response to eCO₂ is greater under water limited conditions (Kimball et al., 1995; Wall et al., 2006). Hence, I predict that the positive effects of eCO₂ on photosynthesis and yield will be stronger under rainfed conditions (water stress) relative to irrigated conditions (hypothesis 4)

To test these hypotheses, Scout and Yitpi were grown at current ambient and future elevated CO₂ under rainfed or irrigated conditions over two growing seasons (2014 and 2015). Irrigation of the dryland field rings created contrasting soil water conditions under current ambient and future elevated CO₂ partial pressures.

4.2 Material and methods

3.2.1 Plant material

The wheat cultivars Scout and Yitpi having a genetically similar background but distinct agronomic features were selected for the experiment. Scout is a high yielding variety with very good grain quality (Pacificseeds, 2009) and has a carbon isotope discrimination gene that putatively increases water use efficiency (WUE). Yitpi is a good early vigour, freely tillering and long maturity line which flowers slightly later than the flowering frame (Seednet, 2005).

3.2.2 Site description

The experiment was conducted at the Australian Free Air CO₂ Enrichment (AGFACE) research facility during 2014 and 2015 field growing seasons. The AGFACE site is located 7 km west of Horsham, Victoria, Australia (36°45'07''S, 142°06'52''E; 127m above sea level), which is a semi-arid region of the Australian wheat belt. The soil at AGFACE site is a Vertosol according to the Australian Soil Classification and has approximately 35% clay at the surface increasing to 60% at 1.4m depth. The region has a Mediterranean climate but with drier and cooler winters. The region receives 448 mm long-term (more than 100 years) average annual rainfall and has a minimum of 8.2°C, and a maximum of 21.5°C long-term average temperature.

3.2.3 Experimental setup and general management

The experimental design included four ambient CO₂ (aCO₂, 400 µl L⁻¹) and four elevated CO₂ (eCO₂, 550 µl L⁻¹) rings of 12 m diameter. Elevated CO₂ rings were equipped with stainless steel pipes injecting CO₂ in the opposite direction of the wind to the atmosphere through 0.3 mm laser drilled holes facing outward. CO₂ concentrations were averaged every minute with infrared gas analysers (IRGAs) (IRGA, SBA-4 model with an Original Equipment Manufacturer board; PP Systems Ltd) positioned at the centre of each ring. Average of 550 µl L⁻¹ of CO₂ concentration was maintained from sunrise to sunset using automated control further described by Mollah et al., (2009). Plants were grown in 4m long and 1.7m wide randomly allocated sub-plots with 0.27 m row spacing. A summary of the climatic conditions during the growing season of this study is given in Fig 4.1.

Agronomic management at both sites was according to local cultural practices, including spraying fungicides and herbicides, as needed. The AGFACE project started in 2007 and the

soil properties were examined before starting the experiment which has been described earlier (Bahrami et al., 2017; Fitzgerald et al., 2016; Mollah et al., 2009). The experiment included multiple cultivars and treatment combinations, but I restricted my study to two commercial cultivars (cv. Scout and cv. Yitpi) that were grown under two water regimes (rainfed and supplemental irrigation). During dry periods, supplemental irrigation was applied to all plants to prevent crop loss. Thus, drought in the current study was within the range of precipitation that supports the crop production.

Meteorological data were collected either with an on-site weather station or from a nearby Bureau of Meteorology (BOM) station (Station #079023, Polkemmet), located about 8 km from the Horsham site. The Polkemmet site data were used to fill in missing values from the AGFACE station. Daily average air temperatures, air humidity, vapour pressure deficit (VPD), soil temperature and rainfall were recorded during growing season in 2014 and 2015 (Figure 4.1). Volumetric soil water content (SWC) was measured at sowing and harvest using a hydraulically operated soil sampler over a range of depths including 100 mm, 200 mm, 300 mm, 400 mm, 600 mm and 1000 mm. Site bulk density was measured from 70 mm diameter \times 75 mm deep sampling rings from each octagonal area.

3.2.4 Biomass and grain yield measurements

Biomass samples were collected at the final harvest. Plant material was air dried before threshing, and then dried at 70 °C, so that biomass and grain yield are expressed at 0% water content. Above ground biomass, tiller number, ear number, harvest index, grain weight, grain number, grain protein, total nitrogen (N) uptake, nitrogen use efficiency (NUE) of grain yield and NUE of biomass were derived from these harvest samples and used to calculate the variables reported.

3.2.5 Leaf gas exchange measurements

Leaf gas exchange measurements were performed for two seasons (2014 and 2015) at the flowering stage using a portable open gas exchange system (LI-6400XT, LI-COR, Lincoln, USA). Light-saturated photosynthetic rate (A_{sat}), stomatal conductance (g_s), the ratio of intercellular to ambient CO₂ (C_i/C_a), and leaf transpiration rate were measured.

Leaf gas exchange measurements were taken around midday (from 10 am to 3 pm) on attached last fully expanded leaves (flag leaf) of the main stem of plants at the flowering stage.

Instantaneous gas exchange measurements were performed at a photosynthetic photon flux density of $1500 \mu\text{mol m}^{-2} \text{s}^{-1}$, $400 \mu\text{l L}^{-1}$ CO_2 partial pressures and field leaf temperatures. Before each measurement, the leaf was allowed to stabilise for 10-20 minutes until it reaches a steady state of CO_2 uptake. The response of the A_{sat} to variations in sub-stomatal CO_2 mole fraction (C_i) (A- C_i response curve) was measured in 8 steps of CO_2 concentrations (50, 100, 230, 330, 420, 650, 1200 and $1800 \mu\text{l L}^{-1}$) at field leaf temperatures. Stimulation in A_{sat} by $e\text{CO}_2$ was determined by comparing A_{sat} measured at CO_2 420 and $650 \mu\text{l L}^{-1}$ during the A- C_i response curves. Photosynthetically active leaves were selected for leaf gas exchange measurements on rainfed plants. One leaf per treatment combination in each ring was used for the leaf gas exchange measurements.

3.2.6 Data analysis

Gas exchange measurements were performed on three to four replicates per line per treatment. Data analysis and plotting were performed using R (R Core Team., 2017). The effect of treatments and their interaction was analysed using linear modelling with two-way ANOVA in base R. Independent treatment effect was performed using t-test.

Plantecophys package based on Farquhar von Caemmerer Berry (FvCB) model in R was used to fit the A- C_i response curves using mesophyll conductance (g_m) and temperature response of photosynthetic parameters measured in the glasshouse grown plants reported in chapter 2 (Duursma, 2015). A_{sat} at C_i of $300 \mu\text{l L}^{-1}$, maximal rate of RuBP carboxylation (V_{cmax}) and maximal rate of RuBP regeneration (J_{max}) for D-ribulose-1,5-bisphosphate carboxylase/oxygenase (Rubisco) at 25°C leaf temperature were estimated using the A- C_i response curves by two methods. In the first method, Photosyn function in plantecophys package was used to estimate A_{sat} at C_i of $300 \mu\text{l L}^{-1}$ and 25°C leaf temperature. The fits were also used to estimate V_{cmax} and J_{max} at 25°C leaf temperature using temperature response parameters measured in the glasshouse-grown plants. In the second method, one Point V_{cmax} and J_{max} were determined using spot gas exchange measurements at common CO_2 ($400 \mu\text{l L}^{-1}$) at field leaf temperatures and then corrected to 25°C leaf temperature using photosynthetic temperature response parameters of the glasshouse-grown plants as follows:

$$\text{One point } V_{\text{cmax}} = (A_c + R_d) \cdot \left[\frac{C_i + K_m}{C_i - \Gamma^*} \right] \quad (1)$$

$$\text{One point } J_{\max} = 4 \cdot (A_j + R_d) \cdot \left[\frac{C_i + 2 \cdot \Gamma^*}{C_i - \Gamma^*} \right] \quad (2)$$

Where, A_c and A_j are photosynthetic rates and C_i is the intercellular CO_2 partial pressure measured at common CO_2 ($400 \mu\text{L L}^{-1}$); Γ^* is the CO_2 compensation point (Bernacchi et al., 2002); K_m is the Michaelis-Menten constant determined using K_c and K_o (Bernacchi et al., 2002); and R_d is dark respiration measured in glasshouse-grown plants. Temperature dependencies of V_{\max} , K_c , K_o , and Γ^* were determined using values in literature (Table 4.1) and Arrhenius equation as follows,

$$f(Tk) = k_{25} \cdot \exp \left[\frac{E_a \cdot (Tk - 298)}{R \cdot 298 \cdot Tk} \right] \quad (3)$$

Where E_a is the activation energy (in J mol^{-1}) and k_{25} is the value of the parameter at 25°C . R is the universal gas constant ($8.314 \text{ J mol}^{-1} \text{ K}^{-1}$) and Tk is the leaf temperature in K. The activation energy term E_a describes the exponential rate of rising enzyme activity with the increase in temperature. A peaked function (Harley et al., 1992) derived Arrhenius function was used to fit the temperature dependence of J_{\max} , and is given by the following equation:

$$f(Tk) = k_{25} \cdot \exp \left[\frac{E_a \cdot (Tk - 298)}{R \cdot 298 \cdot Tk} \right] \cdot \left[\frac{1 + \exp \left(\frac{298 \cdot \Delta S - H_d}{298 \cdot R} \right)}{1 + \exp \left(\frac{Tk \cdot \Delta S - H_d}{Tk \cdot R} \right)} \right] \quad (4)$$

Where E_a is the activation energy and k_{25} is the J_{\max} value at 25°C , H_d is the deactivation energy and S is the entropy term. H_d and ΔS together describe the rate of decrease in the function above the optimum. H_d was set to constant 200 kJ mol^{-1} to avoid over parametrisation.

4.3 Results

Two commercial wheat lines Scout and Yitpi were grown under current ambient ($400 \mu\text{L L}^{-1}$, daytime average) and future elevated ($550 \mu\text{L L}^{-1}$, daytime average) CO_2 conditions for two growth seasons (GS) from April to December in 2014 and 2015. Except for slightly higher total rainfall in 2014 (GS mean, 183mm) relative to 2015 (GS mean, 147mm), the rest of the daily average growth conditions including air temperature (GS mean, $\sim 11^\circ\text{C}$), air humidity (GS mean, $\sim 72\%$), vapor pressure deficit (VPD) (GS mean, $\sim 0.45 \text{ kPa}$), soil temperature (GS mean, $\sim 15^\circ\text{C}$) and radiation profile were similar in 2014 and 2015 (Figure 4.1, Figure S4.2).

4.3.1 Elevated CO_2 did not affect soil water content under irrigated or rainfed conditions

Irrigation successfully created two different soil water conditions during the peak growth period from tillering to flowering stage (August to October) in 2014 and 2015 (Figure 4.2). Volumetric soil water content (SWC, $\text{m}^3 \text{m}^{-3}$) recorded over a range of depths differed from mid to late season (April to November) and was lower under rainfed relative to irrigated conditions mainly at 300 mm in both GS, and only at 400 and 600 mm depth in 2014. The difference in SWC between rainfed and irrigated plots was higher in 2014 relative to 2015. Elevated CO_2 did not affect SWC in any of the two growth seasons under irrigated or rainfed conditions for either of the wheat cultivar (Figure 4.2).

4.3.2 Elevated CO_2 stimulated photosynthesis and grain yield similarly under irrigated or rainfed conditions

Both cultivars had similar light-saturated photosynthetic rates (A_{sat}) and stomatal conductance (g_s) (Figure 4.3). Elevated CO_2 stimulated A_{sat} (measured at growth CO_2) similarly (37%, $p < 0.001$) but did not affect g_s in either growth season or cultivar under rainfed or irrigated conditions. Water stress decreased A_{sat} measured at growth CO_2 only in 2014 (22%, $p = 0.02$) but did not affect A_{sat} measured at common CO_2 despite significant changes in g_s with water availability (Figure 4.3; Tables 4.2, S4.1 and S4.2). Under rainfed conditions, g_s measured at growth CO_2 was lower (-57%, $p < 0.001$) in 2014 and higher (+93%, $p < 0.001$) in 2015 relative to irrigated conditions. Hence, leaf-level photosynthetic water use efficiency (PWUE) increased (+86%, $p < 0.001$) in 2014 and decreased (-43%, $p = 0.009$) in 2015 under rainfed conditions.

Similarly, when measured at common CO_2 , WS decreased g_s in 2014 (-48%, $p = 0.001$) and increased in 2015 (+35%, $p = 0.01$). Hence, leaf-level photosynthetic water use efficiency

(PWUE) increased (+57%, $p < 0.001$) in 2014 and decreased (-19%, $p = 0.002$) in 2015 under rainfed conditions. Despite having carbon isotope discrimination gene Scout had similar PWUE (Tables 4.2, S4.1) and $\delta^{13}\text{C}$ signature (Figure S4.1) relative to Yitpi. However, C_i measured at common CO_2 decreased similarly (15%, $p \text{ value} < 0.001$) in both growing seasons under rainfed conditions (Tables 4.2, S4.1).

4.3.3 Elevated CO_2 reduced photosynthetic capacity only in 2015

Effect of $e\text{CO}_2$ on photosynthetic capacity was determined using instantaneous leaf gas exchange measured at common CO_2 ($400 \mu\text{L L}^{-1}$) as well as the A- C_i response curves performed using leaves which had stable photosynthetic rates. A_{sat} (measured at common CO_2), one point V_{cmax} and one point J_{max} (estimated from instantaneous leaf gas exchange at common CO_2) corrected to 25°C leaf temperature did not change with cultivar, growth CO_2 or irrigation regime (Figure 4.4; Tables 4.2, S4.1 and S4.2).

In contrast, photosynthetic acclimation was observed in 2015 in response to growth at $e\text{CO}_2$ for both cultivars under irrigated and rainfed conditions. In particular, $e\text{CO}_2$ reduced V_{cmax} estimated from A- C_i response curves (-16%, $p = 0.01$) and increased A_{sat} per unit leaf N measured at common CO_2 (+28%, $p = 0.03$) in 2015 in both cultivars under irrigated and rainfed conditions. The reduction in photosynthetic capacity was supported by a reduction in flag leaf N per unit area (-21%, $p = 0.005$) due to growth at $e\text{CO}_2$ in 2015 in both cultivars and irrigation conditions (Tables 4.3, and S4.3). However, J_{max} and A_{sat} at C_i of $300 \mu\text{L L}^{-1}$ estimated from the A- C_i response curves did not change with cultivar, growth CO_2 or irrigation regime (Figure 4.4; Tables 4.2, S4.1 and S4.2).

The correlation between A_{sat} and g_s measured at common CO_2 was stronger in 2015 ($r^2 = 0.84$, $p < 0.001$) relative to 2014 ($r^2 = 0.67$, $p < 0.001$) across all treatments (Figure 4.5a-b). In 2014, irrigated plants had higher A_{sat} and g_s relative to rainfed plants, while in 2015 rainfed plants showed slightly higher A_{sat} and g_s relative to irrigated plants in both cultivars. Overall, growth CO_2 did not significantly change the relationship between A_{sat} and g_s under irrigated or rainfed conditions for both cultivars. There was no correlation between A_{sat} measured at common CO_2 and leaf N across all treatments (Figure 4.5c-d).

In order to test whether variability in leaf gas parameters were driven by SWC, the relationships between the two sets of parameters were plotted (Figure 4.6). In contrast to expectation, soil water content did not correlate with A_{sat} , g_s or C_i measured at common CO_2 (Figure 4.6). To

check whether the lack of correlation was due to changes in leaf N, SWC plotted against A_{sat} per unit leaf N; which also showed no correlation (Figure 4.6).

4.3.4 Water stress equally reduced biomass and grain yield under aCO₂ and eCO₂

The two cultivars Scout and Yitpi generally had similar agronomic characteristics across all treatments and growing seasons, except for higher (+16%, $p = 0.01$) grains per ear and lower (-5%, $p = 0.006$) grain size in Scout relative to Yitpi only in 2015 (Figures 4.7 and 4.8; Tables 4.3 and S4.3).

Elevated CO₂ stimulated biomass, grain yield and grain size (1000 grain weight) in both cultivars in 2015 but not in 2014. Increased biomass (+17 %, $p = 0.05$), grain yield (+12%, $p = 0.2$) and grain size (+6 %, $p = 0.002$) due to eCO₂ in 2015 caused N dilution and led to a reduction in grain protein content (-16 %, $p < 0.001$) (Figures 4.7 and 4.8; Tables 4.3 and S4.3).

Water stress similarly reduced above ground dry matter and grain yield in both cultivars and under both aCO₂ and eCO₂. However, the decrease in above ground dry matter and grain yield due to WS was higher in 2014 (-55% $p < 0.001$ and -62%, $p < 0.001$, respectively) relative to 2015 (-28% $p < 0.001$ and -32%, $p < 0.001$ respectively). Water stress reduced grain yield by decreasing total grain number (-60%, $p < 0.001$ and -30%, $p < 0.001$) as a result of reduced number of tillers (-28%, $p < 0.001$ and -13%, $p < 0.001$), ears (-32%, $p < 0.001$ and -13%, $p = 0.003$) and grains per ear (-40%, $p < 0.001$ and -20%, $p < 0.001$) in 2014 and 2015, respectively (Figures 4.7 and 4.8; Tables 4.3 and S4.3). Water stress reduced flag leaf area more in 2014 (50%, $p < 0.001$) than 2015 (26%, $p < 0.001$) but flag leaf mass per unit area did not change with cultivar, growth CO₂ or irrigation regime in either growth season (Table S4.3).

N uptake was lower (-38%, $p < 0.001$) under rainfed relative to irrigated conditions in both cultivars, growth seasons and CO₂ treatments. Water stress reduced N uptake more in 2014 (-56 %, $p < 0.001$) relative to 2015 (-19 %, $p < 0.001$) in both cultivars and CO₂ treatments. Elevated CO₂ increased nitrogen use efficiency for biomass (NUE_b) more in 2015 (+37%, $p = 0.001$) relative to 2014 (+14%, $p = 0.001$) (Table S4.1). eCO₂ and WS antagonistically affected nitrogen use efficiency for grain yield (NUE_g). eCO₂ increased NUE_g only in 2015 (+22%, $p < 0.001$) while WS reduced NUE_g similarly (-16%, $p = 0.01$) in 2014 and 2015 in both cultivars and CO₂ treatments (Figures 4.8; Tables 4.3 and S4.3).

4.4 Discussion

The current study investigated the interactive effects of eCO₂ and water stress (WS) on soil water content (SWC), photosynthesis, biomass and grain yield in two commercial wheat cultivars growing under dryland field conditions and free air CO₂ enrichment (FACE). The response of photosynthesis, biomass and grain yield to eCO₂ and WS differed between the two growth seasons. Elevated CO₂ stimulated grain yield and reduced photosynthetic capacity to a greater extent in 2015 relative to 2014. The negative impacts of WS were stronger in 2014 and eCO₂ did not protect plants from WS. The latter response was evident in the lack of interaction between the irrigation and CO₂ treatments for any of the measured photosynthetic or yield parameters (Tables 2.4 and 2.3).

4.4.1 Effect of eCO₂ on soil water content

Plants grown at eCO₂ are expected to be more water use efficient which may decrease plant water use leading to higher SWC under eCO₂, while increased biomass due to eCO₂ stimulation may utilise the saved available water ultimately causing no significant changes to soil water content under aCO₂ or eCO₂ (Ainsworth and Rogers, 2007). Hence soil water conservation at eCO₂ may be detected as either increased SWC or increased biomass in the dry plots as a result of an interaction between CO₂ and water treatments.

In the current study, eCO₂ did not affect g_s (measured at common or growth CO₂) or SWC for both cultivars under irrigated or rainfed conditions. Thus, in contrast to the first hypothesis that eCO₂ will conserve soil water by decreasing transpiration via reduced g_s , no effect of eCO₂ on g_s or SWC was observed. Unchanged SWC can be due to a lack of stomatal response to eCO₂ and/or the use of saved water by plants to support increased biomass under eCO₂ (Ainsworth and Rogers, 2007). However, there was no interaction between CO₂ and water treatments on biomass accumulation in the current AGFACE study.

The lack of significant effect of eCO₂ on g_s in the current study may be due to the ability of wheat to acclimate to environmental stresses (Gray et al., 1996; Mehta et al., 2010). Lower leaf area due to WS reduces plant water loss and may enable leaf photosynthesis and stomatal conductance to function at non-stressed levels (Kelly et al., 2016). In addition, environmental factors alter the response of g_s to eCO₂ which may explain the lack of g_s response to eCO₂ (Ainsworth and Rogers, 2007). Recent FACE study in soybean showed that eCO₂ does not always lead to soil water conservation and the variation in soil water correlates with

environmental conditions rather than plant transpiration (Gray et al., 2016). A recent FACE study with the grass understory of a eucalypt woodland also reported no effect of eCO₂ on g_s and SWC (Pathare et al., 2017). The extent to which modest changes in crop transpiration such as those usually brought about by eCO₂ depends on factors such as soil evaporation, LAI, canopy structure and wind, all of which determine the degree of coupling between the canopy and the atmosphere (Ghannoum et al., 2007).

4.4.2 Effect of eCO₂ and WS on photosynthesis

Elevated CO₂ stimulated A_{sat} measured at growth CO₂ with a stronger eCO₂ response in 2015 which was also associated with acclimation evident from reduced V_{cmax} and leaf N content. This suggests that the wheat plants were N limited during the 2015 season even though the rings were fertilised according to standard farming practices in the area. Photosynthetic stimulation by eCO₂ despite acclimation has been consistently observed in FACE studies (Ainsworth and Long, 2005; Leakey et al., 2009; Long et al., 2004). Water stress did not affect A_{sat} (measured at common or growth CO₂) in leaves selected for gas exchange; these usually had openly displayed leaves with stable and good assimilation rates but low g_s (-48% measured at common CO₂) in both cultivars and CO₂ treatments in 2014 when WS was stronger. Also, photosynthetic capacity estimated from A-C_i response curves and spot measurements for A_{sat} at common CO₂ were not affected by WS. Thus, the second hypothesis suggesting that WS may reduce RuBP regeneration capacity (Lawlor and Cornic, 2002; Osakabe et al., 2014; Tezara et al., 1999) in wheat was rejected along with the conclusion that changes in photosynthetic measurements will correlate with changes in biomass and grain yield.

Water stress has been found to reduce photosynthesis through both stomatal and nonstomatal limitations (LAWLOR, 2002; Lawlor and Cornic, 2002; Lawlor and Upreti, 1993; Zhou et al., 2013). As the leaves were selected for good stable photosynthetic rates (i.e., non-rolled leaves), it is possible that the nonstomatal or biochemical limitations were not captured. Given that WS marginally reduced C_i (-15 %), the primary reason for the reduction in net canopy CO₂ uptake may have been the WS-induced leaf rolling and stomatal closure to prevent water loss through transpiration (Clarke, 1986). Both leaf rolling and lower rates of canopy development under WS reduce effective leaf area, and hence overall water use. In turn, this alleviates WS allowing leaves to photosynthesis at non-stressed rates (Kelly et al., 2016).

4.4.3 Elevated CO₂ could not ameliorate WS damage

The observed biomass response to eCO₂ (+17%) in the current study was similar to the reported meta-analysis means for crops around ~18% (Ainsworth and Long, 2005; Kimball, 2016). The biomass and grain yield response to eCO₂ are generally of similar magnitude (Kimball, 2016), however, the observed grain yield response to eCO₂ (+12%) in the current study was not statistically significant and slightly lower than the biomass response.

Many studies have addressed the interactive effects of eCO₂ and WS on growth and yield under different growth conditions. Relative to well watered conditions, the relative response to eCO₂ under WS can be greater (Kimball, 2016; Kimball et al., 1995; Schütz and Fangmeier, 2001) or lower (Fitzgerald et al., 2016; Wu et al., 2004) depending on environmental factors. Stimulation in A_{sat} was similar under irrigated or rainfed conditions in contrast to previous studies that found an increase in the A_{sat} stimulation by eCO₂ under water-limited conditions (Kimball et al., 1995; Wall et al., 2006). Water stress in the current study equally reduced N uptake, biomass and grain yield under aCO₂ or eCO₂, while marginal stimulation in growth, biomass and grain yield by eCO₂ was not enough to ameliorate the large negative effects of WS. Thus, the third hypothesis that eCO₂ response will be stronger under WS was rejected.

Similar growth response eCO₂ under either water regime is indicative of a lack of interaction between eCO₂ and WS. Leaf rolling, which significantly reduced photosynthesis under WS, cannot be reversed by eCO₂ in the absence of substantial soil water conservation. Given that eCO₂ did not lead to soil water saving, WS may have equally reduced biomass and grain yield under both CO₂ treatments. A previous FACE study with wheat in similar conditions has reported reduced eCO₂ stimulation in dry conditions when compared within site, while increased eCO₂ response when compared across sites (Fitzgerald et al., 2016). That study concluded that eCO₂ response varies according to within growth season variation in water, temperature and timing of water or temperature stress. The apparent contradiction in yield responsiveness across the two sites may have been caused by the positive response to pre-anthesis minimum temperatures and pre-anthesis amount of water input and negative dependence on post anthesis high temperatures (Fitzgerald et al., 2016).

4.3.4 Response of photosynthesis, biomass and grain yield differed between the two growth seasons

The elevated CO₂ response of overall parameters including V_{cmax} , flag leaf N per unit leaf area, grain size (1000 grain weight), biomass and grain yield was only observed in 2015 but not in

2014. The absence of significant eCO₂ response in 2014 could be due to stronger WS associated with large variation among replicates evident from higher standard errors for overall parameters in 2014 relative to 2015. With field experiments especially including FACE, it is not uncommon to have fewer replications and higher variability. Strong WS in 2014 may have further increased the variability.

4.4.5 Elevated CO₂ and WS act antagonistically on grain quality

Photosynthetic enhancement by eCO₂ increased biomass and grain yield however the quality of the wheat grain was low due to lower N and consequently lower protein content. Reduction in grain N content accompanied with increased grain yield, due to trade off between yield and quality, is often observed and is consistent with the literature (Pleijel and Uddling, 2012; Taub et al., 2008). In contrast, WS reduced biomass and grain yield but increased grain N and hence the protein concentration, while the nitrogen use efficiency of grain yield (NUEg) was reduced due to decreased N uptake under WS. Thus, in the future climate with elevated CO₂ and limited water, we may see a reduction in yield but not the quality due to counteracting of eCO₂ and WS on grain quality that may nullify each other.

4.5 Conclusions

Elevated CO₂ stimulated photosynthesis with a stronger effect in 2015 and was associated with a reduction in photosynthetic capacity and leaf N content. Water stress reduced photosynthesis due to stomatal closure and leaf rolling to minimize transpiration. Under field conditions, it was not possible to measure rolled and functionally inactive leaves. The selection of functional leaves allowed stable photosynthetic measurements under rainfed conditions. However, this meant that the reduction in photosynthesis due to WS was not captured in these leaves. Biomass, grain yield and grain quality were oppositely affected by elevated CO₂ and WS. Marginal stimulation by eCO₂ could not alleviate the large negative effects of WS but the grain quality was maintained in plants grown under eCO₂ and WS relative to aCO₂ and irrigated conditions. In conclusion, reduction in canopy photosynthesis under WS is largely due to leaf rolling which limits the leaves' ability to access sunlight and minimizes the interaction between eCO₂ and WS as eCO₂ does not affect leaf display in the absence of significant soil water conservation, which was not observed in this study.

Table 4.1 Summary of constants used for estimating gas exchange parameters

Summary of coefficients used from literature to correct gas exchange measurements for leaf temperatures including Michaelis-Menten constant for carboxylation (K_c); Michaelis-Menten constant for oxygenation (K_o); CO_2 compensation point (Γ^*) and their corresponding activation energies (E_a). Parameters used from chapters 2 and 3 include the maximal rate of carboxylation (V_{cmax}) and maximal rate of RuBP regeneration (J_{max}) determined using A- C_i response curves; activation energy for carboxylation (E_{aV}) and activation energy of RuBP regeneration (E_{aJ}). Except for K_c and K_o from tobacco, all other constants are either measured or derived for wheat.

Parameter	Value	Reference
K_c at 25 °C (μbar)	272	(Bernacchi et al., 2002)
E_a for K_c (J mol^{-1})	93724	Silva-Pérez et al., 2017)
K_o at 25 °C (μbar)	166	(Bernacchi et al., 2002)
E_a for K_o (J mol^{-1})	33603	(Silva-Pérez et al., 2017)
Γ^* (μbar)	37.74	(Silva-Pérez et al., 2017)
E_a for Γ^* (J mol^{-1})	24420	(Silva-Pérez et al., 2017)
V_{cmax} at 25 °C ($\mu\text{mol m}^{-2} \text{s}^{-1}$)	197	Chapters 2 and 3
E_{aV} (J mol^{-1})	51500	Chapters 2 and 3
J_{max} at 25 °C ($\mu\text{mol m}^{-2} \text{s}^{-1}$)	194	Chapters 2 and 3
E_{aJ} (J mol^{-1})	39000	Chapters 2 and 3

Table 4.2 Summary of statistics for gas exchange parameters

Summary of statistical analysis using ANOVA test in R for the effects of line, elevated CO₂ and water stress on gas exchange parameters. A_{sat} at C_i of 300 was determined using A-C_i response curves and one-point V_{cmax} and J_{max} were calculated from spot gas exchange measurements at common CO₂. A_{sat} , V_{cmax} , and J_{max} were corrected to 25°C leaf temperature using photosynthetic temperature response of glasshouse grown plants. Photosynthetic water use efficiency (PWUE) was estimated as the ratio of A_{sat}/g_s . Growth CO₂ measurements refer to measurement of ambient CO₂ grown plants at 400 $\mu\text{l L}^{-1}$ and elevated CO₂ grown plants at 650 $\mu\text{l L}^{-1}$. Significance levels are: *** = $p < 0.001$; ** = $p < 0.01$; * = $p < 0.05$; † = $p < 0.1$; ns $p > 1$.

Meas CO ₂ ($\mu\text{l L}^{-1}$)	Parameter	Year	Main Effects			Interactions			
			Line	CO ₂	Water stress	Line*CO ₂	CO ₂ *Water stress	Line*Water stress	Line*CO ₂ *Water stress
Growth CO ₂ (400/650)	A_{sat} ($\mu\text{mol m}^{-2} \text{s}^{-1}$)	2014	ns	**	*	†	ns	*	*
		2015	ns	**	†	ns	ns	ns	ns
	g_s ($\text{mol m}^{-2} \text{s}^{-1}$)	2014	ns	ns	**	ns	ns	ns	ns
		2015	ns	ns	***	ns	ns	ns	ns
	PWUE (A_{sat}/g_s)	2014	ns	†	***	ns	ns	ns	ns
		2015	ns	***	**	ns	*	ns	ns
Common CO ₂ (400)	A_{sat} ($\mu\text{mol m}^{-2} \text{s}^{-1}$)	2014	ns	ns	ns	ns	ns	ns	ns
		2015	ns	ns	†	ns	ns	ns	ns
	A_{sat} per unit N ($\mu\text{mol s}^{-1} \text{g}^{-1}$)	2014	ns	ns	ns	ns	ns	ns	ns
		2015	ns	*	ns	ns	ns	ns	ns
	g_s ($\text{mol m}^{-2} \text{s}^{-1}$)	2014	ns	ns	**	ns	ns	ns	ns
		2015	ns	ns	*	ns	ns	ns	ns
	PWUE (A_{sat}/g_s)	2014	ns	†	***	ns	ns	ns	ns
		2015	ns	ns	**	ns	ns	ns	ns
	C_i ($\mu\text{l L}^{-1}$)	2014	ns	*	***	ns	ns	ns	ns
		2015	ns	ns	***	ns	ns	ns	ns
	One Point V_{cmax} ($\mu\text{mol m}^{-2} \text{s}^{-1}$)	2014	ns	ns	ns	ns	ns	ns	ns
		2015	ns	ns	ns	ns	ns	ns	ns
	One Point J_{max} ($\mu\text{mol m}^{-2} \text{s}^{-1}$)	2014	ns	ns	ns	ns	ns	ns	ns
		2015	ns	ns	ns	ns	ns	ns	ns
Determined from A-C _i curves	A_{sat} at C_i 300 ($\mu\text{mol m}^{-2} \text{s}^{-1}$)	2014	ns	ns	ns	ns	ns	ns	*
		2015	ns	†	ns	ns	ns	ns	ns
	V_{cmax} ($\mu\text{mol m}^{-2} \text{s}^{-1}$)	2014	ns	ns	ns	ns	ns	ns	*
		2015	ns	*	ns	ns	ns	ns	ns
	J_{max} ($\mu\text{mol m}^{-2} \text{s}^{-1}$)	2014	ns	ns	ns	†	†	ns	**
		2015	ns	ns	ns	ns	ns	ns	ns

Table 4.3 Summary of statistics for plant dry matter (DM) and grain yield parameters

Summary of statistical analysis using ANOVA test in R for effect of line, elevated CO₂ and water stress on plant dry mass (DM) and grain yield parameters. Significance levels are: *** = $p < 0.001$; ** = $p < 0.01$; * = $p < 0.05$; † = $p < 0.1$; ns = $p > 1$. Nitrogen (N) use efficiency for grain yield and above ground dry matter produced per unit N is abbreviated as NUEg and NUEb respectively.

Parameter	Year	Main Effects			Interactions			
		Line	CO ₂	Water Stress	Line × CO ₂	CO ₂ × Water Stress	Line × Water Stress	Line × CO ₂ × Water Stress
Flag Leaf Mass Area (g m ⁻²)	2014	ns	ns	ns	ns	ns	ns	ns
	2015	ns	ns	ns	ns	ns	ns	ns
Flag Leaf N (mg g ⁻¹)	2014	ns	*	ns	ns	†	ns	ns
	2015	ns	***	ns	ns	ns	ns	ns
Flag Leaf N per unit Area (g m ⁻²)	2014	ns	ns	ns	ns	ns	ns	ns
	2015	ns	**	ns	ns	ns	ns	ns
Tillers (m ⁻²)	2014	ns	ns	***	ns	ns	ns	ns
	2015	ns	ns	**	ns	ns	ns	ns
Ears (m ⁻²)	2014	ns	ns	***	ns	ns	ns	ns
	2015	ns	ns	**	ns	ns	ns	ns
Grains Per Ear	2014	ns	ns	***	ns	ns	ns	ns
	2015	**	ns	***	ns	ns	ns	ns
Above ground DM (g)	2014	ns	ns	***	ns	ns	ns	ns
	2015	ns	**	***	ns	ns	ns	ns
Grain yield (g)	2014	ns	ns	***	ns	ns	ns	ns
	2015	†	†	***	ns	ns	ns	ns
1000 Grain Weight (g)	2014	ns	ns	*	ns	ns	ns	ns
	2015	***	***	ns	ns	†	ns	ns
Harvest index	2014	ns	ns	**	ns	ns	ns	ns
	2015	*	*	**	†	ns	ns	†
Grain Protein (%)	2014	ns	†	*	ns	ns	ns	ns
	2015	ns	***	***	ns	ns	ns	ns
Total N uptake (g plant ⁻¹)	2014	ns	ns	***	ns	ns	ns	ns
	2015	ns	ns	***	ns	ns	ns	ns
NUEg (g g ⁻¹ N uptake)	2014	ns	ns	*	ns	ns	ns	ns
	2015	ns	***	***	ns	ns	ns	ns
NUEb (g g ⁻¹ N uptake)	2014	ns	**	ns	ns	ns	ns	ns
	2015	ns	**	ns	ns	ns	ns	ns

Daily average weather parameters recorded during growth season (GS)

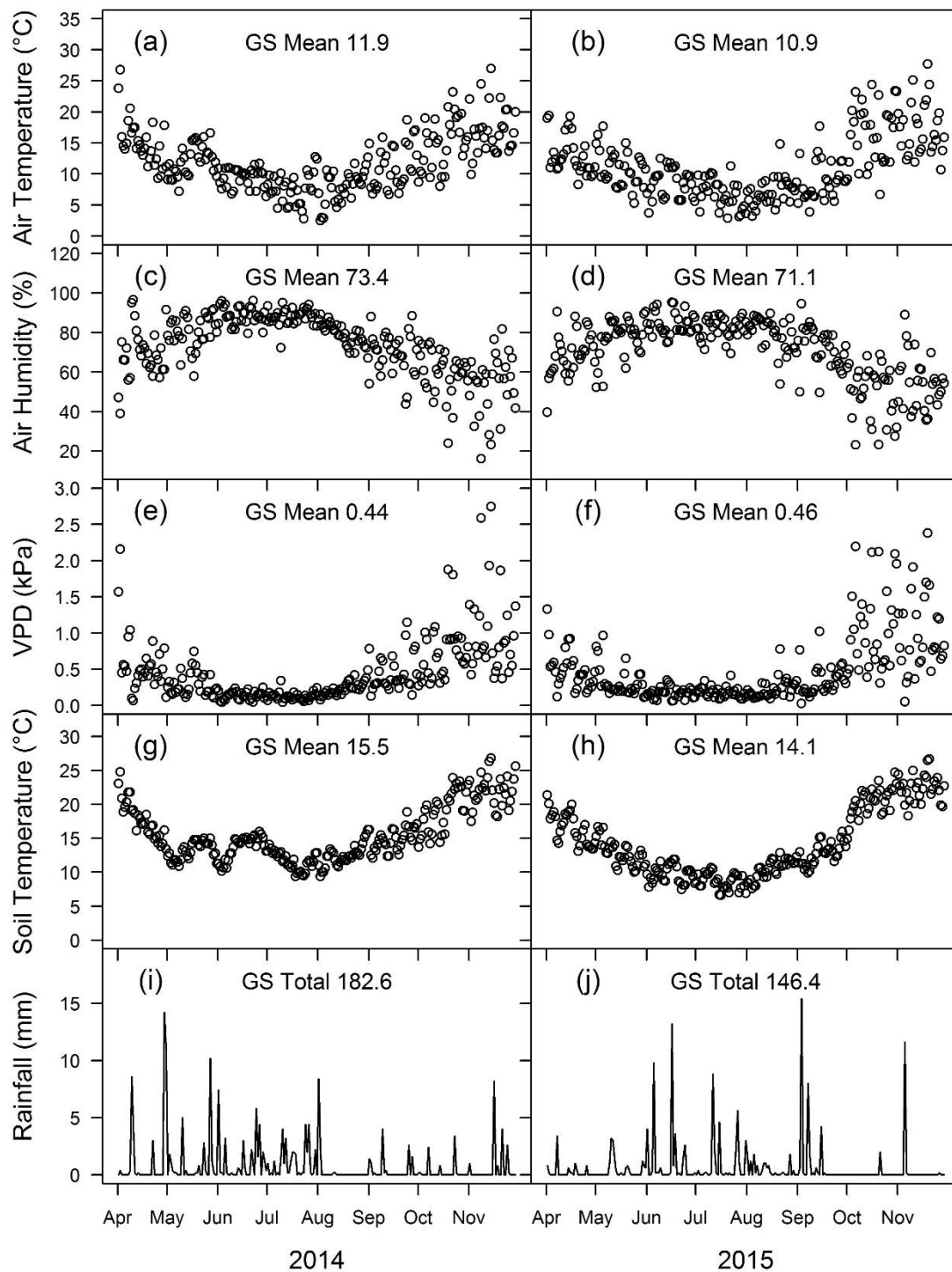


Figure 4.1 Field growth conditions recorded during the growth season (GS) of 2014 and 2015

Environmental conditions during the experimental growth period; air temperature (a and b), relative humidity (c and d), vapour pressure deficit (VPD) (e and f), soil temperature (g and h) and rainfall (i and j) recorded in the year 2014 and 2015. Points are daily averages plotted over the growing season. Growth season (GS) mean or total values are shown.

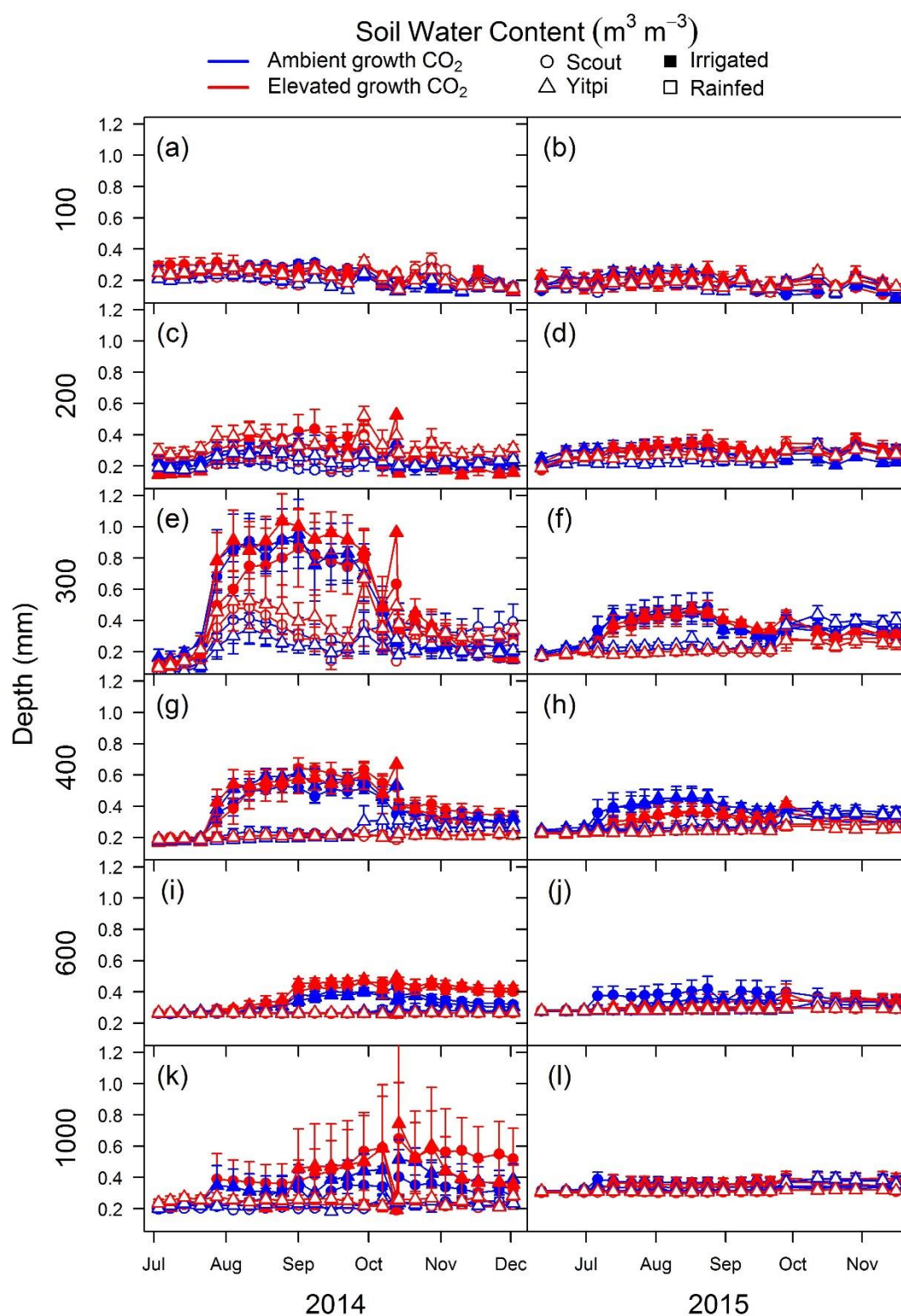


Figure 4.2 Effect of elevated CO_2 and irrigation on soil water content measured at different depths in 2014 and 2015

Soil water content measured at 100, 200, 300, 400, 600 and 1000 (mm) depth for each treatment plot in 2014 and 2015. Ambient and elevated CO_2 treatments are depicted in blue and red, respectively. Scout and Yitpi plots are depicted using circles and triangles, respectively. Open and closed symbols represent rainfed and irrigated plots, respectively. Values are means with standard errors.

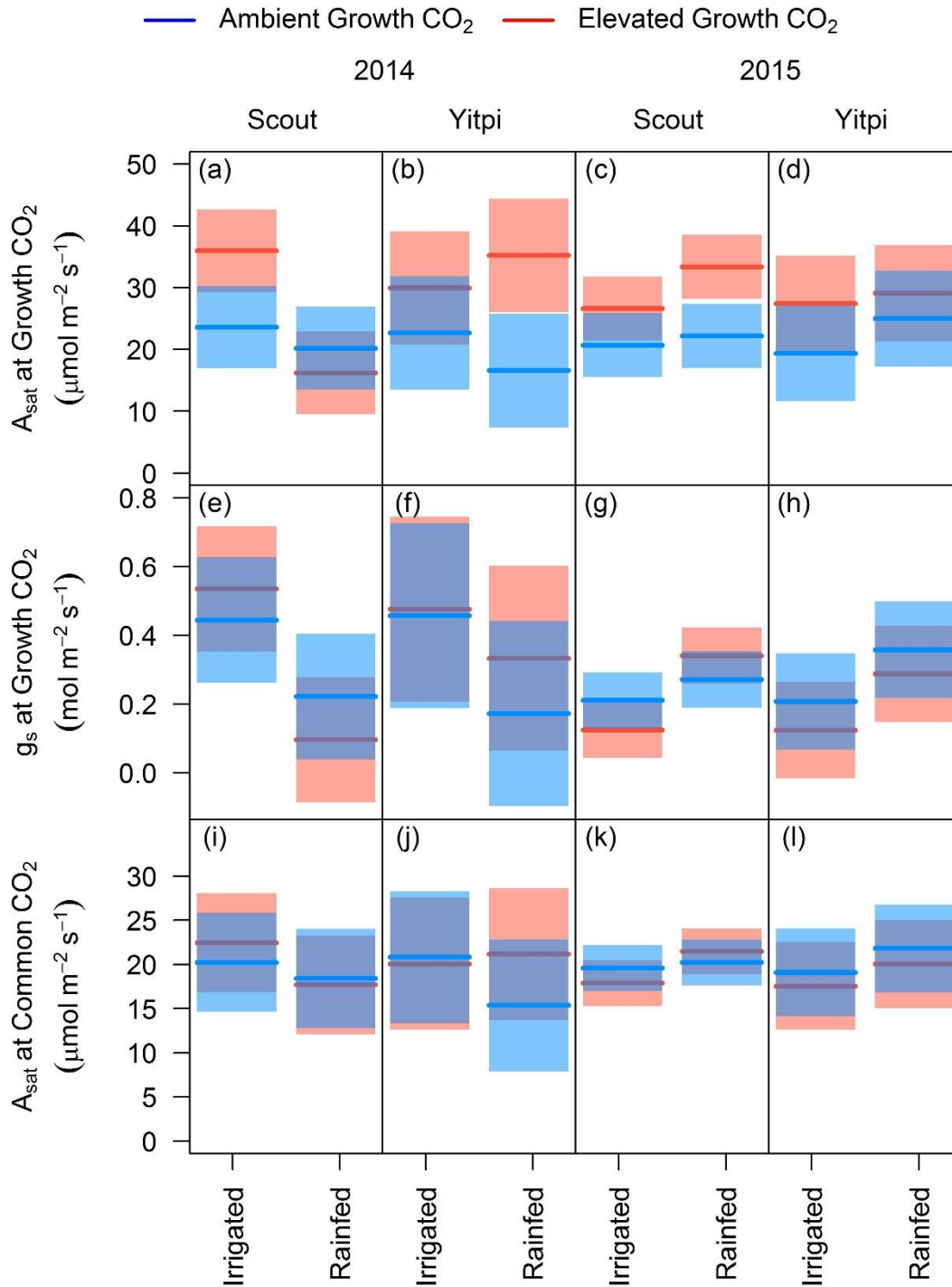


Figure 4.3 Effect of eCO₂ and irrigation on CO₂ assimilation rates (A_{sat}) and stomatal conductance (g_s) measured at common (400 μL^{-1}) and growth CO₂ during 2014 and 2015

Means for temperature corrected A_{sat} (a, b, c, d) measured at growth CO₂; A_{sat} (e, f, g, h) and g_s (i, j, k, l) measured at common CO₂ plotted using visreg package in R. A_{sat} was corrected to 25°C leaf temperature using photosynthetic temperature response of glasshouse grown plants. Lines indicate means and shaded regions represent 95% confidence intervals. Ambient and elevated CO₂ grown plants are depicted in blue and red, respectively. Grouping is based on exposure to water stress and includes irrigated and rainfed plants.

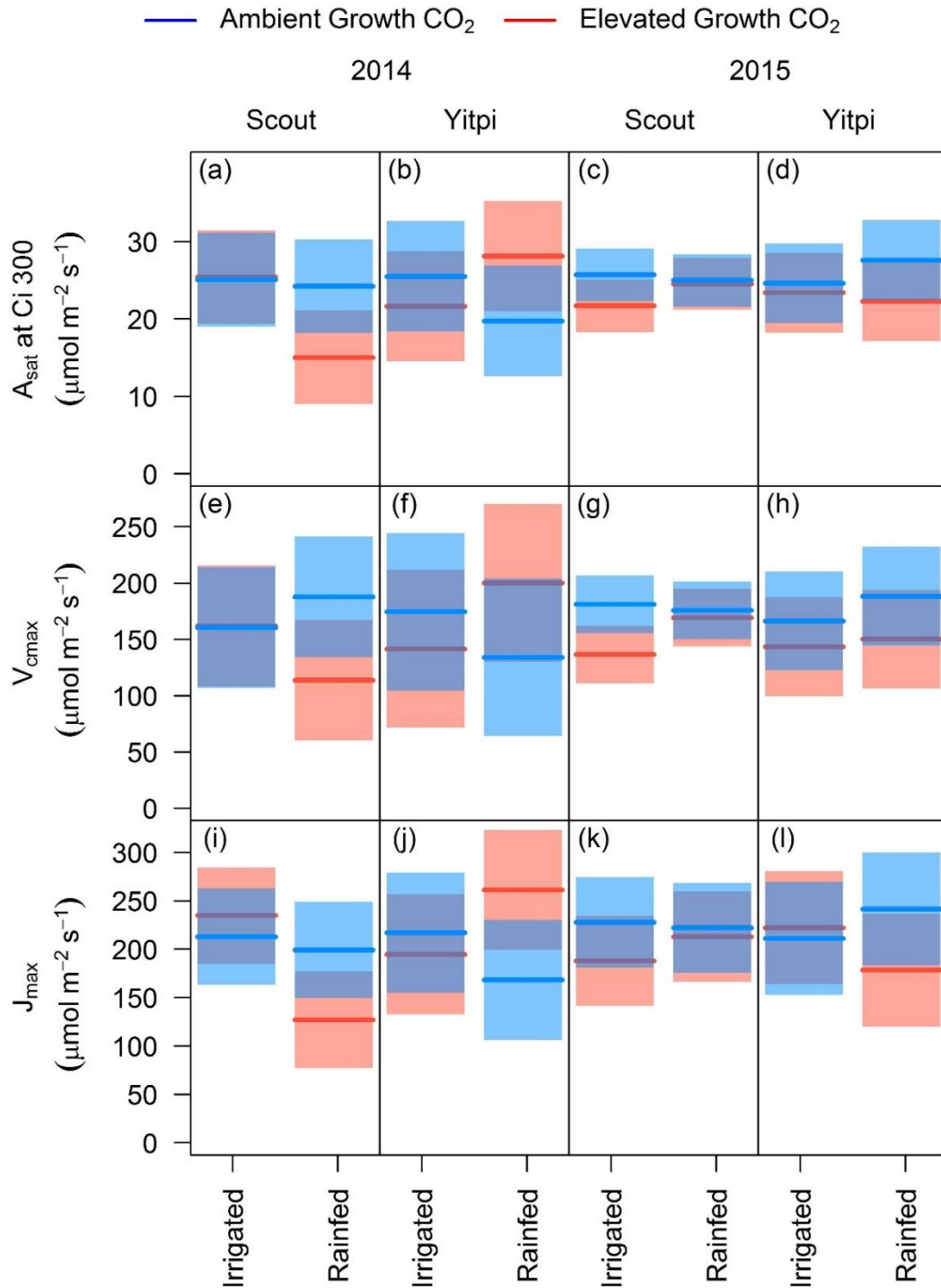


Figure 4.4 Effect of eCO₂ and irrigation on photosynthetic capacity during 2014 and 2015

Means for A_{sat} (at C_i 300) (a, b, c, d), V_{cmax} (e, f, g, h) and J_{max} (i, j, k, l) plotted using visreg package in R. A_{sat} at C_i 300, V_{cmax} and J_{max} were determined using A- C_i response curves. Parameters were corrected to 25°C leaf temperature using coefficients derived from the photosynthetic temperature response of glasshouse-grown plants. Lines indicate means and shaded regions represent 95% confidence intervals. Ambient and elevated CO₂ grown plants are depicted in blue and red, respectively. Grouping is based on exposure to water stress and includes irrigated and rainfed plants.

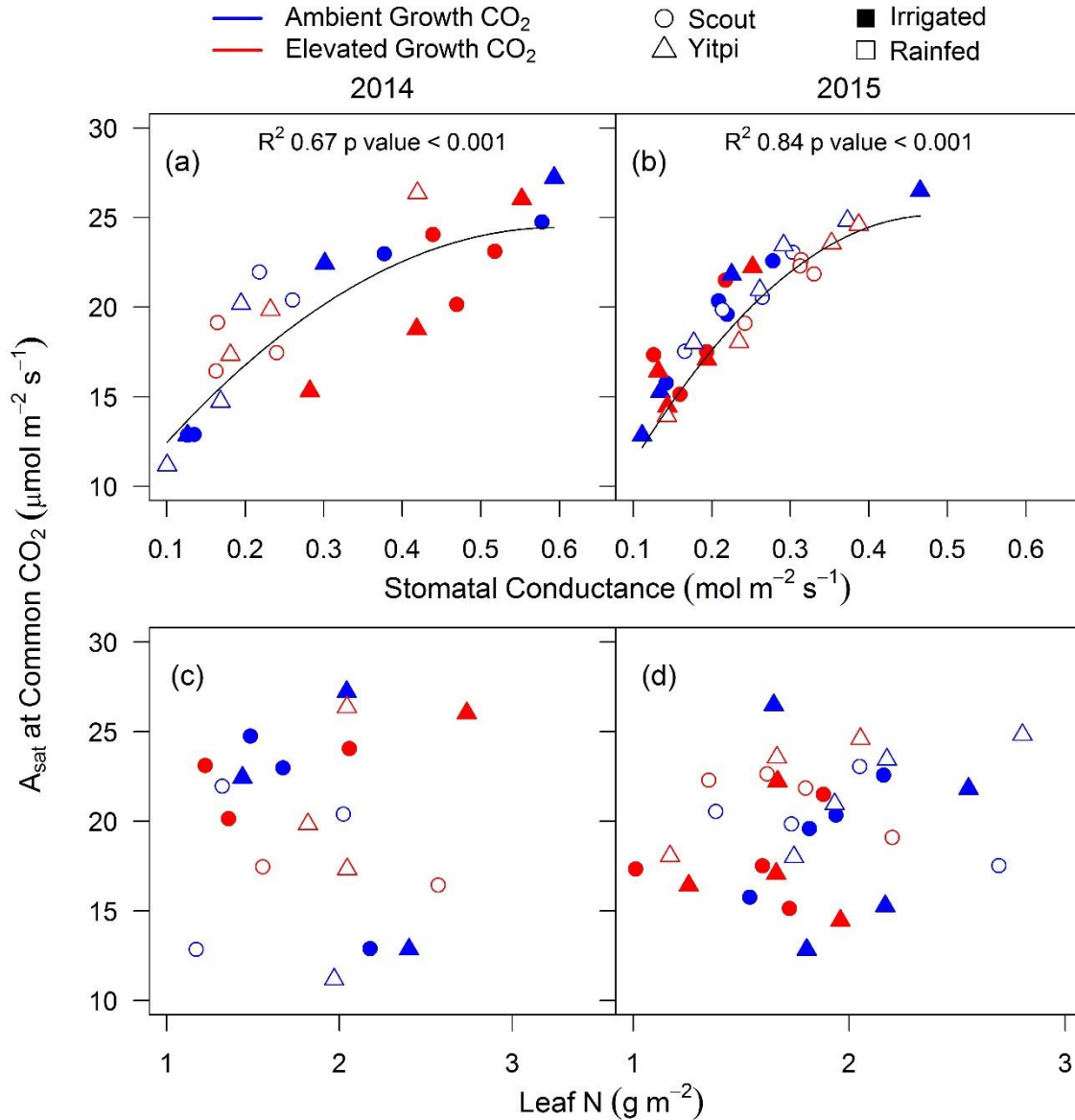


Figure 4.5 Relationships between CO₂ assimilation rates (A_{sat}), stomatal conductance (g_s) and leaf nitrogen (N) content during 2014 and 2015

Relationships between A_{sat} and g_s (a, b) and between A_{sat} and leaf nitrogen content (c, d). A_{sat} was corrected to 25°C leaf temperature using photosynthetic the temperature response of glasshouse-grown plants. Ambient and elevated CO₂ are depicted in blue and red, respectively. Scout and Yitpi are depicted using circles and triangles, respectively. Open and closed symbols represent rainfed and irrigated plants, respectively.

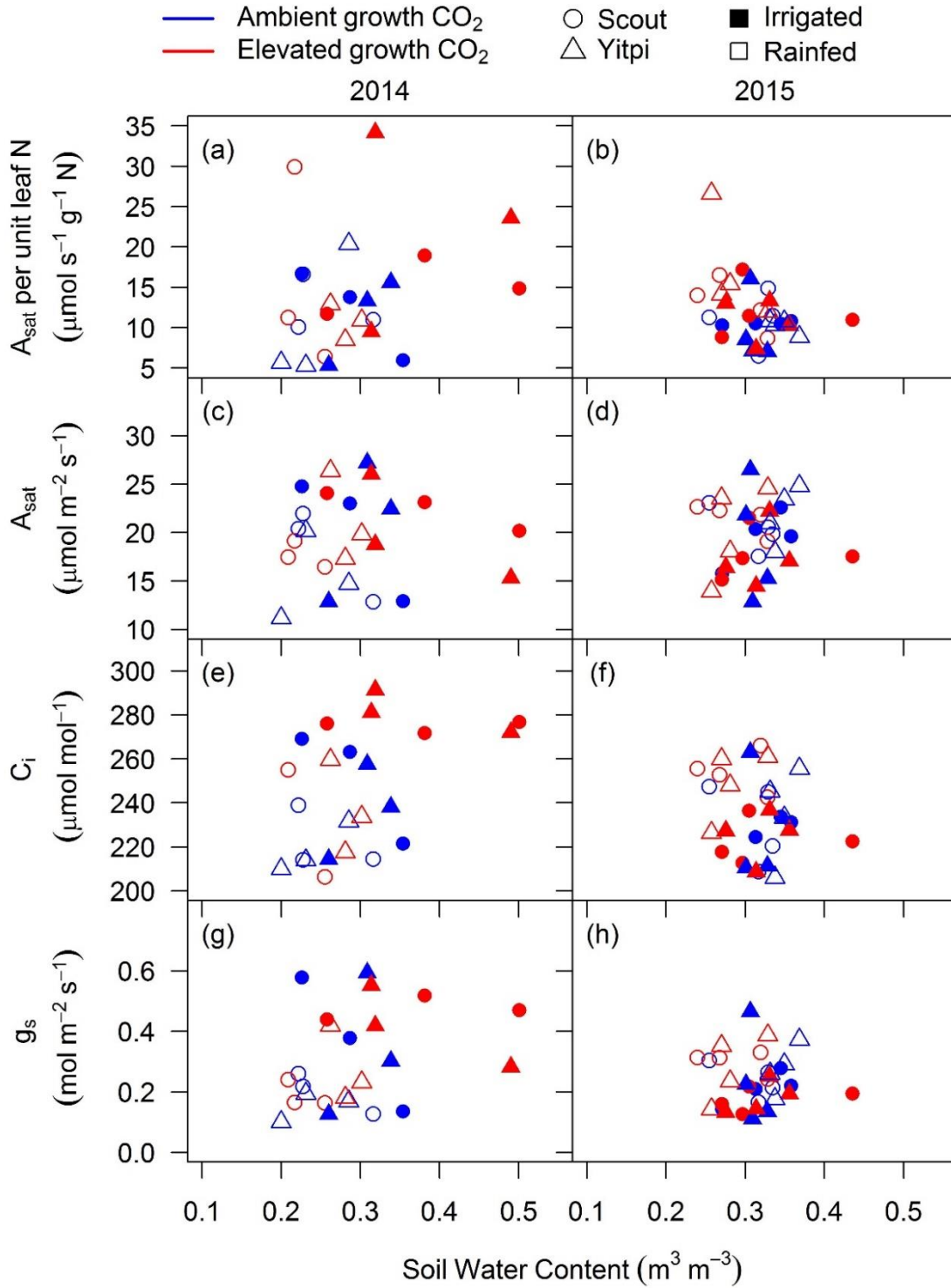


Figure 4.6 Relationships between A_{sat} per unit N, A_{sat} , C_i , g_s (measured at common CO₂) and soil water content

Relationships between A_{sat} per unit leaf nitrogen (N) and soil water content (a, b); A_{sat} and soil water content (c, d); C_i and soil water content (e, f); g_s and soil water content (g, h). A_{sat} was corrected to 25°C leaf temperature using the photosynthetic temperature response of glasshouse-grown plants. Ambient and elevated CO₂ are depicted in blue and red, respectively. Scout and Yitpi are depicted using circles and triangles, respectively. Open and closed symbols represent rainfed and irrigated plants, respectively.

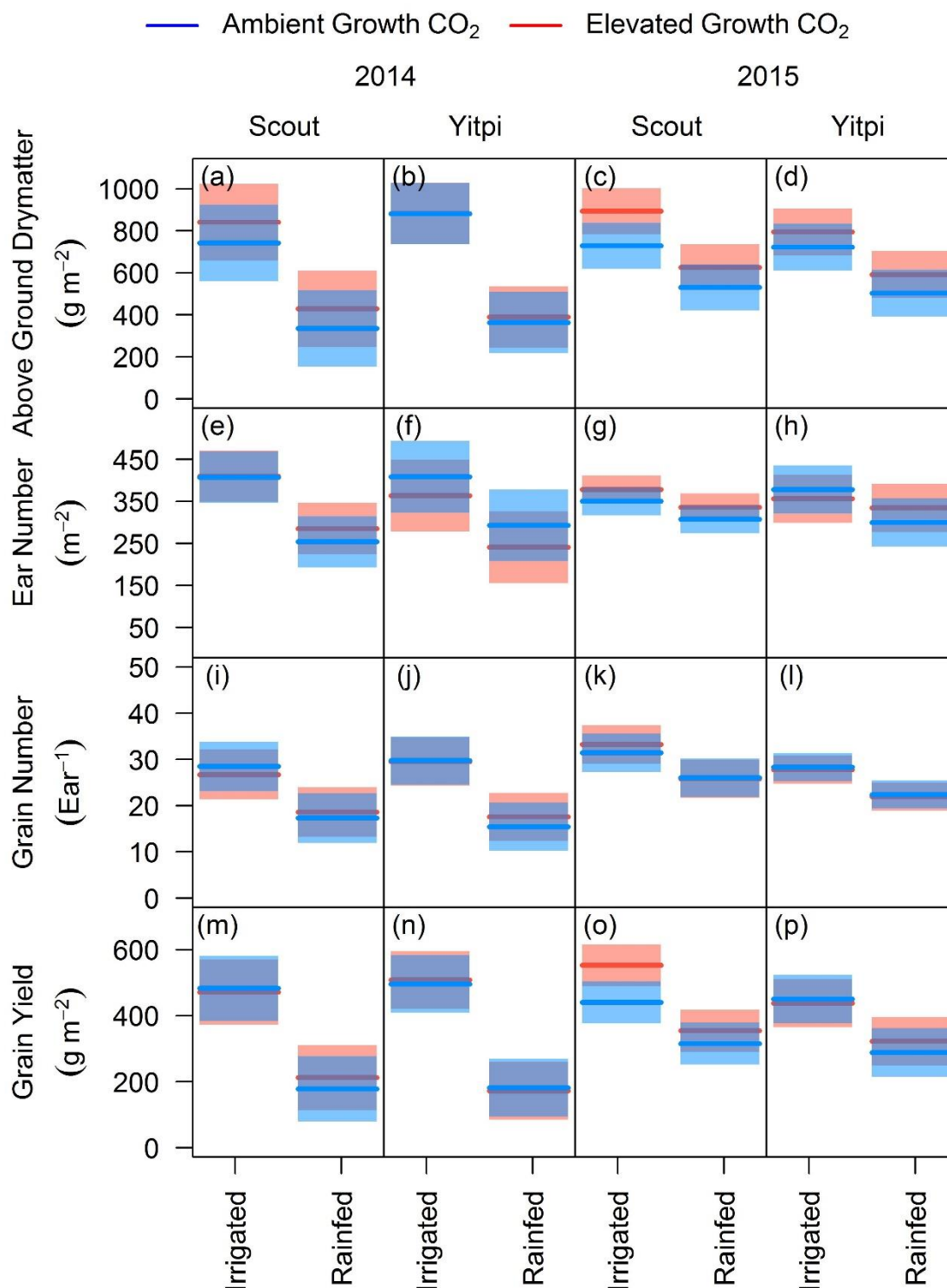


Figure 4.7 Effect of $e\text{CO}_2$ and irrigation on above ground dry matter and grain yield during 2014 and 2015

Means for above ground dry matter (a, b, c, d); grain yield (e, f, g, h), ear number (i, j, k, l) and harvest index (m, n, o, p) plotted using visreg package in R. Lines indicate means and shaded regions depict 95% confidence intervals. Ambient and elevated CO_2 grown plants are depicted in blue and red, respectively. Grouping is based on exposure to water stress and includes irrigated and rainfed plants.

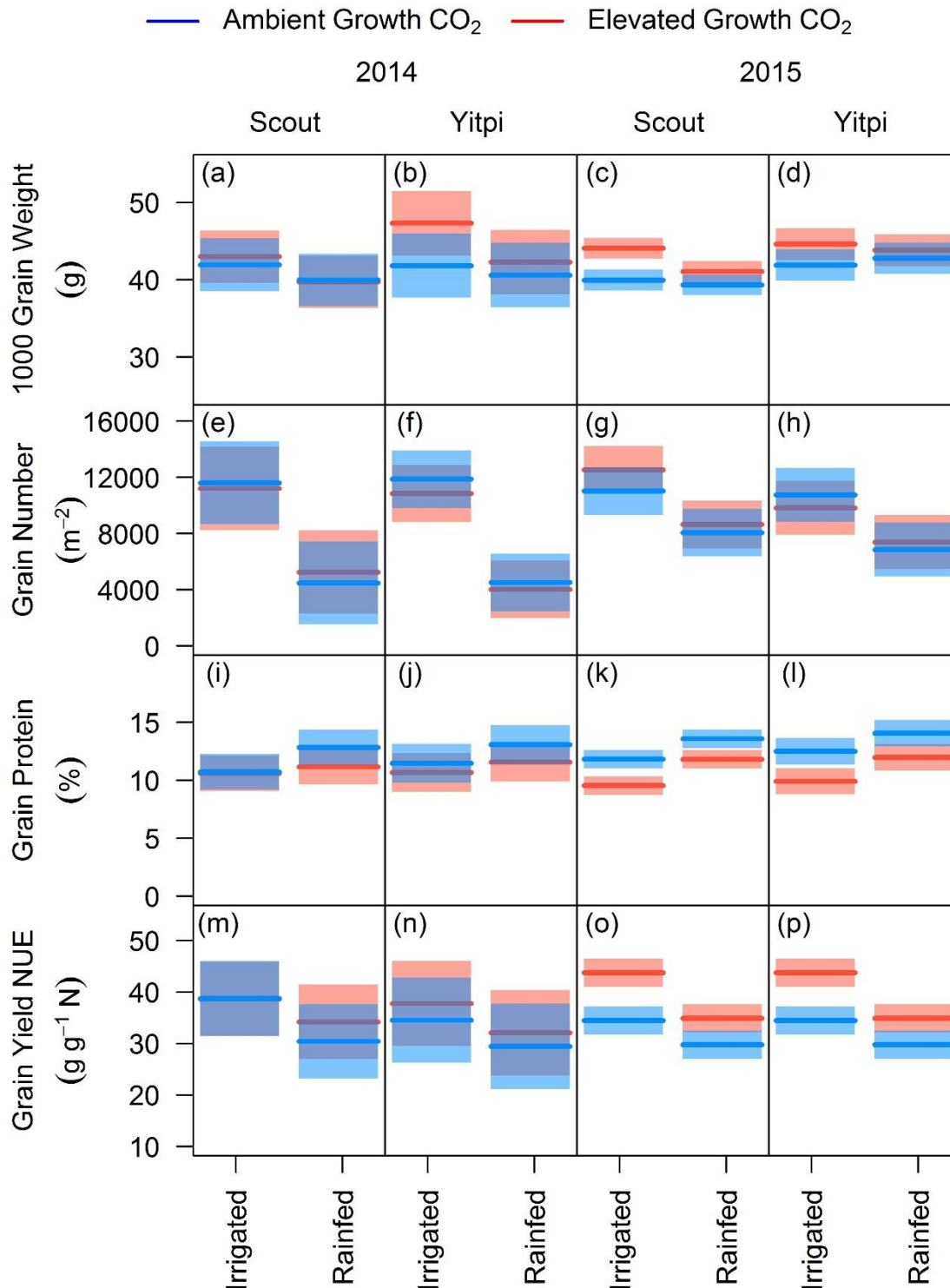


Figure 4.8 Effect of eCO₂ and irrigation on grain size and grain protein during 2014 and 2015

Mean weight for 1000 grains (a, b, c, d); grain number (e, f, g, h); grain protein (i, j, k, l) and grain yield NUE (nitrogen use efficiency) (m, n, o, p) plotted using visreg package in R. Lines indicate means and shaded regions depict 95% confidence intervals. Ambient and elevated CO₂ grown plants are depicted in blue and red, respectively. Grouping is based on exposure to water stress and includes irrigated and rainfed plants.

Table S 4.1 Response of Scout gas exchange parameters to elevated CO₂ and water stress during 2014 and 2015

Summary of leaf gas exchange measured at two CO₂ concentrations (400 and 650 µl L⁻¹) for Scout grown at ambient CO₂ (aCO₂) or elevated CO₂ (eCO₂) under rainfed or irrigated conditions. A_{sat} , V_{cmax} , and J_{max} were corrected to 25°C leaf temperature using photosynthetic temperature response of glass house grown plants. Photosynthetic water use efficiency (PWUE) was estimated as the ratio of A_{sat} and g_s . Values are means ± SE (n= 9-10).

Meas CO ₂	Parameter	2014				2015			
		Irrigated		Rainfed		Irrigated		Rainfed	
		Ambient	Elevated	Ambient	Elevated	Ambient	Elevated	Ambient	Elevated
Common CO ₂ (400)	A_{sat} per unit N (µmol s ⁻¹ g ⁻¹)	12.4 ± 3.3	15.5 ± 2.3	12.8 ± 1.7	15.7 ± 6.9	10.8 ± 0.3	12.7 ± 2.2	11.1 ± 1.7	13.1 ± 1.7
	A_{sat} (µmol m ⁻² s ⁻¹)	20.7 ± 3.8	22.9 ± 1.2	18.9 ± 2.6	17.7 ± 0.6	20.2 ± 1.4	18.7 ± 1.7	20.4 ± 1.4	21.9 ± 1
	g_s (mol m ⁻² s ⁻¹)	0.36 ± 0.13	0.48 ± 0.02	0.2 ± 0.04	0.19 ± 0.03	0.21 ± 0.03	0.17 ± 0.02	0.24 ± 0.03	0.3 ± 0.02
	C_i (µl L ⁻¹)	251 ± 15	275 ± 2	222 ± 8	217 ± 20	228 ± 6	244 ± 8	228 ± 8	233 ± 10
	PWUE (A_{sat}/g_s)	67 ± 16	47 ± 4	94 ± 8	97 ± 13	95 ± 6	106 ± 11	88 ± 7	72 ± 3
Growth CO ₂ (400/650)	A_{sat} (µmol m ⁻² s ⁻¹)	23.9 ± 4.1	37.1 ± 2	20.3 ± 2.5	16.2 ± 2.5	21.5 ± 1.5	28.9 ± 4.3	22.4 ± 2.2	34.4 ± 2.6
	g_s (mol m ⁻² s ⁻¹)	0.44 ± 0.14	0.54 ± 0.02	0.22 ± 0.07	0.1 ± 0.01	0.21 ± 0.03	0.12 ± 0.02	0.27 ± 0.05	0.34 ± 0.04
	PWUE (A_{sat}/g_s)	62 ± 14	67 ± 2	102 ± 18	167 ± 12	102 ± 8	237 ± 53	85 ± 7	101 ± 9
	C_i (µl L ⁻¹)	274 ± 14	466 ± 7	228 ± 23	362 ± 29	232 ± 12	336 ± 20	251 ± 10	442 ± 15
Common CO ₂ (400)	One point V_{cmax} (µmol m ⁻² s ⁻¹)	89 ± 9	94 ± 7	111 ± 23	104 ± 17	109 ± 6	108 ± 12	107 ± 3	99 ± 3
	One point J_{max} (µmol m ⁻² s ⁻¹)	151 ± 23	161 ± 9	159 ± 23	146 ± 15	162 ± 9	146 ± 11	163 ± 6	159 ± 7
Determined using A-C _i curves	A_{sat} at C_i 300 (µmol m ⁻² s ⁻¹)	25 ± 3	25 ± 2	24 ± 1	15 ± 3	26 ± 1	22 ± 2	25 ± 2	25 ± 1
	V_{cmax} (µmol m ⁻² s ⁻¹)	161 ± 32	162 ± 17	188 ± 11	114 ± 27	199 ± 15	169 ± 16	178 ± 19	196 ± 23
	J_{max} (µmol m ⁻² s ⁻¹)	213 ± 32	235 ± 10	199 ± 8	127 ± 26	247 ± 21	219 ± 15	213 ± 26	227 ± 28

Table S 4.2 Response of Yitpi gas exchange parameters to elevated CO₂ and water stress during 2014 and 2015

Summary of leaf gas exchange measured at two CO₂ (400 and 650 $\mu\text{L L}^{-1}$) partial pressures for Yitpi grown at ambient CO₂ (aCO₂) or elevated CO₂ (eCO₂) under rainfed or irrigated conditions. A_{sat} , V_{cmax} , and J_{max} were corrected to 25°C leaf temperature using photosynthetic temperature response of glass house grown plants. Photosynthetic water use efficiency (PWUE) was estimated as the ratio of A_{sat} and g_s . Values are means \pm SE (n= 9-10).

Meas CO ₂	Parameter	2014				2015			
		Irrigated		Rainfed		Irrigated		Rainfed	
		Ambient	Elevated	Ambient	Elevated	Ambient	Elevated	Ambient	Elevated
Common CO ₂ (400)	A_{sat} per unit N ($\mu\text{mol s}^{-1}\text{g}^{-1}$)	11.7 \pm 3.1	22.6 \pm 7.1	10.8 \pm 5.2	10.8 \pm 1.2	10 \pm 2.2	11.6 \pm 1.6	10.2 \pm 0.4	17.1 \pm 3.1
	A_{sat} ($\mu\text{mol m}^{-2}\text{s}^{-1}$)	21.5 \pm 4.2	20.2 \pm 3.1	15.6 \pm 2.2	21.3 \pm 2.6	19.6 \pm 3.1	18.4 \pm 1.9	21.9 \pm 1.5	20.3 \pm 2.7
	g_s ($\text{mol m}^{-2}\text{s}^{-1}$)	0.34 \pm 0.14	0.42 \pm 0.08	0.15 \pm 0.03	0.28 \pm 0.07	0.23 \pm 0.08	0.18 \pm 0.03	0.28 \pm 0.04	0.28 \pm 0.06
	C_i ($\mu\text{L L}^{-1}$)	237 \pm 12	281 \pm 6	219 \pm 7	237 \pm 12	235 \pm 11	242 \pm 7	220 \pm 11	233 \pm 11
	PWUE (A_{sat}/g_s)	74 \pm 16	49 \pm 3	101 \pm 7	81 \pm 10	96 \pm 14	100 \pm 9	82 \pm 7	76 \pm 8
Growth CO ₂ (400/650)	A_{sat} ($\mu\text{mol m}^{-2}\text{s}^{-1}$)	23.1 \pm 4.8	30.5 \pm 4.4	16.9 \pm 2.7	34.9 \pm 2.8	20 \pm 3.4	29.7 \pm 3.5	25 \pm 1.9	29.8 \pm 5.5
	g_s ($\text{mol m}^{-2}\text{s}^{-1}$)	0.46 \pm 0.18	0.48 \pm 0.13	0.17 \pm 0.04	0.33 \pm 0.08	0.21 \pm 0.06	0.12 \pm 0.02	0.36 \pm 0.07	0.29 \pm 0.09
	PWUE (A_{sat}/g_s)	67 \pm 23	68 \pm 11	101 \pm 13	116 \pm 23	106 \pm 15	239 \pm 51	77 \pm 12	123 \pm 27
	C_i ($\mu\text{L L}^{-1}$)	264 \pm 25	482 \pm 17	237 \pm 15	414 \pm 35	232 \pm 12	318 \pm 16	262 \pm 17	411 \pm 37
Common CO ₂ (400)	One point V_{cmax} ($\mu\text{mol m}^{-2}\text{s}^{-1}$)	82 \pm 14	74 \pm 12	84 \pm 31	90 \pm 8	89 \pm 13	81 \pm 8	97 \pm 4	81 \pm 5
	One point J_{max} ($\mu\text{mol m}^{-2}\text{s}^{-1}$)	137 \pm 26	123 \pm 18	114 \pm 29	138 \pm 13	135 \pm 21	114 \pm 13	146 \pm 6	130 \pm 13
Determined using A-Ci curves	A_{sat} at C_i 300 ($\mu\text{mol m}^{-2}\text{s}^{-1}$)	26 \pm 4	22 \pm 4	20 \pm 3	28 \pm 1	25 \pm 3	23 \pm 2	28 \pm 1	22 \pm 3
	V_{cmax} ($\mu\text{mol m}^{-2}\text{s}^{-1}$)	97 \pm 13	86 \pm 12	101 \pm 32	104 \pm 7	106 \pm 13	102 \pm 10	111 \pm 4	95 \pm 5
	J_{max} ($\mu\text{mol m}^{-2}\text{s}^{-1}$)	161 \pm 24	142 \pm 17	139 \pm 26	158 \pm 11	160 \pm 20	143 \pm 14	165 \pm 5	151 \pm 14

Table S 4.3 Response of plant dry matter (DM) and grain yield parameters to elevated CO₂ and water stress

Summary of plant dry mass (DM) and grain yield parameters for Scout and Yitpi grown at ambient CO₂ (aCO₂) or elevated CO₂ (eCO₂) under irrigated or rainfed conditions. Values are means \pm SE (n= 3-4). Nitrogen (N) use efficiency for grain yield and above ground dry matter produced per unit N is abbreviated as NUEg and NUEb respectively.

Line	Parameters	2014				2015			
		Irrigated		Rainfed		Irrigated		Rainfed	
		Ambient	Elevated	Ambient	Elevated	Ambient	Elevated	Ambient	Elevated
Scout	Flag leaf area (m ²)	17 \pm 1	23 \pm 5	14 \pm 1	9 \pm 2	26 \pm 3	29 \pm 3	20 \pm 2	22 \pm 3
	Flag leaf mass area (g m ⁻²)	80 \pm 1	80 \pm 14	78 \pm 7	89 \pm 17	48 \pm 2	57 \pm 8	50 \pm 6	55 \pm 4
	Flag leaf N (mg g ⁻¹)	22.2 \pm 2.5	19.3 \pm 1	19.4 \pm 3.2	17.6 \pm 4.9	38.7 \pm 1.4	27.8 \pm 3.5	39.4 \pm 2.1	31.5 \pm 2.1
	Flag leaf N area (g m ⁻²)	1.8 \pm 0.2	1.5 \pm 0.3	1.5 \pm 0.3	1.6 \pm 0.6	1.9 \pm 0.1	1.6 \pm 0.2	2 \pm 0.3	1.7 \pm 0.2
	Tillers (m ⁻²)	413 \pm 29	444 \pm 34	274 \pm 34	324 \pm 18	367 \pm 9	394 \pm 10	335 \pm 25	364 \pm 30
	Ears (m ⁻²)	408 \pm 28	410 \pm 30	254 \pm 34	286 \pm 16	350 \pm 6	378 \pm 9	307 \pm 21	336 \pm 19
	Grains Per Ear	29 \pm 3	27 \pm 3	17 \pm 1	19 \pm 3	31 \pm 2	33 \pm 2	26 \pm 2	26 \pm 1
	Above ground (g m ⁻²)	742 \pm 78	841 \pm 130	336 \pm 57	429 \pm 41	729 \pm 61	893 \pm 50	531 \pm 55	626 \pm 28
	Total grain number (m ⁻²)	11613 \pm 1271	11216 \pm 2106	4481 \pm 822	5258 \pm 816	11026 \pm 782	12530 \pm 506	8064 \pm 1153	8650 \pm 464
	Grain Yield (g m ⁻²)	483 \pm 40	472 \pm 64	178 \pm 32	213 \pm 39	440 \pm 30	553 \pm 25	315 \pm 40	354 \pm 16
	1000 Grain Weight (g)	41.9 \pm 1.3	43 \pm 1.7	40 \pm 1.3	39.7 \pm 1.8	40 \pm 0.5	44.1 \pm 0.4	39.4 \pm 0.8	41 \pm 0.8
	Harvest Index	0.4 \pm 0	0.4 \pm 0	0.4 \pm 0	0.4 \pm 0	0.4 \pm 0	0.5 \pm 0	0.4 \pm 0	0.4 \pm 0
	Grain Protein (%)	10.7 \pm 0.6	10.6 \pm 0.4	12.8 \pm 0.5	11.2 \pm 1	11.8 \pm 0.3	9.5 \pm 0.1	13.6 \pm 0.4	11.8 \pm 0.6
	Total Nuptake (g)	12.8 \pm 1.8	12.8 \pm 2.9	5.9 \pm 1.2	6.2 \pm 0.5	12.8 \pm 1.1	12.6 \pm 0.4	10.5 \pm 0.9	10.2 \pm 0.2
Yitpi	NUEg (g g ⁻¹ N)	38.7 \pm 2.8	38.6 \pm 2.6	30.4 \pm 1	34.2 \pm 5.4	34.5 \pm 0.8	43.7 \pm 0.8	29.8 \pm 1.5	34.9 \pm 1.7
	NUEb (g g ⁻¹ N)	87 \pm 5	93 \pm 6	79 \pm 2	95 \pm 4	86 \pm 5	118 \pm 11	79 \pm 8	105 \pm 4
	Flag leaf area (m ²)	34 \pm 2	17 \pm 2	14 \pm 4	9 \pm 1	30 \pm 4	27 \pm 2	21 \pm 3	20 \pm 3
	Flag leaf mass area (g m ⁻²)	65 \pm 6	101 \pm 13	103 \pm 23	104 \pm 7	51 \pm 3	55 \pm 7	59 \pm 3	45 \pm 8
	Flag leaf N (mg g ⁻¹)	30 \pm 3.4	11.7 \pm 5	19.2 \pm 4.5	19.1 \pm 1.3	39.6 \pm 1.6	30.4 \pm 2.4	36.4 \pm 2.3	28.5 \pm 2.8
	Flag leaf N area (g m ⁻²)	2 \pm 0.3	1.3 \pm 0.7	2.2 \pm 0.9	2 \pm 0.1	2 \pm 0.2	1.6 \pm 0.1	2.2 \pm 0.2	1.4 \pm 0.3
	Tillers (m ⁻²)	417 \pm 41	392 \pm 48	321 \pm 52	272 \pm 22	432 \pm 17	403 \pm 26	336 \pm 32	359 \pm 10
	Ears (m ⁻²)	408 \pm 41	364 \pm 37	293 \pm 51	241 \pm 22	378 \pm 14	357 \pm 34	300 \pm 35	335 \pm 14
	Grains Per Ear	30 \pm 3	30 \pm 2	15 \pm 1	18 \pm 3	28 \pm 1	28 \pm 2	22 \pm 1	22 \pm 1
	Above ground (g m ⁻²)	881 \pm 47	882 \pm 101	363 \pm 71	390 \pm 22	723 \pm 49	794 \pm 63	503 \pm 56	592 \pm 31
	Total grain number (m ⁻²)	11875 \pm 577	10847 \pm 1407	4508 \pm 922	4026 \pm 591	10764 \pm 748	9827 \pm 854	6849 \pm 1162	7389 \pm 682
	Grain Yield (g m ⁻²)	496 \pm 31	508 \pm 57	182 \pm 37	172 \pm 29	450 \pm 29	438 \pm 36	289 \pm 42	323 \pm 26
	1000 Grain Weight (g)	41.8 \pm 2.1	47.3 \pm 2	40.6 \pm 1.3	42.3 \pm 2.1	41.9 \pm 0.8	44.6 \pm 0.8	42.8 \pm 1.3	43.8 \pm 0.7
	Harvest Index	0.4 \pm 0	0.4 \pm 0	0.4 \pm 0	0.3 \pm 0.1	0.5 \pm 0	0.4 \pm 0	0.4 \pm 0	0.4 \pm 0
	Grain Protein (%)	11.5 \pm 0.7	10.7 \pm 0.4	13.1 \pm 0.4	11.6 \pm 1.2	12.5 \pm 0.2	9.9 \pm 0.3	14.1 \pm 0.4	12 \pm 0.9
	Total Nuptake (g)	14.6 \pm 1.1	13.6 \pm 1.7	6.3 \pm 1.4	5.6 \pm 0.5	13.4 \pm 0.7	10.8 \pm 1.4	10 \pm 1.2	9.5 \pm 0.5
	NUEg (g g ⁻¹ N)	34.5 \pm 3.1	37.8 \pm 2.2	29.5 \pm 1	32.1 \pm 6.5	33.6 \pm 1	41.4 \pm 2.6	28.6 \pm 1.4	34.2 \pm 2.7
	NUEb (g g ⁻¹ N)	83 \pm 5	89 \pm 5	81 \pm 2	97 \pm 8	93 \pm 7	134 \pm 30	80 \pm 6	106 \pm 11

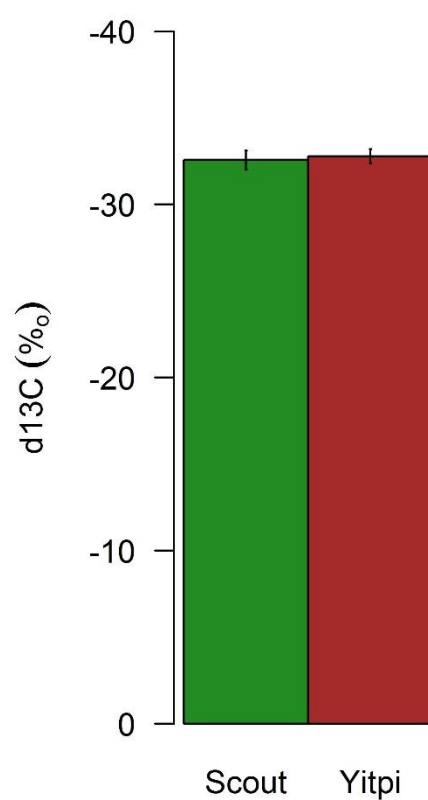


Figure S 4.1 Carbon isotope discrimination values (d13C) for Scout and Yitpi

Carbon isotope discrimination values (d13C) for Scout and Yitpi shown in green and brown respectively.

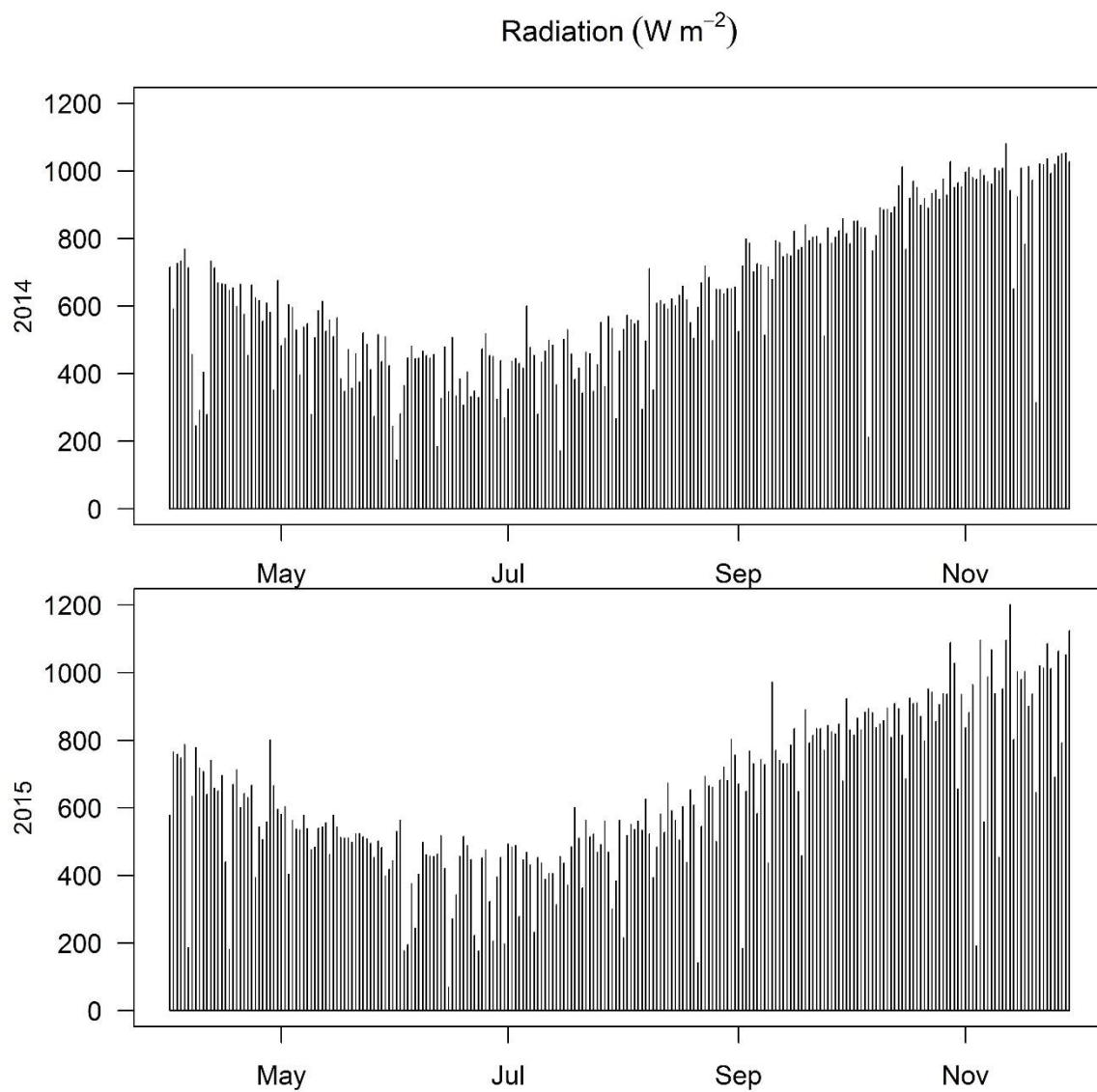


Figure S 4.2 Radiation profile for growth seasons 2014 and 2015

Fifteen-minute averages of Radiation (W m^{-2}) plotted over time for growth seasons in 2014 and 2015

CHAPTER 5

GENERAL DISCUSSION

5.1 Overall thesis summary

Climate change involves rising CO₂ and temperature, varying rainfall patterns as well as increased frequency and duration of heat stress (HS) and water stress (WS). It is important to assess the impact of climate change, including extreme events on crop productivity to manage future food security challenges. Elevated CO₂ (eCO₂) boosts leaf photosynthesis and plant productivity, however plant responses to eCO₂ depend on environmental conditions. The response of wheat to eCO₂ has been investigated in enclosures and in field studies; however, studies accounting for eCO₂ interactions with HS or WS are limited. My PhD project addresses this knowledge gap.

The broad aim of this thesis was to investigate the response of two commercial wheat cultivars with contrasting agronomical traits to future climate with eCO₂ and more extreme events, in order to develop a mechanistic approach that can potentially be incorporated in current crop models, which, so far, fail to predict accurate yields under stressful conditions. Consequently, I investigated the interactive effects of eCO₂ with either heat HS or WS on photosynthesis, crop growth and grain yield of the two wheat cultivars Scout and Yitpi grown either in the glasshouse or in a dryland field.

In the first glasshouse experiment, the two cultivars were grown at current ambient (450 ppm) and future elevated (650 ppm) CO₂ concentrations, 22/14°C day/night temperature, supplied with non-limiting water and nutrients and exposed to 3-day moderate HS cycles at the vegetative (38/14°C) and flowering stage (33/14°C). At aCO₂, both wheat lines showed similar photosynthetic temperature responses; while larger and greater-tillering Yitpi produced slightly more grain yield than early-maturing Scout. Elevated CO₂ stimulated wheat photosynthesis and reduced stomatal conductance despite causing mild photosynthetic acclimation, while moderate HS did not inhibit photosynthesis at 25°C but slightly reduced photosynthesis at 35°C in aCO₂-grown plants. Elevated CO₂ similarly stimulated final biomass and grain yield of the two wheat cultivars not exposed to moderate HS by variably affecting grain size and number. The main distinct outcomes of this chapter were the insignificant effect of moderate HS on wheat yield and the reduced grain nutrient quality of high tillering Yitpi at eCO₂.

In the second glasshouse experiment, a single cultivar Scout was grown at current ambient (419 ppm) and future elevated (654 ppm) CO₂ concentrations, 22/14°C day/night temperature, supplied with non-limiting water and nutrients and exposed to 5-day severe HS cycle at the

flowering stage (39/23°C). Growth at eCO₂ led to downregulation of photosynthetic capacity in Scout measured at common CO₂ and leaf temperature in control plants not exposed to severe HS. Severe HS reduced light saturated CO₂ assimilation rates (A_{sat}) in aCO₂ but not in eCO₂ grown plants. Growth stimulation by eCO₂ protected plants by increasing electron transport capacity under severe HS, ultimately avoiding the damage to maximum efficiency of photosystem II. Elevated CO₂ stimulated biomass and grain yield, while severe HS equally reduced grain yield at both aCO₂ and eCO₂ but had no effect on biomass at final harvest due to stimulated tillering. In conclusion, eCO₂ protected wheat photosynthesis and biomass against severe HS damage at the flowering stage via increased maximal rate of RuBP regeneration (J_{max}), indicating an important interaction between the two components of climate change, however grain yield was reduced by severe HS in both CO₂ treatments due to grain abortion.

The field experiment investigated the interactive effects of eCO₂ and water stress (WS) on two wheat cultivars Scout and Yitpi grown under dryland field conditions using free air CO₂ enrichment (FACE). Plants were grown at two CO₂ concentrations (400 and 550 ppm) under rainfed or irrigated conditions over two growing seasons during 2014 and 2015. Irrigation in dryland field conditions created contrasting soil water conditions under aCO₂ and eCO₂. Elevated CO₂ and WS responses of biomass and grain yield differed in the two growing seasons. Elevated CO₂ stimulated photosynthesis, biomass and grain yield, but reduced photosynthetic capacity evident from lower maximal rate of RuBP carboxylation (V_{cmax}) and flag leaf N only in 2015. Water stress reduced above-ground biomass and grain yield in both cultivars and CO₂ treatment more strongly in 2014 relative to 2015. However, marginal growth stimulation by eCO₂ did not protect plants from WS. Biomass, grain yield and grain quality were antagonistically affected by eCO₂ and WS.

Overall, Scout and Yitpi responded differently to growth conditions in the glasshouse and responded similarly in the field. Under well-watered conditions, Scout and Yitpi slightly benefited from moderate HS but were adversely impacted by severe HS. At the flowering stage, severe HS caused grain abortion decreasing grain yield in both CO₂ treatments. Elevated CO₂ alleviated photosynthetic inhibition but did not stop grain yield damage caused by severe HS. Water stress reduced net photosynthesis, biomass and grain yield in both CO₂ treatments and no interaction between eCO₂ and WS was observed for any of the measured parameters. Grain yield was stimulated by eCO₂ more in the glasshouse than in the field. Grain nutrient quality was reduced by eCO₂ and unaffected by either HS or WS (in both season average).

5.2 Overall thesis conclusions

The current study investigated the interactive effects of elevated atmospheric CO₂ (eCO₂) with heat stress (HS) and water stress (WS) on photosynthesis, biomass and grain yield in two commercial wheat cultivars with contrasting agronomic traits Scout and Yitpi. Based on the results reported in this thesis and the summary outline in the previous section, I have selected to discuss four key overall findings in this general conclusion chapter:

1. *Scout and Yitpi responded to environmental factors differently in the glasshouse experiment and similarly in the field*
2. *Elevated CO₂ interacted with slightly beneficial moderate HS and damaging severe HS under well-watered conditions*
3. *HS will more likely interact with eCO₂ than WS under dryland field conditions*
4. *Elevated CO₂ only marginally benefits wheat plants under severe HS or WS*

5.2.1. Scout and Yitpi responded to environmental factors differently in the glasshouse experiment and similarly in the field

The two commercial wheat cultivars with similar genetic make-up but different agronomic features responded differently to growth conditions. Photosynthetic rates were similar for both cultivars in glasshouse and field conditions, while eCO₂ stimulation was higher in field relative to glasshouse grown plants when measured at growth CO₂ and 25°C leaf temperature (Figure 5.1, Table 5.1), which is in contrast to previous studies that found higher stimulation in photosynthesis in glass house (21%) relative to FACE studies (13%) with wheat (Long et al., 2006). Both cultivars had similar biomass, grain yield and morphological characteristics in the field, while glasshouse grown plants significantly differed in development, biomass, harvest index, grain size and grain number. Scout developed faster and produced fewer but bigger grains in the glasshouse relative to Yitpi. Yitpi produced higher total biomass due to a high tillering phenotype but the harvest index was low relative to Scout producing similar grain yield in both cultivars. In well fertilized glasshouse conditions, Yitpi being a freely tillering cultivar invested more in structural components producing more biomass than Scout, however the biomass was not converted into grains. Glasshouse grown Yitpi had fewer grains per ear and reduced mean grain size relative to glasshouse grown Scout or field grown plants. Consistent with previous studies (Ainsworth et al., 2008; Long et al., 2006) grain yield response to eCO₂ was stronger in glasshouse plants relative to field grown plants (Figure 5.1, Table 5.1).

Higher eCO₂ concentration of 650 (μl L⁻¹) in glasshouse experiments relative to 550 (μl L⁻¹) in field conditions may be a contributing factor for observed differences in eCO₂ response of photosynthesis, biomass and grain yield among the two growth conditions. Another factor may be the greater variability in rainfall and temperature experienced by field grown plants under Australian conditions, as well as the larger heterogeneity in soil nutrient and water supplies. These factor could dampen the expression of the overall growth response to eCO₂ in the field relative to the glasshouse. It is also worth noting that no differences in water use efficiency were detected between the two wheat cultivars in contrast to what was initially reported about Scout having higher water use efficiency due to a carbon isotope gene. *Therefore, it can be concluded that while eCO₂ stimulates grain yield of wheat in both the glasshouse and the field, both Scout and Yitpi are expected to benefit similarly from rising atmospheric CO₂ in the Australian southern wheat belt characterized by dryland fields, and warm and highly variable environments.*

Another important difference between the field and glasshouse experiments was that grain protein levels were generally higher for glasshouse (18-22%) than field (10-12%) grown plants (Table 5.1). In fact the grain protein percentages reported for the grains were higher than what is usually reported for wheat while field values appear within the commonly reported range (Bahrami et al., 2017). Importantly, grain protein decreased in both cultivars in the field and only in Yitpi in the glasshouse experiment. *Reduced grain nutrient quality remains one of the most consistent and serious aspects of climate change on the wheat crop under future eCO₂ climates.*

5.2.2. Elevated CO₂ interacted with slightly beneficial moderate HS and damaging severe HS under well-watered conditions

The interaction of eCO₂ with moderate and severe HS was tested in the glasshouse experiments under well-watered conditions. Moderate HS at vegetative and flowering stage under moderate humidity was not harmful due to evaporative cooling and temperature increases that were below damaging levels (Chapter 2). In the field, leaf temperatures can increase to a level that negatively affect photosynthesis and physiology resulting in decreased in grain yield (Ugarte et al., 2007). Hence, a longer 5-day HS experiment under very high humidity was undertaken to reduce evaporative cooling to allow greater increases in leaf temperatures (Chapter 3). Moderate HS did not affect A_{sat} , while severe HS significantly reduced A_{sat} in aCO₂ grown plants. Interactive effects of eCO₂ and HS on photosynthesis were observed under both

moderate and severe HS. During moderate HS, A_{sat} increased only in eCO₂ grown plants when measured at 35°C relative to 25°C leaf temperature and at growth CO₂ concentration. On exposure to severe HS, A_{sat} decreased under both CO₂ concentrations, however, plants grown at eCO₂ showed complete recovery in A_{sat} , but this was not the case for aCO₂ grown plants. Thus, HS reduced photosynthesis to a greater extent under aCO₂ compared to eCO₂ due to eCO₂ playing a protective role on photosynthesis against HS damage. These results are consistent with previous studies (Wang et al., 2011) that found higher increases in A_{sat} under HS relative to control plants (Figure 5.1). *In conclusion, my results show that the protective effect of eCO₂ against HS may be expressed as either less photosynthetic inhibition at high temperature (moderate HS) or quicker recovery (severe HS).*

Interestingly, moderate HS tended to slightly increase biomass and grain yield and proved beneficial under aCO₂ but not under eCO₂ suggesting interaction between eCO₂ and moderate HS (Figure 5.1 and Table 5.2, 5.3). The absence of positive or negative effect of moderate HS under eCO₂ suggests that under well-watered conditions moderate HS may not have as much impact on plant growth and productivity in future eCO₂ conditions. In contrast, severe HS reduced biomass more under aCO₂ when measured 2 weeks after HS. However, biomass recovered completely under both CO₂ concentrations due to new tiller formation as a consequence of loss of sinks (grain loss due to abortion). Thus, interactive effects of eCO₂ and biomass were observed under both moderate and severe HS. Severe HS at flowering stage under high humidity reduced grain yield, while moderate HS was not non-damaging. Elevated CO₂ prevented biochemical damage but could not ameliorate grain yield damage due to grain abortion (Figure 5.1 and Table 5.2, 5.3). *In conclusion, while moderate and severe HS can have positive, neutral or negative impacts on wheat biomass and grain yield, eCO₂ will unlikely mitigate HS losses in grain yield in contrast to the mitigating effects of eCO₂ at the level of leaf photosynthesis and even plant biomass. This constitutes a serious negative outcome of climate change on wheat yield.*

5.2.3. HS will more likely interact with eCO₂ than WS under dryland field conditions

Elevated CO₂ interacted with moderate and severe HS differently, however, unlike previous studies (Kimball, 2016), I did not observe interactions between eCO₂ and WS for any of the measured parameters under rainfed dryland conditions (Figure 5.1 and Table 5.3). Water stress reduced photosynthesis due to leaf rolling and stomatal closure to prevent transpiration (Clarke, 1986). Rolled and functionally inactive leaves shut down photosynthesis and did not allow leaf

gas exchange measurements. Functionally active leaves used for the gas exchange measurements did not show WS effects on photosynthesis. Hence, leaf rolling and poor stomatal response to eCO_2 may have prevented eCO_2 interaction with WS (Ainsworth and Rogers, 2007). Although crops maintain the flag leaf in better condition than lower leaves, the complexity lies in trying to draw a relation between leaf water potential and the general crop water stress status, particularly when the photosynthesis is measured at leaf level. Alternatively, the lack of interaction between eCO_2 and water stress can also be attributed to the intensity and timing of water stress. The timing of rain/irrigation events and crop water use patterns affect the response to eCO_2 under rainfed conditions (Hatfield et al., 2011). *In conclusion, eCO_2 is unlikely to result in significant water saving or mitigate the negative effects of WS on wheat photosynthesis or grain yield under the generally warmer and drier wheat growing environments of the Australian wheat belt.*

This study also suggests that HS interactions with eCO_2 are more likely than water stress in dryland field conditions. However, considering HS in this study was tested in glasshouse conditions, the outcomes may vary depending on the method of applying HS in the field conditions. Considering the technical difficulties and huge cost of implementing plot scale HS in the field, glasshouse experiments remain valuable to understand the critically important threats of climate change such as HS to crop production in near future.

5.2.4 Elevated CO_2 only marginally benefits wheat plants under severe HS or WS

Elevated CO_2 interactions with HS and WS have been found to be positive, negative or neutral (Coleman et al., 1991; Leakey et al., 2012; Roden and Ball, 1996; Schütz and Fangmeier, 2001; Taub et al., 2008). Variation in the response to eCO_2 in previous studies has been attributed to species and growth environment. In the current study, despite protection of plants by eCO_2 from HS, eCO_2 did not stop large damages caused by severe HS during flowering. In addition, eCO_2 stimulation marginally benefitted plants under WS and did not compensate for WS induced large reductions in grain yield (Figure 5.1 and Table 5.2, 5.3). *Therefore, this study demonstrates that eCO_2 interaction with temperature can benefit plants when HS occurs at the vegetative stage, while losses due to HS during the flowering stage and losses due to WS cannot be alleviated by eCO_2 . Given that HS and WS are more likely to occur late in the growth season during flowering or grain filling stage (Farooq et al., 2011, 2014), the potential for eCO_2 to ameliorate the negative impacts of HS or WS on wheat grain yield is expected to be small or*

negligible under Austrlia's cropping conditions. This the key warning message advanced by my thesis.

5.3 Future prospects and implications

Modelling is a powerful tool to identify future threats to crops and simulation models combined with local-scale climate scenarios can predict impacts of HS and WS on wheat yield. Effects of eCO₂, HS and WS on growth and development are considered a prerequisite to develop simulation models for future climate change studies (O’Leary et al., 2015). Crop simulation models need to be improved to accurately reflect the interactive effects of HS and WS with eCO₂ on plant growth and yield (Asseng et al., 2013). Particularly, the scale up of leaf to canopy photosynthesis will be crucial in improving the accuracy of prediction along with the incorporation of elevated CO₂ and HS.

The photosynthetic rate of a leaf canopy depends on the reflection, transmission and photosynthesis function of the leaves, the position of the leaves with respect to horizon and each other, leaf area index (LAI), the amount of diffused and direct light, the position of the sun and the resistance against the transfer of CO₂ from bulk air to canopy (deWit, 1965).

Scaling leaf photosynthesis to canopy photosynthesis has been attempted using leaf photochemical efficiency and absorbed photosynthetically active radiation (APAR), using average illumination and LAI. This considers the canopy as one whole big leaf, stratifying canopy into sunlit and shade leaves and considering leaf energy balance with environmental gradients (Norman, 1993).

Most of the models estimate canopy photosynthetic uptake driven by radiation interception by the canopy. Major approaches identified for the photosynthesis modelling include the ‘maximum productivity’ approach, the ‘resource use efficiency’ approach, the ‘big leaf’ approach and the ‘sun shade’ approach (Medlyn et al., 2003). The key challenges in scaling up are model identification, parametrization and validation.

Attempts have been made to incorporate temperature response algorithms in crop models (Alderman et al., 2013; Innes et al., 2015) where the mean temperature rise alone is considered in most of the approaches employed. Short term extreme heat waves and mean temperature rise affect wheat growth differently depending on the developmental stage (Farooq et al., 2011). In addition, eCO₂ modulates the temperature response of plant growth (Long, 1991). Therefore, a modelling approach with the potential to incorporate mean temperature rise and short-term heat waves along with the impact of eCO₂ on plant response to heat stress are required.

Experimental data obtained during this project can be used to improve current crop models to incorporate interactions of eCO₂ with HS and WS that can form the basis for scale up from leaf to canopy models. One of the possible ways this can be implicated is to model interactive effects of eCO₂ with HS and WS on photosynthesis at leaf level (using data provided by this study) followed by scale up from leaf to canopy using approaches such as big leaf model or other such radiation use efficiency approaches. Net canopy CO₂ uptake can be simulated by using measured growth conditions, leaf gas exchange, biomass and literature values for missing parameters (Table 5.4). The modelling objective will be to test correlation between change in photosynthesis and change in biomass or grain yield followed by assessing the impact of stresses on the correlation (Figure 5.2).

Thus, current study provides important insights into the interactive effects of eCO₂ with moderate and severe HS under well-watered conditions in the glasshouse, and with WS in dryland field conditions. The photosynthesis and biomass data obtained can be useful in developing mechanistic modelling approach as discussed earlier to improve the accuracy of prediction by incorporating interactive effects of eCO₂ with stresses. Hence, my study has important implications in improving our understanding of future extreme climate on globally important crop wheat and provide the first steps for future research broadly aimed at improving or maintaining the crop productivity in context of climate change and food security.

Consequently, the following experiments are suggested as future follow up works to my PhD project:

1. Model interactive effects of eCO₂, HS and WS on photosynthesis at leaf level followed by scale up to canopy using radiation use efficiency or equivalent approaches.
2. Experiments to characterize HS in field conditions with detailed measurements for photosynthesis and biomass at multiple time points.
3. Experiments to assess WS impact on eCO₂ response under FACE at multiple locations having different soil, nutrient and environmental conditions.
4. Experiments to characterize interactive effects of eCO₂, HS and WS at genetic, biochemical and metabolite level using advanced techniques of molecular characterization.

Table 5.1 Comparative responses to eCO₂ of two wheat cultivars grown in either the glasshouse in the field

Summary of photosynthesis, plant dry mass (DM) and grain yield parameters for Scout and Yitpi grown at aCO₂ or eCO₂ and well-watered and fertilized conditions. Values are means \pm SE (n= 3-4 for field and n= 9-10 for glasshouse). Nitrogen (N) use efficiency for grain yield produced per unit N is abbreviated as NUEg. Value are ranked using a Tukey post hoc test of means within each experiment. Values followed by the same letter are not significantly different at the 5% level.

Parameter	Growth CO ₂	Glasshouse (Ch 2)		Field (Ch 4, Mean 2014-2015)	
		Scout	Yitpi	Scout	Yitpi
<i>A_{sat}</i> at growth CO ₂ ($\mu\text{mol m}^{-2}\text{s}^{-1}$)	aCO ₂	17.6 \pm 0.6a	20 \pm 1.1a	22.7 \pm 2.8a	21.5 \pm 4.1a
	eCO ₂	22.8 \pm 1.5b	23.3 \pm 1.2b	33 \pm 3.1b	30.1 \pm 3.9b
	fold change	1.29	1.16	1.45	1.4
Above ground DM (g plant ⁻¹ for glasshouse) and (g m ⁻² for field)	aCO ₂	14.9 \pm 1.8a	29.8 \pm 3.1bc	735 \pm 69a	802 \pm 48a
	eCO ₂	24.3 \pm 0.8b	16.7 \pm 0.7c	867 \pm 90a	838 \pm 82a
	fold change	1.63	0.56	1.17	1.04
Grains Per Ear	aCO ₂	29 \pm 2ab	22 \pm 2a	30 \pm 2a	29 \pm 2a
	eCO ₂	36 \pm 4b	29 \pm 1ab	30 \pm 2a	29 \pm 2a
	fold change	1.24	1.31	1	1
Total Grain Number (plant ⁻¹ for glasshouse) and (m ⁻² for field)	aCO ₂	230 \pm 15a	328 \pm 32a	11319 \pm 1026a	11319 \pm 662a
	eCO ₂	326 \pm 11a	433 \pm 37b	11873 \pm 1306a	10337 \pm 1130a
	fold change	1.41	1.32	1.04	0.91
Mean Grain Size (mg grain ⁻¹ for glasshouse) and 1000 grain weight (g for	aCO ₂	37 \pm 1b	28 \pm 1a	41 \pm 1a	42 \pm 1a
	eCO ₂	42 \pm 2c	32 \pm 1ab	43 \pm 1ab	45 \pm 1b
	fold change	1.13	1.14	1.04	1.07
Grain yield (g plant ⁻¹ for glasshouse) and (g m ⁻² for field)	aCO ₂	8.5 \pm 0.6a	9.1 \pm 1.0a	461 \pm 35	473 \pm 30
	eCO ₂	14.0 \pm 0.6b	13.7 \pm 1.0b	512 \pm 44	473 \pm 46
	fold change	1.64	1.50	1.11	1
Harvest Index	aCO ₂	0.58 \pm 0.01b	0.31 \pm 0.01a	0.4 \pm 0a	0.45 \pm 0a
	eCO ₂	0.57 \pm 0.01b	0.36 \pm 0.01a	0.45 \pm 0a	0.4 \pm 0a
	fold change	0.98	1.16	1.12	0.88
Grain Protein (%)	aCO ₂	18 \pm 0.6a	22.5 \pm 0.2b	11.2 \pm 0.5a	12 \pm 0.4a
	eCO ₂	18 \pm 1a	18.7 \pm 0.3a	10 \pm 0.2a	10.3 \pm 0.3a
	fold change	1	0.83	0.89	0.85

Table 5.2 Comparative responses of the wheat cultivar Scout to eCO₂ and moderate or severe HS

Summary of photosynthesis, plant dry mass (DM) and grain yield parameters for Scout grown at ambient CO₂ (aCO₂) or elevated CO₂ and exposed to moderate or severe HS at the flowering stage under well-watered and fertilized conditions. Values are means \pm SE (n= 9-10). *A_{sat}* measured at recovery (R) stage after HS at 25°C. Biomass measurements were taken at the recovery (R) stage after HS and at maturity (M) at the final harvest. Value are ranked using a Tukey post hoc test of means within each experiment. Values followed by the same letter are not significantly different at the 5% level.

Parameter	Time Point	Growth CO ₂	Moderate HS		Severe HS	
			Control	HS	Control	HS
<i>A_{sat}</i> at growth CO ₂ (μmol m ⁻² s ⁻¹)	R	aCO ₂	17.6 \pm 0.59	14.8 \pm 1.12	23.1 \pm 1.2b	13.4 \pm 2.6a
		eCO ₂	22.8 \pm 1.55	23.2 \pm 1.9	31.6 \pm 1c	34.6 \pm 1.8d
		fold change	1.29	1.56	1.36	2.58
Total Plant DM (g plant ⁻¹)	R	aCO ₂	16.8 \pm 1.8	16.1 \pm 2.0	34.5 \pm 1.5b	24.1 \pm 1.0a
		eCO ₂	18.3 \pm 1.3	20.0 \pm 2.1	43.6 \pm 2.2d	39.3 \pm 0.9c
		fold change	1.08	1.24	1.26	1.63
	M	aCO ₂	14.9 \pm 1.8a	19.2 \pm 2.7ab	33.7 \pm 1.5a	31.4 \pm 1.1a
		eCO ₂	24.9 \pm 0.8b	17.1 \pm 0.6a	45.5 \pm 2.2b	48.8 \pm 2.2b
		fold change	1.67	0.89	1.35	1.55
Grains Per Ear (plant ⁻¹)	M	aCO ₂	29 \pm 2a	29 \pm 3a	41 \pm 1c	21 \pm 1b
		eCO ₂	36 \pm 4a	26 \pm 1a	41 \pm 1c	17 \pm 1a
		fold change	1.24	0.89	1	0.8
Total Grain Number (plant ⁻¹)	M	aCO ₂	230 \pm 15a	247 \pm 36a	415 \pm 21b	352 \pm 15a
		eCO ₂	326 \pm 11a	237 \pm 8a	511 \pm 20c	384 \pm 30a
		fold change	1.41	0.95	1.23	1.09
Mean Grain Size (mg grain ⁻¹)	M	aCO ₂	37 \pm 1a	43 \pm 1b	44 \pm 1c	32 \pm 1a
		eCO ₂	42 \pm 2b	38 \pm 1a	46 \pm 1c	35 \pm 1b
		fold change	1.13	0.88	1.04	1.09
Grain yield (g plant ⁻¹)	M	aCO ₂	8.5 \pm 0.6a	10.7 \pm 1.7ab	18.1 \pm 0.9c	11.2 \pm 0.4a
		eCO ₂	14.0 \pm 0.6b	9.0 \pm 0.5a	23.5 \pm 1.1d	13.7 \pm 1.1b
		fold change	1.64	0.84	1.29	1.22
Harvest Index	M	aCO ₂	0.58 \pm 0.01a	0.56 \pm 0.01a	0.54 \pm 0.01c	0.36 \pm 0.01b
		eCO ₂	0.57 \pm 0.01a	0.53 \pm 0.01a	0.52 \pm 0.01c	0.28 \pm 0.01a
		fold change	0.98	0.94	0.96	0.7

Table 5.3 Comparative wheat responses to moderate HS, severe HS and WS.

Comparison between the responses of photosynthesis, dry matter (DM) and grain yield parameters to moderate HS (chapter 2), severe HS (chapter 3) and water stress (chapter 4). Values are means \pm SE (n=3/4 for field and n= 9-10 glasshouse grown plants). A_{sat} measured at recovery (R) stage after HS at 25°C leaf temperature and growth CO₂. Biomass and grain yield were measured at maturity. Value are ranked using a Tukey post hoc test of means within each experiment. Values followed by the same letter are not significantly different at the 5% level.

Parameter	Growth CO ₂	Moderate HS (Chapter 2)				Severe HS (Chapter 3)		Water Stress (WS, Chapter 4)			
		Scout		Yitpi		Scout		Scout		Yitpi	
		Control	HS	Control	HS	Control	HS	Control	WS	Control	WS
A_{sat} at growth CO ₂ ($\mu\text{mol m}^{-2}\text{s}^{-1}$)	aCO ₂	17.6 \pm 0.59	14.8 \pm 1.12	20 \pm 1.1a	18.3 \pm 0.81a	23.1 \pm 1.2b	13.4 \pm 2.6a	22.7 \pm 2.8a	21.3 \pm 2.3	21.5 \pm 4.1a	20.9 \pm 2.3
	eCO ₂	22.8 \pm 1.55	23.2 \pm 1.9	23.3 \pm 1.2b	26.7 \pm 1.14c	31.6 \pm 1c	34.6 \pm 1.8d	33 \pm 3.1b	25.3 \pm 2.5	30.1 \pm 3.9b	32.3 \pm 4.1
	fold change	1.29	1.56	1.16	1.45	1.36	2.58	1.45	1.18	1.4	1.54
Above ground DM (g plant ⁻¹ for HS) and (g m ⁻² for WS)	aCO ₂	14.5 \pm 1.1a	18.7 \pm 2.6b	28.8 \pm 2.9a	34.2 \pm 1.5b	9.3 \pm 0.4a	10.3 \pm 0.4b	735 \pm 69b	433 \pm 56a	802 \pm 48b	433 \pm 63a
	eCO ₂	24.3 \pm 0.8c	16.7 \pm 0.7b	37.1 \pm 2.3b	34.7 \pm 3.2b	12.7 \pm 0.7c	18.9 \pm 1.5d	867 \pm 90b	527 \pm 34a	838 \pm 82b	491 \pm 26a
	fold change	1.67	0.89	1.28	1.01	1.36	1.83	1.17	1.21	1.04	1.13
Grain yield (g plant ⁻¹ for HS) and (g m ⁻² for WS)	aCO ₂	8.5 \pm 0.6a	10.7 \pm 1.7ab	18.1 \pm 0.9c	11.2 \pm 0.4a	18.1 \pm 0.9b	11.2 \pm 0.4a	462 \pm 35b	246 \pm 36a	373 \pm 30b	235 \pm 39a
	eCO ₂	14.0 \pm 0.6b	9.0 \pm 0.5a	23.5 \pm 1.1d	13.7 \pm 1.1b	23.5 \pm 1.1c	13.7 \pm 1.1a	512 \pm 44b	283 \pm 27a	473 \pm 46b	247 \pm 27a
	fold change	1.64	0.84	1.29	1.22	1.29	1.22	1.10	1.15	1.26	1.05
Grain Protein (%)	aCO ₂	18 \pm 0.6a	18.1 \pm 0.1a	22.5 \pm 0.2b	20.3 \pm 0.6b	NA		11.2 \pm 0.4b	13.2 \pm 0.4c	12 \pm 0.4b	13.6 \pm 0.4c
	eCO ₂	18 \pm 1a	18 \pm 0.6a	18.7 \pm 0.3a	20.1 \pm 0.8b			10.1 \pm 0.2a	11.5 \pm 0.8b	10.3 \pm 0.3a	11.8 \pm 1ab
	fold change	1	0.99	0.83	0.99			0.90	0.87	0.85	0.86

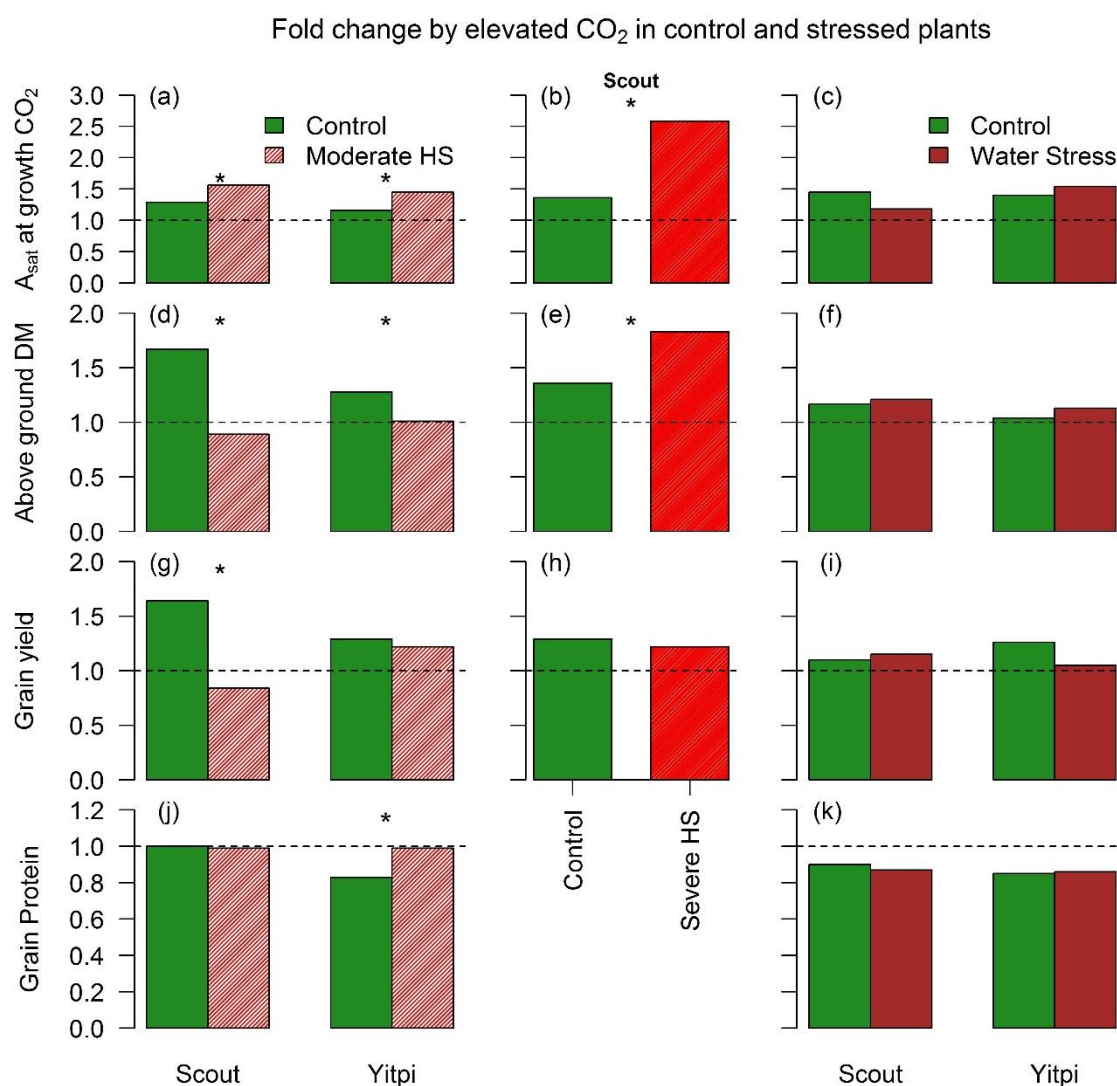


Figure 5.1 Fold change with eCO₂ in control and stresses plants for Photosynthesis, biomass and grain yield per plant

Elevated CO₂ response of A_{sat} measured at growth CO₂ (a, b, c), above ground dry matter (d, e, f), grain yield (g, h, i) and grain protein (j, k) in control, moderately heat stressed, severely heat stressed and water stressed wheat plants. The heat stress data is from glass house experiments (Chapter 2 and 3) and the water stress data is from field experiments (Chapter 4) using free air CO₂ enrichment (FACE). Two cultivars were grown under moderate HS and WS and only one under severe HS.

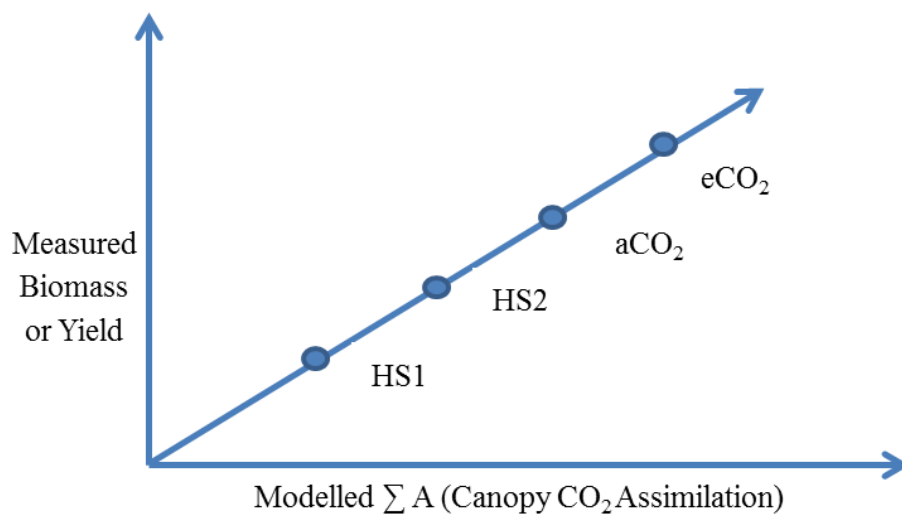


Figure 5.2 Modelling approach to consider interactive effects of eCO₂ with HS and WS

Hypothesized interactive effect between elevated CO₂ and environmental stresses (e.g., heat stress, HS) on the correlation between the changes in measured biomass and modelled canopy CO₂ uptake.

REFERENCES

- AJG Simoes, CA Hidalgo. The Economic Complexity Observatory: An Analytical Tool for Understanding the Dynamics of Economic Development. Workshops at the Twenty-Fifth AAAI Conference on Artificial Intelligence. (2011)
- Ainsworth, E.A., and Long, S.P. (2005). What have we learned from 15 years of free-air CO₂ enrichment (FACE)? A meta-analytic review of the responses of photosynthesis, canopy properties and plant production to rising CO₂. *New Phytol.* 165, 351–372.
- Ainsworth, E.A., and Rogers, A. (2007). The response of photosynthesis and stomatal conductance to rising [CO₂]: mechanisms and environmental interactions. *Plant Cell Environ.* 30, 258–270.
- Ainsworth, E.A., Davey, P.A., Hymus, G.J., Osborne, C.P., Rogers, A., Blum, H., Nösberger, J., and Long, S.P. (2003). Is stimulation of leaf photosynthesis by elevated carbon dioxide concentration maintained in the long term? A test with *Lolium perenne* grown for 10 years at two nitrogen fertilization levels under Free Air CO₂Enrichment (FACE). *Plant Cell Environ.* 26, 705–714.
- Ainsworth, E.A., Leakey, A.D.B., Ort, D.R., and Long, S.P. (2008). FACE-ing the facts: inconsistencies and interdependence among field, chamber and modeling studies of elevated [CO₂] impacts on crop yield and food supply. *New Phytol.* 179, 5–9.
- Alderman, P.D., Quilligan, E., Asseng, S., Ewert, F., and Reynolds, M.P. (2013). Proceedings of the Workshop on Modeling Wheat Response to High Temperature; El Batan, Texcoco, Mexico; 19-21 Jun 2013.
- Alonso, A., Pérez, P., Morcuende, R., and Martínez-Carrasco, R. (2008). Future CO₂ concentrations, though not warmer temperatures, enhance wheat photosynthesis temperature responses. *Physiol. Plant.* 132, 102–112.
- Alonso, A., Pérez, P., and Martínez-Carrasco, R. (2009). Growth in elevated CO₂ enhances temperature response of photosynthesis in wheat. *Physiol. Plant.* 135, 109–120.
- Amthor, J.S. (2001). Effects of atmospheric CO₂ concentration on wheat yield: review of results from experiments using various approaches to control CO₂ concentration. *Field Crops Res.* 73, 1–34.
- Andrews, T.J., and Lorimer, G.H. (1987). 3 - Rubisco: Structure, Mechanisms, and Prospects for Improvement. In *Photosynthesis*, (Academic Press), pp. 131–218.
- Arp, W.J. (1991). Effects of source-sink relations on photosynthetic acclimation to elevated CO₂. *Plant Cell Environ.* 14, 869–875.
- Asseng, S., Ewert, F., Rosenzweig, C., Jones, J.W., Hatfield, J.L., Ruane, A.C., Boote, K.J., Thorburn, P.J., Rötter, R.P., Cammarano, D., et al. (2013). Uncertainty in simulating wheat yields under climate change. *Nat. Clim. Change* 3, 827–832.

- Asseng, S., Ewert, F., Martre, P., Rötter, R.P., Lobell, D.B., Cammarano, D., Kimball, B.A., Ottman, M.J., Wall, G.W., White, J.W., et al. (2015). Rising temperatures reduce global wheat production. *Nat. Clim. Change* 5, 143–147.
- Bahrami, H., De Kok, L.J., Armstrong, R., Fitzgerald, G.J., Bourgault, M., Henty, S., Tausz, M., and Tausz-Posch, S. (2017). The proportion of nitrate in leaf nitrogen, but not changes in root growth, are associated with decreased grain protein in wheat under elevated [CO₂]. *J. Plant Physiol.* 216, 44–51.
- Bányai, J., Karsai, I., Balla, K., Kiss, T., Bedő, Z., and Láng, L. (2014). Heat stress response of wheat cultivars with different ecological adaptation. *Cereal Res. Commun.* 42, 413–425.
- Bathellier, C., Tcherkez, G., Lorimer, G.H., and Farquhar, G.D. (2018). Rubisco is not really so bad. *Plant Cell Environ.* 41, 705–716.
- Bennett, D., Izanloo, A., Reynolds, M., Kuchel, H., Langridge, P., and Schnurbusch, T. (2012). Genetic dissection of grain yield and physical grain quality in bread wheat (*Triticum aestivum* L.) under water-limited environments. *Theor. Appl. Genet.* 125, 255–271.
- Bernacchi, C.J., Portis, A.R., Nakano, H., von Caemmerer, S., and Long, S.P. (2002). Temperature Response of Mesophyll Conductance. Implications for the Determination of Rubisco Enzyme Kinetics and for Limitations to Photosynthesis in Vivo. *Plant Physiol.* 130, 1992–1998.
- Berry, J., and Bjorkman, O. (1980). Photosynthetic Response and Adaptation to Temperature in Higher Plants. *Annu. Rev. Plant Physiol.* 31, 491–543.
- BOM 2014. Annual climate statement 2013. Bureau of Meteorology. Commonwealth of Australia.
- BOM 2017. Annual climate statement 2016. Bureau of Meteorology. Commonwealth of Australia.
- CSIRO and Bureau of Meteorology (BOM) 2015, Climate Change in Australia Information for Australia's Natural Resource Management Regions: Technical Report, CSIRO and Bureau of Meteorology, Australia
- Borjigidai, A., HIKOSAKA, K., HIROSE, T., HASEGAWA, T., OKADA, M., and KOBAYASHI, K. (2006). Seasonal Changes in Temperature Dependence of Photosynthetic Rate in Rice Under a Free-air CO₂ Enrichment. *Ann. Bot.* 97, 549–557.
- Bourgault, M., Dreccer, M.F., James, A.T., and Chapman, S.C. (2013). Genotypic variability in the response to elevated CO₂ of wheat lines differing in adaptive traits. *Funct. Plant Biol.* 40, 172–184.
- Cai, C., Yin, X., He, S., Jiang, W., Si, C., Struik, P.C., Luo, W., Li, G., Xie, Y., Xiong, Y., et al. (2016). Responses of wheat and rice to factorial combinations of ambient and elevated CO₂ and temperature in FACE experiments. *Glob. Change Biol.* 22, 856–874.

- Cardoso- Vilhena, J., and Barnes, J. (2001). Does nitrogen supply affect the response of wheat (*Triticum aestivum* cv. Hanno) to the combination of elevated CO₂ and O₃? *J. Exp. Bot.* *52*, 1901–1911.
- Chaves, M.M., Maroco, J.P., and Pereira, J.S. (2003). Understanding plant responses to drought — from genes to the whole plant. *Funct. Plant Biol.* *30*, 239–264.
- Clarke, J.M. (1986). EFFECT OF LEAF ROLLING ON LEAF WATER LOSS IN *Triticum* spp. *Can. J. Plant Sci.* *66*, 885–891.
- Coleman, J.S., Rochefort, L., Bazzaz, F.A., and Woodward, F.I. (1991). Atmospheric CO₂, plant nitrogen status and the susceptibility of plants to an acute increase in temperature. *Plant Cell Environ.* *14*, 667–674.
- Condon, A.G., Richards, R.A., Rebetzke, G.J., and Farquhar, G.D. (2004). Breeding for high water-use efficiency. *J. Exp. Bot.* *55*, 2447–2460.
- Crous, K.Y., Quentin, A.G., Lin, Y.-S., Medlyn, B.E., Williams, D.G., Barton, C.V.M., and Ellsworth, D.S. (2013). Photosynthesis of temperate *Eucalyptus globulus* trees outside their native range has limited adjustment to elevated CO₂ and climate warming. *Glob. Change Biol.* *19*, 3790–3807.
- Delgado, E., Mitchell, R. a. C., Parry, M. a. J., Driscoll, S.P., Mitchell, V.J., and Lawlor, D.W. (1994). Interacting effects of CO₂ concentration, temperature and nitrogen supply on the photosynthesis and composition of winter wheat leaves. *Plant Cell Environ.* *17*, 1205–1213.
- Dias de Oliveira, E., Bramley, H., Siddique, K.H.M., Henty, S., Berger, J., and Palta, J.A. (2013). Can elevated CO₂ combined with high temperature ameliorate the effect of terminal drought in wheat? *Funct. Plant Biol.* *40*, 160–171.
- Dias de Oliveira, E.A., Siddique, K.H.M., Bramley, H., Stefanova, K., and Palta, J.A. (2015). Response of wheat restricted-tillering and vigorous growth traits to variables of climate change. *Glob. Change Biol.* *21*, 857–873.
- Dreccer, M.F., Wockner, K.B., Palta, J.A., McIntyre, C.L., Borgognone, M.G., Bourgault, M., Reynolds, M., and Miralles, D.J. (2014). More fertile florets and grains per spike can be achieved at higher temperature in wheat lines with high spike biomass and sugar content at booting. *Funct. Plant Biol.* *41*, 482–495.
- Dupont, F.M., Hurkman, W.J., Vensel, W.H., Tanaka, C., Kothari, K.M., Chung, O.K., and Altenbach, S.B. (2006). Protein accumulation and composition in wheat grains: Effects of mineral nutrients and high temperature. *Eur. J. Agron.* *25*, 96–107.
- Duursma, R.A. (2015). Plantecophys - An R Package for Analysing and Modelling Leaf Gas Exchange Data. *PLoS ONE* *10*, e0143346.
- Eckardt, N.A., and Portis, A.R. (1997). Heat Denaturation Profiles of Ribulose-1,5-Bisphosphate Carboxylase/Oxygenase (Rubisco) and Rubisco Activase and the Inability of Rubisco Activase to Restore Activity of Heat-Denatured Rubisco. *Plant Physiol.* *113*, 243–248.

- Ellsworth, D.S., Crous, K.Y., Lambers, H., and Cooke, J. (2015). Phosphorus recycling in photorespiration maintains high photosynthetic capacity in woody species. *Plant Cell Environ.* 38, 1142–1156.
- Evans, J.R., and Caemmerer, S. von (1996). Carbon Dioxide Diffusion inside Leaves. *Plant Physiol.* 110, 339–346.
- Evans, J.R., and Von Caemmerer, S. (2013). Temperature response of carbon isotope discrimination and mesophyll conductance in tobacco. *Plant Cell Environ.* 36, 745–756.
- Evans, J., Sharkey, T., Berry, J., and Farquhar, G. (1986). Carbon Isotope Discrimination measured Concurrently with Gas Exchange to Investigate CO₂ Diffusion in Leaves of Higher Plants. *Funct. Plant Biol.* 13, 281–292.
- Evans, J.R., Kaldenhoff, R., Genty, B., and Terashima, I. (2009). Resistances along the CO₂ diffusion pathway inside leaves. *J. Exp. Bot.* 60, 2235–2248.
- Ewert, F., Rodriguez, D., Jamieson, P., Semenov, M.A., Mitchell, R.A.C., Goudriaan, J., Porter, J.R., Kimball, B.A., Pinter Jr., P.J., Manderscheid, R., et al. (2002). Effects of elevated CO₂ and drought on wheat: testing crop simulation models for different experimental and climatic conditions. *Agric. Ecosyst. Environ.* 93, 249–266.
- Farooq, M., Bramley, H., Palta, J.A., and Siddique, K.H.M. (2011). Heat Stress in Wheat during Reproductive and Grain-Filling Phases. *Crit. Rev. Plant Sci.* 30, 491–507.
- Farooq, M., Hussain, M., and Siddique, K.H.M. (2014). Drought Stress in Wheat during Flowering and Grain-filling Periods. *Crit. Rev. Plant Sci.* 33, 331–349.
- Farquhar, G., and Richards, R. (1984). Isotopic Composition of Plant Carbon Correlates With Water-Use Efficiency of Wheat Genotypes. *Funct. Plant Biol.* 11, 539–552.
- Farquhar, G.D., and Cernusak, L.A. (2012). Ternary effects on the gas exchange of isotopologues of carbon dioxide. *Plant Cell Environ.* 35, 1221–1231.
- Farquhar, G., O’Leary, M., and Berry, J. (1982). On the Relationship Between Carbon Isotope Discrimination and the Intercellular Carbon Dioxide Concentration in Leaves. *Funct. Plant Biol.* 9, 121–137.
- Farquhar, G.D., Caemmerer, S. von, and Berry, J.A. (1980). A biochemical model of photosynthetic CO₂ assimilation in leaves of C₃ species. *Planta* 149, 78–90.
- Farquhar, G.D., Ehleringer, J.R., and Hubick, K.T. (1989). Carbon Isotope Discrimination and Photosynthesis. *Annu. Rev. Plant Physiol. Plant Mol. Biol.* 40, 503–537.
- Fischer, R.A. (1980). Influence of water stress on crop yield in semiarid regions. *Influ. Water Stress Crop Yield Semiarid Reg.*
- Fischer, R.A. (1985). Number of kernels in wheat crops and the influence of solar radiation and temperature. 15.
- Fitzgerald, G.J., Tausz, M., O’Leary, G., Mollah, M.R., Tausz-Posch, S., Seneweera, S., Mock, I., Löw, M., Partington, D.L., McNeil, D., et al. (2016). Elevated atmospheric [CO₂]

can dramatically increase wheat yields in semi-arid environments and buffer against heat waves. *Glob. Change Biol.* 22, 2269–2284.

Flexas, J., and Medrano, H. (2002). Drought-inhibition of Photosynthesis in C3 Plants: Stomatal and Non-stomatal Limitations Revisited. *Ann. Bot.* 89, 183–189.

Flexas, J., Bota, J., Loreto, F., Cornic, G., and Sharkey, T.D. (2004). Diffusive and Metabolic Limitations to Photosynthesis under Drought and Salinity in C3 Plants. *Plant Biol.* 6, 269–279.

García, G.A., Dreccer, M.F., Miralles, D.J., and Serrago, R.A. (2015). High night temperatures during grain number determination reduce wheat and barley grain yield: a field study. *Glob. Change Biol.* 21, 4153–4164.

Ghannoum, O., Searson, M.J., and Conroy, J.P. (2007). Nutrient and water demands of plants under global climate change. In *Agroecosystems in a Changing Climate*, p.

Ghannoum, O., Phillips, N.G., Sears, M.A., Logan, B.A., Lewis, J.D., Conroy, J.P., and Tissue, D.T. (2010). Photosynthetic responses of two eucalypts to industrial-age changes in atmospheric [CO₂] and temperature. *Plant Cell Environ.* 33, 1671–1681.

Gray, G.R., Savitch, L.V., Ivanov, A.G., and Huner, N. (1996). Photosystem II Excitation Pressure and Development of Resistance to Photoinhibition (II. Adjustment of Photosynthetic Capacity in Winter Wheat and Winter Rye). *Plant Physiol.* 110, 61–71.

Gray, S.B., Dermody, O., Klein, S.P., Locke, A.M., McGrath, J.M., Paul, R.E., Rosenthal, D.M., Ruiz-Vera, U.M., Siebers, M.H., Strellner, R., et al. (2016). Intensifying drought eliminates the expected benefits of elevated carbon dioxide for soybean. *Nat. Plants* 2, nplants2016132.

Grossman-Clarke, S., Pinter, P.J., Kartschall, T., Kimball, B.A., Hunsaker, D.J., Wall, G.W., Garcia, R.L., and LaMorte, R.L. (2001). Modelling a spring wheat crop under elevated CO₂ and drought. *New Phytol.* 150, 315–335.

Haque, M.S., Kjaer, K.H., Rosenqvist, E., Sharma, D.K., and Ottosen, C.-O. (2014). Heat stress and recovery of photosystem II efficiency in wheat (*Triticum aestivum* L.) cultivars acclimated to different growth temperatures. *Environ. Exp. Bot.* 99, 1–8.

Harley, P.C., Thomas, R.B., Reynolds, J.F., and Strain, B.R. (1992). Modelling photosynthesis of cotton grown in elevated CO₂. *Plant Cell Environ.* 15, 271–282.

Hatfield, J.L., and Prueger, J.H. (2015). Temperature extremes: Effect on plant growth and development. *Weather Clim. Extrem.* 10, Part A, 4–10.

Hatfield, J., Boote, K., Kimball, B., Ziska, L., Izaurralde, R., Ort, D., Thomson, A., and Wolfe, D. (2011). *Climate Impacts on Agriculture: Implications for Crop Production*. Publ. USDA-ARS UNL Fac.

Hochman, Z., Gobbett, D.L., and Horan, H. (2017). Climate trends account for stalled wheat yields in Australia since 1990. *Glob. Change Biol.* n/a-n/a.

Hocking, P.J., and Meyer, C.P. (Commonwealth S. and I.R.O. (1991). Effects of CO₂ enrichment and nitrogen stress on growth and partitioning of dry matter and nitrogen in wheat and maize. *Aust. J. Plant Physiol.* Aust.

Hogan, K.P., Smith, A.P., and Ziska, L.H. (1991). Potential effects of elevated CO₂ and changes in temperature on tropical plants. *Plant Cell Environ.* *14*, 763–778.

Högy, P., Wieser, H., Köhler, P., Schwadorf, K., Breuer, J., Franzaring, J., Muntifer, R., and Fangmeier, A. (2009). Effects of elevated CO₂ on grain yield and quality of wheat: results from a 3-year free-air CO₂ enrichment experiment. *Plant Biol.* *11*, 60–69.

Holzworth, D.P., Huth, N.I., deVoil, P.G., Zurcher, E.J., Herrmann, N.I., McLean, G., Chenu, K., van Oosterom, E.J., Snow, V., Murphy, C., et al. (2014). APSIM – Evolution towards a new generation of agricultural systems simulation. *Environ. Model. Softw.* *62*, 327–350.

Huang, Y., Eglinton, G., Ineson, P., Bol, R., and Harkness, D.D. (1999). The effects of nitrogen fertilisation and elevated CO₂ on the lipid biosynthesis and carbon isotopic discrimination in birch seedlings (*Betula pendula*). *Plant Soil* *216*, 35–45.

Hunsaker, D.J., Kimball, B.A., Pinter Jr., P.J., Wall, G.W., LaMorte, R.L., Adamsen, F.J., Leavitt, S.W., Thompson, T.L., Matthias, A.D., and Brooks, T.J. (2000). CO₂ enrichment and soil nitrogen effects on wheat evapotranspiration and water use efficiency. *Agric. For. Meteorol.* *104*, 85–105.

Hunsaker, D.J. (U.S.W.C.L., Kimball, B.A., Pinter, P.J., LaMorte, R.L., and Wall, G.W. (1996). Carbon dioxide enrichment and irrigation effects on wheat evapotranspiration and water use efficiency. *Trans. ASAE USA*.

IPCC, 2014: Climate Change 2014: Synthesis Report. Contributions of Working Group I, Working Group II and Working Group III, special Report on Renewable Energy Sources and Climate Change Mitigation and Special Report on Managing the Risks of Extreme Events and Disasters to Advance Climate Change Adaptation to the Fifth Assessment Report (AR5). IPCC, Geneva, Switzerland, 80 pp.

Innes, P.J., Tan, D.K.Y., Van Ogtrop, F., and Amthor, J.S. (2015). Effects of high-temperature episodes on wheat yields in New South Wales, Australia. *Agric. For. Meteorol.* *208*, 95–107.

Jauregui, I., Aroca, R., Garnica, M., Zamarreño, Á.M., García-Mina, J.M., Serret, M.D., Parry, M., Irigoyen, J.J., and Aranjuelo, I. (2015). Nitrogen assimilation and transpiration: key processes conditioning responsiveness of wheat to elevated [CO₂] and temperature. *Physiol. Plant.* *155*, 338–354.

Jordan, D.B., and Ogren, W.L. (1984). The CO₂/O₂ specificity of ribulose 1,5-bisphosphate carboxylase/oxygenase. *Planta* *161*, 308–313.

Keating, B.A., Carberry, P.S., Hammer, G.L., Probert, M.E., Robertson, M.J., Holzworth, D., Huth, N.I., Hargreaves, J.N.G., Meinke, H., Hochman, Z., et al. (2003). An overview of APSIM, a model designed for farming systems simulation. *Eur. J. Agron.* *18*, 267–288.

- Keeling, R.F., Piper, S.C., Bollenbacher, A.F., and Walker, J.S. (2009). Atmospheric Carbon Dioxide Record from Mauna Loa (Oak Ridge National Laboratory).
- Kelly, J.W.G., Duursma, R.A., Atwell, B.J., Tissue, D.T., and Medlyn, B.E. (2016). Drought \times CO₂ interactions in trees: a test of the low-intercellular CO₂ concentration (C_i) mechanism. *New Phytol.* *209*, 1600–1612.
- Keys, A.J. (1986). Rubisco: Its Role in Photorespiration. *Philos. Trans. R. Soc. Lond. B. Biol. Sci.* *313*, 325–336.
- Kimball, B.A. (1983). Carbon Dioxide and Agricultural Yield: An Assemblage and Analysis of 430 Prior Observations. *Agron. J.* *75*, 779–788.
- Kimball, B.A. (2016). Crop responses to elevated CO₂ and interactions with H₂O, N, and temperature. *Curr. Opin. Plant Biol.* *31*, 36–43.
- Kimball, B.A., Pinter Jr., P.J., Garcia, R.L., La Morte, R.L., Wall, G.W., Hunsaker, D.J., Wechsung, G., Wechsung, F., and Kartschall, T. (1995). Productivity and water use of wheat under free-air CO₂ enrichment. *Glob. Change Biol.* *1*, 429–442.
- Kimball, B.A., LaMorte, R.L., Pinter, P.J., Wall, G.W., Hunsaker, D.J., Adamsen, F.J., Leavitt, S.W., Thompson, T.L., Matthias, A.D., and Brooks, T.J. (1999). Free-air CO₂ enrichment and soil nitrogen effects on energy balance and evapotranspiration of wheat. *Water Resour. Res.* *35*, 1179–1190.
- Krenzer, E.G., and Moss, D.N. (1975). Carbon Dioxide Enrichment Effects Upon Yield and Yield Components in Wheat. *Crop Sci.* *15*, 71–74.
- Lanigan, G.J., Betson, N., Griffiths, H., and Seibt, U. (2008). Carbon Isotope Fractionation during Photorespiration and Carboxylation in Senecio. *Plant Physiol.* *148*, 2013–2020.
- LAWLOR, D.W. (2002). Limitation to Photosynthesis in Water-stressed Leaves: Stomata vs. Metabolism and the Role of ATP. *Ann. Bot.* *89*, 871–885.
- Lawlor, D.W., and Cornic, G. (2002). Photosynthetic carbon assimilation and associated metabolism in relation to water deficits in higher plants. *Plant Cell Environ.* *25*, 275–294.
- Lawlor, D.W., and Upreti, D.C. (1993). Effects of Water Stress on Photosynthesis of Crops and the Biochemical Mechanism. In *Photosynthesis: Photoreactions to Plant Productivity*, Y.P. Abrol, P. Mohanty, and Govindjee, eds. (Springer Netherlands), pp. 419–449.
- Leakey, A.D., Bishop, K.A., and Ainsworth, E.A. (2012). A multi-biome gap in understanding of crop and ecosystem responses to elevated CO₂. *Curr. Opin. Plant Biol.* *15*, 228–236.
- Leakey, A.D.B., Ainsworth, E.A., Bernacchi, C.J., Rogers, A., Long, S.P., and Ort, D.R. (2009). Elevated CO₂ effects on plant carbon, nitrogen, and water relations: six important lessons from FACE. *J. Exp. Bot.* *60*, 2859–2876.
- Liao, M., Fillery, I.R.P., and Palta, J.A. (2004). Early vigorous growth is a major factor influencing nitrogen uptake in wheat. *Funct. Plant Biol.* *31*, 121–129.

Lobell, D.B., and Gourdji, S.M. (2012). The Influence of Climate Change on Global Crop Productivity. *Plant Physiol.* 160, 1686–1697.

Long, S.P. (1991). Modification of the response of photosynthetic productivity to rising temperature by atmospheric CO₂ concentrations: Has its importance been underestimated? *Plant Cell Environ.* 14, 729–739.

Long, S.P., and Bernacchi, C.J. (2003). Gas exchange measurements, what can they tell us about the underlying limitations to photosynthesis? Procedures and sources of error. *J. Exp. Bot.* 54, 2393–2401.

Long, S.P., Ainsworth, E.A., Rogers, A., and Ort, D.R. (2004). RISING ATMOSPHERIC CARBON DIOXIDE: Plants FACE the Future. *Annu. Rev. Plant Biol.* 55, 591–628.

Long, S.P., Ainsworth, E.A., Leakey, A.D.B., Nösberger, J., and Ort, D.R. (2006). Food for Thought: Lower-Than-Expected Crop Yield Stimulation with Rising CO₂ Concentrations. *Science* 312, 1918–1921.

Lorimer, G.H., and Andrews, T.J. (1973). Plant Photorespiration—An Inevitable Consequence of the Existence of Atmospheric Oxygen. *Nature* 243, 359–360.

Lu, C., and Zhang, J. (1998). Effects of water stress on photosynthesis, chlorophyll fluorescence and photoinhibition in wheat plants. *Funct. Plant Biol.* 25, 883–892.

Medlyn, B., Barrett, D., Landsberg, J., Sands, P., and Clement, R. (2003). Conversion of canopy intercepted radiation to photosynthate: review of modelling approaches for regional scales. *Funct. Plant Biol.* 30, 153–169.

Medlyn, B.E., Dreyer, E., Ellsworth, D., Forstreuter, M., Harley, P.C., Kirschbaum, M.U.F., Le Roux, X., Montpied, P., Strassmeyer, J., Walcroft, A., et al. (2002). Temperature response of parameters of a biochemically based model of photosynthesis. II. A review of experimental data. *Plant Cell Environ.* 25, 1167–1179.

Mehta, P., Allakhverdiev, S.I., and Jajoo, A. (2010). Characterization of photosystem II heterogeneity in response to high salt stress in wheat leaves (*Triticum aestivum*). *Photosynth. Res.* 105, 249–255.

Miglietta, F., Giuntoli, A., and Bindi, M. (1996). The effect of free air carbon dioxide enrichment (FACE) and soil nitrogen availability on the photosynthetic capacity of wheat. *Photosynth. Res.* 47, 281–290.

Mitchell, R. a. C., Mitchell, V.J., Driscoll, S.P., Franklin, J., and Lawlor, D.W. (1993). Effects of increased CO₂ concentration and temperature on growth and yield of winter wheat at two levels of nitrogen application. *Plant Cell Environ.* 16, 521–529.

Mollah, M., Norton, R., and Huzzey, J. (2009). Australian grains free-air carbon dioxide enrichment (AGFACE) facility: design and performance. *Crop Pasture Sci.* 60, 697–707.

Morison, J.I.L., and Lawlor, D.W. (1999). Interactions between increasing CO₂ concentration and temperature on plant growth. *Plant Cell Environ.* 22, 659–682.

Mosse, J. (1990). Nitrogen-to-protein conversion factor for ten cereals and six legumes or oilseeds. A reappraisal of its definition and determination. Variation according to species and to seed protein content. *J. Agric. Food Chem.* 38, 18–24.

Mulholland, B.J., Craigan, J., Black, C.R., Colls, J.J., Atherton, J., and Landon, G. (1998). Growth, light interception and yield responses of spring wheat (*Triticum aestivum* L.) grown under elevated CO₂ and O₃ in open-top chambers. *Glob. Change Biol.* 4, 121–130.

Nie, G.Y., Long, S.P., Garcia, R.L., Kimball, B.A., Lamorte, R.L., Pinter, P.J., Wall, G.W., and Webber, A.N. (1995). Effects of free-air CO₂ enrichment on the development of the photosynthetic apparatus in wheat, as indicated by changes in leaf proteins. *Plant Cell Environ.* 18, 855–864.

Niinemets, Ü., Oja, V., and Kull, O. (1999). Shape of leaf photosynthetic electron transport versus temperature response curve is not constant along canopy light gradients in temperate deciduous trees. *Plant Cell Environ.* 22, 1497–1513.

NOAA National Centers for Environmental Information, State of the Climate: Global Climate Report for Annual 2016, published online January 2017, retrieved on December 2, 2017 from <https://www.ncdc.noaa.gov/sotc/global/201613>

Norman, J.M. (1993). 4 - Scaling Processes between Leaf and Canopy Levels. In *Scaling Physiological Processes*, J.R.E.B. Field, ed. (San Diego: Academic Press), pp. 41–76.

Ogren, W.L. (1984). Photorespiration: Pathways, Regulation, and Modification. *Annu. Rev. Plant Physiol.* 35, 415–442.

O’Leary, G.J., Christy, B., Nuttall, J., Huth, N., Cammarano, D., Stöckle, C., Basso, B., Shcherbak, I., Fitzgerald, G., Luo, Q., et al. (2015). Response of wheat growth, grain yield and water use to elevated CO₂ under a Free-Air CO₂ Enrichment (FACE) experiment and modelling in a semi-arid environment. *Glob. Change Biol.* 21, 2670–2686.

Osakabe, Y., Osakabe, K., Shinozaki, K., and Tran, L.-S.P. (2014). Response of plants to water stress. *Front. Plant Sci.* 5, 1–8.

Osborne, C.P., Roche, J.L., Garcia, R.L., Kimball, B.A., Wall, G.W., Pinter, P.J., Morte, R.L.L., Hendrey, G.R., and Long, S.P. (1998). Does Leaf Position within a Canopy Affect Acclimation of Photosynthesis to Elevated CO₂? Analysis of a Wheat Crop under Free-Air CO₂ Enrichment. *Plant Physiol.* 117, 1037–1045.

Pacificseeds, 2009. LongReach Scout Wheat. <https://www.pacificseeds.com.au/images/Icons/Products/Wheat/SNSWVICA/ScoutVICA.pdf> (Accessed 15 January 2017).

Pathare, V.S., Crous, K.Y., Cooke, J., Creek, D., Ghannoum, O., and Ellsworth, D.S. (2017). Water availability affects seasonal CO₂-induced photosynthetic enhancement in herbaceous species in a periodically dry woodland. *Glob. Change Biol.* 23, 5164–5178.

Pleijel, H., and Uddling, J. (2012). Yield vs. Quality trade-offs for wheat in response to carbon dioxide and ozone. *Glob. Change Biol.* 18, 596–605.

- Poorter, H. (1993). Interspecific variation in the growth response of plants to an elevated ambient CO₂ concentration. *Vegetatio* 104–105, 77–97.
- Porter, J.R., and Gawith, M. (1999). Temperatures and the growth and development of wheat: a review. *Eur. J. Agron.* 10, 23–36.
- Portis, A.R., and Salvucci, M.E. (2002). The discovery of Rubisco activase – yet another story of serendipity. *Photosynth. Res.* 73, 257–264.
- Prasad, P.V.V., and Djanaguiraman, M. (2014). Response of floret fertility and individual grain weight of wheat to high temperature stress: sensitive stages and thresholds for temperature and duration. *Funct. Plant Biol.* 41, 1261–1269.
- Prasad, P.V.V., Pisipati, S.R., Ristic, Z., Bukovnik, U., and Fritz, A.K. (2008). Impact of Nighttime Temperature on Physiology and Growth of Spring Wheat. *Crop Sci.* 48, 2372–2380.
- Rawson, H. (1992). Plant Responses to Temperature Under Conditions of Elevated CO₂. *Aust. J. Bot.* 40, 473–490.
- Roden, J.S., and Ball, M.C. (1996). The Effect of Elevated [CO₂] on Growth and Photosynthesis of Two Eucalyptus Species Exposed to High Temperatures and Water Deficits. *Plant Physiol.* 111, 909–919.
- Rogers, A., and Humphries, S.W. (2000). A mechanistic evaluation of photosynthetic acclimation at elevated CO₂. *Glob. Change Biol.* 6, 1005–1011.
- Rosenzweig, C., Iglesias, A., Yang, X.B., Epstein, P.R., and Chivian, E. (2001). Climate Change and Extreme Weather Events; Implications for Food Production, Plant Diseases, and Pests. *Glob. Change Hum. Health* 2, 90–104.
- Sadras, V., and Dreccer, M.F. (2015). Adaptation of wheat, barley, canola, field pea and chickpea to the thermal environments of Australia. *Crop Pasture Sci.* 66, 1137–1150.
- Sage, R.F. (1994). Acclimation of photosynthesis to increasing atmospheric CO₂: The gas exchange perspective. *Photosynth. Res.* 39, 351–368.
- Sage, R.F., and Kubien, D.S. (2007). The temperature response of C₃ and C₄ photosynthesis. *Plant Cell Environ.* 30, 1086–1106.
- Sage, R.F., and Sharkey, T.D. (1987). The Effect of Temperature on the Occurrence of O₂ and CO₂ Insensitive Photosynthesis in Field Grown Plants 1. *Plant Physiol.* 84, 658–664.
- Schütz, M., and Fangmeier, A. (2001). Growth and yield responses of spring wheat (*Triticum aestivum* L. cv. Minaret) to elevated CO₂ and water limitation. *Environ. Pollut.* 114, 187–194.
- Seneweera, S. (2011). Effects of elevated CO₂ on plant growth and nutrient partitioning of rice (*Oryza sativa* L.) at rapid tillering and physiological maturity. *J. Plant Interact.* 6, 35–42.

- Seneweera, S.P., and Conroy, J.P. (1997). Growth, grain yield and quality of rice (*Oryza sativa* L.) in response to elevated CO₂ and phosphorus nutrition. *Soil Sci. Plant Nutr.* *43*, 1131–1136.
- Shanmugam, S., Kjaer, K.H., Ottosen, C.-O., Rosenqvist, E., Kumari Sharma, D., and Wollenweber, B. (2013). The Alleviating Effect of Elevated CO₂ on Heat Stress Susceptibility of Two Wheat (*Triticum aestivum* L.) Cultivars. *J. Agron. Crop Sci.* *199*, 340–350.
- Sharkey, T.D. (1985). Photosynthesis in intact leaves of C₃ plants: Physics, physiology and rate limitations. *Bot. Rev.* *51*, 53–105.
- Sharkova, V.E. (2001). The Effect of Heat Shock on the Capacity of Wheat Plants to Restore Their Photosynthetic Electron Transport after Photoinhibition or Repeated Heating. *Russ. J. Plant Physiol.* *48*, 793–797.
- Sharma, D.K., Andersen, S.B., Ottosen, C.-O., and Rosenqvist, E. (2014). Wheat cultivars selected for high Fv/Fm under heat stress maintain high photosynthesis, total chlorophyll, stomatal conductance, transpiration and dry matter. *Physiol. Plant.* n/a-n/a.
- Sharma-Natu, P., Khan, F.A., and Ghildiyal, M.C. (1998). Photosynthetic acclimation to elevated CO₂ in wheat cultivars. *Photosynthetica* *34*, 537–543.
- Silva-Pérez, V., Furbank, R.T., Condon, A.G., and Evans, J.R. (2017). Biochemical model of C₃ photosynthesis applied to wheat at different temperatures. *Plant Cell Environ.* *40*, 1552–1564.
- Sionit, N., Mortensen, D.A., Strain, B.R., and Hellmers, H. (1981). Growth Response of Wheat to CO₂ Enrichment and Different Levels of Mineral Nutrition. *Agron. J.* *73*, 1023–1027.
- Spieritz, J.H.J., Hamer, R.J., Xu, H., Primo-Martin, C., Don, C., and van der Putten, P.E.L. (2006). Heat stress in wheat (*Triticum aestivum* L.): Effects on grain growth and quality traits. *Eur. J. Agron.* *25*, 89–95.
- Stone, P., and Nicolas, M. (1994). Wheat Cultivars Vary Widely in Their Responses of Grain Yield and Quality to Short Periods of Post-Anthesis Heat Stress. *Funct. Plant Biol.* *21*, 887–900.
- Stone, P., and Nicolas, M. (1996). Effect of Timing of Heat Stress During Grain Filling on Two Wheat Varieties Differing in Heat Tolerance. II. Fractional Protein Accumulation. *Funct. Plant Biol.* *23*, 739–749.
- Stone, P.J., and Nicolas, M.E. (1998). The effect of duration of heat stress during grain filling on two wheat varieties differing in heat tolerance: grain growth and fractional protein accumulation. *Funct. Plant Biol.* *25*, 13–20.
- Taiz, L., and Zeiger, E. (2010). *Plant Physiology* (Sinauer Associates).
- Taub, D.R., Miller, B., and Allen, H. (2008). Effects of elevated CO₂ on the protein concentration of food crops: a meta-analysis. *Glob. Change Biol.* *14*, 565–575.

- Tcherkez, G.G.B., Farquhar, G.D., and Andrews, T.J. (2006). Despite slow catalysis and confused substrate specificity, all ribulose biphosphate carboxylases may be nearly perfectly optimized. *Proc. Natl. Acad. Sci.* *103*, 7246–7251.
- Tezara, W., Mitchell, V.J., Driscoll, S.D., and Lawlor, D.W. (1999). Water stress inhibits plant photosynthesis by decreasing coupling factor and ATP. *Nature* *401*, 914–917.
- Ugarte, C., Calderini, D.F., and Slafer, G.A. (2007). Grain weight and grain number responsiveness to pre-anthesis temperature in wheat, barley and triticale. *Field Crops Res.*
- Von Caemmerer, S. (2013). Steady-state models of photosynthesis. *Plant Cell Environ.* *36*, 1617–1630.
- Wahid, A., Gelani, S., Ashraf, M., and Foolad, M.R. (2007). Heat tolerance in plants: An overview. *Environ. Exp. Bot.* *61*, 199–223.
- Walker, A.P., Beckerman, A.P., Gu, L., Kattge, J., Cernusak, L.A., Domingues, T.F., Scales, J.C., Wohlfahrt, G., Wullschlegel, S.D., and Woodward, F.I. (2014). The relationship of leaf photosynthetic traits – V_cmax and J_{max} – to leaf nitrogen, leaf phosphorus, and specific leaf area: a meta-analysis and modeling study. *Ecol. Evol.* *4*, 3218–3235.
- Wall, G.W., Garcia, R.L., Kimball, B.A., Hunsaker, D.J., Pinter, P.J.J., Long, S.P., Osborne, C.P., Hendrix, D.L., Wechsung, F., and Wechsung, G. (2006). Interactive effects of elevated carbon dioxide and drought on wheat. *Agron. J.*
- Wang, D., Heckathorn, S.A., Barua, D., Joshi, P., Hamilton, E.W., and LaCroix, J.J. (2008). Effects of elevated CO₂ on the tolerance of photosynthesis to acute heat stress in C₃, C₄, and CAM species. *Am. J. Bot.* *95*, 165–176.
- Wang, D., Heckathorn, S.A., Wang, X., and Philpott, S.M. (2011). A meta-analysis of plant physiological and growth responses to temperature and elevated CO₂. *Oecologia* *169*, 1–13.
- Wardlaw, I.F., and Moncur, L. (1995). The Response of Wheat to High Temperature Following Anthesis. I. The Rate and Duration of Kernel Filling. *Funct. Plant Biol.* *22*, 391–397.
- Wardlaw, I.F., Blumenthal, C., Larroque, O., and Wrigley, C.W. (2002). Contrasting effects of chronic heat stress and heat shock on kernel weight and flour quality in wheat. *Funct. Plant Biol.* *29*, 25–34.
- Wechsung, G., Wechsung, F., Wall, G.W., Adamsen, F.J., Kimball, B.A., Pinter JR., P.J., Lamorte, R.L., Garcia, R.L., and Kartschall, T. (1999). The effects of free-air CO₂ enrichment and soil water availability on spatial and seasonal patterns of wheat root growth. *Glob. Change Biol.* *5*, 519–529.
- Welch, J.R., Vincent, J.R., Auffhammer, M., Moya, P.F., Dobermann, A., and Dawe, D. (2010). Rice yields in tropical/subtropical Asia exhibit large but opposing sensitivities to minimum and maximum temperatures. *Proc. Natl. Acad. Sci.* *107*, 14562–14567.
- Wu, A., Song, Y., Oosterom, V., J, E., and Hammer, G.L. (2016). Connecting Biochemical Photosynthesis Models with Crop Models to Support Crop Improvement. *Front. Plant Sci.* *7*.

- Wu, A., Doherty, A., Farquhar, G.D., and Hammer, G.L. (2017). Simulating daily field crop canopy photosynthesis: an integrated software package. *Funct. Plant Biol.*
- Wu, D.-X., Wang, G.-X., Bai, Y.-F., and Liao, J.-X. (2004). Effects of elevated CO₂ concentration on growth, water use, yield and grain quality of wheat under two soil water levels. *Agric. Ecosyst. Environ.* *104*, 493–507.
- Yamasaki, T., Yamakawa, T., Yamane, Y., Koike, H., Satoh, K., and Katoh, S. (2002). Temperature Acclimation of Photosynthesis and Related Changes in Photosystem II Electron Transport in Winter Wheat. *Plant Physiol.* *128*, 1087–1097.
- Yin, X., and Struik, P.C. (2009). C₃ and C₄ photosynthesis models: An overview from the perspective of crop modelling. *NJAS - Wagening. J. Life Sci.* *57*, 27–38.
- Yin, X., Belay, D.W., van der Putten, P.E.L., and Struik, P.C. (2014). Accounting for the decrease of photosystem photochemical efficiency with increasing irradiance to estimate quantum yield of leaf photosynthesis. *Photosynth. Res.* *122*, 323–335.
- Zelitch, I. (1973). Plant Productivity and the Control of Photorespiration. *Proc. Natl. Acad. Sci. U. S. A.* *70*, 579–584.
- Zhang, H., Turner, N.C., Simpson, N., and Poole, M.L. (2010). Growing-season rainfall, ear number and the water-limited potential yield of wheat in south-western Australia. *Crop Pasture Sci.* *61*, 296–303.
- Zhou, S., Duursma, R.A., Medlyn, B.E., Kelly, J.W.G., and Prentice, I.C. (2013). How should we model plant responses to drought? An analysis of stomatal and non-stomatal responses to water stress. *Agric. For. Meteorol.* *182–183*, 204–214.
- Zhu, C., Ziska, L., Zhu, J., Zeng, Q., Xie, Z., Tang, H., Jia, X., and Hasegawa, T. (2012). The temporal and species dynamics of photosynthetic acclimation in flag leaves of rice (*Oryza sativa*) and wheat (*Triticum aestivum*) under elevated carbon dioxide. *Physiol. Plant.* *145*, 395–405.
- Ziska, L.H., Morris, C.F., and Goins, E.W. (2004). Quantitative and qualitative evaluation of selected wheat varieties released since 1903 to increasing atmospheric carbon dioxide: can yield sensitivity to carbon dioxide be a factor in wheat performance? *Glob. Change Biol.* *10*, 1810–1819.
- Zivcak, M., Brestic, M., Balatova, Z., Drevenakova, P., Olsovska, K., Kalaji, H.M., Yang, X., and Allakhverdiev, S.I. (2013). Photosynthetic electron transport and specific photoprotective responses in wheat leaves under drought stress. *Photosynth. Res.* *117*, 529–546.